

Parameter Estimation in Land Surface Models: Challenges and Opportunities with Data Assimilation and Machine Learning

Nina Raoult¹, Natalie Douglas², Natasha MacBean³, Jana Kolassa⁴, Tristan Quaife², Andrew G. Roberts⁵, Rosie A. Fisher⁶, Istem Fer⁷, Cédric Bacour⁸, Katherine Dagon⁹, Linnia Hawkins¹⁰, Nuno Carvalhais¹¹, Elizabeth Cooper¹², Michael Dietze⁵, Pierre Gentine¹⁰, Thomas Kaminski¹³, Daniel Kennedy⁹, Hannah M Liddy¹⁰, David Moore¹⁴, Philippe Peylin⁸, Ewan Pinnington¹⁵, Benjamin M Sanderson¹⁶, Marko Scholze¹⁷, Christian Seiler¹⁸, Thomas Luke Smallman¹⁹, Noemi Vergopolan²⁰, Toni Viskari²¹, Mathew Williams¹⁹, and John Zobitz²²

¹University of Exeter

²University of Reading

³Western University

⁴NASA Goddard Spaceflight Center

⁵Boston University

⁶CICERO Center for International Climate Research

⁷Finnish Meteorological Institute

⁸LSCE

⁹National Center for Atmospheric Research

¹⁰Columbia University

¹¹Max Planck Institute for Biogeochemistry

¹²UK Centre for Ecology & Hydrology

¹³The Inversion Lab

¹⁴The University of Arizona

¹⁵ECMWF

¹⁶CICERO Centre for International Climate Research

¹⁷Lund University

¹⁸Queen's University

¹⁹University of Edinburgh

²⁰Rice University

²¹Joint Research Centre

²²Augsburg University

October 08, 2024

Abstract

Accurately predicting terrestrial ecosystem responses to climate change is crucial for addressing global challenges. This relies on mechanistic modelling of ecosystem processes through Land Surface Models (LSMs). Despite their importance, LSMs face significant uncertainties due to poorly constrained parameters, especially in carbon cycle predictions. This paper reviews the progress made in using data assimilation (DA) for LSM parameter optimisation, focusing on carbon-water-vegetation inter-

actions, as well as discussing the technical challenges faced by the community. These challenges include identifying sensitive model parameters and their prior distributions, characterising errors due to observation biases and model-data inconsistencies, developing observation operators to interface between the model and the observations, tackling spatial and temporal heterogeneity as well as dealing with large and multiple datasets, and including the spin-up and historical period in the assimilation window. We then outline how machine learning (ML) can help address these issues, proposing different avenues for future work that integrate ML and DA to reduce uncertainties in LSMs. We conclude by highlighting future priorities, including the need for international collaborations, to fully leverage the wealth of available Earth observation datasets, harness machine learning advances, and enhance the predictive capabilities of LSMs.

Parameter Estimation in Land Surface Models: Challenges and Opportunities with Data Assimilation and Machine Learning

⁴ Nina Raoult^{1*}, Natalie Douglas², Natasha MacBean³, Jana Kolassa^{4,5}, Tristan Quaife², Andrew G. Roberts⁶, Rosie Fisher⁷, Istem Fer⁸, Cédric Bacour⁹, Katherine Dagon¹⁰, Linnia Hawkins¹¹, Nuno Carvalhais^{12,13,14}, Elizabeth Cooper¹⁵, Michael C. Dietze¹⁶, Pierre Gentine¹¹, Thomas Kaminski¹⁸, Daniel Kennedy¹⁹, Hannah M. Liddy^{20, 21}, David J.P. Moore²², Philippe Peylin⁹, Ewan Pinnington²³, Benjamin Sanderson⁷, Marko Scholze²⁴, Christian Seiler²⁵, T. Luke Smallman²⁶, Noemi Vergopolan²⁷, Toni Viskari²⁸, Mathew Williams²⁶, John Zobitz²⁹

¹⁰

¹¹ ¹Department of Mathematics and Statistics, Faculty of Environment, Science and Economy, University of Exeter, Exeter, UK

¹³ ²National Centre for Earth Observation, Department of Meteorology, University of Reading, Reading, UK

¹⁴ ³Departments of Geography and Environment & Biology, Western University, Canada

¹⁵ ⁴Global Modeling and Assimilation Office, NASA Goddard Space Flight Center, Greenbelt, MD, USA

¹⁶ ⁵Science Systems and Applications, Inc., Lanham, MD, USA

¹⁷ ⁶Computing and Data Sciences, Boston University, Boston, MA 02215 USA

¹⁸ ⁷CICERO, Norway

¹⁹ ⁸Finnish Meteorological Institute, Helsinki, Finland

²⁰ ⁹Laboratoire des Sciences du Climat et de l'Environnement, LSCE/IPSL, CEA-CNRS-UVSQ, Gif-sur-Yvette, France

²¹ ¹⁰NSF National Center for Atmospheric Research, Boulder, CO, USA

²² ¹¹Earth and Environmental Engineering Department, Columbia University, New York, NY 10027, USA

²³ ¹²Max Planck Institute for Biogeochemistry, Hans Knöll Strasse 10, 07745 Jena, Germany;

²⁴ ¹³Departamento de Ciências e Engenharia do Ambiente, DCEA, Faculdade de Ciências e Tecnologia, FCT,

²⁵ Universidade Nova de Lisboa, 2829-516 Caparica, Portugal

²⁶ ¹⁴ELLIS Unit Jena, Jena, Germany

²⁷ ¹⁵UK Centre for Ecology and Hydrology, Wallingford, UK

²⁸ ¹⁶Department of Earth & Environment, Boston University, Boston, MA 02215 USA

²⁹ ¹⁷Earth and Environmental Engineering Department, Columbia University, New York, NY 10027, USA

³⁰ ¹⁸The Inversion Lab, Hamburg, Germany

³¹ ¹⁹NSF National Center for Atmospheric Research, Boulder, CO, USA

³² ²⁰Columbia Climate School, Columbia University, New York, NY, USA

³³ ²¹NASA Goddard Institute for Space Studies, New York, NY, USA.

³⁴ ²²School of Natural Resources and the Environment, University of Arizona, Tucson, AZ, 85721, USA

³⁵ ²³European Centre for Medium-Range Weather Forecasts, Shinfield Park, Reading, UK

³⁶ ²⁴Department of Physical Geography and Ecosystem Science, Lund University, Lund, Sweden

³⁷ ²⁵School of Environmental Studies, Queen's University, Kingston, ON, K7L3N6, Canada

³⁸ ²⁶School of GeoSciences and National Centre for Earth Observation, University of Edinburgh, Edinburgh, EH9 3FF

³⁹ ²⁷Earth Environment and Planetary Sciences, Rice University, Houston, TX 77006, USA

⁴⁰ ²⁸European Commission Joint Research Center, Ispra, 21027 VA, Italy

⁴¹ ²⁹Department of Mathematics, Statistics, and Computer Science, Augsburg University, Minneapolis, MN 55454 USA

⁴² *now at European Centre for Medium-Range Weather Forecasts, Shinfield Park, Reading, UK

1 Key points (max 140 characters each)

2 ● Data assimilation has been shown to be a powerful tool for reducing land surface model
3 parametric uncertainty.

4 ● Machine learning can facilitate parameter estimation by enhancing computational
5 efficiency and replacing poorly represented processes.

6 ● Collaboration is key to advancing land surface model calibration and data assimilation,
7 promoting knowledge exchange and standard methods.

8 Abstract (max 250 words)

9 Accurately predicting terrestrial ecosystem responses to climate change is crucial for
10 addressing global challenges. This relies on mechanistic modelling of ecosystem processes
11 through Land Surface Models (LSMs). Despite their importance, LSMs face significant
12 uncertainties due to poorly constrained parameters, especially in carbon cycle predictions. This
13 paper reviews the progress made in using data assimilation (DA) for LSM parameter
14 optimisation, focusing on carbon-water-vegetation interactions, as well as discussing the
15 technical challenges faced by the community. These challenges include identifying sensitive
16 model parameters and their prior distributions, characterising errors due to observation biases
17 and model-data inconsistencies, developing observation operators to interface between the
18 model and the observations, tackling spatial and temporal heterogeneity as well as dealing with
19 large and multiple datasets, and including the spin-up and historical period in the assimilation
20 window. We then outline how machine learning (ML) can help address these issues, proposing
21 different avenues for future work that integrate ML and DA to reduce uncertainties in LSMs. We
22 conclude by highlighting future priorities, including the need for international collaborations, to
23 fully leverage the wealth of available Earth observation datasets, harness machine learning
24 advances, and enhance the predictive capabilities of LSMs.

25 Plain language summary (max 200 words)

26 Improving the accuracy of land surface models (LSMs) is crucial for reducing uncertainties in
27 climate change projections. Parameter data assimilation, which fine-tunes model parameters to
28 better match observed data, is key to enhancing LSM performance. However, the complexity of
29 LSMs poses challenges for global optimisation. Advances in computational power, novel
30 datasets, and machine learning (ML) offer promising solutions to improve these models. ML can
31 streamline the data assimilation process, handling large datasets and reducing computational
32 demands. This article discusses the progress made in LSM parameter estimation and the
33 challenges faced by the community. We then discuss how machine learning can help address
34 these challenges and outline future priorities. International collaboration, fostered by initiatives
35 like the Analysis, Integration and Modeling of the Earth System Land Data Assimilation Working
36 Group and the International Land Model Forum, is essential for accelerating progress,
37 facilitating knowledge exchange, and developing standardised methods for more accurate
38 climate modelling.

¹ 1. Introduction and premise

² Our world faces unprecedented climate change, water scarcity, and food security challenges. To
³ tackle these issues effectively, we need to predict the responses of terrestrial ecosystem
⁴ dynamics to future global change. This strongly relies on our ability to accurately model the
⁵ underlying processes at the global scale. Such global-scale, mechanistic or process-based
⁶ models of the terrestrial biosphere, often embedded in Earth system models (wherein they are
⁷ called Land Surface Models – LSMs; Blyth et al., 2021), mathematically represent complex
⁸ interacting ecosystem vegetation, carbon, water and energy cycling processes over half-hourly
⁹ to centennial time scales. Thus, for a given atmospheric CO₂ or anthropogenic emissions
¹⁰ scenario (including emissions from land use change), LSMs are used to predict the response of
¹¹ terrestrial ecosystems to climate change, rising CO₂ and land use change, and the resultant
¹² feedbacks to climate. LSMs are also indispensable tools in assessing climate change mitigation
¹³ strategies, for example, to assess how effective nature-based solutions such as reforestation
¹⁴ will be in curbing rising CO₂ emissions.

¹⁵

¹⁶ Representing all the requisite processes corresponding to interacting vegetation,
¹⁷ biogeochemistry, water and energy cycles mechanistically (and accurately) in LSMs over a wide
¹⁸ range of timescales, from sub-daily flux exchanges with the atmosphere to decadal-century
¹⁹ timescales representative of changes in biomass and soil carbon pools required for
²⁰ carbon-climate feedbacks, is critical for robust and reliable projections (Watson-Parris, 2021).
²¹ However, LSMs are highly complex and subject to large uncertainties, both in terms of missing
²² processes, inadequate representation of processes, and poorly constrained parameters.
²³ Furthermore, when trying to address model structural uncertainty, implementing new processes
²⁴ tends to introduce additional parameters and, therefore, more parameter uncertainty. As a
²⁵ result, LSMs often diverge significantly in their representation of many terrestrial processes
²⁶ (Gier et al., 2024; Green et al., 2024; Varney et al., 2024). Consequently, their predictions of
²⁷ important ecosystem responses under future climate change scenarios often vary widely. For
²⁸ example, LSMs disagree on the magnitude of the land carbon sink (Koven et al., 2022; Shi et
²⁹ al., 2024), and the potential constraints on CO₂ fertilisation due to water (Green et al., 2019) and
³⁰ nutrient (Davies-Barnard et al., 2022) limitations.

³¹

³² Parametric uncertainty is one of the largest sources of uncertainty in all types of land models (simple,
³³ intermediate and full complexity models), particularly for predictions of carbon cycling,
³⁴ vegetation dynamics and climate-carbon cycle feedbacks (Booth et al., 2012; Dietze, 2017;
³⁵ Fisher et al., 2019; Smallman et al., 2021). Indeed, it has been shown for one LSM that even
³⁶ perturbing a single carbon flux related parameter within its range of uncertainty can result in a
³⁷ projection spread in atmospheric CO₂ by 2100 that is larger than running the model under
³⁸ different emissions scenarios (Booth et al., 2012). We urgently need to reduce this uncertainty
³⁹ to ensure we can utilise the full potential of LSMs—parameter optimisation is one way to
⁴⁰ achieve this.

⁴¹

⁴² Many processes in LSMs (as well as processes in ecosystem models, see Table A1 for all
⁴³ process-based models mentioned in the paper) are controlled by parameters that represent the

1 functioning of individual elements of the system. While some of these parameters can be
2 directly observed (e.g. photosynthetic capacity, wood density, rooting depth, hydraulic and
3 thermal properties of snow and soil, bark thickness, tissue nutrient stoichiometry), many
4 parameters either cannot be easily measured (e.g., rooting depth) or are essentially only
5 “effective” parameters in that they have no physical meaning. Even those parameters that can
6 be directly measured can often only be observed at scales that differ from the grid resolution of
7 most global-scale LSM simulations (typically 0.5 degrees or greater). As a result, LSM
8 predictions – particularly for vegetation and carbon cycle related processes – can be highly
9 sensitive to parameter choices (in addition to model parameterisation or structural uncertainties)
10 (Booth et al., 2012; Buotte et al., 2021; Exbrayat et al., 2014; Fisher et al., 2019; Oberpriller et
11 al., 2022; Smallman et al., 2021; Zaehle, Friedlingstein, et al., 2010).

12

13 Historically, LSM parameters have simply been manually tuned (adjusted by hand to produce
14 more realistic model behaviour or to better fit a given important model variable to a given
15 dataset). Manual tuning of LSM parameters was often the only option given the required rapid
16 pace of LSM development, the lack of available data at the correct scales for LSM parameter
17 optimisation, or the computational demand of optimising the large number of parameters
18 (typically >200) in LSMs with many complex, interacting processes. However, in the last two
19 decades, the hurdles associated with performing rigorous LSM parameter optimisation (as
20 opposed to tuning) have diminished to the point that it has become feasible: many datasets
21 have become available at LSM-relevant scales, and the computational cost of running LSMs
22 has decreased (although it remains a challenge – see Sect. 3). LSM groups have therefore
23 started to optimise a selection of parameters using statistically robust data assimilation (DA)
24 methods.

25

26 DA methods are powerful as they allow observational data to be combined with numerical
27 methods to optimise estimates of chosen variables at the time of observations, either to update
28 the state (state estimation) or to optimise internal parameters (parameter estimation) while
29 accounting for uncertainties in both the model and the data (Rayner et al., 2019). However, the
30 distinct requirements of LSMs compared to the atmospheric and ocean components of ESMs
31 result in subtle but important differences in how DA techniques are applied. The atmospheric
32 and ocean components of ESMs rely on fluid dynamic models, where the underlying
33 fundamental laws are relatively well understood, even if complex to simulate, and many of the
34 model parameters are known physical quantities that can be observed. Therefore, DA activities
35 using atmospheric or ocean components of ESMs have thus far been heavily focused on
36 numerical weather forecasting (NWP) and reanalysis applications, for which estimating and
37 correcting the optimal model state at each time step is the primary goal (de Rosnay et al., 2022;
38 Hersbach et al., 2018; Zuo et al., 2019). In LSMs, however, parametric and structural
39 uncertainties dominate their spread (Bonan & Doney, 2018; Draper, 2021; Luo et al., 2015).
40 LSM parameters are often linked to biological processes and organismal traits and are
41 dependent on plant functional type (PFT). Therefore, these parameters have a wide range of
42 possible values where they have been measured (in addition to a lack of data on parameters for
43 some PFTs and the role of “effective” parameters as discussed above). Characterising and

1 simplifying the diversity of life into relatively few parameters is thus a challenge faced in LSM
2 development that is less of an issue for atmospheric and ocean modeling.

3 Early efforts in global model calibration in the 1990s and 2000s focused on optimising
4 vegetation and carbon cycle parameters of simplified or intermediate complexity land, carbon, or
5 ecosystem models. These studies, such as Knorr & Heimann's (1995) work optimising
6 parameters of the Simple Diagnostic Biosphere Model (SDBM) using site CO₂ measurements,
7 laid the groundwork for DA-focused land model parameter optimisation. Knorr & Heimann's
8 (1995) study was followed by further studies constrain carbon flux related processes in simple
9 and intermediate complexity ecosystem models like BETHY (Rayner et al., 2005; Scholze et al.,
10 2007), using frameworks referred to carbon cycle data assimilation systems (CCDASs). Parallel
11 to this, there was significant progress in using local eddy-covariance flux tower measurements
12 to optimise parameters related to photosynthesis, respiration, and energy flux in ecosystem
13 models at the site level (e.g., Moore et al., 2008; Sacks et al., 2006; Y.-P. Wang et al., 2001;
14 Williams et al., 2005). Two key intercomparison projects, OptIC and REFLEX, played a pivotal
15 role in assessing various data assimilation techniques for parameter estimation in simple and
16 intermediate complexity land, carbon cycle or ecosystem models (Fox et al., 2009; Trudinger et
17 al., 2007).

18 Parameter optimisation of computational expensive land models using DA started in the late
19 2000s (Medvigy et al., 2009; Rayner, 2010; Santaren et al., 2007). These studies used similar
20 data (*in situ* fluxes and biomass) and similar experimental configurations (site scale
21 optimisations) as past studies with simple and intermediate complexity models but often with
22 different DA methods due to the increase in computational expense of running much more
23 complex models (Sect. 2). Building on the formative DA work with the SDBM (Kaminski et al.,
24 2002) and BETHY models (Rayner et al., 2005), other LSM groups also started using global
25 networks of *in situ* atmospheric CO₂ mole concentration data for constraining regional to global
26 scale surface net CO₂ exchange (Kaminski et al., 2013; Peylin et al., 2016; Schürmann et al.,
27 2016). Testing of DA configuration at site scale (data type, sampling interval, record length, and
28 combinations of data - e.g., carbon fluxes and stocks or carbon fluxes) continued with all types
29 of land models (Bastrikov et al., 2018; Bloom et al., 2016; Bloom & Williams, 2015; Braswell et
30 al., 2005; Dietze et al., 2014; Keenan et al., 2013; Medvigy et al., 2009; Moore et al., 2008;
31 Ricciuto et al., 2008, 2011; Santaren et al., 2014; Thum et al., 2017; Weng et al., 2011; Weng &
32 Luo, 2011; Wutzler & Carvalhais, 2014; Xu et al., 2006). One example was the emergence of
33 "multi-site" experiments – parameter estimation studies in which data from multiple sites (often
34 grouped by PFT) were included simultaneously in the assimilation, with the retrieved
35 parameters then compared to those from assimilations with only individual site data (see Sect.
36 3.4 for further discussion). These were initially performed against data from the global
37 FLUXNET network for a range of intermediate and full complexity LSMs, including many LSMs
38 used within ESMs (e.g., Carvalhais et al., 2008, 2010; Groenendijk et al., 2011; Kato et al.,
39 2013; Knorr et al., 2010; Wu et al., 2018; Xiao et al., 2014, ORCHIDEE: Kuppel et al., 2012,
40 2014; JULES: Alton, 2013; Raoult et al., 2016; Noah: Chaney et al., 2016; CLM: Post et al.,
41 2017). With the advent of satellite products, remote sensing indicators of vegetation dynamics
42 (phenology and photosynthetic uptake) began to be employed to constrain model parameters at
43 various spatial scales, including reflectance (Shiklomanov et al., 2021); vegetation indices

1 (Migliavacca et al., 2009; NDVI – MacBean et al., 2015), FAPAR (Bacour et al., 2015; Forkel et
2 al., 2014, 2019; Kaminski et al., 2012; Knorr et al., 2010; Stöckli et al., 2008; Zobitz et al., 2014),
3 solar-induced fluorescence (SIF; (Bacour et al., 2019; Forkel et al., 2019; Knorr et al., 2024;
4 MacBean et al., 2018; Norton et al., 2018, 2019; J. Wang et al., 2021), aboveground biomass
5 and burned area (Forkel et al., 2019). Over the past decade, parameter estimation has
6 advanced to constrain the terrestrial carbon, water, and energy cycles simultaneously, driven by
7 new remote sensing data on total column-integrated CO_2 fluxes (XCO_2), satellite-derived
8 vegetation optical depth, soil moisture, snow cover, and river flow measurements, which have
9 been successfully integrated, for example, into BETHY (Scholze et al., 2016), the new
10 community D&B model developed by the European Space Agency (ESA)'s Carbon Cluster
11 (Knorr et al., 2024); JULES (Pinnington et al., 2018, 2021), and ORCHIDEE (Raoult et al.,
12 2021). Further details on the history of parameter optimisation in all types of land models are
13 provided in Rayner (2010), Kaminski et al. (2013), Scholze et al. (2017), Rayner et al. (2019),
14 Baatz et al. (2021), and MacBean, Bacour, et al. (2022).

15 While substantial progress in complex LSM parameter optimisation has been made (particularly
16 for constraining parameters of short timescale vegetation dynamics and carbon fluxes, as
17 described above), a number of challenges hindering objective calibration of the full
18 high-dimensional LSM parameter space remain. Despite advances in the use of analytical
19 techniques to dramatically reduce the time for LSM simulations (Luo et al., 2022; Sun et al.,
20 2023), these highly complex models still have computational requirements – even for one global
21 scale simulation – that are too high for efficient multi-site to global DA experiments. This is true
22 even for “offline” simulations (i.e., LSM simulations forced with climate reanalysis data, as
23 opposed to “online” cases when LSMs are run within the whole ESM). High dimensionality and
24 computational cost make it difficult to calibrate LSMs using conventional statistical approaches
25 like Markov Chain Monte Carlo. Methods used with simpler models often fail with LSMs due to
26 their complexity. These challenges have also meant that LSMs currently struggle to fully
27 leverage the large amount of data from ground networks and Earth observation platforms for
28 calibration.

29

30 As an LSM community, thus far, we have no overall strategy for how to proceed towards a
31 system that allows for objective parameter estimation. However, this field is rapidly expanding
32 and we are in a unique position to learn from each other, especially in relation to the technical
33 challenges we face with computational expensive LSM parameter DA. Efforts to build a Land
34 Data Assimilation Community (<https://land-da-community.github.io/>) by the Analysis, Integration
35 and Modeling of the Earth System (AIMES) Land Data Assimilation Working Group (MacBean,
36 Liddy, et al., 2022) and the International Land Model Forum (ILMF –
37 <https://hydro-jules.org/international-land-modeling-forum-ilmf>) have precipitated this sharing of
38 knowledge through online workshops and town halls. Capitalising on this momentum is vital
39 given the importance of this problem. The rapid advancements in machine learning (ML) and
40 the increasing availability of global earth observations and networks of *in situ* data create new
41 opportunities for advancing land/earth system modelling with the help of DA.

42

43 In this paper, we summarise the current state of parameter estimation in land surface modelling,

1 starting with DA methods, before outlining the different challenges and opportunities our
2 community faces. We then highlight how some of these challenges can be potentially addressed
3 by capitalising on emerging ML techniques and increasing computational capabilities. Finally,
4 we propose future priorities for advancing the field given the urgent need for more accurate and
5 precise LSM projections. We focus on the techniques and challenges related to optimising
6 carbon-vegetation-water interactions in full complexity LSMs but also discuss parameter DA and
7 ML methods applied to intermediate complexity land, carbon cycle and ecosystem models.

8

9 This paper complements Kumar et al. (2022) which addresses land surface model data
10 assimilation in the context of state estimation, with a focus on vegetation and hydrology
11 processes. A water cycle-focused perspective, tackling both state and parameter estimation, is
12 offered by De Lannoy et al. (2022).

13 2. Data assimilation methods for parameter 14 estimation in land surface models

15

16 LSMs have many parameters that need to be calibrated to accurately reflect the real world
17 (ideally based on observations) and to increase confidence in their future projections. Expert
18 knowledge and empirical measurements of some LSM parameters provide approximate values
19 or their respective ranges. However, due to uncertainties in observations and processes, and
20 the conceptual nature of most parameters, the exact values of LSM parameters are inherently
21 difficult to determine. Instead, we make use of the abundance of observational data indirectly
22 related to the parameters via the processes they are related to, and thus the problem of
23 parameter estimation in LSMs becomes the solution to the inverse problem (Tarantola, 1987,
24 2005): *find the parameter set Θ given the observations y such that $y \approx G(\Theta)$* . In the context of
25 parameter estimation, G includes a mapping from parameters to states and propagates states
26 through time via a forward model as well as an observation operator (Kaminski & Mathieu,
27 2017) that maps states to observation space.

28

29 Typically, a unique solution to the exact inverse problem does not exist and often the logical step
30 is to cast the approximate inverse problem into a loss minimisation effort that locates the
31 argument of a cost function that minimises the discrepancy between y and $G(\Theta)$. However,
32 many techniques of this type only provide point estimates (i.e., a single solution), which have
33 significant limitations when applied to LSM calibration. LSMs are inherently complex, involving
34 many interacting processes, uncertain observations, and non-linear relationships. By focusing
35 only on the best-fit parameters, point estimates ignore the range of plausible values that could
36 explain the data equally well. This can lead to overconfident predictions, underestimating the
37 variability and uncertainty in model outcomes, which is crucial for understanding the full
38 spectrum of possible future climate scenarios. Instead, we want to be able to account for
39 uncertainties in the model, data, and parameters, and reduce the uncertainty in the parameters
40 by creating observationally-constrained posterior distributions.

41

1 Hence, an approach more desirable for its ability to quantify the uncertainty in the estimated
2 parameters and its inherent natural regularisation, is the Bayesian approach. Bayesian methods
3 include information on the prior distribution of the parameters $p(\Theta)$ to define an entire posterior
4 distribution:

5
$$p(\Theta|y) \propto p(y|\Theta)p(\Theta) \quad (1)$$

6 where Θ is regarded as a random variable as opposed to a fixed value to be estimated. In this
7 case, the maximum a posteriori (MAP) estimate - the argument that maximises the posterior
8 distribution (i.e., its mode) - provides a point estimate for Θ and is equivalent to a loss
9 minimisation estimate regularised with prior parameter information under Gaussian
10 assumptions. Under such assumptions, maximising the posterior distribution corresponds to
11 minimising the so-called variational cost function:

12
$$J(\Theta) = \frac{1}{2}[(G(\Theta) - y)^T R^{-1}(G(\Theta) - y) + (\Theta - \Theta_b)^T B^{-1}(\Theta - \Theta_b)], \quad (2)$$

13 where R and B are the model/data and prior error covariance matrix, respectively, and Θ_b are
14 the prior parameter values.

15

16 With the emergence of novel ground and satellite observation sets came the advent and
17 development of techniques to implement them in a field of mathematics originally coined Data
18 Assimilation (DA) (Talagrand & Courtier, 1987). Along with the differences in the aforementioned
19 approaches to solving the inverse problem, these methods also differ in the nature of the
20 temporal assimilation of the available observations. DA methods that assimilate all available
21 observations over a given time window are known as batch (or offline/smoothers) techniques
22 whereas those that incorporate the observations at the time they become available are referred
23 to as sequential (or online/filters). There is some confusion in the community regarding the
24 terminology used when describing DA methods, for example, the false dichotomies sometimes
25 used between “variational and sequential” and “optimisation-based versus Bayesian” - these
26 dichotomies have been marred over time with hybridisation and the continual development of
27 the techniques. Rayner et al. (2019) have made a significant effort to harmonise the notation
28 and clarify overlapping terminology within the community.

29

30 Although DA is primarily used in numerical weather forecasting to correct the model state, in
31 LSMs, DA is often employed to reduce parametric uncertainty, a process referred to as
32 parameter data assimilation (PDA). Techniques used in numerical weather forecasting can be
33 adapted for parameter estimation in LSMs. One of the key methods is 4DVar, which involves
34 minimising Eq. 2 (called 4DVar to contrast with 3DVar, where the observations are instead
35 compared to a single model output at a time). The next part of this section looks a little deeper
36 into methods used to reduce this cost function, as well as outlining alternative DA methods that
37 extract the full posterior distribution.

38

39 **Methods for reducing cost functions:**

40 Methods commonly used to minimise the cost (e.g., Eq. 2) require numerical optimisation due to
41 their complex structure and these can usually be grouped into local gradient-descent or global
42 random search techniques. Although more computationally efficient, gradient-descent methods
43 require the gradient of the cost function (either exact, which requires differentiating the entire
44 LSM - see Sect. 3.7, or approximated when exact is not possible or desirable) and they can

1 result in the location of a local minimum. A common gradient-based minimisation method used
2 in LSM parameter estimation is the quasi-Newton algorithm L-BFGS-B (limited memory
3 Broyden–Fletcher–Goldfarb–Shanno algorithm with bound constraints - Byrd et al., 1995). This
4 approach can leverage exact gradients derived from either the tangent linear (forward sensitivity
5 propagation) or adjoint (backward sensitivity propagation) of the model. These gradients can be
6 obtained by hand or using automatic differentiation software (Gelbrecht et al., 2023; Griewank,
7 1997). While L-BFGS-B is powerful when exact gradients are available, practical
8 challenges—such as the complexity and computational burden of maintaining the tangent
9 linear/adjoint (see Sect. 3.7)—often necessitate alternatives. To address this, approximate
10 gradient methods can be employed. One approach is to estimate gradients using finite
11 difference, calculating the change in model output relative to changes in parameters. This
12 method is especially useful for parameters related to threshold functions, such as those
13 controlling phenology. However, the choice of perturbation size to be applied to each parameter
14 individually is crucial, as inappropriate values can lead to inaccuracies. In cases where gradient
15 information is difficult to obtain or unreliable, derivative-free methods offer a solution. The
16 Nelder-Mead simplex algorithm (Nelder & Mead, 1965), for instance, iteratively adjusts a
17 simplex (geometric shape) in parameter space to converge towards the minimum of a cost
18 function, eliminating the need for direct gradient calculations. Additionally, more advanced
19 approaches, such as the ensemble-based 4DVar (4DEnVar) algorithm proposed by Liu et al.
20 (2008) use an ensemble of model trajectories to approximate gradient information via a control
21 variable transform.

22

23 Alternatively, global search methods can be used to minimise the cost function. These methods
24 use techniques that try to scan the entire parameter space in some defined way to avoid this
25 pitfall but often require heavy computational power to do so. These global search methods can
26 be categorised as Monte Carlo (MC), since they are methods that make use of repeated trials
27 (or sampling) generated using random numbers (Owen, 2013). An example of such a method is
28 the genetic algorithm (Goldberg & Holland, 1988; Haupt & Haupt, 2004), which is based on the
29 laws of natural selection and belongs to the class of evolutionary algorithms.

30

31 Although these gradient-descent and global search methods are very efficient in finding an
32 optimal point-estimate of the parameters that minimise the given cost function, usually they do
33 not directly offer information about the posterior error statistics. Nevertheless, it is possible to
34 exploit information about the curvature of the cost function (via the Hessian) at the optimum to
35 obtain such information, but this is typically more complicated than deriving gradient information
36 and more costly in the case of global search.

37

38 **Methods to extract the full posterior distribution:**

39 In contrast to methods that obtain point-estimates for the parameters, other approaches aim to
40 extract useful information from the full posterior distribution $P(\Theta|y)$, usually at a much higher
41 computational expense and tend to be applied to computationally inexpensive LSMs, carbon
42 cycle, and ecosystem models. Similarly to global search algorithms for objective function
43 optimisation, as opposed to gradient-descent methods, these techniques are often Monte Carlo
44 in nature and hence also derivative-free (black-box).

1
2 Techniques include importance sampling (Kloek & Van Dijk, 1978), a relatively simple approach
3 that samples random values from the prior and accumulates accepted parameterisations based
4 on importance weights and aims to estimate expectations of interest such as mean, variance,
5 etc. This approach can run into limitations when the problem becomes more complicated (e.g.
6 dimensionality increases or target distribution gets more complex), as demonstrated by Ziehn et
7 al. (2012). When the computational budget permits, Markov Chain Monte Carlo (MCMC;
8 Hastings, 1970) algorithms have emerged as the gold standard for quantifying uncertainty in the
9 solution of Bayesian inverse problems. This class of iterative algorithms seeks to draw samples
10 from the posterior distribution $P(\Theta|y)$, which can in turn be used to estimate posterior statistics of
11 interest. The cost of such comprehensive uncertainty quantification is that standard MCMC
12 algorithms often require a large number ($> 10^4$ – 10^7) of iterations that build on previously
13 accepted values and so must be performed serially (i.e., not taking advantage of parallel
14 high-performance computing). This essentially means that the full LSM must be run using a new
15 parameter vector during each iteration, and while it is possible to run different
16 information-sharing chains in parallel to accelerate sampling around a global optimum (Vrugt,
17 2016), within chain iterative model evaluations still precludes parallelisation.

18
19 Particle filters provide an alternative to MCMC for sampling from the posterior distribution,
20 particularly in time-evolving systems. They represent the posterior using a set of particles,
21 updating them with each new data point. While computationally intensive and prone to particle
22 degeneracy, particle filters are useful for real-time tracking of system states and time-varying
23 parameters. However, many of the parameters in land surface models are linked to biological
24 processes and thus are subject to change over time due to acclimation, phenotypic plasticity,
25 adaptation and evolution. While some attempts have been made to explore the seasonal
26 variability in parameters (Rowland et al., 2014; Verbeeck et al., 2011), the majority of the
27 literature in land model parameter estimation so far operates on the assumption that parameters
28 are fixed in time. As such, particle filters are rarely used in PDA (Speich et al., 2021) (unless
29 part of joint state-parameter DA, for example, Zhang et al., 2017).

30

31 Applications in LSMs:

32 Due to the high number of required model evaluations, MCMC methods have primarily been
33 applied to computationally inexpensive land, carbon cycle, and ecosystem models, or to
34 calibrate isolated processes such as fitting parameters of a two-pool model of substrate
35 dependence in plant respiration (Jones et al., 2024) or parameters of the wetlands CH4
36 emissions module in the second generation dynamic global vegetation model LPJ-GUESS
37 (Kallingal et al., 2024). For example, MCMC methods have been used to estimate parameters
38 of the Simplified PnET (SIPNET) ecosystem model (Fer et al., 2018; M. Liu et al., 2015; Sacks
39 et al., 2006), TECOS (Xu et al., 2006), FöBAAR forest carbon cycle model (Keenan et al.,
40 2012), BETHY (Knorr & Kattge, 2005) and the DALEC suite of intermediate complexity
41 ecosystem models (Famiglietti et al., 2021; Keenan et al., 2011; D. Lu et al., 2017). DALEC is
42 also at the heart of the cutting-edge CARbon DAta MOdel fraMework (CARDAMOM) where the
43 full potential of MCMC-based carbon parameter estimation is performed (Bloom et al., 2016;
44 Exbrayat, Smallman, et al., 2018; Smallman et al., 2021).

1
2 While computationally expensive LSMs build on this foundation, their complexity and parameter
3 volume have made MCMC methods computationally prohibitive. Consequently, 4DVar has been
4 the preferred approach for these models. When the tangent linear or adjoint models have been
5 available (e.g., Bacour et al., 2015; Knorr et al., 2024; Kuppel et al., 2012; Raoult et al., 2016;
6 Schürmann et al., 2016), these have been directly used to minimise the cost function and
7 calculate the Hessian. Alternatively, the Nelder-Mead simplex algorithm (Pinnington et al.,
8 2018), finite differences (Bacour et al., 2019; Bastrikov et al., 2018; MacBean et al., 2015) and
9 4DEnVar (Pinnington et al., 2020) have all been used to circumvent the need of such models.
10 While some Monte Carlo approaches have been used to calibrate complex LSM
11 parameters—either for global search methods to minimise the cost function or to extract the full
12 posterior distribution—these are typically applied at the site scale and fall short of full global
13 calibrations. Examples include the adaptive population importance sampler used to calibrate the
14 JSBACH model (Mäkelä et al., 2019), the genetic algorithm used to calibrate ORCHIDEE
15 (Bastrikov et al., 2018), and multichain MCMC method DiffeRential Evolution Adaptive
16 Metropolis (DREAM(zs)) (Vrugt et al., 2009) used with CLM (Post et al., 2017) and LPJ-GUESS
17 (Bagnara et al., 2019).

18 3. Challenges

19 3.1 Selecting parameters and their prior distributions

20 A big challenge in parameter estimation studies is defining the experiment, starting with
21 selecting the parameters to be constrained and the prior distributions over which they are
22 allowed to vary. A common first step is to select from the (potentially quite large) number of
23 model parameters, a subset that is deemed the most influential in some sense. The excluded
24 parameters are then fixed at their nominal values, yielding a parameter space of reduced
25 dimension. This challenge is amplified by large numbers of interconnected parameters
26 influencing different parts of the model as parameters with strong enough covariances need to
27 be considered jointly. Furthermore, the strong co-variations between parameters and forcing
28 and boundary conditions further complicate the parameter selection process. It is vital to identify
29 the key internal parameters that have the most impact on a given model output because i) PDA
30 techniques are computationally demanding, scaling with the number of parameters used in the
31 optimisation, and ii) due to the high degree of equifinality in most parameter spaces (i.e.,
32 different parameter vectors giving the same fit to the observed data), attempting to estimate an
33 excessive number of parameters can lead to overfitting and a severe degradation in model
34 performance when the model is run in predictive mode. In other words, increasing model
35 complexity for improved prediction is only justified when there are adequate observational
36 constraints to its parameters (Famiglietti et al., 2021). Note that identifying key internal
37 parameters is not a solution in itself to the equifinality issue - it is still possible to have only two
38 key parameters and end up at equifinality.

39

1 Which model output and metric is tested fundamentally affects the crucial parameter selection if
2 relying primarily on sensitivity analysis. Furthermore, parameter sensitivity is often a function of
3 the parameter prior distributions, about which for many parameters we may have poor
4 knowledge. Indeed, a key distinction between a traditional sensitivity analysis, which may vary
5 all parameters by the same arbitrary amount (e.g. +/- 10%), and an uncertainty partitioning
6 analysis is whether the prior distributions accurately represent our knowledge about model
7 parameters prior to calibration (direct data constraints, formal expert elicitation, etc.) (Dietze et
8 al., 2014; LeBauer et al., 2013; Raczka et al., 2018).

9

10 The most common parameter sensitivity experiment is a one-factor-at-a-time parameter
11 perturbation experiment. However, this does not account for covariance between parameters,
12 which can vary along ecological tradeoffs and are known to strongly impact LSM outputs
13 (Prihodko et al., 2008). One solution to combat this is to use spatial pattern correlations as a
14 metric for parameter selection to ensure that the parameters selected are not highly correlated
15 (Dagon et al., 2020). More sophisticated methods include using the adjoint model to determine
16 local sensitivities and global sensitivity methods such as Morris (Morris, 1991) and the
17 variance-based Sobol (Saltelli et al., 2008; Sobol', 2001) and Fourier amplitude sensitivity tests
18 (FAST; Cukier et al., 1973). These methods have been applied to wide range of LSMs including
19 CABLE (Lu et al., 2013), CLASSIC (Deepak et al., 2024), CLM4.5(FATES) (Massoud et al.,
20 2019), JULES (Pianosi et al., 2017), Noah-MP (Wang et al., 2023) and ORCHIDEE
21 (Dantec-Nédélec et al., 2017; Novick et al., 2022). However, these methods can be hard to
22 implement (see Sect. 3.7 for the discussion about adjoint models) or require a large number of
23 model runs (e.g., $O(10,000)$ for Sobol). Nevertheless, once the adjoint or ensemble exists, it is
24 relatively easy to test the sensitivity of different model outputs.

25

26 In complex LSMs, even after selecting the most influential parameters, the large number of
27 vegetation (e.g., 15 plant functional types in ORCHIDEE) and soil texture classes (e.g., 13
28 USDA textural classes) used to represent the diversity of terrestrial ecosystems quickly
29 increases the dimensionality of global calibrations, as each parameter can be varied
30 independently. One way to tackle this issue is to assume that the parameter differences among
31 different groups vary proportionally and, therefore, optimise a parameter scaling factor instead
32 of targeting each parameter per group (Fer et al., 2018; McNeall et al., 2024). However, for
33 some plant traits, the "within functional type" uncertainty can be as large as the "across
34 functional type" uncertainty (e.g., Trugman et al., 2020), possibly due to the traits being either
35 weakly constrained by available data or genuinely plastic traits that vary spatially. In the latter
36 case, this variability suggests that localising parameters rather than using PFT-specific
37 parameterisations may be more appropriate. As such, methods that allow for independent
38 tuning of parameters within each PFT, or even localisation of parameters, may be necessary.
39 Scaling factors can also be used to target processes without needing to deeply explore detailed
40 parameterisations (e.g., Raoult et al., 2021) used a factor to scale the bare soil resistance to
41 evapotranspiration parameterisation in ORCHIDEE).

42

43 Selecting parameters is only one part of the problem - choosing the prior distributions is equally
44 important. In the existing LSM calibration literature, it is very common to assume uniform prior

1 distributions, either explicitly within Bayesian calibrations or implicitly when selecting uniform
2 range restrictions within parameter estimation using a naive objective function (unlike, for
3 example, classic variational DA techniques such as 4DVar which use an explicit Gaussian prior).
4 In these cases, uniform ranges are often based on informal “expert judgment” or ad hoc trial and
5 error. In some cases, parameter uncertainty ranges can be obtained from *in situ* measurements,
6 such as the TRY database (Kattge et al., 2020). Alternatively, the range can be set based on the
7 operational value of the parameter (e.g., $\pm 20\%$) - although this should only be done as a last
8 resort. When selecting ranges, extra considerations are needed to ensure that the ranges make
9 physical sense (e.g., not sampling negative values if the parameter needs to be positive), that
10 parameter dependencies are maintained (e.g., two parameters whose ratio should not surpass
11 a given threshold, or multiple parameters that must sum to one) and that plausible relationships
12 are retained (e.g., longevity of wood should be longer than that of foliage).

13

14 While uniform distributions are frequently chosen due to the lack of a more specific prior
15 distribution, and often to ensure the range is broad enough to cover edge cases, this approach
16 has significant drawbacks. Uniform priors rarely represent our actual prior knowledge of a
17 system, as they imply that all values within a range are equally likely, but values even a little bit
18 outside that range are impossible. In practice, parameter values in certain parts of parameter
19 space are often known a priori to be more plausible than others. An alternative to assuming
20 uniform prior distributions is to select from any of a plethora of other distributions, with such
21 choices usually driven by a combination of structural constraints (e.g., using zero-bound
22 distributions for non-negative parameters), formal syntheses and meta-analyses of trait data,
23 and structured expert-elicitation exercises (Dietze, 2017; Dietze et al., 2014; LeBauer et al.,
24 2013). However, selecting an inappropriate distribution can be as problematic as using a
25 uniform distribution, especially given that the true prior distribution is often not well known at the
26 start of the calibration process. This highlights the importance of conducting formal prior
27 predictive checks to validate assumptions before proceeding.

28

29 Priors constructed from trait data, where available, can often be quite well constrained, acting as
30 a form of data fusion (i.e. combining multiple constraints) and helping to constrain subsequent
31 calibrations to biologically-plausible parts of parameters space. Indeed, accounting for prior trait
32 knowledge can lead to very different conclusions about what parameters need to be included in
33 a calibration, as there are cases where very sensitive parameters may be well constrained a
34 priori (e.g., the parameter controlling the maximum rate of carboxylation - V_{Cmax}) while in other
35 cases much less sensitive, but unconstrained, parameters may plausibly span multiple orders of
36 magnitude and thus contribute more to overall model predictive uncertainty (Dietze, 2017;
37 LeBauer et al., 2013).

38

39 Informative non-uniform priors do not have to assume parameter independence; multivariate
40 priors can be constructed to capture known correlation structures and trait trade-offs, both
41 within- and across-PFTs (Shiklomanov et al., 2018). However, quantifying these correlations can
42 be a challenge, and so error covariances are often omitted in PDA, neglecting natural parameter
43 relationships. This simplification can result in an ill-posed inversion problem.

44

1 Finally, adopting informative non-uniform priors makes it easier to take advantage of the iterative
2 nature of Bayesian inference, where the posteriors from one round of model calibration can be
3 used as priors in the next round without requiring the recalibration of models to earlier data
4 constraints. Not only does this greatly simplify the updating of model calibrations as new data
5 becomes available, but it offers considerable computational advantages.

6

7 It is important to stress that no matter the method used for parameter estimation, solutions only
8 exist in the parameter space defined by the parameter selection and authorised prior ranges
9 (Williamson et al., 2013). Changing the number of parameters, their prior distributions, and/or
10 the model process representation will require new calibrations since the solution may differ due
11 to new parameter interactions and the equifinality of solutions.

12 3.2 Characterisation of model and data/observation errors

13 The state-of-the-art way to account for model and observation errors is through a Bayesian
14 framework. However, properly characterising these errors (especially data bias) can be a
15 challenge and potential model-data biases are not always properly treated with this formalism
16 (Cameron et al., 2022; MacBean et al., 2016). Model discrepancy, or model process error, refers
17 to the inherent inability of a model to replicate observations (Wu et al., 2023), stemming from
18 factors such as missing processes, choice of process representation, ecosystem heterogeneity,
19 stochastic processes (e.g., dispersal, recruitment, mortality, disturbance), biases in the model
20 forcing data, uncertainties in the initial model state, and the resolution of numerical solvers.
21 Observation error encompasses sampling variability, instrument inaccuracies, and any errors
22 involved in deriving the data products making up the observations. Furthermore, observation
23 error also usually includes a modelling step from the raw data measurement to any given
24 physical quantity (see Sect. 3.3). Due to the difficulty in separating model and observation
25 errors, they have often been combined in past studies. In fact, the mathematical formalisation
26 commonly used in PDA assumes that observation errors include model errors, thereby treating
27 model discrepancy as part of the observational error.

28

29 Although common, combining model error with data error can lead to an overestimation of
30 predictive uncertainty (van Oijen, 2017). Another approach to deal with model error is to ignore
31 it (i.e. assume the model structure is correct), however, this means only the input uncertainty is
32 propagated. A final approach is to treat model uncertainty as a separate parameter needing
33 calibration. If a prior for the model error uncertainties can be specified explicitly, model and data
34 error terms can theoretically be fitted separately. However, in practice, specifying an informative
35 prior on the model error term is challenging due to incomplete theoretical understanding of the
36 underpinning processes (Brynjarsdóttir & O'Hagan, 2014). Fortunately, it is often much easier to
37 specify an informative prior on the observation error, as these are frequently reported in data
38 products or estimable via sampling theory, and this is often useful to allow model error to be
39 separately identifiable.

40

41 There are a number of arguments for keeping process and observation error distinct. Model
42 process error propagates in space and time when making predictions, while observation error

1 does not. Additionally, addressing a large process error requires improving the model structure,
2 while addressing a large observation error calls for improving data quality. Furthermore,
3 calibrating models using cost functions that rely solely on fixed a priori observation errors can
4 distort parameter uncertainty estimates as well as the relative weight assigned to different data
5 constraints, as there's often no inherent reason to assume that model skill at predicting a
6 variable is proportional to the accuracy of its measurement. Indeed, it is easy to point to
7 examples where the uncertainty in our ability to model something differs in rank order from our
8 ability to measure that same thing (e.g., at local scale, model predictions of net ecosystem
9 exchange (NEE) are more uncertain than gross primary productivity (GPP: the flux of carbon
10 absorbed into the land surface due to photosynthesis), but observations of GPP are more
11 uncertain than NEE).

12

13 Quantifying both observation and model process error correlations, such as autocorrelated
14 measurement error, presents an additional challenge. These correlations yield non-diagonal
15 covariance structures, which are rarely well understood and are often ignored. Nevertheless,
16 accounting for these correlated errors has been shown to improve data assimilation results
17 (Waller et al., 2016), for example, by increasing the information content of observations (Stewart
18 et al., 2008). Since observation error correlations are more prevalent in dense observation
19 networks (Bannister et al., 2020), strategies to mitigate not modelling them include observation
20 thinning (reducing the number of observations assimilated in data-rich regions) and
21 super-lobbing (combining many observations into one (Lorenc, 1981)). Another common
22 approach to inflate variances is to reduce the weight of observations in data assimilation
23 (Chevallier, 2007; Kuppel et al., 2013). However, all these approaches are subjective and
24 potentially reject meaningful information (Cameron et al., 2022).

25

26 Finally, addressing systematic errors in models and data is becoming increasingly crucial as the
27 volume of data grows. With larger datasets, random errors tend to average out, leaving
28 systematic errors to dominate. These errors have long been recognised by the LSM calibration
29 community, such as when a model's ability to predict one variable worsens after assimilating
30 data for another. However, the underlying causes and potential solutions have not been widely
31 appreciated. Since all models are approximations, systematic errors in both models and data
32 require greater attention. To combat these biases, various approaches are emerging, ranging
33 from incorporating simple linear bias correction factors in the cost function (Cameron et al.,
34 2022; Fer et al., 2018) to more complex and flexible statistical models of bias, applied either
35 within the assimilation process or post-hoc (Kennedy & O'Hagan, 2001; Oberpriller et al., 2021).
36 Additionally, hybrid models that integrate machine learning with process-based models are
37 being explored as a means to address these challenges (see Sect. 4.2).

38

39 Ultimately, interconnected efforts, such as the characterisation of data errors together with the
40 data providers, post-PDA analysis of remaining model-data discrepancies, multi-model PDA
41 protocols that highlight relative model structural errors, and novel PDA algorithms are all
42 valuable in providing ways forward for discerning errors in data from those in model structure.

¹ 3.3 Developing observation operators

² The term “observation operator” refers to any transformation of the modelled quantity used to
³ allow comparison against observations (Kaminski & Mathieu, 2017). Note that what are often
⁴ called observations are themselves complex transformations of raw data measurements used to
⁵ estimate physical quantities comparable to the LSM output. For example, radiances observed
⁶ by a satellite at the top of the atmosphere can be translated into any number of land surface
⁷ data products, such as leaf area index. This processing can also be seen as a complex model,
⁸ such as the inversion of a radiative transfer scheme. Furthermore, these data are usually
⁹ prepared in such a way that they are available on the model grid.

¹⁰

¹¹ In some cases, it is possible to assume a one-to-one relationship between the model output and
¹² assimilated data, in which case the observation operator is the identity matrix. However, in all
¹³ other cases, an observation operator is required for DA, and the choice of observation operator
¹⁴ can significantly impact the results (Cooper et al., 2019). A common use of an observation
¹⁵ operator is to bridge the spatial scale between model and observations, either by aggregating
¹⁶ the gridded observations to the resolution of the model or vice-versa (Pinnington et al., 2021).
¹⁷ More complex examples of spatial scaling operators utilise a weighted averaging process to
¹⁸ match a more detailed description of the observation, such as modelling the point spread
¹⁹ function of satellite data, or the footprint of an eddy-covariance flux measurement. For example,
²⁰ Vergopolan et al. (2020) introduced a cluster-based observation operator that maps the
²¹ Gaussian footprint of satellite observations to the sub-grid scale of high-resolution LSMs. This
²² enables efficiently assimilating coarse soil moisture observations while bridging the spatial scale
²³ mismatch with fine-scale LSMs and ground observations (Vergopolan et al., 2021). In an
²⁴ application with flux tower data, Pinnington et al. (2017) partitioned the fluxes to observe
²⁵ different parts of the forest and run separate assimilation experiments for logged and unlogged
²⁶ forest stands.

²⁷

²⁸ In another example, atmospheric transport is used to map surface fluxes of gas species, such
²⁹ as CO₂, into atmospheric concentrations of that species at sampling points. In this way, flask
³⁰ measurements of CO₂ have been used to constrain parameters in models of the terrestrial
³¹ biosphere (Bacour et al., 2023; Kaminski et al., 2002, 2012; Knorr & Heimann, 1995; Peylin et
³² al., 2016; Rayner et al., 2005, 2011; Scholze et al., 2007) and to evaluate simulated net CO₂
³³ fluxes after optimising against eddy-covariance data (Kuppel et al., 2014). For non-reactive
³⁴ species, it is sufficient to have data on winds to drive the observation operator, but for reactive
³⁵ species such as CH₄, the process is more complex as atmospheric chemistry needs to be
³⁶ included.

³⁷

³⁸ Observation operators are also used to predict observed quantities that are not directly
³⁹ computed by the model itself. A recent example is the assimilation of SIF data, which is typically
⁴⁰ assumed to be a proxy for GPP. Examples of SIF observation operators include simple linear
⁴¹ relationships with GPP (Bloom et al., 2020; MacBean et al., 2018) through to more complex
⁴² operators based on the underlying photochemistry and radiative transfer in the canopy, either
⁴³ using empirical simplifications of those processes (Bacour et al., 2019) or using fully

1 mechanistic models for the operator (Norton et al., 2019). Another example is vegetation optical
2 depth which has been used to constrain above-ground biomass and leaf area index (Scholze et
3 al., 2019).

4

5 Scholze et al. (2016, 2019) also developed observation operators to map surface soil moisture
6 (SSM) retrievals to simulated volumetric soil moisture of the surface layer of BETHY, which were
7 also used by Wu et al. (2018, 2020, 2024). SSM is subject to large biases, which therefore
8 necessitates this type of transformation. Numerous models employ methods to map SSM to the
9 climatology of their model, for example through cumulative density function (CDF) matching.
10 Another approach is to focus solely on dynamics (e.g., dry downs, Raoult et al., 2021). The
11 dynamics approach is often used when assimilating vegetation indices, FAPAR or leaf area
12 index (LAI) — retrievals are normalised to estimate the seasonality of phenology instead of the
13 absolute values (MacBean et al., 2015). The optimisation then focuses on a reduced set of
14 phenology-related parameters, rather than including those related to photosynthesis (Bacour et
15 al., 2015).

16

17 Forward modelling of remote sensing data — i.e., the process of simulating remote sensing data
18 directly from the LSM outputs rather than assimilating processed satellite products — like in the
19 example of SIF, is the opposite approach to the assimilation of high-level satellite products such
20 as LAI or GPP. A key argument for taking this approach is that assumptions in the retrieval
21 process used in these products are likely inconsistent with the assumptions embedded in the
22 land surface model they are being assimilated into. A clear example of this is the use of satellite
23 GPP products which typically employ a production efficiency approach (e.g. the MODIS GPP
24 product, Running et al., 2021) whereas land surface models often use limiting-rate enzyme
25 kinetic schemes derived from those of Farquhar et al. (1980) and Collatz et al. (1992).
26 Furthermore, satellite-derived GPP estimates typically use environmental drivers such as
27 downwelling shortwave radiation which will almost certainly differ from those used to drive the
28 land surface model they are being assimilated into. Finally, there are often substantial
29 differences between the satellite-derived estimates (e.g. of GPP or LAI) where the assimilation
30 of any one product is likely biased with respect to the ‘truth’ (which is the primary reason for
31 using the seasonal dynamics rather than the actual values of time series data, as discussed in
32 the previous paragraph). Consequently, discrepancies between these high-level observations
33 and the values of the same variables predicted by a LSM may differ due to these factors and be
34 non-trivial to characterise.

35

36 It is appealing, therefore, to assimilate low-level products like SIF or canopy reflectance (Quaife
37 et al., 2008). For canopy reflectance, this typically requires the use of radiative transfer models
38 and is analogous to so-called “radiance assimilation” which is used extensively in numerical
39 weather prediction. In that way, any systematic error between the model and the observations
40 can be attributed to the land model (including the radiative transfer model) itself. For example,
41 Shiklomanov et al. (2021) modified the existing canopy radiative transfer model in the
42 Ecosystem Demography v2 model (ED2) to predict full hyperspectral waveforms, instead of just
43 aggregate visible, near-infrared, and thermal bands, and then used this observation operator to
44 calibrate ED2 against airborne AVIRIS imaging spectroscopy across the eastern temperate US.

1 Meunier et al. (2022) later used this observation operator in the development of a novel tropical
2 liana PFT. However, low-level satellite products often exhibit variability across domains that are
3 not inherently resolved by the land model, leading to some level of compromise between i)
4 adding complexity to the land model, ii) having an observation operator that is not completely
5 consistent with the underlying model or, iii) accepting that some of the variability in the
6 observations themselves will not be resolved. In the examples of SIF and canopy reflectance,
7 both vary with the relative geometry of the sun and sensor - correctly capturing that directional
8 variability using an observation operator that is physically consistent with the description of the
9 radiative transfer regime implemented in global land surface models (which typically only predict
10 total fluxes, i.e. integrated across the viewing hemisphere) is not currently possible.
11 Nevertheless, the selection and processing of observation data can help mitigate some of these
12 issues. For example, space-time binning of space-borne SIF data across multiple observation
13 geometries can limit the impact of directional effects and potentially increase the consistency
14 between model assumptions and the observed variables.

15

16 As observation operators become more complex, especially in the case of radiative transfer
17 calculations, they also become more computationally expensive. This is a clear example of
18 where machine learning may offer a unique opportunity within DA applications, as discussed in
19 Sect. 4.3.

20 3.4 Tackling spatial and temporal heterogeneity

21 The large variability in the surface properties of terrestrial ecosystems, arising from diverse
22 climates, soil properties, and variations in plant and soil species composition, plasticity, and
23 evolution, is an additional challenge in LSM parameter estimation. Calibration of the model at
24 one location may not be applicable at another. Moreover, most LSMs are too computationally
25 demanding to support calibration across large spatial domains. As such, it is important to
26 develop strategies to ensure results offer a good compromise across different locations, as well
27 as perform rigorous evaluation checks against data not used in the calibration.

28

29 A common approach to tackle this spatial heterogeneity is to perform “multi-site” optimisations,
30 grouping sites and performing a single optimisation over this group to obtain a more generic set
31 of parameters. The multi-site approach has been shown to be very effective, at times
32 out-performing site-specific optimisations (Kuppel et al., 2012; Raoult et al., 2016). Another
33 approach is to average the results of single-site optimisations. While usually less effective than
34 multi-site optimisations, this is often a more practical solution and can still result in an improved
35 parameter set. For example, Olivera-Guerra et al. (2024) found that the median values of
36 optimised parameters improved simulated land-surface temperature performance.

37

38 Both these approaches can be thought of as end-members (all sites the same versus all sites
39 different) in a continuum representing the statistical independence of calibrations across sites.
40 While only just beginning to be utilised to calibrate ecosystem models (Dokoochaki et al., 2022;
41 Fer, Shiklomanov, et al., 2021), hierarchical models have a long history of use in ecology as a
42 way of capturing this continuum, allowing parameters to vary across space and through time,

1 but constraining that variability with multivariate statistical models that describe that variability.
2 Since the across-site and within-site calibrations are fit simultaneously, this would allow LSM
3 models to “borrow strength” across sites (e.g., reducing equifinality as described above) without
4 forcing parameters to be the same everywhere. Hierarchical models also provide a formal
5 framework for accounting for the fact that out-of-sample predictions are more uncertain
6 (because their parameter vectors need to be predicted) than in-sample predictions at sites
7 where parameter vectors are known. To date, existing hierarchical ecosystem model calibrations
8 have assumed a simple “random effects” structure (i.e. different sites are drawn from the same
9 across-site distribution), but there are important opportunities to explore hierarchical models
10 with across-site spatiotemporal covariances (i.e., sites closer together should be more similar)
11 and across-site covariates (i.e., parameters that explain, and help predict, parameter variability).

12 A further alternative is the use of intermediate complexity models (e.g., DALEC), which, due to
13 their reduced computational complexity, can retrieve parameters at the pixel scale utilising
14 spatially continuous information from Earth Observation (EO) data and thus derive unique
15 information about the spatial variability of key underlying parameters, such as tissue residence
16 times (Bloom et al., 2016) and the impact of fire (Exbrayat, Smallman, et al., 2018). The
17 parameters and emergent ecosystem properties estimated from these models provide valuable
18 insights into the spatial variability and magnitude of parameters. This can reduce the parameter
19 space that needs to be searched when calibrating larger models. Furthermore, these optimised
20 parameters can be inserted into more complex models, enhancing their performance and
21 helping to better understand their internal dynamics (Caen et al., 2022).

22 Similarly, the interannual variability of atmospheric conditions means we also need to be careful
23 which period is used for the assimilation. Ideally, we want to calibrate over multiple years to
24 capture both the seasonal cycle and this interannual variability, while still retaining a number of
25 years for evaluation (although using different sites for calibration and evaluation can help to
26 relax this latter requirement). However, in practice, we are often limited by short time series
27 (e.g., only a few years for some *in situ* experiments and recently launched satellite missions),
28 data gaps, and the availability of meteorological forcing for corresponding periods, particularly
29 for *in situ* datasets.

30 3.5 Dealing with large and multiple observational datasets

31 Although EO instruments can provide global gridded datasets with which to calibrate the
32 models, fully exploiting these opportunities is challenging. Running experiments at the same
33 resolution as the satellite products (e.g., 500m MODIS resolution; Justice et al., 2002) requires
34 a lot of computational power and time, and we do not always have access to matching
35 meteorological forcing data. The resolution of products to be assimilated may also not be
36 meaningful for the objectives of the experiment. Additionally, when assimilating more than one
37 remote sensing data constraint, we must address multiple competing resolutions. This requires
38 decisions about scaling (see Sect. 3.3), determining which products are to be upscaled
39 (aggregated) versus downscaled (interpolated). Generally, satellite products are scaled to

1 match the chosen model grid, usually dictated by the resolution of the forcing data, although this
2 scaling can result in an over-generalisation or loss of information.

3

4 Furthermore, the quality of EO data can differ hugely across different regions since they are
5 impacted by atmospheric conditions (e.g., cloud cover) and topography, as well as the different
6 data processing algorithms and calibration/validation strategies used to develop the different
7 products. This can lead to regional and biome biases in the products that are very hard to
8 circumvent due to measurement limitations, potentially generating structural model biases.
9 Therefore, for many LSMs, it is common to select representative pixels for optimisation (e.g.,
10 MacBean et al., 2015), although defining what is representative is a challenge in itself. Once
11 selected, the representative pixel approach helps to i) reduce the dimensionality of the problem,
12 allowing for efficient and multi-data-stream calibrations, ii) focus on points with close to
13 homogenous coverage to be able to calibrate class-specific parameters (e.g., plant functional
14 types), and iii) define a different evaluation set of pixels with which to assess the optimisations,
15 especially sites with additional ground data. After selecting representative pixels, multi-pixel
16 optimisations are performed (as described in Sect. 3.4), focusing on estimating parameters for
17 different ecosystem/edaphic conditions by spanning the various model plant functional types
18 and soil textures all over the globe.

19

20 Another way to include more constraints to an optimisation is by calibrating against multiple data
21 streams. There is now an unprecedented wealth of *in situ* and EO data available, with even
22 more satellite missions and *in situ* field measurement sites being planned (Balsamo et al., 2018;
23 Ustin & Middleton, 2021). Different data streams offer information over different footprints and at
24 different spatial and temporal resolutions offering unique opportunities to constrain different
25 processes in the models. As LSMs become more complex through increased process
26 representation and greater interconnectedness between the different terrestrial cycles (e.g.,
27 water, energy, carbon, nitrogen), multi-data stream optimisations are becoming paramount to
28 provide adequate constraints since parameters are likely to impact different parts of the model.
29 By selecting only one specific data stream in an optimisation, we risk degrading the model's
30 overall predictive capacity if some of the optimised parameters are loosely constrained (Bacour
31 et al., 2015, 2023).

32

33 There are two possible approaches when assimilating multiple data streams. We can either
34 calibrate against each data stream in turn, often referred to as "stepwise" assimilation, or
35 include all data streams in one single optimisation, known as "simultaneous" assimilation.
36 Although mathematically equivalent when the posterior parameter uncertainties are properly
37 estimated and propagated in the stepwise case (MacBean et al., 2016; Peylin et al., 2016),
38 simultaneous assimilation is often preferable, since it ensures consistency (Kaminski et al.,
39 2012) and avoids issues linked to accurately propagating the information gained about the
40 parameter values from one step to the next. However, simultaneous optimisations may not
41 always be practical, especially when running a computationally demanding LSM experiment,
42 which is why the stepwise approach is often the pragmatic choice. In particular, there may be
43 technical difficulties associated with the different number of observations for each data stream
44 and the characterisation of error correlations between them (Bacour et al., 2023). Nevertheless,

1 it must be stressed that issues with unbalanced data streams are not solely due to imbalance
2 but stem from the model's inability to accommodate both data sources when structural errors
3 exist in either the model or the data (Oberpriller et al., 2021). In fact, properly quantifying and
4 accounting for the uncertainty in the model structural error and data bias leads to better results
5 than using ad-hoc methods such as reweighting different data streams (Cameron et al., 2022)
6 (see Sect. 3.2).

7 3.6 Including the spin-up and transient historical period in the 8 assimilation to better constrain land carbon sink projections

9 Many LSM simulations include both a spin-up phase that brings the prognostic variables
10 including vegetation state, soil carbon pools, and soil moisture content into equilibrium prior to
11 the industrial revolution (c. 1750). This is followed by a transient historical simulation where the
12 model is driven by changing climate forcing, rising CO₂ levels, nitrogen deposition, and
13 prescribed land management and land cover change since the equilibrium time point up to the
14 present day. Even with transient forcings, this historical period is likely not accurately simulated,
15 in part due to the lack of accurate historical climate and land use forcing data, in part because
16 “slow” carbon cycling parameters (e.g. carbon allocation or turnover rates) that control the
17 magnitude of the equilibrium carbon stock are poorly constrained, and in part because the
18 effects of key global change drivers on carbon storage (including recovery from disturbance) are
19 often missing or not reliably represented in models. The result is a large spread in the
20 magnitude and dynamics of various carbon pools and fluxes which underpin the current and
21 future projections of the land carbon sink (Arora et al., 2020; Friedlingstein et al., 2023).

22
23 To obtain reliable estimates of the current or future land carbon sink and trend in atmospheric
24 CO₂ we need accurate simulations of global carbon stock trajectories (i.e., *changes* in carbon
25 stocks). The trend in carbon stocks depends on the magnitude of carbon stocks post spin-up,
26 which in turn is strongly controlled by soil carbon pool turnover rates (Exbrayat, Bloom, et al.,
27 2018) (in addition to other parameters involved in soil carbon decomposition that moderate that
28 turnover rate). This is because for the CENTURY type model (Parton et al., 1987) used in many
29 LSMs, heterotrophic respiration is partly dependent on the size of carbon stocks. Global
30 sensitivity analyses (Sect. 3.1) of soil carbon cycle models performed for multiple different
31 biomes worldwide have rarely been performed (though see Huang et al., 2018) due to the
32 computational expense of running long-timescale simulations needed to model carbon stock
33 trajectories. For the same reason, relatively few past parameter DA studies with computationally
34 expensive LSMs at multi-site or global scale have included these slow-acting carbon cycle
35 parameters in their assimilation experiments. However, we know from past DA studies that
36 optimising “fast” carbon cycle flux related parameters related to photosynthesis, phenology, and
37 ecosystem respiration has limited impact on regional to global scale carbon stocks (MacBean,
38 Bacour, et al., 2022), as expected, while “slow” carbon cycle process parameters (such as those
39 related to carbon allocation to different biomass pools, or biomass and soil carbon pool turnover
40 times) are important for constraining long-term carbon stock trajectories (Thum et al., 2017).

41

1 To optimise the “slow” acting carbon cycle parameters involved in carbon allocation, biomass
2 turnover and soil carbon cycling, LSM assimilation experiments would need to include the
3 spin-up and transient runs in the assimilation, which would be prohibitively costly given the
4 computational cost of LSM runs. Therefore, neither the spin-up or transient period (prior to the
5 assimilation window) are usually included in LSM assimilations (Peylin et al., 2016; Raoult et al.,
6 2016; Schürmann et al., 2016). This presents challenges for obtaining accurate model estimates
7 of carbon fluxes and stocks because an incorrect initial carbon stock will likely result in biased
8 parameter retrievals that are accounting for the model errors contributing to the incorrect initial
9 carbon stock. Note this is not the case for carbon cycle and ecosystem models that have much
10 faster run times and who have therefore been able to include biomass and soil carbon turnover
11 rates and other related “slow” carbon cycling parameters in their optimisations (e.g.,
12 CARDAMOM-DALEC – Bloom et al., 2016).

13

14 To make up for incorrect carbon pool magnitudes and the fact that including spin-up and
15 transient in the assimilation is not yet feasible, most past carbon cycle parameter DA studies
16 have included scalars on the initial C pools in the optimisation, resulting in an improved fit to
17 NEE and atmospheric CO₂ data (e.g., η , Carvalhais et al. (2008, 2010); K_{soilC} in ORCHIDEE
18 PDA studies, e.g., Peylin et al. (2016); f_{slow} in CCDAS studies, Castro-Morales et al. (2019;
19 Schürmann et al., (2016)). These scalars alter the initial carbon pool size to account for model
20 and forcing errors mentioned above that contribute to incorrect soil carbon stock sizes. Studies
21 differ in how many such scalars to include, both in terms of which carbon pools to relax (all C
22 pools as in Santaren et al. (2007) versus slow and/or passive as in Peylin et al. (2016), whether
23 to scale aboveground biomass or not (Carvalhais et al., 2010), and to how many to use spatially
24 in global simulations (1 in CCDAS, Castro-Morales et al. (2019), Schürmann et al. (2016),
25 versus 30 regional factors used in ORCHIDEE studies, Bacour et al. (2023), Peylin et al.
26 (2016)). Other options for avoiding spin-up include directly initialising models with carbon stock
27 observations, and including parameter calibration within iterative state DA approaches.
28 However, in all of these cases, calibrating the “right” model parameters to the “wrong” model
29 pools is going to produce poor fits, complex sets of compensating errors, and potentially
30 incorrect hypothesis testing around alternative model structures.

31

32 Adjusting initial carbon stocks without optimising the “slow” carbon cycle parameters to which
33 the equilibrium carbon stock magnitude is sensitive is only useful if the purpose of the carbon
34 cycle assimilation experiment is to update model estimates of *current* carbon budgets. If the
35 desired goal is an accurate prediction of *future* carbon stock trajectories – for predicting carbon
36 mitigation potentials or carbon-climate feedbacks under different scenarios of climate and
37 disturbance trajectories – then simply adjusting initial carbon stocks is insufficient. In longer runs
38 (up to 2100 or 2300) those “slow” carbon cycling parameters that resulted in the original
39 incorrect carbon stock magnitude will start to push the model back to that original (inaccurate)
40 equilibrium, resulting in an artificial trend in the modelled carbon pools (and resultant biases in
41 carbon fluxes and land carbon sink estimates). Thus, for long term projections of carbon-climate
42 feedbacks, all parameters that are important for carbon pool trajectories need to be included in
43 the assimilations. This means that longer time windows (lasting several hundreds to thousands
44 of years) governing the periods over which these “slower” carbon cycle parameters operate will

1 need to be included in the assimilation experiments (Raiho et al., 2021; Thum et al., 2017). This
2 will materially increase the computational cost of an experiment enough to be prohibitive for
3 computationally expensive LSMs with current simulation protocols and assimilation algorithms.
4 Methods for increasing the simulation speed (e.g., model emulation - see Sect. 4.2) will
5 potentially solve the issue of prohibitive computational cost for these longer-term assimilation
6 experiments. One opportunity for accelerating the spin-up is by adopting the matrix approach,
7 where carbon balance equations are expressed as a single matrix equation without altering any
8 processes of the original model, which has now been applied to multiple LSMs and used for
9 both parameter sensitivity analyses and data assimilation (Hararuk et al., 2014; Huang et al.,
10 2018; Luo et al., 2022; Tao et al., 2020, 2024). Intermediate complexity ecosystem models may
11 be able to assist by providing much constrained priors of soil carbon pool turnover times (and
12 other parameters to which equilibrium/initial carbon stock magnitude are sensitive) (Bloom et al.,
13 2016).

14

15 This problem is specific to long-term, slowly changing carbon (and other nutrient like nitrogen
16 and phosphorus) stocks: e.g., for water storage (e.g., soil moisture), usually only a few years
17 are required either for spin-up or to adjust to a given perturbation. Therefore, for
18 hydrology-focused simulations both the spin-up and historical period spanning the perturbation
19 from equilibrium can be included in the experiment. In fact, by including this shorter spinup, the
20 assimilation also gives an estimate of the initial state (e.g., soil moisture, Pinnington et al.,
21 (2021); snow albedo, Raoult et al. (2023)). While carbon cycling is interlinked with water and
22 energy cycles, long-term carbon stock trajectories are insensitive to short-term fluctuations in
23 soil moisture.

24

25 In addition to longer assimilation time windows, assimilating measurements of aboveground
26 biomass or soil C stocks in conjunction with carbon fluxes provides a useful additional constraint
27 on carbon pools magnitude and trajectory (Thum et al., 2017). However, data on soil carbon
28 stocks are relatively scarce compared to carbon fluxes, highly uncertain, and often difficult to
29 link to the conceptual carbon pools in many CENTURY-type models (Parton et al. (1987),
30 though this is changing, Abramoff et al. (2018)). Additionally, these datasets often contain only
31 one or a few time points. While assimilating some information on carbon stocks is better than
32 not having any data, constraining long-term changes in C stocks will require multiple
33 observations of both above- and belowground C stocks over time (Raiho et al., 2021) (or data
34 representing rates of carbon cycling) in addition to nighttime and soil respiration data that so far
35 have typically not been utilised in LSM DA studies. Just how long a time series we need to
36 include to accurately estimate slow carbon cycle parameters will likely depend upon which
37 parameters are important for estimating future carbon stock trajectories over the timescales of
38 interest and the uncertainties associated with observations. More parameter sensitivity studies
39 are needed to assess which slow carbon cycling parameters control carbon stock trajectories at
40 different temporal scales (Raczka et al., 2018). Ideally, these sensitivity studies should be
41 performed with different scenarios of global change drivers, as changing inputs may alter the
42 relative importance of slow carbon cycling parameters. The community can learn from the
43 calibration and validation activities of soil biogeochemical models being approved for use in
44 voluntary carbon markets (Mathers et al., 2023).

¹ 3.7 Choice and implementation of minimisation algorithms

² To perform optimisations effectively, careful consideration must be given to the choice of
³ algorithm and its implementation. As discussed in Sect. 2, various algorithms are available,
⁴ each with distinct characteristics, such as local versus global optimisation, each having different
⁵ computational demands. Additionally, every algorithm comes with a variety of configurable
⁶ options. For instance, a Genetic Algorithm implementation by (Scrucca, 2013) offers a range of
⁷ functions for parent selection (6 options), crossover (5 options), and mutation (3 options),
⁸ resulting in 90 possible combinations. Users can also adjust crossover and mutation
⁹ probabilities. The success of the optimisation process greatly depends on how the optimisation
¹⁰ is implemented, which may vary on a case-by-case basis. Systematically testing all possible
¹¹ combinations is unfeasible due to the large computational demand of an LSM. A more efficient
¹² approach is to use an emulator (see Sect. 4.1) rather than an LSM to find an optimal
¹³ experimental design (Dagon et al., 2020); once the design has been identified, the optimisation
¹⁴ can be carried out using the LSM.

¹⁵ Furthermore, for gradient-based methods, implementing and maintaining the tangent linear or
¹⁶ adjoint model is a huge challenge in LSM DA. For complex LSMs, which are historically coded
¹⁷ in Fortran, the tangent linear and adjoint models can take years to develop, even when using
¹⁸ automatic differentiation software, since the code first needs to be cleaned and structural
¹⁹ adjustments need to be made to ensure the code is differentiable without changing the
²⁰ fundamental physics. For example, this may require replacing look-up tables with their
²¹ continuous formulations and reformulating minimum and maximum calculations to allow a
²² smooth transition at the edge (Schürmann et al., 2016). The years taken to derive the tangent
²³ linear/adjoint models mean they quickly become outdated, especially with big community
²⁴ models like JULES and ORCHIDEE, where new processes are added approximately every six
²⁵ months. For JULES, the adjoint was developed for v2.2 of the model (Raoult et al., 2016),
²⁶ whereas JULES is currently at v7.3 at the time of writing. Similarly, while the tangent linear
²⁷ exists for ORCHIDEE, it exists for an old version of the model (AR5) that predates the addition
²⁸ of a multi-layered soil hydrology scheme and nitrogen cycle. To address this issue, the
²⁹ ORCHIDEE DA team has been developing a tool to do the required preprocessing of any
³⁰ version of ORCHIDEE so the tangent linear version of the model can be easily derived using
³¹ Transformation of Algorithms in Fortran (Giering, 2010). On the other hand, BETHY's lower
³² complexity has allowed it to be kept compliant with automatic differentiation software for
³³ decades, which provided efficient derivative code of the up-to-date version of the model. This is
³⁴ also the case for its successor D&B (Knorr et al., 2024), which is the model component of the
³⁵ European Space Agency supported TCASS system, and for the Nanjing University Carbon
³⁶ Assimilation System (NUCAS, Zhu et al., 2023). Alternatively, models written directly in an
³⁷ auto-differentiable language (Julia or python-JAX; see Sect. 5.4) alleviate this issue (Gelbrecht
³⁸ et al., 2023; C. Shen et al., 2023). Although these languages have slower computational
³⁹ performance than Fortran, these new languages often also facilitate the use of graphic
⁴⁰ processing units (GPU), e.g., through packages like pyTorch (Paszke et al., 2019).

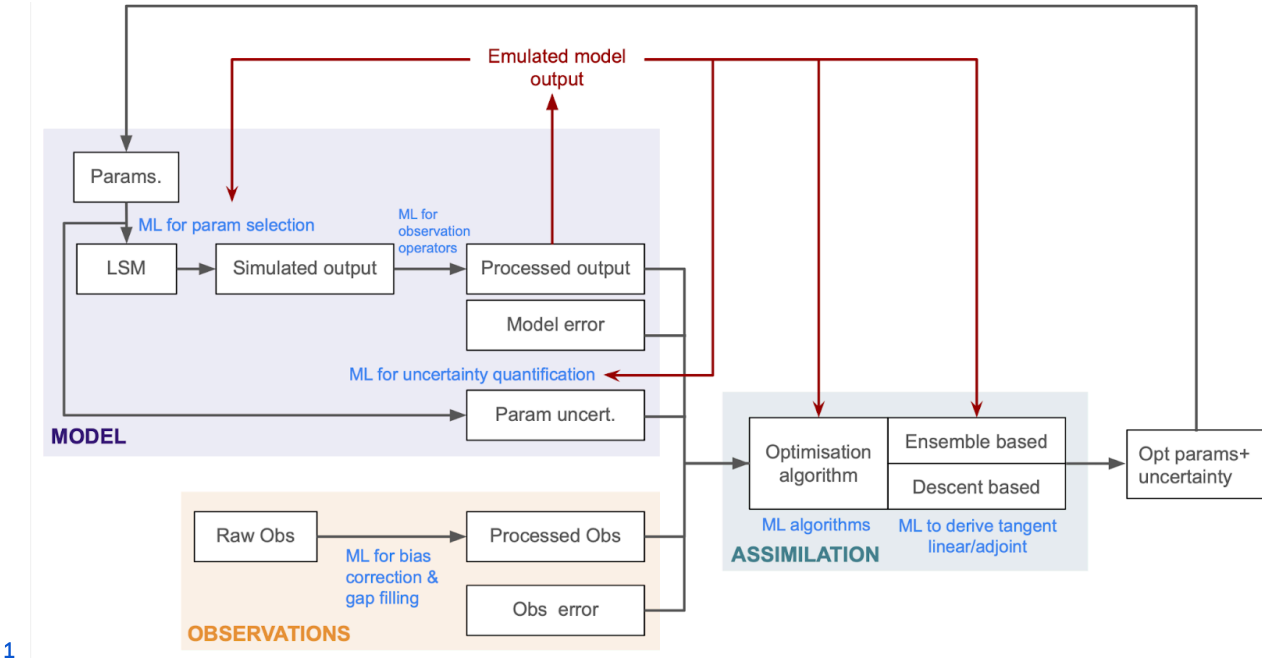
1 As discussed in Sect. 2, in the absence of the tangent linear or adjoint model, one can use finite
2 differences. However, this necessitates the selection of an appropriate step size for accuracy
3 and convergence speed, which will differ based on the sensitivities of the parameter estimated.
4 Other methods to bypass the need for tangent linear and adjoint models include LAVENDAR's
5 ensemble 4DVar approach (Pinnington et al., 2020) or the use of emulators, which can be used
6 to either avoid gradient-based approaches in favour of Monte Carlo ones, make numerical
7 approximations of gradients viable, or both (e.g., Hamiltonian MCMC). However, these
8 algorithms also come with a number of hyperparameters that need to be selected including the
9 number of ensembles and convergence criteria.

10 4. Opportunities through machine learning for 11 parameter estimation

12 Despite the challenges and knowledge gaps discussed above, our community has never been
13 in a better position to calibrate land surface models and rigorously diagnose their uncertainties.
14 We now have access to large observational datasets at high spatio-temporal resolutions and
15 increased computational capacity and efficiency. These factors, combined with recent advances
16 in machine learning (ML), potentially allow us to make significant progress in model calibration.
17

18 The recent surge in ML has been evident in every aspect of society with the most relevant
19 examples coming from numerical weather prediction (Lam et al., 2023) or remote sensing (Lary
20 et al., 2016). These examples can help us identify ways in which ML can assist with land PDA.
21 In this section, we specifically focus on how ML can help us address the current challenges and
22 limitations in land PDA outlined above, as well as areas where ML has the potential to improve
23 the DA workflow (Fig. 1). With the large number of studies currently being published in the field
24 of machine learning, we only provide a short overview of the relevant literature. In the context of
25 ML for PDA, we can broadly group the existing studies and applications into four categories: i)
26 the use of ML to emulate the relationship between LSM parameters and its outputs or
27 performance (Sect. 4.1), ii) the creation of 'hybrid models' in which ML replaces or complements
28 a component of a larger LSM (Sect. 4.2), iii) the use of ML to improve or pre-process
29 observation datasets prior to their use in PDA (Sect. 4.3), and iv) the use of ML to optimise the
30 parameter estimation process itself (Sect. 4.4).

31



1

2 **Figure 1:** Examples of where ML can facilitate each part of the land surface model PDA workflow

3 4.1 Parameter perturbation emulators

4 The computational cost of high-complexity LSMs hinders the use of the more computationally
 5 demanding PDA techniques such as MCMC. However, machine learning methods can mitigate
 6 a portion of these computational burdens. By building a statistical relationship between input
 7 parameter settings and the LSM output or an aggregate of the LSM output (for instance over
 8 time or space), the LSM output can be estimated for a new set of input parameters. The
 9 statistical relationship serves as a computationally efficient surrogate model for the expensive
 10 LSM and is most frequently called an emulator (although this term is not exclusive to this
 11 application), while surrogate, meta-model, or reduced-order model are also used to refer to this
 12 tool. Indeed, emulators already have a rich history in climate sciences (Knutti et al., 2003;
 13 Sanderson et al., 2008; Watson-Parris, 2021).

14

15 Parameter Sampling Strategies

16 The training of an emulator requires an ensemble of LSM simulations with perturbations to the
 17 input parameters often called a perturbed parameter ensemble (PPE, see McNeall et al. (2024)
 18 and Kennedy et al. (2024) for PPEs constructed for JULES and CLM, respectively). The design
 19 of the initial PPE depends on the intended use; for uncertainty quantification, it is often
 20 preferable to sparsely sample the entire parameter space using Latin hypercube sampling
 21 (McKay et al., 1979). However, for calibration applications, it can be more cost effective to use a
 22 non-random and targeted sampling strategy, such as active learning which tries to optimise the
 23 selection of the next sample (e.g., Zhao & Kowalski, 2022). Alternatively, an Ensemble Kalman
 24 Filter approach (Evensen, 2003) can be used to place the initial design points in regions of
 25 significant posterior mass to optimise the calibration process (e.g., (Cleary et al., 2021). When
 26 building emulators for model calibration it can be particularly effective to treat this as an iterative

1 design process, whereby an initial set of parameter vectors (e.g., Latin hypercube) is used to
2 generate a rough idea of where in parameter space the optimum lies, then additional parameter
3 vectors are sampled from this region, refining the emulator in a way conceptually similar to a
4 nested grid in parameter space (Fer et al., 2018). How to optimally propose points in parameter
5 space remains an important research question.

6

7 Emulation Methods

8 There are many ML methods appropriate for emulating the LSM response to parameter
9 modifications. When it comes to the calibration problem specifically, an alternative to emulating
10 the LSM output is to directly emulate the cost function itself (i.e., the response surface of model
11 error as a function of parameter value) which is much lower dimensional and often much
12 smoother than the model output itself (Cheng et al., 2023, 2024; Dagon et al., 2020; Fer et al.,
13 2018; Fer, Shiklomanov, et al., 2021).

14

15 Gaussian processes are commonly applied as they are well-suited to interpolate non-linear
16 surfaces in data-scarce settings and moreover provide a measure of prediction uncertainty that
17 can be used to quantify the emulator uncertainty. However, since the computational cost of
18 Gaussian processes dramatically increases with the size of the dataset, they are less feasible
19 for larger datasets. One option is to develop sparse Gaussian processes, as demonstrated by
20 Baker et al. (2022). Running JULES at a 1km resolution over Great Britain, they exploit the fact
21 that LSMs typically do not exchange information laterally between grid cells (river routing is
22 generally done as a separate step) to select a subset of coordinates representative of different
23 parameter settings and forcing data regimes.

24

25 Another popular method for emulating LSMs are neural networks (NNs), as they are
26 straightforward and fast to implement (Hatfield et al., 2021), with fast evaluation speeds and
27 good predictive skill within the bounds of the training data. However, NNs are sensitive to biases
28 in the selection of the training data as well as the tuning of the algorithm hyperparameters,
29 which means that they generally cannot extrapolate to scenarios beyond the training data or be
30 transferred to new datasets without performance degradation (Shwartz-Ziv & Armon, 2022). (D.
31 Lu & Ricciuto, 2019) used singular value decomposition with Bayesian optimisation to create a
32 reduced number of surrogate models for carbon modelling parameter perturbation. Their
33 approach showed minimal accuracy loss, making it effective for extensive parameter space
34 exploration and uncertainty quantification. Other examples of NNs used to emulate LSMs
35 include, Dagon et al. (2020), where a series of artificial feed-forward NNs were trained to
36 emulate CLM5 output given important biophysical parameter values and Meyer et al. (2022),
37 where an NN was trained to emulate the ensemble mean of several urban LSMs combining the
38 strengths of the different into one ML model. While artificial NNs do not provide a probabilistic
39 prediction, new methods are emerging such as neural processes (e.g., (Garnelo et al., 2018) or
40 randomised prior networks (Bhouri et al., 2023). Regression trees can also be extended to
41 include probabilistic prediction such as with NGBoost (Duan et al., 2020) or XGBoost (Donnerer,
42 2024), as used for example to emulate ELM-FATES (Li et al., 2023). XGBoost has been shown
43 to generally outperform NNs while requiring little parameter tuning and is able to achieve robust
44 performance even when extrapolating to scenarios beyond the training data (Grinsztajn et al.,

1 2022; Shwartz-Ziv & Armon, 2022). A disadvantage of tree-based methods is their slower
2 evaluation speeds and the fact that they are not differentiable, which can limit their usability for
3 certain applications (e.g., coupled DA, Hatfield et al., 2021). Long-Short Term Memory (LSTM)
4 methods, which for example have been applied to ECLand (Boussetta et al., 2021), include
5 memory mechanisms by leveraging long-term dependencies in the training data time series,
6 allowing them to effectively emulate model processes across different time scales without
7 performance loss at longer lead times (as is the case for XGBoost for example, (Wesselkamp et
8 al., 2024). This makes them particularly suited for the emulation of large-scale forecasting
9 systems that encompass physical processes acting at different time scales (e.g., Datta &
10 Faroughi, 2023; Guo et al., 2021; Wesselkamp et al., 2024).

11

12 Computational Cost Reduction

13 Once an emulator is trained it becomes computationally feasible to apply PDA techniques that
14 require a large number of samples from a prior parameter distribution, e.g., MCMC. Fer et al.,
15 (2018) showed how emulators sped up an MCMC optimisation for the relatively simple SIPNET
16 model by over two orders of magnitude (>100x). Further applying their method to the more
17 complex Ecosystem Demography model v2 (ED2), whose complexity precluded it from a direct
18 application of the MCMC methodology for parameter tuning, they found that emulators helped
19 achieve a >20,000x increase in speed (27 hr versus a predicted 74 years by traditional MCMC).
20 Similarly, Sawada (2020) and Cleary et al. (2021) both used emulators to perform Bayesian
21 inversion using the otherwise costly MCMC approach to sample the approximate posterior
22 parameter distribution after calibration. Torres-Rojas et al. (2022) combine surrogate modelling
23 with a multi-objective Pareto efficiency analysis to infer LSM's optimal subgrid parameters at 1%
24 of the computational cost. The emulators were trained on forward model runs used to initially
25 calibrate the model using Ensemble Kalman sampling - a derivative-free optimisation method.
26 Coining the method "Calibrate, emulate, sample", Cleary et al. (2021) showed how the method
27 could be successfully applied to models of different complexity, while other groups have also
28 demonstrated the suitability of ensemble approaches for parameter selection (e.g., Couvreux et
29 al., 2021).

30

31 History Matching

32 Emulators are commonly used in the field of uncertainty quantification, and one key method
33 from this field that is gaining traction in land surface modelling is the so-called history matching
34 (HM) method (Hourdin et al., 2023). This method is not about finding the most likely parameter
35 values, but rather ruling out implausible ones based on some given metrics (Williamson et al.,
36 2013). Using emulators to facilitate computation, HM is commonly applied using successive
37 iterations (also known as iterative refocusing) to reduce parameter space and retain the least
38 implausible parameters. Like the cost function used in variational DA, the implausibility takes the
39 observation and model structure errors into account. While these errors are still hard to
40 determine (Peatier et al., 2023), it is arguably less dangerous to get them wrong here than in the
41 DA case - if the errors are overestimated, HM gives a clear diagnostic of this being the case, for
42 example, by ruling out little to no parameter space. If the errors are underestimated, HM will rule
43 everything out, suggesting the errors have been misspecified, whereas, in other optimisation
44 approaches, we would still get a solution even if one does not exist. HM also allows the user to

1 test many different metrics to see if parameters can capture specific features, similar to
2 multi-objective optimisations, giving a clear diagnosis of model structure error. HM has
3 successfully been tested with some of the major high-complexity LSMs: CLM (Dagon et al.,
4 2020), JULES (Baker et al., 2022; McNeall et al., 2024), and ORCHIDEE (Raoult, Beylat, et al.,
5 2024), for example. These studies highlight how HM can be used to identify sensitive
6 parameters, redefine ranges of variation and identify non-Gaussian relationships between
7 parameters. This information could potentially be used to determine the prior error covariances
8 (i.e., to set up the background error covariance matrix in variational DA) or provide ecological
9 constraints to an optimisation.

10 4.2 Hybrid modelling

11 ML can also be used in a hybrid modelling approach to substitute components of the physical
12 model with an ML approximation (Eyring et al., 2024). The appeal of the hybrid approach is that
13 it can address known model inadequacies and computational bottlenecks in a targeted manner
14 while retaining the use of physical process knowledge and constraints where they are reliable.
15 For example, the hybrid approach can mitigate model structural errors, by replacing model
16 processes that are missing or poorly understood with data-driven substitutes, assuming
17 adequate data exists (Arsenault et al., 2018; Reichstein et al., 2019). At the same time, the
18 hybrid approach can add physical constraints to the ML model components, thus maintaining
19 physical consistency and interpretability (e.g., Beucler et al., 2021; Kraft et al., 2022; Reichstein
20 et al., 2019). ML and process models can be combined in a number of different ways, including
21 i) substituting a specific model parameterisation with an ML approximation, ii) deriving spatial
22 parameterisations that better capture observed physical behaviour, iii) training on model-data
23 residuals to predict process-model biases and characterise structural errors, and iv) replace
24 computationally costly parts of the model. Hybrid modelling has been implemented successfully
25 in a number of LSM applications, including for streamflow (Yang et al., 2019), evapotranspiration
26 (W. L. Zhao et al., 2019), subsurface flow (N. Wang et al., 2020), rainfall-runoff modelling (Xie et
27 al., 2021), as well as more generally for the prediction of sea surface temperatures (de Bézenac
28 et al., 2019), atmospheric convection (Gentine et al., 2018), and high impact weather events
29 (McGovern et al., 2017). As with all parameter estimation methods, hybrid modelling can be
30 subject to parameters compensating for model structural errors or errors in parameters outside
31 the calibration set (see also Sect. 4.2). This can be counteracted through the use of multivariate
32 independent observation constraints in the calibration.

33

34 Substitution of Uncertain or Missing Parameterisations and Processes

35 In the context of land DA, hybrid modelling has been used to improve the representation of
36 complex processes, such as the representation of human processes and their impact, which are
37 often not represented in their full complexity or missing completely in traditional LSMs. ML
38 approaches trained in an aggregate manner (e.g., one NN trained on all locations) and using a
39 combination of observations and process-model outputs can effectively account for human
40 processes by mapping observations into the model climatology (thus removing global biases).
41 At the same time, they can retain the independent information on human processes that is
42 inherent in the observations but typically removed in traditional bias correction approaches (e.g.,

1 Kumar et al., 2012). Kolassa et al. (2017) used an artificial NN observation operator trained on
2 brightness temperature observations from the Soil Moisture Active Passive (SMAP) mission and
3 GEOS land model outputs to assimilate soil moisture information, which introduced the impact
4 of irrigation and tile drainage in a model that does not normally represent these processes.
5 Assem et al. (2017) developed a Deep Convolutional NN, trained on historic water flow and
6 water level observations, to predict water flow in urban areas from runoff estimates generated
7 by a physical LSM. Hybrid modelling can also be used in cases when the naturally occurring
8 physical processes are poorly understood. For example, Arsenault et al. (2018) used an ANN
9 with a combination of remote sensing observations and model predicted states to generate
10 improved estimates of snow depth within the Land Information System.

11

12 Improved Spatial Parameterisations

13 Hybrid modelling techniques have also been used successfully to generate model
14 parameterisations that better capture the parameter spatial distribution and thus the observed
15 physical behaviour (Tao et al., 2020, 2024). Process-model parameterisations can be limited by
16 observation sparsity, which can lead to ad hoc decisions when assigning parameter values
17 globally. Similarly, many global LSMs significantly simplify biogeochemical and physical
18 mechanisms into empirical parametric functions. Hybrid modelling can address these issues by
19 mapping environmental variables into model parameters or using high-resolution, high-fidelity
20 model simulations to derive new parameterisations for coarse-resolution models (e.g., Gentine
21 et al., 2018). Bao et al. (2023) replaced the traditional PFT-based parameterisation of a light use
22 efficiency model with an ecosystem-property-based parameterisation derived from a multi-layer
23 perceptron NN to better capture the spatial variability of GPP within PFTs. Several studies have
24 used a hybrid ML approach to improve the representation of evapotranspiration in LSMs, either
25 by directly estimating evapotranspiration (Zhao et al., 2019) from observations or by inferring
26 related prognostic variables, such as the stomatal and aerodynamic resistances (ElGhawi et al.,
27 2023), or transpiration stress (Koppa et al., 2022). In each case, the hybrid model was able to
28 learn unknown latent processes and thus outperform traditional physics-based schemes.

29

30 Model Error Identification/Characterisation

31 Additionally, hybrid modelling implementations can serve as effective diagnostic tools to identify
32 model errors. For an independently evaluated ML approximation, systematic differences
33 between predictions from a physical model component and its ML counterpart can provide
34 insights into missing or flawed model process representations as well as identify inadequate
35 model parameters (e.g., McGovern et al., 2017), especially when the ML model is not only
36 trained to represent the model outputs but uses other observational constraints in the learning
37 phase. For example, Finn et al. (2023) and Gregory et al. (2023) used an ML trained on
38 model-data residuals to predict model biases and characterise structural errors, while Gregory
39 et al. (2024) extended this approach to implement an online bias correction within a DA
40 framework. Similarly, Farchi et al. (2021, 2023) integrated a deep-learning step into a DA
41 framework to create a hybrid model that dynamically learns and corrects model errors at each
42 DA time step.

43

44

1 Computational Cost Reduction

2 Finally, hybrid modelling can be used to replace computationally costly parts of the model. For
3 example, emulating the spinup, which can account for up to 98% of computational time in
4 complex LSMs, would greatly alleviate challenges linked to this bottleneck (see Sect. 3.6). A
5 successful undertaking by Sun et al. (2023) showed how bagging decision trees (an ensemble
6 ML method based on (Breiman, 1996) could be used to emulate the spin-up of the ORCHIDEE
7 LSM. Koppa et al. (2022) developed a deep learning-based hybrid model combining a
8 process-based land surface model with remotely-sensed observations to estimate global
9 evaporation. They showed how hybrid models can significantly improve predictive accuracy
10 while reducing the computational cost.

11

12 Data Requirements

13 Hybrid modelling has the potential to be very powerful, but it is also susceptible to issues linked
14 to equifinality (Kraft et al., 2022; Sawada, 2020). We note that any ML approaches need
15 substantial data to perform well and thus the ML components in the hybrid part need to be
16 targeting processes for which data is plentiful. ML approaches often have a large number of
17 parameters in their training which gives them a larger degree of flexibility that can compensate
18 for errors in physical models, but can also lead to overfitting.

19 4.3 Observation Processing

20 There are many examples of using ML to improve or pre-process the observational datasets
21 that can be assimilated into LSMs, especially from the field of remote sensing. Many of these
22 novel datasets have yet to be exploited in the LSM parameter estimation studies, presenting
23 exciting new opportunities.

24

25 Observation Operators

26 One such application is the use of ML-generated observation operators to translate
27 satellite-observed radiances into model states or parameters (see challenges raised in Sect.
28 3.3). The use of ML techniques in this context has several advantages: i) ML-based observation
29 operators are relatively simple to implement compared to physically-based approaches, which
30 often involve the inversion of radiative transfer models, ii) they are able to easily accommodate
31 the simultaneous assimilation of multiple observation types, iii) they can inherently correct
32 climatological biases between model and observations, and iv) they facilitate the assimilation of
33 radiance observations rather than retrieval products, thus reducing errors stemming from
34 possible inconsistencies between retrieval algorithm assumptions and models. Due to these
35 advantages, ML-based observation operators have been applied in several land data
36 assimilation studies, including for soil moisture (Kolassa et al., 2017; Rodríguez-Fernández et
37 al., 2019), leaf area index (Durbha et al., 2007), snow water equivalent (Kwon et al., 2019), and
38 as a combined forward model for soil moisture and LAI (Shan et al., 2022).

39

40 Retrieval Algorithms

41 Similarly, ML approaches have been used to develop data-driven retrieval algorithms in cases
42 where physical retrieval algorithms are very complex. For example, Chen et al. (2022), Gentine

1 & Alejomhammad (2018), Shen et al. (2022) and Zhang et al. (2018) each used ML to estimate
2 SIF from MODIS radiances, OCO-2, and TROPOMI observations, respectively. Alejomhammad
3 et al. (2017) developed an ML approach to retrieve global, monthly GPP estimates from
4 GOME-2 SIF observations only.

5

6 **Gap-Filling**

7 ML approaches can also be used to improve observation datasets by making them more
8 suitable for data assimilation applications. One approach is to use ML to generate gap-filled
9 observations or generate higher temporal resolution datasets. For example, Yatheendradas &
10 Kumar (2022) used an ML approach to create a gap-filled, high-resolution dataset of observed
11 snow cover fraction and Fang et al. (2019) used a deep learning Long Short-Term Memory
12 framework to predict daily “SMAP Level-3 like” soil moisture estimates from atmospheric forcing
13 data and static physiographic attributes. Vekuri et al. (2023) used extreme gradient boosting to
14 gap-fill eddy covariance data reducing the northern biases in the data found after using more
15 traditional gap-filling methods. Nevertheless, one must exert caution when using gap-filled data
16 (or other model-derived data, such as retrieval products) for parameter estimation, since they
17 are dependent on the assumptions of the selected gap-filling method. Furthermore, gap-filled
18 data can artificially inflate sample size, which leads to falsely precise parameter estimates.

19

20 **Upscaling**

21 Another approach is to use ML to map local observations to the global scale to mitigate
22 representativeness issues that can arise from the assimilation of local observations. For
23 example, studies by Beer et al. (2010), Joiner et al. (2018), Jung et al. (2011) and Tramontana
24 et al. (2016) all have used ML approaches in combination with remote sensing observations to
25 generate global estimates of carbon and energy fluxes from local flux-tower observations.
26 Vergopolan et al. (2021) used a high-resolution LSM and an ML Bayesian merging scheme
27 trained on in-situ soil moisture data to learn LSM and SMAP satellite biases and obtain 30m
28 satellite-based soil moisture estimates over the contiguous United States. One caveat to using
29 ML to upscale point observations is that large discrepancies can exist between different data
30 products based on the same observations, highlighting the need for thorough evaluation and
31 uncertainty assessment of ML-based products.

32

33 **Derived Quantities**

34 Finally, ML can be used to improve the algorithms used to generate observation datasets. For
35 example, Tramontana et al. (2020) used a combined neural network approach that accounts for
36 the influence of soil property and micrometeorological drivers to generate improved estimates of
37 the partitioning of observed NEE into GPP and ecosystem respiration (RECO), while Zeng et al.
38 (2022) used an ML approach to separate the natural and anthropogenic contributions to
39 satellite-estimated evapotranspiration.

40 **4.4 Optimisation process**

41 Since optimisation is a key component to both ML and DA, there are many algorithms common
42 to both fields including gradient-based and evolutionary algorithms (Sect. 2). Indeed, the strong

1 mathematical similarities between ML and DA mean that both fields can learn from each other
2 and share methodologies (Geer, 2021). ML approaches can be used to improve optimisation
3 algorithms themselves by helping speed up the search process and improve the quality of
4 solutions (Song et al., 2019). Furthermore, ML can be used to automatically choose the setting
5 of adjustable parameters found in some optimisation algorithms. For example, clustering
6 methods can be used to set the population size, crossover probability and mutation probability
7 parameters in genetic algorithms (Zhang et al., 2007) and maintain population diversity.
8 Tree-based random forest models have been used to dynamically construct, search, and prune
9 the parameter space to efficiently optimise ML structure and hyperparameters (Akiba et al.,
10 2019). ML techniques can also be used to choose the best-performing algorithm for a particular
11 optimisation problem (Kerschke et al., 2019). While the emerging ML methods are promising,
12 they are very novel and - to the best of our knowledge - have not yet been applied to optimising
13 the parameter estimation algorithm hyperparameters themselves.

14

15 Finally, a novel and emerging use of ML is the use of large language models (e.g. ChatGPT).
16 Modern open-source coding languages like Julia and Python through the Google JAX library
17 (Bradbury et al., 2018) can be automatically differentiated to generate the tangent linear model
18 (see Sect. 2). Many high-complexity LSMs are written in Fortran code; large language models
19 can help translate Fortran code to more modern languages (Zhou et al., 2024), facilitating the
20 derivative of such models. Alternatively, we can use neural networks to emulate the tangent
21 linear and adjoint models since neural networks can be differentiated trivially (Hatfield et al.,
22 2021).

23

24 Table 1: Summary of challenges outlined in Sect. 3 and their ML opportunities

PDA challenge	ML opportunity
Selecting parameters and their prior distributions (Sect. 3.1)	
<ul style="list-style-type: none">- Identifying which model parameters to optimise is challenging, due to high dimensionality and strong parameter covariances.- Choosing prior distributions for parameters is crucial yet difficult, requiring detailed structural insights and data.	<ul style="list-style-type: none">- Emulators can reduce the computational demand of running models with many different parameter settings needed for sensitivity analyses (Sect. 4.1).- Emulators can be used to facilitate uncertainty quantification, for example, through history matching (Sect. 4.1).
Characterisation of model and data/observation errors (Sect. 3.2)	
<ul style="list-style-type: none">- Model errors are difficult to quantify due to uncertainties in process representation, missing processes, and the challenge of specifying an informative prior.- Quantifying data errors is tricky because of sampling variability, instrument inaccuracies, and complex error correlations that are often ignored.	<ul style="list-style-type: none">- Hybrid modelling can be used to replace model processes that are missing or poorly understood, helping to diagnose model structural errors (Sect. 4.2).- ML methods can be used to generate improved estimates of derived quantities, thus reducing observation errors (Sect. 4.3).

Developing observation operators (Sect. 3.3)	
<ul style="list-style-type: none"> - Matching model outputs to observations require transformations that can introduce biases. 	<ul style="list-style-type: none"> - ML-generated observation operators can be used to directly translate satellite-observed radiances into model states or parameters (Sect. 4.3).
Tackling spatial and temporal heterogeneity (Sect. 3.4)	
<ul style="list-style-type: none"> - Variability in surface properties, driven by diverse climates, soils, and ecosystems, complicates parameter estimation across locations. - High computational demands make it difficult to calibrate LSMs across large spatial domains. - Temporal variability and short data series hinder the capture of both seasonal cycles and long-term trends. 	<ul style="list-style-type: none"> - Hybrid modelling can be used to improve spatial parameterisations (Sect. 4.2). - Emulators can help reduce the computational demand of running the model over large domains (Sect. 4.1). - Long Short-Term Memory encoder-decoder networks consider long-term dependencies and therefore may help capture seasonal and interannual trends (Sect. 4.1).
Dealing with large and multiple observational datasets (Sect. 3.5)	
<ul style="list-style-type: none"> - Scaling satellite products to match model grids can lead to information loss. - Products may be subject to regional biases due to varying data quality and processing methods. - Assimilating multiple data streams in model calibrations presents challenges in consistency, error characterisation, and balancing different data sources. 	<ul style="list-style-type: none"> - ML methods can be used to upscale sparse observational data (e.g., flux tower observations) or map satellite observations to a model grid (Sect. 4.3). - ML can be applied to improve the algorithms used to produce observational datasets (Sect. 4.3). - ML-based observation operators are able to easily accommodate multiple observation types and adjust their respective impacts in the assimilation (Sect. 4.3).
Including the historical period in the assimilation window (Sect. 3.6)	
<ul style="list-style-type: none"> - Spin-up and transient parts of model runs can be computationally demanding. 	<ul style="list-style-type: none"> - Hybrid modelling can be used to replace computationally costly parts of the model (Sect. 4.2).
Choice and implementation of minimisation algorithms (Sect. 3.7)	
<ul style="list-style-type: none"> - Algorithms requiring a large number of model runs are computationally costly and therefore rarely applied to complex LSMs. - For different algorithms, there can be a large number of configuration options and tuneable hyperparameters. 	<ul style="list-style-type: none"> - ML can enhance computational efficiency, enabling the use of algorithms that require numerous model runs (Sect. 4.1). - ML can help find the best configurations and hyperparameters to use when optimising (Sect. 4.4).

<ul style="list-style-type: none"> - Maintaining tangent linear/adjoint models for gradient-based optimisation in complex LSMs is challenging. 	<ul style="list-style-type: none"> - Large language models can be used to translate LSMs to modern coding languages that are easier to differentiate and can better exploit GPU. Alternatively, we can emulate the LSM using NNs, which are easily differentiable (Sect. 4.4).
---	---

¹ 5. Future priorities

² Moving beyond the ML avenues outlined in the previous section and summarised in Table 1,
³ here, we discuss the opportunities and future priorities where land PDA promises to have some
⁴ large impacts, building on recent successes. We argue that more funding for technical DA
⁵ studies and software engineering support would significantly aid this work.

⁶ 5.1 Testing novel datasets and experimental configurations

⁷ In addition to the traditional datasets used to optimise LSM parameters, our data-rich world
⁸ offers access to a wide array of data streams enabling new and exciting constraints on multiple
⁹ different processes in LSMs (as have been used for parameter DA in smaller scale ecosystem
¹⁰ and ecology models). These include (to name a few):

- ¹¹ • **Manipulation experiments:** For example, elevated CO₂ experiments can be used to constrain the fertilisation effect at nitrogen-limited sites (Thomas et al., 2017; Jiang et al., 2020; Mahmud et al., 2018; Raoult, Edouard-Rambaut, et al., 2024).
- ¹⁴ • **Data about soil carbon stocks:** Data from the International Soil Carbon Network (Harden et al., 2018; Nave et al., 2016) and the global soil respiration database (Jian et al., 2021) can provide valuable insights. Similarly, soil radiocarbon measurements (Lawrence et al., 2020) can help constrain rates of soil carbon cycling (Shi et al., 2020) and carbon isotope concentrations can be used to improve simulated soil organic matter decomposition (Mäkelä et al., 2022).
- ²⁰ • **Tree ring data:** Annual biomass increments derived from tree ring widths can help infer carbon accumulation (Babst et al., 2014; Jeong et al., 2021). Similarly, tree ring isotopic data (carbon and oxygen) can act as constraints for leaf physiology and growth (Barichivich et al., 2021).
- ²⁴ • **Other aboveground biomass products:** Products from the ESA BIOMASS mission (Quegan et al., 2019) help constrain carbon allocation and woody biomass turnover parameters (Smallman et al., 2021). Similarly, land-use and land-cover products (e.g., MapBiomas Collection 3.1, based on Landsat) can be used to create regrowth curves (Heinrich et al., 2021, 2023), which together with forest inventory data, can help constrain disturbance processes.
- ³⁰ • **Additional remote sensing datasets:** New datasets, such as full-waveform lidar data from the GEDI (Global Ecosystem Dynamics Investigation) mission (Dubayah et al., 2020), can help constrain canopy structural parameters, including canopy height (Potapov et al., 2021). Similarly, improved observations of land surface temperature and total

1 surface/groundwater content from GRACE instruments also can offer additional
2 constraints on the energy and water cycles.

3 • **Trace gas flux measurements:** Carbonyl sulfide measurements (Whelan et al., 2018)
4 can be used to constrain GPP and stomatal conductance (Abadie et al., 2023). There is
5 also a growing number of nitrous oxide flux measurements (Nicolini et al., 2013), which
6 can be used to calibrate LSMs that include nitrogen cycles. Methane flux measurements,
7 such as those over peatlands ((Salmon et al., 2022), can also be utilised to improve the
8 representation of methane production processes.

9 By combining these data and implementing novel DA approaches described in this paper, we
10 can aspire to assess how this information influences both short-term and long-term forecasts
11 and reduces model discrepancies. The focus should be on refining core processes driving
12 ecosystem-scale carbon and water fluxes and testing their responses to global change, beyond
13 just fitting historical data.

14

15 As with all past carbon cycle DA studies, before novel datasets can be reliably used in a DA
16 experiment, it will take time to test the best approaches for how to best use these data streams
17 within a DA experimental framework. It should be standard practice to run synthetic DA
18 experiments to test which observational characteristics (temporal sampling interval, record
19 length, observation uncertainty, choice of minimisation algorithm and its configuration, etc. –
20 Sect. 3.7) are required to retrieve the correct parameter values with the strong assumption that
21 there is no modelling bias. Synthetic experiments, also known as “twin” experiments, use
22 “pseudo data” that have been output from the model and modified according to known
23 observational characteristics (see REFLEX and Optic experiments; Trudinger et al., 2007; Fox
24 et al., 2009). As these data are model outputs, the “true” value of the parameters is known.
25 Synthetic DA experiments can also be used prior to data collection, where they can help
26 optimise sampling over space, time, and sampling design. Indeed, calibration has yet to be
27 adequately integrated into the broader literature on model-driven observing system simulation
28 experiments. To improve this, advocating for standardised community benchmark protocols and
29 datasets could address different challenges, such as assessing resistance to noise and
30 evaluating forcing variability. Results from such community-driven experimental setups could
31 reveal common challenges and development opportunities, enhancing the robustness and
32 effectiveness of DA methods across the field (see Sect. 5.4).

33

34 Additional tests of DA experimental configuration that are rarely performed (or rarely reported in
35 the literature) should include testing i) how parameters retrieved at individual sites compare to
36 parameters retrieved when including multiple sites in the assimilation (Kuppel et al., 2012;
37 Raoult et al., 2016) or using hierarchical approaches (Fer, Shiklomanov, et al., 2021; Tian et al.,
38 2020)(see Sect. 3.4), ii) the utility of PFT dependent parameters versus alternative approaches
39 for grouping parameters (e.g., regionally dependent PFTs - e.g. Dahlin et al., 2017; Bao et al.,
40 2023), iii) how retrieved parameters vary with the forcing dataset used in the simulations, iv)
41 how retrieved values depend on which parameters and/or PFTs are optimised or which terms to
42 include in the cost function, and v) how retrieved parameters vary in space and time within PFTs
43 and what this tells us about missing processes, among other factors. A critical test of any
44 parameterisation process is that the newly trained model must have improved predictive skill for

1 independent data. For example, Famiglietti et al. (2021) demonstrated that different data
2 combinations impact the resultant predictive skill and that the amount of data used in model
3 calibration must be commensurate with the complexity of the model. Such technical tests are
4 required each time a new process is optimised or a novel dataset is used in the assimilation.
5 Building DA frameworks to include this technical testing will give confidence in using retrieved
6 parameter values in operational versions of the models.

7 5.2 Moving towards land surface–atmospheric transport and full 8 Earth system model coupling in data assimilation

9 Atmospheric CO₂ mole fraction measurements collected at tall towers around the world have
10 proven valuable in improving NEE predictions at regional to global scales within a carbon cycle
11 DA framework (Bacour et al., 2023; Castro-Morales et al., 2019; Kaminski et al., 2002, 2012,
12 2013; Knorr & Heimann, 1995; Koffi et al., 2012; Peylin et al., 2016; Rayner et al., 2005;
13 Scholze et al., 2007, 2016; Schürmann et al., 2016). While atmospheric CO₂ data provide a
14 direct constraint on net surface CO₂ exchange, reliable representation of terrestrial carbon
15 sources and sinks ideally requires accurate simulations of the gross carbon fluxes. However,
16 while global scale estimates of GPP are available for model evaluation or assimilation purposes
17 (Joiner et al., 2018; Nelson et al., 2024) the currently available RECO products are still subject
18 to large uncertainties. For instance, empirically upscaled RECO from eddy covariance
19 measurements provided by FLUXCOM are inconsistent with inversion-based products in the
20 tropics, possibly due to low sampling density in the region (Jung et al., 2020). *In situ* data are
21 sparse and site history does not reflect larger-scale disturbance adequately. One benefit of
22 assimilating atmospheric CO₂ concentration data is that it is one of the only datasets that can
23 provide a large spatial scale constraint (albeit indirect) on RECO because it is heavily influenced
24 by soil carbon stocks; thus, assimilating atmospheric CO₂ data presents an opportunity to
25 improve the representation of both soil carbon flux and stock trajectories in LSMs, which is
26 crucial for future predictions regarding the carbon sink capacity of terrestrial ecosystems.

27
28 However, the assimilation of atmospheric CO₂ data requires coupling LSMs with atmospheric
29 transport models in order to scale the simulated land surface fluxes to atmospheric CO₂
30 concentrations at specified vertical levels (for station data) or integrated over the atmospheric
31 column (for space-borne data). The observational constraints of atmospheric CO₂ data on LSM
32 parameters is also more "diffuse" than when assimilating surface observations. This is due to
33 the inclusion of additional modelling errors associated with the atmospheric model itself (physics
34 and spatial/vertical discretisation) and with the other CO₂ fluxes required as inputs (mainly
35 ocean fluxes, fossil fuel emissions, and biomass burning). The coupling also presents technical
36 and computational challenges. Compared to LSMs, the derivation of the tangent linear and
37 adjoint models of atmospheric transport models is more straightforward (Kaminski et al., 1999;
38 Meirink et al., 2008; Rödenbeck et al., 2003), but their implementation increases the
39 computational load. One approach to overcome this issue is to use pre-calculated transport
40 fields of the sensitivity of mean atmospheric concentrations at selected stations to the surface
41 net CO₂ flux (see Peylin et al. (2016); or Bacour et al. (2023) for further details). However, this
42 method has limited spatial and temporal coverage due to the finite time period of the

1 precalculated sensitivities (estimating these sensitivities is also technically and computationally
2 expensive). Assimilation of space-borne retrievals of XCO₂ (column-averaged carbon dioxide)
3 with global coverage and pre-computed transport in SDBM and BETHY was demonstrated by
4 Kaminski et al. (2010) and Kaminski & Mathieu (2017). Recent advances in the utilisation of
5 graphics accelerators (Chevallier et al., 2023) offer hope for a significant reduction in
6 computational times and the development of full coupling between LSMs and atmospheric
7 transport models in the near future.

8

9 While coupling to an atmospheric transport model at least permits the use of atmospheric CO₂
10 data in parameter DA experiments, the ultimate goal for LSM parameter calibration is within a
11 fully coupled ESM. This would allow representation of carbon-climate and land-atmosphere
12 feedbacks within the optimisations. To date, there has been limited assessment of whether
13 posterior parameter values from offline DA experiments compare to retrieved values from fully
14 coupled runs (nor how retrieved values vary when different offline climate reanalysis forcing
15 products are used). To achieve this goal, LSM DA groups should learn from advances made in
16 the NWP community (de Rosnay et al., 2022). As discussed at length in this review, while
17 computational cost has so far been a prohibiting factor in achieving full ESM coupling, new ML
18 techniques for model emulation (Sect. 4.1) (Watson-Parris et al., 2021) and automatic
19 differentiation of model code (Gelbrecht et al., 2023) should help considerably in alleviating this
20 problem (see Sect. 3.7 for remaining challenges).

21 5.3 Identifying and improving structural errors and model 22 representation

23 The best estimates of different parameters are very dependent on the experimental setup and
24 so few of the optimised parameter values are actually used in the operational version of each
25 LSM—although this is something to strive for in future efforts. Indeed, even when calibrated
26 parameters have been shown to improve model performance, getting them to be the new
27 defaults in coupled models is non-trivial (Kyker-Snowman et al., 2022). Instead, the main
28 strength of parameter estimation for LSMs and, therefore, its main purpose thus far, has been to
29 identify structural errors. If we cannot match observations within the bounds of their known
30 uncertainties by simply changing the parameter values, this suggests that a process is poorly
31 represented or missing from the model. This critical information is then fed back to the model
32 developers to ensure changes are made to the model, before restarting the cycle of model
33 calibration. Although this exchange is key in developing any LSM, it is rarely published.
34 Nevertheless, a few documented examples from the ORCHIDEE land surface model workflow
35 exist. MacBean et al. (2015) demonstrated that temperate broadleaved temperature thresholds
36 for senescence in the ORCHIDEE LSM were too low. The newly optimised parameters have
37 since been included in ORCHIDEE trunk versions. Salmon et al. (2022) found that when
38 constraining parameters of the ORCHIDEE LSM against methane emissions in northern
39 peatlands, the process providing enough active carbon for methanogenesis was missing. Raoult
40 et al. (2023) found by assimilating MODIS snow albedo over Greenland that a three-layered ice
41 sheet model was insufficient to simulate accurately both the snow albedo and runoff rates,
42 leading to further discretisation of the model.

1
2 However, careful consideration is needed to avoid equating the status quo of making changes to
3 models—often involving increased complexity—with progress in model development. While
4 identifying and addressing structural errors is crucial, introducing new processes or refining
5 existing ones can sometimes lead to models that are more complex without necessarily
6 improving their predictive power. It is important to strike a balance between enhancing model
7 accuracy and maintaining model parsimony. Overly complex models can become difficult to
8 validate and manage, potentially obscuring rather than clarifying underlying processes.
9 Therefore, the goal should be to make thoughtful adjustments that improve model performance
10 while ensuring that the added complexity is justified by significant improvements in accuracy or
11 functionality. This approach ensures that models remain robust and efficient and that any
12 modifications contribute meaningfully to their overall effectiveness.

13
14 As parameter estimation methods and systems become more developed, we can run more
15 experiments to quantify and reduce uncertainty due to poorly constrained parameters using
16 different driving datasets and versions of the model that account for different representations of
17 processes. In the wider climate science literature, there exist promising approaches to provide
18 objective assessments of structural and parametric components of model error (Peatier et al.,
19 2023). Moreover, the proposed move to more modular LSMs (Fisher & Koven, 2020) will also
20 allow for different processes in the model to be isolated and calibrated sequentially, reducing the
21 scale of parameter subspaces to be calibrated and enabling better testing of alternative
22 hypotheses (e.g., different stomatal optimisation theories) and facilitate collaboration across
23 different modelling groups.

24 5.4 International collaboration: intercomparison studies and 25 shared toolboxes

26 Efforts by AIMES and ILMF to build a Land Data Assimilation Community have significantly
27 advanced knowledge sharing through online workshops and town halls, highlighting the
28 importance of continued collaboration. The goal is to facilitate cross-group interaction for DA
29 methods training, knowledge exchange on technical DA developments and calibrated model
30 intercomparison projects. The learning curve associated with learning DA for land surface
31 modelling is steep. This is exacerbated by the lack of community-wide educational materials
32 (although some resources exist, see <https://land-da-community.github.io/training/> for a selective
33 list, last accessed 27th August 2024). Understanding of DA methods is also hampered by the
34 fact that technical studies testing different DA configurations are generally buried in
35 supplementary materials or not published at all. Parameter DA system intercomparison studies
36 would help to determine how much parameter uncertainty is contributing to the spread in model
37 projections. This would signal to the wider LSM community that parameter uncertainty
38 quantification and reduction are needed to improve future projections of carbon-climate
39 feedbacks and land-atmosphere interactions. One desirable outcome may be to create and
40 share statistical toolboxes utilising community cyberinfrastructure, for example, following the
41 pioneering example of PEcAn (Predictive Ecosystem Analyzer; Fer, Gardella, et al., 2021;
42 LeBauer et al., 2013), which offers a complete end-to-end informatic structure, as well as

1 open-source land surface model benchmarking tools (iLAMB: Collier et al., 2018; Seiler et al.,
2 2022). While LSMs with established DA systems may not switch to a community toolbox, such
3 shared toolboxes will facilitate knowledge sharing, intercomparison studies and training of early
4 career researchers. Simultaneously, if LSMs with established DA systems made more of their
5 tools available within established community toolboxes, it would help reduce redundant
6 research efforts and make the adoption of such tools easier. This is one of the big lessons we
7 can learn as a community from the recent boom in ML. In addition to the improved hardware
8 (e.g., GPUs), new algorithms and huge datasets, one of the reasons ML has been so successful
9 is because the research has been done with a collaborative spirit and developed using
10 open-source frameworks (e.g., TensorFlow, PyTorch, JAX).

11 5.5 Propagation of error reductions to constrain climate 12 predictions

13 Many studies have successfully constrained parameter uncertainty in LSMs, leading to reduced
14 uncertainty in contemporary land-atmosphere carbon fluxes. However, this reduction in
15 uncertainty has not been fully propagated to constrain future projections. There is a clear
16 opportunity to take this extra step to enable observationally constrained probabilistic statements
17 to be made about the future of the land biosphere. Such efforts are already commonplace in
18 ensembles of reduced complexity models (Sanderson, 2020; Smith et al., 2024), where large
19 ensembles of future projections are computationally trivial, but the difficulty of spinning up slow
20 carbon pool processes and ocean circulation in ESMs remains a challenge for probabilistic
21 coupled projections with ESMs (without flux corrections, (Irvine et al., 2013)). However, with
22 increased computational power, we are acquiring the capability to run LSMs as ensembles
23 rather than relying on a single realisation, thereby enabling us to better capture the uncertainty
24 of model predictions (Arora et al., 2023).

25
26 By sampling from the posterior distributions after a PDA experiment, we can generate ensemble
27 simulations which can be used to explore future scenarios and idealised experiments (e.g.
28 1%/yr CO₂ concentration increase) and quantify constrained distributions of carbon-climate-CO₂
29 feedbacks. For example, by weighting the probability of each of the ensemble members, we can
30 create probability density functions of future land carbon storage for different locations, thus
31 narrowing the associated uncertainty of the future land sink and subsequently leading to more
32 accurate calculations of carbon budget estimates. Although this can easily be done for simpler
33 models where MCMC can be applied, for computational demanding models, there are two
34 critical yet distinct questions in this area that need addressing. The first is how to generate joint
35 posterior distributions for large models, which likely requires the use of emulators (see Sect.
36 4.1). The second is how to intelligently select parameter vectors from those distributions.
37 Currently, simple models might propagate uncertainty by using 100-1000 ensemble members,
38 but protocols like that used in the Coupled Model Intercomparison Project (CMIP) are not yet
39 adopting such large ensembles, again due to computational expense and constraints on data
40 storage. As a climate community, we should be striving to move towards using data-constrained
41 ensemble simulations in CMIP or the TRENDY model intercomparison project (Sitch et al.,
42 2024) to quantify uncertainties in model predictions reported in the Intergovernmental Panel on

¹ Climate Change (IPCC) 8th Assessment Report, the annual Global Carbon Budget (GCB) and
² other emerging frameworks quantifying land carbon trajectories. Therefore, we must develop
³ methods to maximise the propagation and partitioning of uncertainty with a limited number of
⁴ ensemble runs. Constraining parameter uncertainty via improved DA and ML techniques should
⁵ also help to reduce inter-model spread in CMIP and TRENDY, as model differences are likely
⁶ partly attributable to variations in parameter values between models.

⁷

⁸ Other international frameworks that oversee policies and socioeconomic management of
⁹ terrestrial carbon stocks – such as the voluntary carbon market and national emissions reporting
¹⁰ for Nationally Determined Contributions under the Paris Agreement – already require estimates
¹¹ of model uncertainty; however, so far the models used in voluntary carbon market offset project
¹² verification tend to be of simple to intermediate complexity, and not full complexity LSMs. Better
¹³ estimating uncertainty in LSMs via methods such as parameter DA should therefore facilitate
¹⁴ their use in a wider range of policy and carbon management initiatives.

¹⁵ 6. Summary and conclusion

¹⁶ Improving the accuracy of land surface models (LSMs) is of vital importance since land surface
¹⁷ feedbacks on climate change represent one of the largest sources of uncertainty in climate
¹⁸ change projections. Parameter data assimilation is critical for enhancing the performance and
¹⁹ reliability of these LSMs. This process involves determining the best estimates of model
²⁰ parameters, and their uncertainties, that best align the model outputs with observed data.
²¹ Effective parameter estimation helps in capturing the complex dynamics of land-atmosphere
²² interactions and improves the model's ability to simulate real-world phenomena. However, LSMs
²³ used to predict future climate scenarios (e.g., when coupled to Earth System Models) are
²⁴ complex in nature leading to many challenges when performing global scale optimisations.
²⁵ Nevertheless, advances in computational capability, novel datasets and emerging technologies
²⁶ offer promising avenues for improving parameter accuracy and model calibration.

²⁷ Machine learning (ML) clearly has a pivotal part to play in the future of land surface model data
²⁸ assimilation, helping to streamline the assimilation process, manage large datasets and speed
²⁹ up otherwise computationally demanding processes. International collaboration is crucial in this
³⁰ endeavour, as shared knowledge and resources can significantly accelerate the advancement
³¹ of LSM calibration and data assimilation. Efforts to build a Land Data Assimilation Community,
³² such as those by the AIMES Land Data Assimilation Working Group and the International Land
³³ Model Forum, have already made substantial progress in facilitating cross-group interactions.
³⁴ These collaborative platforms are essential for training, knowledge exchange, and the
³⁵ development of standardised methodologies, ultimately leading to more accurate LSMs.

¹ Acknowledgements

² This manuscript is the result of efforts by the Analysis, Integration, and Modeling of the Earth
³ System (AIMES) Land DA Working Group annual virtual workshops
⁴ (<https://aimesproject.org/lawg/>) and initiatives to build a Land DA Community
⁵ (<https://land-da-community.github.io>). NR has been supported by a H2020 Marie
⁶ Skłodowska-Curie Actions grant (no. 101026422). ND and TQ would like to acknowledge
⁷ funding from the UKRI National Centre for Earth Observation, under the International Science
⁸ Programme (NE/X006328/1). AR and MD acknowledge funding from NSF MSB 2406258 and
⁹ MD further acknowledges funding from NASA CMS 80NSSC21K0965. KD, LH and PG would
¹⁰ like to acknowledge funding from the National Science Foundation (NSF) Science and
¹¹ Technology Center (STC) Learning the Earth with Artificial Intelligence and Physics (LEAP),
¹² Award # 2019625-STC. KD further acknowledges support from the U.S. Department of Energy,
¹³ Office of Biological & Environmental Research (BER), under Award DE-SC0022070, the
¹⁴ National Science Foundation (NSF) under IA 1947282, and the National Center for Atmospheric
¹⁵ Research (NCAR) through Cooperative Agreement No. 1852977 NM acknowledges support
¹⁶ from the Wolfe-Western Fellowship At-Large for Outstanding Newly Recruited Research
¹⁷ Scholars Endowment Fund. IF acknowledges funding from the Research Council of Finland
¹⁸ (grant number 337552) and Horizon Europe, HORIZON-MISS-2022-SOIL-01-05. TLS was
¹⁹ funded by the National Centre for Earth Observation, under the LTSS programme
²⁰ (NE/R016518/1) and the UK's EO Climate Information Service (NE/X019071/1). MS
²¹ acknowledges support from three Swedish strategic research areas: Modelling the Regional
²² and Global Earth system (MERGE), the e-science collaboration (eSSENCE), and Biodiversity
²³ and Ecosystems in a Changing Climate (BECC).

²⁴ Open research

²⁵ **Data Availability statement:** This article discusses the challenges and priorities in the field of
²⁶ parameter estimation for land data assimilation, and the opportunities offered by machine
²⁷ learning—it does not include the specific use of any particular software or results involving
²⁸ specific data products.

²⁹

¹ Appendix

² The process-based models mentioned through the paper are listed in Table A1. This list cover
³ wide spectrum of land models ranging in complexity and computational demand, including
⁴ LSMs that simulate interactions between carbon, water, and energy cycles, often incorporating
⁵ other biogeochemical cycles (e.g., nitrogen cycling) and dynamic vegetation processes;
⁶ stand-alone DGVMs that have more complex representation of vegetation demography
⁷ (so-called vegetation demographic models, VDMs) but may not fully represent energy and
⁸ hydrology components; and ecosystem models that primarily represent carbon cycling and
⁹ simple representations of vegetation and hydrology processes but may lack the full mechanistic
¹⁰ representation of energy and hydrological processes or vegetation dynamics seen in LSMs and
¹¹ VDMs.

¹² **Table A1.** References for the process-based models mentioned in this article.

Acronym	Full name	Model reference
BETHY	Biosphere Energy Transfer Hydrology	Knorr (2000)
CABLE	Community Atmosphere Biosphere Land Exchange	Kowalczyk et al., (2006)
CARDAMOM	CARbon DATA MOdel fraMework	Bloom et al. (2016); Smallman et al. (2021)
CLASSIC	Canadian Land Surface Scheme Including Biogeochemical Cycles	Melton et al. (2020)
CLM	Community Land Model	Lawrence et al. (2019)
D&B	DALEC & BETHY	Knorr et al. (2024)
DALEC	Data Assimilation Linked Ecosystem Carbon	Williams et al. (2005)
ED	Ecosystem Demography	Ma et al. (2022); Moorcroft et al. (2001)
ECLand	European Centre for Medium-range Weather Forecasts Land model (based on CHTESSEL: Carbon-Hydrology Tiled Scheme for Surface Exchanges over Land)	Boussetta et al. (2021)

FATES	Functionally Assembled Terrestrial Ecosystem Simulator	Fisher et al. (2015); Koven et al. (2020)
FöBAAR	Forest Biomass, Assimilation, Allocation and Respiration	Keenan et al. (2012)
JULES	Joint UK Land Environment Simulator	Best et al. (2011); Clark et al. (2011)
JSBACH	Jena Scheme for Biosphera-Atmosphere Coupling in Hamburg	Mauritsen et al (2019); Reick et al. (2021)
LPJ-GUESS	Lund-Potsdam-Jena General Ecosystem Simulator	Smith (2007)
Noah	-	Ek et al. (2003)
ORCHIDEE	Organising Carbon and Hydrology In Dynamic Ecosystems	Krinner et al. (2005); Vuichard et al. (2019); Zaehle, Friend, et al. (2010)
SDBM	Simple Diagnostic Biosphere Model	Knorr & Heimann (1995)
SIPNET	Simplified Photosynthesis and Evapotranspiration	Braswell et al. (2005)
TECOS	terrestrial ecosystem	Xu et al., (2006)

1 References

2 Abadie, C., Maignan, F., Remaud, M., Kohonen, K.-M., Sun, W., Kooijmans, L., Vesala, T.,
3 Seibt, U., Raoult, N., Bastrikov, V., Belviso, S., & Peylin, P. (2023). Carbon and water fluxes
4 of the boreal evergreen needleleaf forest biome constrained by assimilating ecosystem
5 carbonyl sulfide flux observations. *Journal of Geophysical Research. Biogeosciences*,
6 128(7), e2023JG007407. <https://doi.org/10.1029/2023jg007407>

7 Abramoff, R., Xu, X., Hartman, M., O'Brien, S., Feng, W., Davidson, E., Finzi, A., Moorhead, D.,
8 Schimel, J., Torn, M., & Mayes, M. A. (2018). The Millennial model: in search of measurable
9 pools and transformations for modeling soil carbon in the new century. *Biogeochemistry*,
10 137(1-2), 51–71. <https://doi.org/10.1007/s10533-017-0409-7>

11 Akiba, T., Sano, S., Yanase, T., Ohta, T., & Koyama, M. (2019). Optuna: A Next-generation
12 Hyperparameter Optimization Framework. In *arXiv [cs.LG]*. arXiv.
13 <http://arxiv.org/abs/1907.10902>

14 Alejomhammad, S. H., Fang, B., Konings, A. G., Aires, F., Green, J. K., Kolassa, J., Miralles, D.,
15 Prigent, C., & Gentine, P. (2017). Water, Energy, and Carbon with Artificial Neural Networks
16 (WECANN): A statistically-based estimate of global surface turbulent fluxes and gross
17 primary productivity using solar-induced fluorescence. *Biogeosciences*, 14(18), 4101–4124.
18 <https://doi.org/10.5194/bg-14-4101-2017>

19 Alton, P. B. (2013). From site-level to global simulation: Reconciling carbon, water and energy
20 fluxes over different spatial scales using a process-based ecophysiological land-surface
21 model. *Agricultural and Forest Meteorology*, 176, 111–124.
22 <https://doi.org/10.1016/j.agrformet.2013.03.010>

23 Arora, V. K., Katavouta, A., Williams, R. G., Jones, C. D., Brovkin, V., Friedlingstein, P.,
24 Schwinger, J., Bopp, L., Boucher, O., Cadule, P., Chamberlain, M. A., Christian, J. R.,
25 Delire, C., Fisher, R. A., Hajima, T., Ilyina, T., Joetzjer, E., Kawamiya, M., Koven, C. D., ...
26 Ziehn, T. (2020). Carbon–concentration and carbon–climate feedbacks in CMIP6 models
27 and their comparison to CMIP5 models. *Biogeosciences*, 17(16), 4173–4222.
28 <https://doi.org/10.5194/bg-17-4173-2020>

29 Arora, V. K., Seiler, C., Wang, L., & Kou-Giesbrecht, S. (2023). Towards an ensemble-based
30 evaluation of land surface models in light of uncertain forcings and observations.
31 *Biogeosciences*, 20(7), 1313–1355. <https://doi.org/10.5194/bg-20-1313-2023>

32 Arsenault, K. R., Kumar, S. V., Geiger, J. V., Wang, S., Kemp, E., Mocko, D. M., Beaudoing, H.
33 K., Getirana, A., Navari, M., Li, B., Jacob, J., Wegiel, J., & Peters-Lidard, C. D. (2018). The
34 Land surface Data Toolkit (LDT v7.2) – a data fusion environment for land data assimilation
35 systems. *Geoscientific Model Development*, 11(9), 3605–3621.
36 <https://doi.org/10.5194/gmd-11-3605-2018>

37 Assem, H., Ghariba, S., Makrai, G., Johnston, P., Gill, L., & Pilla, F. (2017). Urban water flow
38 and water level prediction based on deep learning. In *Machine Learning and Knowledge
39 Discovery in Databases* (pp. 317–329). Springer International Publishing.
40 https://doi.org/10.1007/978-3-319-71273-4_26

41 Baatz, R., Hendricks Franssen, H. J., Euskirchen, E., Sihi, D., Dietze, M., Ciavatta, S., Fennel,
42 K., Beck, H., De Lannoy, G., Pauwels, V. R. N., Raiho, A., Montzka, C., Williams, M.,
43 Mishra, U., Poppe, C., Zacharias, S., Lausch, A., Samaniego, L., Van Looy, K., ...

1 Vereecken, H. (2021). Reanalysis in earth system science: Toward terrestrial ecosystem
2 reanalysis. *Reviews of Geophysics* (Washington, D.C.: 1985), 59(3), e2020RG000715.
3 <https://doi.org/10.1029/2020rg000715>

4 Babst, F., Bouriaud, O., Alexander, R., Trouet, V., & Frank, D. (2014). Toward consistent
5 measurements of carbon accumulation: A multi-site assessment of biomass and basal area
6 increment across Europe. *Dendrochronologia*, 32(2), 153–161.
7 <https://doi.org/10.1016/j.dendro.2014.01.002>

8 Bacour, C., MacBean, N., Chevallier, F., Léonard, S., Koffi, E. N., & Peylin, P. (2023).
9 Assimilation of multiple datasets results in large differences in regional- to global-scale NEE
10 and GPP budgets simulated by a terrestrial biosphere model. *Biogeosciences*, 20(6),
11 1089–1111. <https://doi.org/10.5194/bg-20-1089-2023>

12 Bacour, C., Maignan, F., MacBean, N., Porcar-Castell, A., Flexas, J., Frankenberg, C., Peylin,
13 P., Chevallier, F., Vuichard, N., & Bastrikov, V. (2019). Improving estimates of gross primary
14 productivity by assimilating solar-induced fluorescence satellite retrievals in a terrestrial
15 biosphere model using a process-based SIF model. *Journal of Geophysical Research: Biogeosciences*, 124(11), 3281–3306. <https://doi.org/10.1029/2019jg005040>

17 Bacour, C., Peylin, P., MacBean, N., Rayner, P. J., Delage, F., Chevallier, F., Weiss, M.,
18 Demarty, J., Santaren, D., Baret, F., Berveiller, D., Dufrêne, E., & Prunet, P. (2015). Joint
19 assimilation of eddy covariance flux measurements and FAPAR products over temperate
20 forests within a process-oriented biosphere model. *Journal of Geophysical Research: Biogeosciences*, 120(9), 1839–1857. <https://doi.org/10.1002/2015JG002966>

22 Bagnara, M., Silveyra Gonzalez, R., Reifenberg, S., Steinkamp, J., Hickler, T., Werner, C.,
23 Dormann, C. F., & Hartig, F. (2019). An R package facilitating sensitivity analysis, calibration
24 and forward simulations with the LPJ-GUESS dynamic vegetation model. *Environmental Modelling & Software: With Environment Data News*, 111, 55–60.
26 <https://doi.org/10.1016/j.envsoft.2018.09.004>

27 Baker, E., Harper, A. B., Williamson, D., & Challenor, P. (2022). Emulation of high-resolution
28 land surface models using sparse Gaussian processes with application to JULES.
29 *Geoscientific Model Development*, 15(5), 1913–1929.
30 <https://doi.org/10.5194/gmd-15-1913-2022>

31 Balsamo, G., Agusti-Panareda, A., Albergel, C., Arduini, G., Beljaars, A., Bidlot, J., Blyth, E.,
32 Bousserez, N., Boussetta, S., Brown, A., Buizza, R., Buontempo, C., Chevallier, F.,
33 Choulga, M., Cloke, H., Cronin, M. F., Dahoui, M., De Rosnay, P., Dirmeyer, P. A., ... Zeng,
34 X. (2018). Satellite and in situ observations for advancing global Earth surface modelling: A
35 review. *Remote Sensing*, 10(12), 2038. <https://doi.org/10.3390/rs10122038>

36 Bannister, R. N., Chipilski, H. G., & Martinez-Alvarado, O. (2020). Techniques and challenges in
37 the assimilation of atmospheric water observations for numerical weather prediction
38 towards convective scales. *Quarterly Journal of the Royal Meteorological Society*,
39 146(726), 1–48. <https://doi.org/10.1002/qj.3652>

40 Bao, S., Alonso, L., Wang, S., Gensheimer, J., De, R., & Carvalhais, N. (2023). Toward robust
41 parameterizations in ecosystem-level photosynthesis models. *Journal of Advances in
42 Modeling Earth Systems*, 15(8). <https://doi.org/10.1029/2022ms003464>

43 Barichivich, J., Peylin, P., Launois, T., Daux, V., Risi, C., Jeong, J., & Luysaert, S. (2021). A
44 triple tree-ring constraint for tree growth and physiology in a global land surface model.

1 *Biogeosciences*, 18(12), 3781–3803. <https://doi.org/10.5194/bg-18-3781-2021>

2 Bastrikov, V., MacBean, N., Bacour, C., Santaren, D., Kuppel, S., & Peylin, P. (2018). Land
3 surface model parameter optimisation using in situ flux data: Comparison of gradient-based
4 versus random search algorithms (a case study using ORCHIDEE v1. 9.5. 2). *Geoscientific
5 Model Development*, 11(12), 4739–4754. <https://gmd.copernicus.org/articles/11/4739/2018/>

6 Beer, C., Reichstein, M., Tomelleri, E., Ciais, P., Jung, M., Carvalhais, N., Rödenbeck, C., Arain,
7 M. A., Baldocchi, D., Bonan, G. B., Bondeau, A., Cescatti, A., Lasslop, G., Lindroth, A.,
8 Lomas, M., Luyssaert, S., Margolis, H., Oleson, K. W., Roupsard, O., ... Papale, D. (2010).
9 Terrestrial gross carbon dioxide uptake: global distribution and covariation with climate.
10 *Science (New York, N.Y.)*, 329(5993), 834–838. <https://doi.org/10.1126/science.1184984>

11 Best, M. J., Pryor, M., Clark, D. B., Rooney, G. G., Essery, R., Ménard, C. B., & Harding R.
12 (2011). The Joint UK Land Environment Simulator (JULES), model description—Part 1:
13 energy and water fluxes. *Geoscientific Model Development*, 4(3), 677–699.
14 <https://gmd.copernicus.org/articles/4/677/2011/>

15 Beucler, T., Pritchard, M., Rasp, S., Ott, J., Baldi, P., & Gentine, P. (2021). Enforcing analytic
16 constraints in neural networks emulating physical systems. *Physical Review Letters*, 126(9),
17 098302. <https://doi.org/10.1103/PhysRevLett.126.098302>

18 Bhouri, M. A., Joly, M., Yu, R., Sarkar, S., & Perdikaris, P. (2023). Scalable Bayesian
19 optimization with randomized prior networks. *Computer Methods in Applied Mechanics and
20 Engineering*, 417, 116428. <https://doi.org/10.1016/j.cma.2023.116428>

21 Bloom, A. A., Bowman, K. W., Liu, J., Konings, A. G., Worden, J. R., Parazoo, N. C., Meyer, V.,
22 Reager, J. T., Worden, H. M., Jiang, Z., Quetin, G. R., Smallman, T. L., Exbrayat, J.-F., Yin,
23 Y., Saatchi, S. S., Williams, M., & Schimel, D. S. (2020). Lagged effects regulate the
24 inter-annual variability of the tropical carbon balance. *Biogeosciences*, 17(24), 6393–6422.
25 <https://doi.org/10.5194/bg-17-6393-2020>

26 Bloom, A. A., Exbrayat, J.-F., van der Velde, I. R., Feng, L., & Williams, M. (2016). The decadal
27 state of the terrestrial carbon cycle: Global retrievals of terrestrial carbon allocation, pools,
28 and residence times. *Proceedings of the National Academy of Sciences of the United
29 States of America*, 113(5), 1285–1290. <https://doi.org/10.1073/pnas.1515160113>

30 Bloom, A. A., & Williams, M. (2015). Constraining ecosystem carbon dynamics in a data-limited
31 world: integrating ecological “common sense” in a model–data fusion framework.
32 *Biogeosciences*, 12(5), 1299–1315. <https://doi.org/10.5194/bg-12-1299-2015>

33 Blyth, E. M., Arora, V. K., Clark, D. B., Dadson, S. J., De Kauwe, M. G., Lawrence, D. M.,
34 Melton, J. R., Pongratz, J., Turton, R. H., Yoshimura, K., & Yuan, H. (2021). Advances in
35 land surface modelling. *Current Climate Change Reports*, 7(2), 45–71.
36 <https://doi.org/10.1007/s40641-021-00171-5>

37 Bonan, G. B., & Doney, S. C. (2018). Climate, ecosystems, and planetary futures: The challenge
38 to predict life in Earth system models. *Science (New York, N.Y.)*, 359(6375).
39 <https://doi.org/10.1126/science.aam8328>

40 Booth, B. B. B., Jones, C. D., Collins, M., Totterdell, I. J., Cox, P. M., Sitch, S., Huntingford, C.,
41 Betts, R. A., Harris, G. R., & Lloyd, J. (2012). High sensitivity of future global warming to
42 land carbon cycle processes. *Environmental Research Letters*, 7(2), 024002.
43 <https://doi.org/10.1088/1748-9326/7/2/024002>

44 Boussetta, S., Balsamo, G., Arduini, G., Dutra, E., McNorton, J., Choulga, M., Agustí-Panareda,

1 A., Beljaars, A., Wedi, N., Munoz-Sabater, J., de Rosnay, P., Sandu, I., Hadade, I., Carver,
2 G., Mazzetti, C., Prudhomme, C., Yamazaki, D., & Zsoter, E. (2021). ECLand: The ECMWF
3 land surface modelling system. *Atmosphere*, 12(6), 723.
4 <https://doi.org/10.3390/atmos12060723>

5 Bradbury, J., Frostig, R., Hawkins, P., Johnson, M. J., Leary, C., Maclaurin, D., Necula, G.,
6 Paszke, A., VanderPlas, J., Wanderman-Milne, S., & Zhang, Q. (2018). JAX: *composable*
7 *transformations of Python+NumPy programs* (Version 0.3.13). <http://github.com/google/jax>

8 Braswell, B. H., Sacks, W. J., Linder, E., & Schimel, D. S. (2005). Estimating diurnal to annual
9 ecosystem parameters by synthesis of a carbon flux model with eddy covariance net
10 ecosystem exchange observations. *Global Change Biology*, 11(2), 335–355.
11 <https://doi.org/10.1111/j.1365-2486.2005.00897.x>

12 Breiman, L. (1996). Bagging predictors. *Machine Learning*, 24(2), 123–140.
13 <https://doi.org/10.1007/bf00058655>

14 Brynjarsdóttir, J., & O'Hagan, A. (2014). Learning about physical parameters: the importance of
15 model discrepancy. *Inverse Problems*, 30(11), 114007.
16 <https://doi.org/10.1088/0266-5611/30/11/114007>

17 Buotte, P. C., Koven, C. D., Xu, C., Shuman, J. K., Goulden, M. L., Levis, S., & Kueppers L.
18 (2021). Capturing functional strategies and compositional dynamics in vegetation
19 demographic models. *Biogeosciences*, 18(14), 4473–4490.
20 <https://bg.copernicus.org/articles/18/4473/2021/bg-18-4473-2021.html>

21 Byrd, R. H., Lu, P., Nocedal, J., & Zhu, C. (1995). A limited memory algorithm for bound
22 constrained optimization. *SIAM Journal on Scientific Computing: A Publication of the*
23 *Society for Industrial and Applied Mathematics*, 16(5), 1190–1208.
24 <https://doi.org/10.1137/0916069>

25 Caen, A., Smallman, T. L., de Castro, A. A., Robertson, E., von Randow, C., Cardoso, M., &
26 Williams, M. (2022). Evaluating two land surface models for Brazil using a full carbon cycle
27 benchmark with uncertainties. *Climate Resilience and Sustainability*, 1(1).
28 <https://doi.org/10.1002/clr2.10>

29 Cameron, D., Hartig, F., Minnuno, F., Oberpriller, J., Reineking, B., Van Oijen, M., & Dietze, M.
30 (2022). Issues in calibrating models with multiple unbalanced constraints: the significance
31 of systematic model and data errors. *Methods in Ecology and Evolution*, 13(12),
32 2757–2770. <https://doi.org/10.1111/2041-210x.14002>

33 Carvalhais, N., Reichstein, M., Ciais, P., Collatz, G. J., Mahecha, M. D., Montagnani, L., Papale,
34 D., Rambal, S., & Seixas, J. (2010). Identification of vegetation and soil carbon pools out of
35 equilibrium in a process model via eddy covariance and biometric constraints:
36 ECOSYSTEM C POOLS APART FROM EQUILIBRIUM. *Global Change Biology*, 16(10),
37 2813–2829. <https://doi.org/10.1111/j.1365-2486.2010.02173.x>

38 Carvalhais, N., Reichstein, M., Seixas, J., James Collatz, G., Pereira, J. S., Berbigier, P.,
39 Carrara, A., Granier, A., Montagnani, L., Papale, D., Rambal, S., Sanz, M. J., & Valentini, R.
40 (2008). Implications of the carbon cycle steady state assumption for biogeochemical
41 modeling performance and inverse parameter retrieval. *Global Biogeochemical Cycles*,
42 22(2). <https://doi.org/10.1029/2007GB003033>

43 Castro-Morales, K., Schürmann, G., Köstler, C., Rödenbeck, C., Heimann, M., & Zaehle, S.
44 (2019). Three decades of simulated global terrestrial carbon fluxes from a data assimilation

1 system confronted with different periods of observations. *Biogeosciences* , 16(15),
2 3009–3032. <https://doi.org/10.5194/bg-16-3009-2019>

3 Chaney, N. W., Herman, J. D., Ek, M. B., & Wood, E. F. (2016). Deriving global parameter
4 estimates for the Noah land surface model using FLUXNET and machine learning. *Journal*
5 *of Geophysical Research: Atmospheres*, 121(22), 13,218–13,235.
6 <https://doi.org/10.1002/2016JD024821>

7 Cheng, Y., Wang, W., Dettò, M., Fisher, R., & Shoemaker, C. (2024). Calibrating tropical forest
8 coexistence in ecosystem demography models using Multi-objective optimization through
9 population-based parallel surrogate search. *Journal of Advances in Modeling Earth*
10 *Systems*, 16(8), e2023MS004195. <https://doi.org/10.1029/2023ms004195>

11 Cheng, Y., Xia, W., Dettò, M., & Shoemaker, C. A. (2023). A framework to calibrate ecosystem
12 demography models within earth system models using parallel surrogate global
13 optimization. *Water Resources Research*, 59(1), e2022WR032945.
14 <https://doi.org/10.1029/2022wr032945>

15 Chen, X., Huang, Y., Nie, C., Zhang, S., Wang, G., Chen, S., & Chen, Z. (2022). A long-term
16 reconstructed TROPOMI solar-induced fluorescence dataset using machine learning
17 algorithms. *Scientific Data*, 9(1), 427. <https://doi.org/10.1038/s41597-022-01520-1>

18 Chevallier, F. (2007). Impact of correlated observation errors on inverted CO₂ surface fluxes
19 from OCO measurements. *Geophysical Research Letters*, 34(24).
20 <https://doi.org/10.1029/2007gl030463>

21 Chevallier, F., Lloret, Z., Cozic, A., Takache, S., & Remaud, M. (2023). Toward high-resolution
22 global atmospheric inverse modeling using graphics accelerators. *Geophysical Research*
23 *Letters*, 50(5). <https://doi.org/10.1029/2022gl102135>

24 Clark, D. B., Mercado, L. M., Sitch, S., Jones, C. D., Gedney, N., Best, M. J., & Cox P. (2011).
25 The Joint UK Land Environment Simulator (JULES), model description—Part 2: carbon
26 fluxes and vegetation dynamics. *Geoscientific Model Development*, 4(3), 701–722.
27 <https://gmd.copernicus.org/articles/4/701/2011/>

28 Cleary, E., Garbuno-Íñigo, A., Lan, S., Schneider, T., & Stuart, A. M. (2021). Calibrate, emulate,
29 sample. *Journal of Computational Physics*, 424, 109716.
30 <https://doi.org/10.1016/j.jcp.2020.109716>

31 Collatz, G. J., Ribas-Carbo, M., & Berry, J. A. (1992). Coupled photosynthesis-stomatal
32 conductance model for leaves of C₄ plants. *Functional Plant Biology: FPB*, 19(5), 519.
33 <https://doi.org/10.1071/pp9920519>

34 Collier, N., Hoffman, F. M., Lawrence, D. M., Keppel-Aleks, G., Koven, C. D., Riley, W. J., Mu,
35 M., & Randerson, J. T. (2018). The international land model benchmarking (ILAMB) system:
36 Design, theory, and implementation. *Journal of Advances in Modeling Earth Systems*,
37 10(11), 2731–2754. <https://doi.org/10.1029/2018ms001354>

38 Cooper, E. S., Dance, S. L., García-Pintado, J., Nichols, N. K., & Smith, P. J. (2019).
39 Observation operators for assimilation of satellite observations in fluvial inundation
40 forecasting. *Hydrology and Earth System Sciences*, 23(6), 2541–2559.
41 <https://doi.org/10.5194/hess-23-2541-2019>

42 Couvreux, F., Hourdin, F., Williamson, D., Roehrig, R., Volodina, V., Villefranque, N., Rio, C.,
43 Audouin, O., Salter, J., Bazile, E., Brient, F., Favot, F., Honnert, R., Lefebvre, M.-P.,
44 Madeleine, J.-B., Rodier, Q., & Xu, W. (2021). Process-based climate model development

1 harnessing machine learning: I. a calibration tool for parameterization improvement. *Journal*
2 *of Advances in Modeling Earth Systems*, 13(3). <https://doi.org/10.1029/2020ms002217>

3 Cukier, R. I., Fortuin, C. M., Shuler, K. E., Petschek, A. G., & Schaibly, J. H. (1973). Study of the
4 sensitivity of coupled reaction systems to uncertainties in rate coefficients. I Theory. *The*
5 *Journal of Chemical Physics*, 59(8), 3873–3878. <https://doi.org/10.1063/1.1680571>

6 Dagon, K., Sanderson, B. M., Fisher, R. A., & Lawrence, D. M. (2020). A machine learning
7 approach to emulation and biophysical parameter estimation with the Community Land
8 Model, version 5. *Advances in Statistical Climatology Meteorology and Oceanography*, 6(2),
9 223–244. <https://doi.org/10.5194/ascmo-6-223-2020>

10 Dahlin, K. M., Ponte, D. D., Setlock, E., & Nagelkirk, R. (2017). Global patterns of drought
11 deciduous phenology in semi-arid and savanna-type ecosystems. *Ecography*, 40(2),
12 314–323. <https://doi.org/10.1111/ecog.02443>

13 Dantec-Nédélec, S., Ottlé, C., Wang, T., Guglielmo, F., Maignan, F., Delbart, N., Valdayskikh, V.,
14 Radchenko, T., Nekrasova, O., Zakharov, V., & Jouzel, J. (2017). Testing the capability of
15 ORCHIDEE land surface model to simulate Arctic ecosystems: Sensitivity analysis and
16 site-level model calibration. *Journal of Advances in Modeling Earth Systems*, 9(2),
17 1212–1230. <https://doi.org/10.1002/2016ms000860>

18 Datta, P., & Faroughi, S. A. (2023). A multihead LSTM technique for prognostic prediction of soil
19 moisture. *Geoderma*, 433(116452), 116452.
20 <https://doi.org/10.1016/j.geoderma.2023.116452>

21 Davies-Barnard, T., Zaehle, S., & Friedlingstein, P. (2022). Assessment of the impacts of
22 biological nitrogen fixation structural uncertainty in CMIP6 earth system models.
23 *Biogeosciences*, 19(14), 3491–3503. <https://doi.org/10.5194/bg-19-3491-2022>

24 de Bézenac, E., Pajot, A., & Gallinari, P. (2019). Deep learning for physical processes:
25 incorporating prior scientific knowledge. *Journal of Statistical Mechanics*, 2019(12), 124009.
26 <https://doi.org/10.1088/1742-5468/ab3195>

27 Deepak, R., Seiler, C., & Monahan, A. H. (2024). A global sensitivity analysis of parameter
28 uncertainty in the CLASSIC model. *Atmosphere-Ocean*, 0(0), 1–13.
29 <https://doi.org/10.1080/07055900.2024.2396426>

30 De Lannoy, G. J. M., Bechtold, M., Albergel, C., Brocca, L., Calvet, J.-C., Carrassi, A., Crow, W.,
31 T., de Rosnay, P., Durand, M., Forman, B., Geppert, G., Girotto, M., Hendricks Franssen,
32 H.-J., Jonas, T., Kumar, S., Lievens, H., Lu, Y., Massari, C., Pauwels, V. R. N., ...
33 Steele-Dunne, S. (2022). Perspective on satellite-based land data assimilation to estimate
34 water cycle components in an era of advanced data availability and model sophistication.
35 *Frontiers in Water*, 4. <https://doi.org/10.3389/frwa.2022.981745>

36 de Rosnay, P., Browne, P., de Boisséson, E., Fairbairn, D., Hirahara, Y., Ochi, K., Schepers, D.,
37 Weston, P., Zuo, H., Alonso-Balmaseda, M., Balsamo, G., Bonavita, M., Borman, N.,
38 Brown, A., Chrust, M., Dahoui, M., Chiara, G., English, S., Geer, A., ... Rabier, F. (2022).
39 Coupled data assimilation at ECMWF: current status, challenges and future developments.
40 *Quarterly Journal of the Royal Meteorological Society*, 148(747), 2672–2702.
41 <https://doi.org/10.1002/qj.4330>

42 Dietze, M. C. (2017). *Ecological Forecasting*. Princeton University Press.
43 <https://doi.org/10.1515/9781400885459>

44 Dietze, M. C., Serbin, S. P., Davidson, C., Desai, A. R., Feng, X., Kelly, R., Kooper, R., LeBauer,

1 D., Mantooth, J., McHenry, K., & Wang, D. (2014). A quantitative assessment of a terrestrial
2 biosphere model's data needs across North American biomes. *Journal of Geophysical*
3 *Research. Biogeosciences*, 119(3), 286–300. <https://doi.org/10.1002/2013jg002392>

4 Dokoochaki, H., Morrison, B. D., Raiho, A., Serbin, S. P., Zarada, K., Dramko, L., & Dietze, M.
5 (2022). Development of an open-source regional data assimilation system in PEcAn v.
6 1.7.2: application to carbon cycle reanalysis across the contiguous US using SIPNET.
7 *Geoscientific Model Development*, 15(8), 3233–3252.
8 <https://doi.org/10.5194/gmd-15-3233-2022>

9 Donnerer, C. (n.d.). *xgboost-distribution: Probabilistic prediction with XGBoost*. Github.
10 Retrieved August 15, 2024, from <https://github.com/CDonnerer/xgboost-distribution>

11 Draper, C. S. (2021). Accounting for land model error in numerical weather prediction ensemble
12 systems: toward ensemble-based coupled land/atmosphere data assimilation. *Journal of*
13 *Hydrometeorology*, 22(8), 2089–2104. <https://doi.org/10.1175/jhm-d-21-0016.1>

14 Duan, T., Anand, A., Ding, D. Y., Thai, K. K., Basu, S., Ng, A., & Schuler, A. (13–18 Jul 2020).
15 NGBoost: Natural Gradient Boosting for Probabilistic Prediction. In H. D. Iii & A. Singh
16 (Eds.), *Proceedings of the 37th International Conference on Machine Learning* (Vol. 119,
17 pp. 2690–2700). PMLR. <https://proceedings.mlr.press/v119/duan20a.html>

18 Dubayah, R., Blair, J. B., Goetz, S., Fatoyinbo, L., Hansen, M., Healey, S., Hofton, M., Hurt, G.,
19 Kellner, J., Luthcke, S., Armston, J., Tang, H., Duncanson, L., Hancock, S., Jantz, P.,
20 Marselis, S., Patterson, P. L., Qi, W., & Silva, C. (2020). The Global Ecosystem Dynamics
21 Investigation: High-resolution laser ranging of the Earth's forests and topography. *Egyptian*
22 *Journal of Remote Sensing and Space Sciences*, 1, 100002.
23 <https://doi.org/10.1016/j.srs.2020.100002>

24 Durbha, S. S., King, R. L., & Younan, N. H. (2007). Support vector machines regression for
25 retrieval of leaf area index from multiangle imaging spectroradiometer. *Remote Sensing of*
26 *Environment*, 107(1-2), 348–361. <https://doi.org/10.1016/j.rse.2006.09.031>

27 Ek, M. B., Mitchell, K. E., Lin, Y., Rogers, E., Grunmann, P., Koren, V., Gayno, G., & Tarpley, J.
28 D. (2003). Implementation of Noah land surface model advances in the National Centers for
29 Environmental Prediction operational mesoscale Eta model. *Journal of Geophysical*
30 *Research*, 108(D22). <https://doi.org/10.1029/2002jd003296>

31 ElGhawi, R., Kraft, B., Reimers, C., Reichstein, M., Körner, M., Gentine, P., & Winkler, A. J.
32 (2023). Hybrid modeling of evapotranspiration: inferring stomatal and aerodynamic
33 resistances using combined physics-based and machine learning. *Environmental Research*
34 *Letters*, 18(3), 034039. <https://doi.org/10.1088/1748-9326/acbbe0>

35 Evensen, G. (2003). The Ensemble Kalman Filter: theoretical formulation and practical
36 implementation. *Ocean Dynamics*, 53(4), 343–367.
37 <https://doi.org/10.1007/s10236-003-0036-9>

38 Exbrayat, J.-F., Bloom, A. A., Falloon, P., Ito, A., Smallman, T. L., & Williams, M. (2018).
39 Reliability ensemble averaging of 21st century projections of terrestrial net primary
40 productivity reduces global and regional uncertainties. *Earth System Dynamics*, 9(1),
41 153–165. <https://doi.org/10.5194/esd-9-153-2018>

42 Exbrayat, J.-F., Pitman, A. J., & Abramowitz, G. (2014). Response of microbial decomposition to
43 spin-up explains CMIP5 soil carbon range until 2100. *Geoscientific Model Development*,
44 7(6), 2683–2692. <https://doi.org/10.5194/gmd-7-2683-2014>

1 Exbrayat, J.-F., Smallman, T. L., Bloom, A. A., Hutley, L. B., & Williams, M. (2018). Inverse
2 determination of the influence of fire on vegetation carbon turnover in the pantropics. *Global*
3 *Biogeochemical Cycles*, 32(12), 1776–1789. <https://doi.org/10.1029/2018gb005925>

4 Eyring, V., Collins, W. D., Gentine, P., Barnes, E. A., Barreiro, M., Beucler, T., Bocquet, M.,
5 Bretherton, C. S., Christensen, H. M., Dagon, K., Gagne, D. J., Hall, D., Hammerling, D.,
6 Hoyer, S., Iglesias-Suarez, F., Lopez-Gomez, I., McGraw, M. C., Meehl, G. A., Molina, M.
7 J., ... Zanna, L. (2024). Pushing the frontiers in climate modelling and analysis with
8 machine learning. *Nature Climate Change*, 14(9), 916–928.
9 <https://doi.org/10.1038/s41558-024-02095-y>

10 Famiglietti, C. A., Smallman, T. L., Levine, P. A., Flack-Prain, S., Quetin, G. R., Meyer, V.,
11 Parazoo, N. C., Stettz, S. G., Yang, Y., Bonal, D., Bloom, A. A., Williams, M., & Konings, A.
12 G. (2021). Optimal model complexity for terrestrial carbon cycle prediction. *Biogeosciences*
13 , 18(8), 2727–2754. <https://doi.org/10.5194/bg-18-2727-2021>

14 Fang, K., Pan, M., & Shen, C. (2019). The value of SMAP for long-term soil moisture estimation
15 with the help of deep learning. *IEEE Transactions on Geoscience and Remote Sensing: A*
16 *Publication of the IEEE Geoscience and Remote Sensing Society*, 57(4), 2221–2233.
17 <https://doi.org/10.1109/tgrs.2018.2872131>

18 Farchi, A., Chrust, M., Bocquet, M., Laloyaux, P., & Bonavita, M. (2023). Online model error
19 correction with neural networks in the incremental 4D-Var framework. *Journal of Advances*
20 *in Modeling Earth Systems*, 15(9), e2022MS003474.
21 <https://doi.org/10.1029/2022ms003474>

22 Farchi, A., Laloyaux, P., Bonavita, M., & Bocquet, M. (2021). Using machine learning to correct
23 model error in data assimilation and forecast applications. *Quarterly Journal of the Royal*
24 *Meteorological Society. Royal Meteorological Society (Great Britain)*, 147(739), 3067–3084.
25 <https://doi.org/10.1002/qj.4116>

26 Farquhar, G. D., von Caemmerer, S., & Berry, J. A. (1980). A biochemical model of
27 photosynthetic CO₂ assimilation in leaves of C 3 species. *Planta*, 149(1), 78–90.
28 <https://doi.org/10.1007/BF00386231>

29 Fer, I., Gardella, A. K., Shiklomanov, A. N., Campbell, E. E., Cowdery, E. M., De Kauwe, M. G.,
30 Desai, A., Duveneck, M. J., Fisher, J. B., Haynes, K. D., Hoffman, F. M., Johnston, M. R.,
31 Kooper, R., LeBauer, D. S., Mantooth, J., Parton, W. J., Poulter, B., Quaife, T., Raiho, A., ...
32 Dietze, M. C. (2021). Beyond ecosystem modeling: A roadmap to community
33 cyberinfrastructure for ecological data-model integration. *Global Change Biology*, 27(1),
34 13–26. <https://doi.org/10.1111/gcb.15409>

35 Fer, I., Kelly, R., Moorcroft, P. R., Richardson, A. D., Cowdery, E. M., & Dietze, M. C. (2018).
36 Linking big models to big data: efficient ecosystem model calibration through Bayesian
37 model emulation. *Biogeosciences* , 15(19), 5801–5830.
38 <https://doi.org/10.5194/bg-15-5801-2018>

39 Fer, I., Shiklomanov, A., Novick, K. A., Gough, C. M., Altaf Arain, M., Chen, J., Murphy, B.,
40 Desai, A. R., & Dietze, M. C. (2021). Capturing site-to-site variability through Hierarchical
41 Bayesian calibration of a process-based dynamic vegetation model. In *bioRxiv* (p.
42 2021.04.28.441243). <https://doi.org/10.1101/2021.04.28.441243>

43 Finn, T. S., Durand, C., Farchi, A., Bocquet, M., Chen, Y., Carrassi, A., & Dansereau, V. (2023).
44 Deep learning subgrid-scale parametrisations for short-term forecasting of sea-ice

1 dynamics with a Maxwell elasto-brittle rheology. *The Cryosphere*, 17(7), 2965–2991.
2 <https://doi.org/10.5194/tc-17-2965-2023>

3 Fisher, R. A., & Koven, C. D. (2020). Perspectives on the future of land surface models and the
4 challenges of representing complex terrestrial systems. *Journal of Advances in Modeling
Earth Systems*, 12(4). <https://doi.org/10.1029/2018ms001453>

5 Fisher, R. A., Muszala, S., Verteinstein, M., Lawrence, P., Xu, C., McDowell, N. G., Knox, R. G.,
6 Koven, C., Holm, J., Rogers, B. M., Spessa, A., Lawrence, D., & Bonan, G. (2015). Taking
7 off the training wheels: the properties of a dynamic vegetation model without climate
8 envelopes, CLM4.5(ED). *Geoscientific Model Development*, 8(11), 3593–3619.
9 <https://doi.org/10.5194/gmd-8-3593-2015>

10 Fisher, R. A., Wieder, W. R., Sanderson, B. M., Koven, C. D., Oleson, K. W., Xu, C., Fisher, J.
11 B., Shi, M., Walker, A. P., & Lawrence, D. M. (2019). Parametric controls on vegetation
12 responses to biogeochemical forcing in the CLM5. *Journal of Advances in Modeling Earth
13 Systems*, 11(9), 2879–2895. <https://doi.org/10.1029/2019ms001609>

14 Forkel, M., Carvalhais, N., Schaphoff, S., v. Bloh, W., Migliavacca, M., Thurner, M., & Thonicke,
15 K. (2014). Identifying environmental controls on vegetation greenness phenology through
16 model–data integration. *Biogeosciences*, 11(23), 7025–7050.
17 <https://doi.org/10.5194/bg-11-7025-2014>

18 Forkel, M., Drüke, M., Thurner, M., Dorigo, W., Schaphoff, S., Thonicke, K., von Bloh, W., &
19 Carvalhais, N. (2019). Constraining modelled global vegetation dynamics and carbon
20 turnover using multiple satellite observations. *Scientific Reports*, 9(1), 18757.
21 <https://doi.org/10.1038/s41598-019-55187-7>

22 Fox, A., Williams, M., Richardson, A. D., Cameron, D., Gove, J. H., Quaife, T., Ricciuto, D.,
23 Reichstein, M., Tomelleri, E., Trudinger, C. M., & Van Wijk, M. T. (2009). The REFLEX
24 project: Comparing different algorithms and implementations for the inversion of a terrestrial
25 ecosystem model against eddy covariance data. *Agricultural and Forest Meteorology*,
26 149(10), 1597–1615. <https://doi.org/10.1016/j.agrformet.2009.05.002>

27 Friedlingstein, P., O’Sullivan, M., Jones, M. W., Andrew, R. M., Bakker, D. C. E., Hauck, J.,
28 Landschützer, P., Le Quéré, C., Luijckx, I. T., Peters, G. P., Peters, W., Pongratz, J.,
29 Schwingshackl, C., Sitch, S., Canadell, J. G., Ciais, P., Jackson, R. B., Alin, S. R., Anthoni,
30 P., ... Zheng, B. (2023). Global Carbon Budget 2023. *Earth System Science Data*, 15(12),
31 5301–5369.
32 <https://doi.org/10.5194/essd-15-5301-202310.5194/essd-15-5301-2023-supplement>

33 Garnelo, M., Schwarz, J., Rosenbaum, D., Viola, F., Rezende, D. J., Ali Eslami, S. M., & Teh, Y.
34 W. (2018). Neural Processes. In *arXiv [cs.LG]*. arXiv. <http://arxiv.org/abs/1807.01622>

35 Geer, A. J. (2021). Learning earth system models from observations: machine learning or data
36 assimilation? *Philosophical Transactions. Series A, Mathematical, Physical, and
37 Engineering Sciences*, 379(2194), 20200089. <https://doi.org/10.1098/rsta.2020.0089>

38 Gelbrecht, M., White, A., Bathiany, S., & Boers, N. (2023). Differentiable programming for Earth
39 system modeling. *Geoscientific Model Development*, 16(11), 3123–3135.
40 <https://doi.org/10.5194/gmd-16-3123-2023>

41 Gentine, P., & Alejomahmad, S. H. (2018). Reconstructed solar-induced fluorescence: A
42 machine learning vegetation product based on MODIS surface reflectance to reproduce
43 GOME-2 solar-induced fluorescence. *Geophysical Research Letters*, 45(7), 3136–3146.

1 <https://doi.org/10.1002/2017GL076294>

2 Gentine, P., Pritchard, M., Rasp, S., Reinaudi, G., & Yacalis, G. (2018). Could machine learning
3 break the convection parameterization deadlock? *Geophysical Research Letters*, 45(11),
4 5742–5751. <https://doi.org/10.1029/2018gl078202>

5 Gier, B. K., Schlund, M., Friedlingstein, P., Jones, C. D., Jones, C., Zaehle, S., & Eyring, V.
6 (2024). Representation of the terrestrial carbon cycle in CMIP6. In *arXiv [physics.ao-ph]*.
7 arXiv. <https://doi.org/10.5194/egusphere-2024-277>

8 Giering, R. (2010). *Transformation of algorithms in Fortran Version 1.15 (TAF Version 1.9. 70)*.

9 Goldberg, D. E., & Holland, J. H. (1988). Genetic Algorithms and Machine Learning. *Machine
Learning*, 3(2/3), 95–99. <https://doi.org/10.1023/a:1022602019183>

10 Green, J. K., Seneviratne, S. I., Berg, A. M., Findell, K. L., Hagemann, S., Lawrence, D. M., &
11 Gentine, P. (2019). Large influence of soil moisture on long-term terrestrial carbon uptake.
12 *Nature*, 565(7740), 476–479. <https://doi.org/10.1038/s41586-018-0848-x>

13 Green, J. K., Zhang, Y., Luo, X., & Keenan, T. F. (2024). Systematic underestimation of canopy
14 conductance sensitivity to drought by Earth System Models. *AGU Advances*, 5(1),
15 e2023AV001026. <https://doi.org/10.1029/2023av001026>

16 Gregory, W., Bushuk, M., Adcroft, A., Zhang, Y., & Zanna, L. (2023). Deep learning of
17 systematic sea ice model errors from data assimilation increments. *Journal of Advances in
Modeling Earth Systems*, 15(10), e2023MS003757. <https://doi.org/10.1029/2023ms003757>

18 Gregory, W., Bushuk, M., Zhang, Y., Adcroft, A., & Zanna, L. (2024). Machine learning for online
19 sea ice bias correction within global ice-ocean simulations. *Geophysical Research Letters*,
20 51(3), e2023GL106776. <https://doi.org/10.1029/2023gl106776>

21 Griewank, A. (1997). *On Automatic Differentiation*.
22 https://www.researchgate.net/publication/2703247_On_Automatic_Differentiation

23 Grinsztajn, L., Oyallon, E., & Varoquaux, G. (2022). Why do tree-based models still outperform
24 deep learning on tabular data? In *arXiv [cs.LG]*. arXiv. <http://arxiv.org/abs/2207.08815>

25 Groenendijk, M., Dolman, A. J., Ammann, C., Arneth, A., Cescatti, A., Dragoni, D., Gash, J. H.
26 C., Gianelle, D., Gioli, B., Kiely, G., Knohl, A., Law, B. E., Lund, M., Marcolla, B., van der
27 Molen, M. K., Montagnani, L., Moors, E., Richardson, A. D., Roupsard, O., ... Wohlfahrt, G.
28 (2011). Seasonal variation of photosynthetic model parameters and leaf area index from
29 global Fluxnet eddy covariance data. *Journal of Geophysical Research: Biogeosciences*,
30 116(G4). <https://doi.org/10.1029/2011JG001742>

31 Guo, Y., Yu, X., Xu, Y.-P., Chen, H., Gu, H., & Xie, J. (2021). AI-based techniques for multi-step
32 streamflow forecasts: application for multi-objective reservoir operation optimization and
33 performance assessment. *Hydrology and Earth System Sciences*, 25(11), 5951–5979.
34 <https://doi.org/10.5194/hess-25-5951-2021>

35 Hararuk, O., Xia, J., & Luo, Y. (2014). Evaluation and improvement of a global land model
36 against soil carbon data using a Bayesian Markov chain Monte Carlo method. *Journal of
37 Geophysical Research. Biogeosciences*, 119(3), 403–417.
38 <https://doi.org/10.1002/2013jg002535>

39 Harden, J. W., Hugelius, G., Ahlström, A., Blankinship, J. C., Bond-Lamberty, B., Lawrence, C.
40 R., Loisel, J., Malhotra, A., Jackson, R. B., Ogle, S., Phillips, C., Ryals, R., Todd-Brown, K.,
41 Vargas, R., Vergara, S. E., Cotrufo, M. F., Keiluweit, M., Heckman, K. A., Crow, S. E., ...
42 Nave, L. E. (2018). Networking our science to characterize the state, vulnerabilities, and

1 management opportunities of soil organic matter. *Global Change Biology*, 24(2),
2 e705–e718. <https://doi.org/10.1111/gcb.13896>

3 Hastings, W. K. (1970). Monte Carlo sampling methods using Markov chains and their
4 applications. *Biometrika*, 57(1), 97–109. <https://doi.org/10.1093/biomet/57.1.97>

5 Hatfield, S., Chantry, M., Dueben, P., Lopez, P., Geer, A., & Palmer, T. (2021). Building
6 tangent-linear and adjoint models for data assimilation with neural networks. *Journal of*
7 *Advances in Modeling Earth Systems*, 13(9). <https://doi.org/10.1029/2021ms002521>

8 Haupt, R. L., & Haupt, S. E. (2004). *Practical genetic algorithms* (2nd ed.) [PDF]. John Wiley &
9 Sons. <https://doi.org/10.1002/0471671746>

10 Heinrich, V. H. A., Dalagnol, R., Cassol, H. L. G., Rosan, T. M., de Almeida, C. T., Silva Junior,
11 C. H. L., Campanharo, W. A., House, J. I., Sitch, S., Hales, T. C., Adami, M., Anderson, L.
12 O., & Aragão, L. E. O. C. (2021). Large carbon sink potential of secondary forests in the
13 Brazilian Amazon to mitigate climate change. *Nature Communications*, 12(1), 1785.
14 <https://doi.org/10.1038/s41467-021-22050-1>

15 Heinrich, V. H. A., Vancutsem, C., Dalagnol, R., Rosan, T. M., Fawcett, D., Silva-Junior, C. H. L.,
16 Cassol, H. L. G., Achard, F., Jucker, T., Silva, C. A., House, J., Sitch, S., Hales, T. C., &
17 Aragão, L. E. O. C. (2023). The carbon sink of secondary and degraded humid tropical
18 forests. *Nature*, 615(7952), 436–442. <https://doi.org/10.1038/s41586-022-05679-w>

19 Hersbach, H., de Rosnay, P., Bell, B., Schepers, D., Simmons, A., Soci, C., Abdalla, S.,
20 Alonso-Balmaseda, M., Balsamo, G., Bechtold, P., Berrisford, P., Bidlot, J.-R., de
21 Boisséson, E., Bonavita, M., Browne, P., Buizza, R., Dahlgren, P., Dee, D., Dragani, R., ...
22 Zuo, H. (2018). Operational global reanalysis: progress, future directions and synergies with
23 NWP | ERA Report Series. *ECMWF*.
24 <https://www.ecmwf.int/en/elibrary/80922-operational-global-reanalysis-progress-future-directions-and-synergies-nwp>

25

26 Hourdin, F., Ferster, B., Deshayes, J., Mignot, J., Musat, I., & Williamson, D. (2023). Toward
27 machine-assisted tuning avoiding the underestimation of uncertainty in climate change
28 projections. *Science Advances*, 9(29), eadf2758. <https://doi.org/10.1126/sciadv.adf2758>

29 Huang, Y., Zhu, D., Ciais, P., Guenet, B., Huang, Y., Goll, D. S., Guimbertea, M., Jornet-Puig,
30 A., Lu, X., & Luo, Y. (2018). Matrix-based sensitivity assessment of soil organic carbon
31 storage: A case study from the ORCHIDEE-MICT model. *Journal of Advances in Modeling*
32 *Earth Systems*, 10(8), 1790–1808. <https://doi.org/10.1029/2017MS001237>

33 Irvine, P. J., Gregoire, L. J., Lunt, D. J., & Valdes, P. J. (2013). An efficient method to generate a
34 perturbed parameter ensemble of a fully coupled AOGCM without flux-adjustment.
35 *Geoscientific Model Development*, 6(5), 1447–1462.
36 <https://doi.org/10.5194/gmd-6-1447-2013>

37 Jeong, J., Barichivich, J., Peylin, P., Haverd, V., McGrath, M. J., Vuichard, N., Evans, M. N.,
38 Babst, F., & Luyssaert, S. (2021). Using the International Tree-Ring Data Bank (ITRDB)
39 records as century-long benchmarks for global land-surface models. *Geoscientific Model*
40 *Development*, 14(9), 5891–5913.
41 <https://doi.org/10.5194/gmd-14-5891-202110.5194/gmd-14-5891-2021-supplement>

42 Jiang, M., Medlyn, B. E., Drake, J. E., Duursma, R. A., Anderson, I. C., Barton, C. V. M., Boer,
43 M. M., Carrillo, Y., Castañeda-Gómez, L., Collins, L., Crous, K. Y., De Kauwe, M. G., Dos
44 Santos, B. M., Emmerson, K. M., Facey, S. L., Gherlenda, A. N., Gimeno, T. E., Hasegawa,

1 S., Johnson, S. N., ... Ellsworth, D. S. (2020). The fate of carbon in a mature forest under
2 carbon dioxide enrichment. *Nature*, 580(7802), 227–231.
3 <https://doi.org/10.1038/s41586-020-2128-9>

4 Jian, J., Vargas, R., Anderson-Teixeira, K., Stell, E., Herrmann, V., Horn, M., Kholod, N.,
5 Manzon, J., Marchesi, R., Paredes, D., & Bond-Lamberty, B. (2021). A restructured and
6 updated global soil respiration database (SRDB-V5). *Earth System Science Data*, 13(2),
7 255–267. <https://doi.org/10.5194/essd-13-255-2021>

8 Joiner, J., Yoshida, Y., Zhang, Y., Duveiller, G., Jung, M., Lyapustin, A., Wang, Y., & Tucker, C. J.
9 (2018). Estimation of Terrestrial Global Gross Primary Production (GPP) with Satellite
10 Data-Driven Models and Eddy Covariance Flux Data. *Remote Sensing*, 10(9), 1346.
11 <https://doi.org/10.3390/rs10091346>

12 Jones, S., Mercado, L. M., Bruhn, D., Raoult, N., & Cox, P. M. (2024). Night-time decline in plant
13 respiration is consistent with substrate depletion. *Communications Earth & Environment*,
14 5(1), 1–9. <https://doi.org/10.1038/s43247-024-01312-y>

15 Jung, M., Reichstein, M., Margolis, H. A., Cescatti, A., Richardson, A. D., Arain, M. A., Arneth,
16 A., Bernhofer, C., Bonal, D., Chen, J., Gianelle, D., Gobron, N., Kiely, G., Kutsch, W.,
17 Lasslop, G., Law, B. E., Lindroth, A., Merbold, L., Montagnani, L., ... Williams, C. (2011).
18 Global patterns of land-atmosphere fluxes of carbon dioxide, latent heat, and sensible heat
19 derived from eddy covariance, satellite, and meteorological observations. *Journal of*
20 *Geophysical Research*, 116(G00J07). <https://doi.org/10.1029/2010jg001566>

21 Jung, M., Schwalm, C., Migliavacca, M., Walther, S., Camps-Valls, G., Koirala, S., Anthoni, P.,
22 Besnard, S., Bodesheim, P., Carvalhais, N., Chevallier, F., Gans, F., Goll, D. S., Haverd, V.,
23 Köhler, P., Ichii, K., Jain, A. K., Liu, J., Lombardozzi, D., ... Reichstein, M. (2020). Scaling
24 carbon fluxes from eddy covariance sites to globe: synthesis and evaluation of the
25 FLUXCOM approach. *Biogeosciences*, 17(5), 1343–1365.
26 <https://doi.org/10.5194/bg-17-1343-2020>

27 Justice, C., Townshend, J., Vermote, E., Masuoka, E., Wolfe, R., Saleous, N., Roy, D., &
28 Morisette, J. (2002). An overview of MODIS Land data processing and product status.
29 *Remote Sensing of Environment*, 83, 3–15. [https://doi.org/10.1016/S0034-4257\(02\)00084-6](https://doi.org/10.1016/S0034-4257(02)00084-6)

30 Kallingal, J. T., Scholze, M., Miller, P. A., Lindström, J., Rinne, J., Aurela, M., Vestin, P., &
31 Weslien, P. (2024). Assimilating multi-site eddy-covariance data to calibrate the CH₄
32 wetland emission module in a terrestrial ecosystem model. In *EGUsphere* (pp. 1–32).
33 <https://doi.org/10.5194/egusphere-2024-373>

34 Kaminski, T., Heimann, M., & Giering, R. (1999). A coarse grid three-dimensional global inverse
35 model of the atmospheric transport: 1. Adjoint model and Jacobian matrix. *Journal of*
36 *Geophysical Research*, 104(D15), 18535–18553. <https://doi.org/10.1029/1999jd900147>

37 Kaminski, T., Knorr, W., Rayner, P., & Heimann, M. (2002). Assimilating atmospheric data into a
38 terrestrial biosphere model: A case study of the seasonal cycle. *Global Biogeochem.*
39 *Cycles*, 16(4), 1066. <https://doi.org/10.1029/2001GB001463>

40 Kaminski, T., Knorr, W., Scholze, M., Gobron, N., Pinty, B., Giering, R., & Mathieu, P.-P. (2012).
41 Consistent assimilation of MERIS FAPAR and atmospheric CO₂ into a terrestrial vegetation
42 model and interactive mission benefit analysis. *Biogeosciences*, 9(8), 3173–3184.
43 <https://doi.org/10.5194/bg-9-3173-2012>

44 Kaminski, T., Knorr, W., Schürmann, G., Scholze, M., Rayner, P. J., Zaehle, S., Blessing, S.,

1 Dorigo, W., Gayler, V., Giering, R., Gobron, N., Grant, J. P., Heimann, M., Hooker-Stroud,
2 A., Houweling, S., Kato, T., Kattge, J., Kelley, D., Kemp, S., ... Ziehn, T. (2013). The
3 BETHY/JSBACH Carbon Cycle Data Assimilation System: experiences and challenges.
4 *Journal of Geophysical Research. Biogeosciences*, 118(4), 1414–1426.
5 <https://doi.org/10.1002/jgrg.20118>

6 Kaminski, T., & Mathieu, P.-P. (2017). Reviews and syntheses: Flying the satellite into your
7 model: on the role of observation operators in constraining models of the Earth system and
8 the carbon cycle. *Biogeosciences*, 14(9), 2343–2357.
9 <https://doi.org/10.5194/bg-14-2343-2017>

10 Kaminski, T., Scholze, M., & Houweling, S. (2010). Quantifying the benefit of A-SCOPE data for
11 reducing uncertainties in terrestrial carbon fluxes in CCDAS. *Tellus. Series B, Chemical and
12 Physical Meteorology*, 62(5), 784–796. <https://doi.org/10.1111/j.1600-0889.2010.00483.x>

13 Kato, T., Knorr, W., Scholze, M., Veenendaal, E., Kaminski, T., Kattge, J., & Gobron, N. (2013).
14 Simultaneous assimilation of satellite and eddy covariance data for improving terrestrial
15 water and carbon simulations at a semi-arid woodland site in Botswana. *Biogeosciences*,
16 10(2), 789–802. <https://doi.org/10.5194/bg-10-789-2013>

17 Kattge, J., Bönisch, G., Díaz, S., Lavorel, S., Prentice, I. C., Leadley, P., Tautenhahn, S.,
18 Werner, G. D. A., Aakala, T., Abedi, M., Acosta, A. T. R., Adamidis, G. C., Adamson, K.,
19 Aiba, M., Albert, C. H., Alcántara, J. M., Alcázar C, C., Aleixo, I., Ali, H., ... Wirth, C. (2020).
20 TRY plant trait database - enhanced coverage and open access. *Global Change Biology*,
21 26(1), 119–188. <https://doi.org/10.1111/gcb.14904>

22 Keenan, T. F., Carbone, M. S., Reichstein, M., & Richardson, A. D. (2011). The model-data
23 fusion pitfall: assuming certainty in an uncertain world. *Oecologia*, 167(3), 587–597.
24 <https://doi.org/10.1007/s00442-011-2106-x>

25 Keenan, T. F., Davidson, E. A., Munger, J. W., & Richardson, A. D. (2013). Rate my data:
26 quantifying the value of ecological data for the development of models of the terrestrial
27 carbon cycle. *Ecological Applications: A Publication of the Ecological Society of America*,
28 23(1), 273–286. <https://doi.org/10.1890/12-0747.1>

29 Keenan, T. F., Davidson, E., Moffat, A. M., Munger, W., & Richardson, A. D. (2012). Using
30 model-data fusion to interpret past trends, and quantify uncertainties in future projections, of
31 terrestrial ecosystem carbon cycling. *Global Change Biology*, 18(8), 2555–2569.
32 <https://doi.org/10.1111/j.1365-2486.2012.02684.x>

33 Kennedy, D., Dagon, K., Lawrence, D. M., Fisher, R. A., Sanderson, B. M., Collier, N., Hoffman,
34 F. M., Koven, C. D., Levis, S., Oleson, K. W., Zariski, C. M., Cheng, Y., Foster, A., Lu, X.,
35 Fowler, M., Hawkins, L., Kavoo, T., Kluzeck, E. B., Kumar, S., ... Luo, Y. (2024).
36 One-at-a-time parameter perturbation ensemble of the community land model, version 5.1.
37 In *ESS Open Archive*. <https://doi.org/10.22541/essar.172745082.24089296/v1>

38 Kennedy, M. C., & O'Hagan, A. (2001). Bayesian Calibration of Computer Models. *Journal of the
39 Royal Statistical Society Series B: Statistical Methodology*, 63(3), 425–464.
40 <https://doi.org/10.1111/1467-9868.00294>

41 Kerschke, P., Hoos, H. H., Neumann, F., & Trautmann, H. (2019). Automated Algorithm
42 Selection: Survey and Perspectives. *Evolutionary Computation*, 27(1), 3–45.
43 https://doi.org/10.1162/evco_a_00242

44 Kloek, T., & Van Dijk, H. K. (1978). Bayesian estimates of equation system parameters: an

1 application of integration by Monte Carlo. *Econometrica: Journal of the Econometric Society*.
2
3 https://www.jstor.org/stable/1913641?casa_token=1EgxpT-njfMAAAAAA:EPHlIE24zFcUOWFrDS_G8r0LMGluWx60_Ft7yeBlx9XViRf0sI27b3uD1MmKewRbJkO2Lcgb7G3kDQS-sQBi1vl tqRAyTEHOyQfEkAYw1W6Dtalc-PGm

6 Knorr, W. (2000). Annual and interannual CO₂ exchanges of the terrestrial biosphere:
7 process-based simulations and uncertainties: CO₂ exchanges of the terrestrial biosphere.
8 *Global Ecology and Biogeography: A Journal of Macroecology*, 9(3), 225–252.
9 <https://doi.org/10.1046/j.1365-2699.2000.00159.x>

10 Knorr, W., & Heimann, M. (1995). Impact of drought stress and other factors on seasonal land
11 biosphere CO₂ exchange studied through an atmospheric tracer transport model. *Tellus. Series B, Chemical and Physical Meteorology*, 47(4), 471–489.
13 <https://doi.org/10.1034/j.1600-0889.47.issue4.7.x>

14 Knorr, W., Kaminski, T., Scholze, M., Gobron, N., Pinty, B., Giering, R., & Mathieu, P.-P. (2010).
15 Carbon cycle data assimilation with a generic phenology model. *Journal of Geophysical Research*, 115(G4). <https://doi.org/10.1029/2009jg001119>

17 Knorr, W., & Kattge, J. (2005). Inversion of terrestrial ecosystem model parameter values
18 against eddy covariance measurements by Monte Carlo sampling. *Global Change Biology*,
19 11(8), 1333–1351. <https://doi.org/10.1111/j.1365-2486.2005.00977.x>

20 Knorr, W., Williams, M., Thum, T., Kaminski, T., Voßbeck, M., Scholze, M., Quaife, T.,
21 Smallmann, L., Steele-Dunne, S., Vreugdenhil, M., Green, T., Zähle, S., Aurela, M., Bouvet,
22 A., Buechi, E., Dorigo, W., El-Madany, T., Migliavacca, M., Honkanen, M., ... Drusch, M.
23 (2024). A comprehensive land surface vegetation model for multi-stream data assimilation,
24 D&B v1.0. In *EGUsphere*. <https://doi.org/10.5194/egusphere-2024-1534>

25 Knutti, R., Stocker, T. F., Joos, F., & Plattner, G.-K. (2003). Probabilistic climate change
26 projections using neural networks. *Climate Dynamics*, 21(3), 257–272.
27 <https://doi.org/10.1007/s00382-003-0345-1>

28 Koffi, E. N., Rayner, P. J., Scholze, M., & Beer, C. (2012). Atmospheric constraints on gross
29 primary productivity and net ecosystem productivity: Results from a carbon-cycle data
30 assimilation system. *Global Biogeochemical Cycles*, 26(1).
31 <https://doi.org/10.1029/2010gb003900>

32 Kolassa, J., Reichle, R. H., Liu, Q., Cosh, M., Bosch, D. D., Caldwell, T. G., Colliander, A.,
33 Collins, C. H., Jackson, T. J., Livingston, S. J., Moghaddam, M., & Starks, P. J. (2017). Data
34 assimilation to extract soil moisture information from SMAP observations. *Remote Sensing*,
35 9(11), 1179. <https://doi.org/10.3390/rs9111179>

36 Koppa, A., Rains, D., Hulsman, P., Poyatos, R., & Miralles, D. G. (2022). A deep learning-based
37 hybrid model of global terrestrial evaporation. *Nature Communications*, 13(1), 1912.
38 <https://doi.org/10.1038/s41467-022-29543-7>

39 Koven, C. D., Arora, V. K., Cadule, P., Fisher, R. A., Jones, C. D., Lawrence, D. M., Lewis, J.,
40 Lindsay, K., Mathesius, S., Meinshausen, M., Mills, M., Nicholls, Z., Sanderson, B. M.,
41 Séférian, R., Swart, N. C., Wieder, W. R., & Zickfeld, K. (2022). Multi-century dynamics of
42 the climate and carbon cycle under both high and net negative emissions scenarios. *Earth
43 System Dynamics*, 13(2), 885–909. <https://doi.org/10.5194/esd-13-885-2022>

44 Koven, C. D., Knox, R. G., Fisher, R. A., Chambers, J. Q., Christoffersen, B. O., Davies, S. J.,

1 Detto, M., Dietze, M. C., Faybushenko, B., Holm, J., Huang, M., Kovenock, M., Kueppers, L.
2 M., Lemieux, G., Massoud, E., McDowell, N. G., Muller-Landau, H. C., Needham, J. F.,
3 Norby, R. J., ... Xu, C. (2020). Benchmarking and parameter sensitivity of physiological and
4 vegetation dynamics using the Functionally Assembled Terrestrial Ecosystem Simulator
5 (FATES) at Barro Colorado Island, Panama. *Biogeosciences*, 17(11), 3017–3044.
6 <https://doi.org/10.5194/bg-17-3017-2020>

7 Kowalczyk, E. A., Wang, Y. P., Law, R. M., Davies, H. L., McGregor, J. L., Abramowitz, G. S.
8 (2006). *The CSIRO Atmosphere Biosphere Land Exchange (CABLE) model for use in*
9 *climate models and as an offline model*. Aspendale, Vic., CSIRO Marine and Atmospheric
10 Research. <https://doi.org/10.4225/08/58615C6A9A51D>

11 Kraft, B., Jung, M., Körner, M., Koirala, S., & Reichstein, M. (2022). Towards hybrid modeling of
12 the global hydrological cycle. *Hydrology and Earth System Sciences*, 26(6), 1579–1614.
13 <https://doi.org/10.5194/hess-26-1579-2022>

14 Krinner, G., Viovy, N., de Noblet-Ducoudré, N., Ogée, J., Polcher, J., Friedlingstein, P., Ciais, P.,
15 Sitch, S., & Prentice, I. C. (2005). A dynamic global vegetation model for studies of the
16 coupled atmosphere-biosphere system: DVGM FOR COUPLED CLIMATE STUDIES.
17 *Global Biogeochemical Cycles*, 19(1). <https://doi.org/10.1029/2003gb002199>

18 Kumar, S., Kolassa, J., Reichle, R., Crow, W., de Lannoy, G., de Rosnay, P., MacBean, N.,
19 Giroto, M., Fox, A., Quaife, T., Draper, C., Forman, B., Balsamo, G., Steele-Dunne, S.,
20 Albergel, C., Bonan, B., Calvet, J.-C., Dong, J., Liddy, H., & Ruston, B. (2022). An agenda
21 for land data assimilation priorities: Realizing the promise of terrestrial water, energy, and
22 vegetation observations from space. *Journal of Advances in Modeling Earth Systems*,
23 14(11). <https://doi.org/10.1029/2022ms003259>

24 Kumar, S. V., Reichle, R. H., Harrison, K. W., Peters-Lidard, C. D., Yatheendradas, S., &
25 Santanello, J. A. (2012). A comparison of methods for a priori bias correction in soil
26 moisture data assimilation: BIAS CORRECTION IN SOIL MOISTURE DATA
27 ASSIMILATION. *Water Resources Research*, 48(3). <https://doi.org/10.1029/2010wr010261>

28 Kuppel, S., Chevallier, F., & Peylin, P. (2013). Quantifying the model structural error in carbon
29 cycle data assimilation systems. *Geoscientific Model Development*, 6(1), 45–55.
30 <https://gmd.copernicus.org/articles/6/45/2013/>

31 Kuppel, S., Peylin, P., Chevallier, F., Bacour, C., Maignan, F., & Richardson, A. D. (2012).
32 Constraining a global ecosystem model with multi-site eddy-covariance data.
33 *Biogeosciences*, 9(10), 3757–3776. <https://doi.org/10.5194/bg-9-3757-2012>

34 Kuppel, S., Peylin, P., Maignan, F., Chevallier, F., Kiely, G., Montagnani, L., & Cescatti, A.
35 (2014). Model–data fusion across ecosystems: From multisite optimizations to global
36 simulations. *Geoscientific Model Development*, 7(6), 2581–2597.
37 <https://gmd.copernicus.org/articles/7/2581/2014/>

38 Kwon, Y., Forman, B. A., Ahmad, J. A., Kumar, S. V., & Yoon, Y. (2019). Exploring the utility of
39 machine learning-based passive microwave brightness temperature data assimilation over
40 terrestrial snow in High Mountain Asia. *Remote Sensing*, 11(19), 2265.
41 <https://doi.org/10.3390/rs11192265>

42 Kyker-Snowman, E., Lombardozzi, D. L., Bonan, G. B., Cheng, S. J., Dukes, J. S., Frey, S. D.,
43 Jacobs, E. M., McNellis, R., Rady, J. M., Smith, N. G., Thomas, R. Q., Wieder, W. R., &
44 Grandy, A. S. (2022). Increasing the spatial and temporal impact of ecological research: A

1 roadmap for integrating a novel terrestrial process into an Earth system model. *Global
2 Change Biology*, 28(2), 665–684. <https://doi.org/10.1111/gcb.15894>

3 Lam, R., Sanchez-Gonzalez, A., Willson, M., Wirnsberger, P., Fortunato, M., Alet, F., Ravuri, S.,
4 Ewalds, T., Eaton-Rosen, Z., Hu, W., Merose, A., Hoyer, S., Holland, G., Vinyals, O., Stott,
5 J., Pritzel, A., Mohamed, S., & Battaglia, P. (2023). Learning skillful medium-range global
6 weather forecasting. *Science*, 382(6677), 1416–1421.
7 <https://doi.org/10.1126/science.adz2336>

8 Lary, D. J., Alavi, A. H., Gandomi, A. H., & Walker, A. L. (2016). Machine learning in
9 geosciences and remote sensing. *Geoscience Frontiers*, 7(1), 3–10.
10 <https://doi.org/10.1016/j.gsf.2015.07.003>

11 Lawrence, C. R., Beem-Miller, J., Hoyt, A. M., Monroe, G., Sierra, C. A., Stoner, S., Heckman,
12 K., Blankinship, J. C., Crow, S. E., McNicol, G., Trumbore, S., Levine, P. A., Vindušková, O.,
13 Todd-Brown, K., Rasmussen, C., Hicks Pries, C. E., Schädel, C., McFarlane, K., Doetterl,
14 S., ... Wagai, R. (2020). An open-source database for the synthesis of soil radiocarbon
15 data: International Soil Radiocarbon Database (ISRaD) version 1.0. *Earth System Science
16 Data*, 12(1), 61–76. <https://doi.org/10.5194/essd-12-61-2020>

17 Lawrence, D. M., Fisher, R. A., Koven, C. D., Oleson, K. W., Swenson, S. C., Bonan, G., Collier,
18 N., Ghimire, B., van Kampenhout, L., Kennedy, D., Kluzek, E., Lawrence, P. J., Li, F., Li, H.,
19 Lombardozzi, D., Riley, W. J., Sacks, W. J., Shi, M., Vertenstein, M., ... Zeng, X. (2019).
20 The community land model version 5: Description of new features, benchmarking, and
21 impact of forcing uncertainty. *Journal of Advances in Modeling Earth Systems*, 11(12),
22 4245–4287. <https://doi.org/10.1029/2018ms001583>

23 LeBauer, D. S., Wang, D., Richter, K. T., Davidson, C. C., & Dietze, M. C. (2013). Facilitating
24 feedbacks between field measurements and ecosystem models. *Ecological Monographs*,
25 83(2), 133–154. <https://doi.org/10.1890/12-0137.1>

26 Li, L., Fang, Y., Zheng, Z., Shi, M., Longo, M., Koven, C. D., Holm, J. A., Fisher, R. A.,
27 McDowell, N. G., Chambers, J., & Leung, L. R. (2023). A machine learning approach
28 targeting parameter estimation for plant functional type coexistence modeling using
29 ELM-FATES (v2.0). *Geoscientific Model Development*, 16(14), 4017–4040.
30 <https://doi.org/10.5194/gmd-16-4017-202310.5194/gmd-16-4017-2023-supplement>

31 Liu, C., Xiao, Q., & Wang, B. (2008). An ensemble-based four-dimensional variational data
32 assimilation scheme. Part I: Technical formulation and preliminary test. *Monthly Weather
33 Review*, 136(9), 3363–3373. <https://doi.org/10.1175/2008mwr2312.1>

34 Liu, M., He, H., Ren, X., Sun, X., Yu, G., Han, S., Wang, H., & Zhou, G. (2015). The effects of
35 constraining variables on parameter optimization in carbon and water flux modeling over
36 different forest ecosystems. *Ecological Modelling*, 303, 30–41.
37 <https://doi.org/10.1016/j.ecolmodel.2015.01.027>

38 Lorenc, A. C. (1981). A global three-dimensional multivariate statistical interpolation scheme.
39 *Monthly Weather Review*, 109(4), 701–721.
40 [https://doi.org/10.1175/1520-0493\(1981\)109<0701:agtdms>2.0.co;2](https://doi.org/10.1175/1520-0493(1981)109<0701:agtdms>2.0.co;2)

41 Lu, D., & Ricciuto, D. (2019). Efficient surrogate modeling methods for large-scale Earth system
42 models based on machine-learning techniques. *Geoscientific Model Development*, 12(5),
43 1791–1807. <https://doi.org/10.5194/gmd-12-1791-2019>

44 Lu, D., Ricciuto, D., Walker, A., Safta, C., & Munger, W. (2017). Bayesian calibration of

1 terrestrial ecosystem models: a study of advanced Markov chain Monte Carlo methods.
2 *Biogeosciences*, 14, 4295–4314. <https://doi.org/10.5194/BG-14-4295-2017>

3 Luo, Y., Huang, Y., Sierra, C. A., Xia, J., Ahlström, A., Chen, Y., Hararuk, O., Hou, E., Jiang, L.,
4 Liao, C., Lu, X., Shi, Z., Smith, B., Tao, F., & Wang, Y.-P. (2022). Matrix approach to land
5 carbon cycle modeling. *Journal of Advances in Modeling Earth Systems*, 14(7).
6 <https://doi.org/10.1029/2022ms003008>

7 Luo, Y., Keenan, T. F., & Smith, M. (2015). Predictability of the terrestrial carbon cycle. *Global
8 Change Biology*, 21(5), 1737–1751. <https://doi.org/10.1111/gcb.12766>

9 Lu, X., Wang, Y.-P., Ziehn, T., & Dai, Y. (2013). An efficient method for global parameter
10 sensitivity analysis and its applications to the Australian community land surface model
11 (CABLE). *Agricultural and Forest Meteorology*, 182-183, 292–303.
12 <https://doi.org/10.1016/j.agrformet.2013.04.003>

13 MacBean, N., Bacour, C., Raoult, N., Bastrikov, V., Koffi, E. N., Kuppel, S., Maignan, F., Ottlé,
14 C., Peaucelle, M., Santaren, D., & Peylin, P. (2022). Quantifying and reducing uncertainty in
15 global carbon cycle predictions: Lessons and perspectives from 15 years of data
16 assimilation studies with the ORCHIDEE terrestrial biosphere model. *Global
17 Biogeochemical Cycles*, 36(7), e2021GB007177. <https://doi.org/10.1029/2021gb007177>

18 MacBean, N., Liddy, H., Quaife, T., Kolassa, J., & Fox, A. (2022). Building a land data
19 assimilation community to tackle technical challenges in quantifying and reducing
20 uncertainty in land model predictions. *Bulletin of the American Meteorological Society*,
21 103(3), E733–E740. <https://doi.org/10.1175/bams-d-21-0228.1>

22 MacBean, N., Maignan, F., Bacour, C., Lewis, P., Peylin, P., Guanter, L., Köhler, P.,
23 Gómez-Dans, J., & Disney, M. (2018). Strong constraint on modelled global carbon uptake
24 using solar-induced chlorophyll fluorescence data. *Scientific Reports*, 8(1), 1973.
25 <https://doi.org/10.1038/s41598-018-20024-w>

26 MacBean, N., Maignan, F., Peylin, P., Bacour, C., Bréon, F.-M., & Ciais, P. (2015). Using satellite
27 data to improve the leaf phenology of a global terrestrial biosphere model. *Biogeosciences* ,
28 12(23), 7185–7208. <https://doi.org/10.5194/bg-12-7185-2015>

29 MacBean, N., Peylin, P., Chevallier, F., Scholze, M., & Schürmann, G. (2016). Consistent
30 assimilation of multiple data streams in a carbon cycle data assimilation system.
31 *Geoscientific Model Development*, 9(10), 3569–3588.
32 <https://doi.org/10.5194/gmd-9-3569-2016>

33 Mahmud, K., Medlyn, B. E., Duursma, R. A., Campany, C., & De Kauwe, M. G. (2018). Inferring
34 the effects of sink strength on plant carbon balance processes from experimental
35 measurements. *Biogeosciences* , 15(13), 4003–4018.
36 <https://doi.org/10.5194/bg-15-4003-2018>

37 Mäkelä, J., Arppe, L., Fritze, H., Heinonsalo, J., Karhu, K., Liski, J., Oinonen, M., Straková, P., &
38 Viskari, T. (2022). Implementation and initial calibration of carbon-13 soil organic matter
39 decomposition in the Yasso model. *Biogeosciences*, 19(17), 4305–4313.
40 <https://doi.org/10.5194/bg-19-4305-2022>

41 Mäkelä, J., Knauer, J., Aurela, M., Black, A., Heimann, M., Kobayashi, H., Lohila, A.,
42 Mammarella, I., Margolis, H., Markkanen, T., Susiluoto, J., Thum, T., Viskari, T., Zaehle, S.,
43 & Aalto, T. (2019). Parameter calibration and stomatal conductance formulation comparison
44 for boreal forests with adaptive population importance sampler in the land surface model

1 JSBACH. *Geoscientific Model Development*, 12(9), 4075–4098.
2 <https://doi.org/10.5194/gmd-12-4075-2019>

3 Ma, L., Hurtt, G., Ott, L., Sahajpal, R., Fisk, J., Lamb, R., & Sullivan. (2022). Global evaluation
4 of the Ecosystem Demography model (ED v3. 0). *Geoscientific Model Development*, 15(5),
5 1971–1994. <https://gmd.copernicus.org/articles/15/1971/2022/>

6 Massoud, E. C., Xu, C., Fisher, R. A., Knox, R. G., Walker, A. P., Serbin, S. P., Christoffersen, B.
7 O., Holm, J. A., Kueppers, L. M., Ricciuto, D. M., Wei, L., Johnson, D. J., Chambers, J. Q.,
8 Koven, C. D., McDowell, N. G., & Vrugt, J. A. (2019). Identification of key parameters
9 controlling demographically structured vegetation dynamics in a land surface model:
10 CLM4.5(FATES). *Geoscientific Model Development*, 12(9), 4133–4164.
11 <https://doi.org/10.5194/gmd-12-4133-2019>

12 Mathers, C., Black, C. K., Segal, B. D., Gurung, R. B., Zhang, Y., Easter, M. J., Williams, S.,
13 Motew, M., Campbell, E. E., Brummitt, C. D., Paustian, K., & Kumar, A. A. (2023). Validating
14 DayCent-CR for cropland soil carbon offset reporting at a national scale. *Geoderma*,
15 438(116647), 116647. <https://doi.org/10.1016/j.geoderma.2023.116647>

16 Mauritsen, T., Bader, J., & Becker, T. (2019). *Developments in the MPI-M Earth System Model
version 1.2 (MPI-ESM1.2) and Its Response to Increasing CO₂*.
17 <https://doi.org/10.1029/2018ms001400>

18 McGovern, A., Elmore, K. L., Gagne, D. J., II, Haupt, S. E., Karstens, C. D., Lagerquist, R.,
19 Smith, T., & Williams, J. K. (2017). Using artificial intelligence to improve real-time
20 decision-making for high-impact weather. *Bulletin of the American Meteorological Society*,
21 98(10), 2073–2090. <https://doi.org/10.1175/bams-d-16-0123.1>

22 McKay, M. D., Beckman, R. J., & Conover, W. J. (1979). A Comparison of Three Methods for
23 Selecting Values of Input Variables in the Analysis of Output from a Computer Code.
24 *Technometrics: A Journal of Statistics for the Physical, Chemical, and Engineering
Sciences*, 21(2), 239–245. <https://doi.org/10.2307/1268522>

25 McNeall, D., Robertson, E., & Wiltshire, A. (2024). Constraining the carbon cycle in
26 JULES-ES-1.0. *Geoscientific Model Development*, 17(3), 1059–1089.
27 <https://doi.org/10.5194/gmd-17-1059-2024>

28 Medvigy, D., Wofsy, S. C., Munger, J. W., Hollinger, D. Y., & Moorcroft, P. R. (2009). Mechanistic
29 scaling of ecosystem function and dynamics in space and time: Ecosystem Demography
30 model version 2. *Journal of Geophysical Research: Biogeosciences*, 114(G1).
31 <https://doi.org/10.1029/2008JG000812>

32 Meirink, J. F., Bergamaschi, P., & Krol, M. C. (2008). Four-dimensional variational data
33 assimilation for inverse modelling of atmospheric methane emissions: method and
34 comparison with synthesis inversion. *Atmospheric Chemistry and Physics*, 8(21),
35 6341–6353. <https://doi.org/10.5194/acp-8-6341-2008>

36 Melton, J. R., Arora, V. K., Wisernig-Cojoc, E., Seiler, C., Fortier, M., Chan, E., & Teckentrup, L.
37 (2020). CLASSIC v1.0: the open-source community successor to the Canadian Land
38 Surface Scheme (CLASS) and the Canadian Terrestrial Ecosystem Model (CTEM) – Part 1:
39 Model framework and site-level performance. *Geoscientific Model Development*, 13(6),
40 2825–2850. <https://doi.org/10.5194/gmd-13-2825-2020>

41 Meunier, F., Visser, M. D., Shiklomanov, A., Dietze, M. C., Guzmán Q, J. A., Sanchez-Azofeifa,
42 G. A., De Deurwaerder, H. P. T., Krishna Moorthy, S. M., Schnitzer, S. A., Marvin, D. C.,

1 Longo, M., Liu, C., Broadbent, E. N., Almeyda Zambrano, A. M., Muller-Landau, H. C.,
2 Detto, M., & Verbeeck, H. (2022). Liana optical traits increase tropical forest albedo and
3 reduce ecosystem productivity. *Global Change Biology*, 28(1), 227–244.
4 <https://doi.org/10.1111/gcb.15928>

5 Meyer, D., Grimmond, S., Dueben, P., Hogan, R., & van Reeuwijk, M. (2022). Machine learning
6 emulation of urban land surface processes. *Journal of Advances in Modeling Earth
7 Systems*, 14(3), e2021MS002744. <https://doi.org/10.1029/2021ms002744>

8 Migliavacca, M., Meroni, M., Busetto, L., Colombo, R., Zenone, T., Matteucci, G., Manca, G., &
9 Seufert, G. (2009). Modeling gross primary production of agro-forestry ecosystems by
10 assimilation of satellite-derived information in a process-based model. *Sensors (Basel,
11 Switzerland)*, 9(2), 922–942. <https://doi.org/10.3390/s90200922>

12 Moorcroft, P. R., Hurtt, G. C., & Pacala, S. W. (2001). A method for scaling vegetation dynamics:
13 the ecosystem demography model (ED). *Ecological Monographs*.
14 [https://doi.org/10.1890/0012-9615\(2001\)071\[0557:AMFSVD\]2.0.CO;2](https://doi.org/10.1890/0012-9615(2001)071[0557:AMFSVD]2.0.CO;2)

15 Moore, D. J. P., Hu, J., Sacks, W. J., Schimel, D. S., & Monson, R. K. (2008). Estimating
16 transpiration and the sensitivity of carbon uptake to water availability in a subalpine forest
17 using a simple ecosystem process model informed by measured net CO₂ and H₂O fluxes.
18 *Agricultural and Forest Meteorology*, 148(10), 1467–1477.
19 <https://doi.org/10.1016/j.agrformet.2008.04.013>

20 Morris, M. D. (1991). Factorial sampling plans for preliminary computational experiments.
21 *Technometrics: A Journal of Statistics for the Physical, Chemical, and Engineering
22 Sciences*, 33(2), 161–174. <https://doi.org/10.1080/00401706.1991.10484804>

23 Nave, L., Johnson, K., van Ingen, C., Agarwal, D., Humphrey, M., & Beekwilder, N. (2016).
24 *International Soil Carbon Network (ISCN) Database v3-1*.
25 <https://doi.org/10.17040/ISCN/1305039>

26 Nelder, J. A., & Mead, R. (1965). A simplex method for function minimization. *The Computer
27 Journal*, 7(4), 308–313. <https://doi.org/10.1093/comjnl/7.4.308>

28 Nelson, J. A., Walther, S., Gans, F., Kraft, B., Weber, U., Novick, K., Buchmann, N., Migliavacca,
29 M., Wohlfahrt, G., Šigut, L., Ibrom, A., Papale, D., Göckede, M., Duveiller, G., Knohl, A.,
30 Hörtnagl, L., Scott, R. L., Zhang, W., Hamdi, Z. M., ... Jung, M. (2024). X-BASE: the first
31 terrestrial carbon and water flux products from an extended data-driven scaling framework,
32 FLUXCOM-X. In *EGUspHERE*. <https://doi.org/10.5194/egusphere-2024-165>

33 Nicolini, G., Castaldi, S., Fratini, G., & Valentini, R. (2013). A literature overview of
34 micrometeorological CH₄ and N₂O flux measurements in terrestrial ecosystems.
35 *Atmospheric Environment (Oxford, England: 1994)*, 81, 311–319.
36 <https://doi.org/10.1016/j.atmosenv.2013.09.030>

37 Norton, A. J., Rayner, P. J., Koffi, E. N., & Scholze, M. (2018). Assimilating solar-induced
38 chlorophyll fluorescence into the terrestrial biosphere model BETHY-SCOPE v1.0: model
39 description and information content. *Geoscientific Model Development*, 11(4), 1517–1536.
40 <https://doi.org/10.5194/gmd-11-1517-2018>

41 Norton, A. J., Rayner, P. J., Koffi, E. N., Scholze, M., Silver, J. D., & Wang, Y.-P. (2019).
42 Estimating global gross primary productivity using chlorophyll fluorescence and a data
43 assimilation system with the BETHY-SCOPE model. *Biogeosciences*, 16(15), 3069–3093.
44 <https://doi.org/10.5194/bg-16-3069-2019>

1 Novick, K. A., Ficklin, D. L., Baldocchi, D., Davis, K. J., Ghezzehei, T. A., Konings, A. G.,
2 MacBean, N., Raoult, N., Scott, R. L., Shi, Y., Sulman, B. N., & Wood, J. D. (2022).
3 Confronting the water potential information gap. *Nature Geoscience*, 15(3), 158–164.
4 <https://doi.org/10.1038/s41561-022-00909-2>

5 Oberpriller, J., Cameron, D. R., Dietze, M. C., & Hartig, F. (2021). Towards robust statistical
6 inference for complex computer models. *Ecology Letters*, 24(6), 1251–1261.
7 <https://doi.org/10.1111/ele.13728>

8 Oberpriller, J., Herschlein, C., Anthoni, P., Arneth, A., Krause, A., Rammig, A., & Hartig. (2022).
9 Climate and parameter sensitivity and induced uncertainties in carbon stock projections for
10 European forests (using LPJ-GUESS 4.0). *Geoscientific Model Development*, 15(16),
11 6495–6519. <https://gmd.copernicus.org/articles/15/6495/2022/>

12 Olivera-Guerra, L.-E., Ottlé, C., Raoult, N., & Peylin, P. (2024). *Assimilating ESA-CCI Land
13 Surface Temperature into the ORCHIDEE Land Surface Model: Insights from a multi-site
14 study across Europe*. <https://doi.org/10.5194/egusphere-2024-546>

15 Owen, A. B. (2013). *Monte Carlo theory, methods and examples*. 16, 19–22.
16 https://scholar.google.com/citations?view_op=view_citation&hl=en&citation_for_view=owV8q1cAAAAJ:tOudhMTPpwUC

18 Parton, W. J., Schimel, D. S., Cole, C. V., & Ojima, D. S. (1987). Analysis of factors controlling
19 soil organic matter levels in Great Plains grasslands. *Soil Science Society of America
20 Journal. Soil Science Society of America*, 51(5), 1173–1179.
21 <https://doi.org/10.2136/sssaj1987.03615995005100050015x>

22 Paszke, A., Gross, S., Massa, F., Lerer, A., Bradbury, J., Chanan, G., Killeen, T., Lin, Z.,
23 Gimelshein, N., Antiga, L., Desmaison, A., Köpf, A., Yang, E., DeVito, Z., Raison, M.,
24 Tejani, A., Chilamkurthy, S., Steiner, B., Fang, L., ... Chintala, S. (2019). PyTorch: An
25 imperative style, high-performance deep learning library. *Neural Information Processing
26 Systems*, *abs/1912.01703*.
27 <https://papers.nips.cc/paper/9015-pytorch-an-imperative-style-high-performance-deep-learn>
28 ing-library

29 Peatier, S., Sanderson, B. M., & Terray, L. (2023). On the spatial calibration of imperfect climate
30 models. In *EGUsphere*. <https://doi.org/10.5194/egusphere-2023-2269>

31 Peylin, P., Bacour, C., MacBean, N., Leonard, S., Rayner, P., Kuppel, S., Koffi, E., Kane, A.,
32 Maignan, F., Chevallier, F., Ciais, P., & Prunet, P. (2016). A new stepwise carbon cycle data
33 assimilation system using multiple data streams to constrain the simulated land surface
34 carbon cycle. *Geoscientific Model Development*, 9(9), 3321–3346.
35 <https://doi.org/10.5194/gmd-9-3321-2016>

36 Pianosi, F., Iwema, J., Rosolem, R., & Wagener, T. (2017). A multimethod global sensitivity
37 analysis approach to support the calibration and evaluation of land surface models. In
38 *Sensitivity Analysis in Earth Observation Modelling* (pp. 125–144). Elsevier.
39 <https://doi.org/10.1016/b978-0-12-803011-0.00007-0>

40 Pinnington, E., Amezcuia, J., Cooper, E., Dadson, S., Ellis, R., Peng, J., Robinson, E., Morrison,
41 R., Osborne, S., & Quaife, T. (2021). Improving soil moisture prediction of a high-resolution
42 land surface model by parameterising pedotransfer functions through assimilation of SMAP
43 satellite data. *Hydrology and Earth System Sciences*, 25(3), 1617–1641.
44 <https://doi.org/10.5194/hess-25-1617-2021>

1 Pinnington, E. M., Casella, E., Dance, S. L., Lawless, A. S., Morison, J. I. L., Nichols, N. K.,
2 Wilkinson, M., & Quaife, T. L. (2017). Understanding the effect of disturbance from selective
3 felling on the carbon dynamics of a managed woodland by combining observations with
4 model predictions. *J. Geophys. Res. Biogeosci.*, 122, 886–902.
5 <https://doi.org/10.1002/2017JG003760>

6 Pinnington, E., Quaife, T., & Black, E. (2018). Impact of remotely sensed soil moisture and
7 precipitation on soil moisture prediction in a data assimilation system with the JULES land
8 surface model. *Hydrology and Earth System Sciences*, 22(4), 2575–2588.
9 <https://hess.copernicus.org/articles/22/2575/2018/>

10 Pinnington, E., Quaife, T., Lawless, A., Williams, K., Arkebauer, T., & Scoby, D. (2020). The
11 Land Variational Ensemble Data Assimilation Framework: LAVENDAR v1.0.0. *Geoscientific
12 Model Development*, 13(1), 55–69. <https://doi.org/10.5194/gmd-13-55-2020>

13 Post, H., Vrugt, J. A., Fox, A., Vereecken, H., & Hendricks Franssen, H.-J. (2017). Estimation of
14 Community Land Model parameters for an improved assessment of net carbon fluxes at
15 European sites: Estimation of CLM Parameters. *Journal of Geophysical Research.
16 Biogeosciences*, 122(3), 661–689. <https://doi.org/10.1002/2015jg003297>

17 Potapov, P., Li, X., Hernandez-Serna, A., Tyukavina, A., Hansen, M. C., Kommareddy, A.,
18 Pickens, A., Turubanova, S., Tang, H., Silva, C. E., Armston, J., Dubayah, R., Blair, J. B., &
19 Hofton, M. (2021). Mapping global forest canopy height through integration of GEDI and
20 Landsat data. *Remote Sensing of Environment*, 253(112165), 112165.
21 <https://doi.org/10.1016/j.rse.2020.112165>

22 Prihodko, L., Denning, A. S., Hanan, N. P., Baker, I., & Davis, K. (2008). Sensitivity, uncertainty
23 and time dependence of parameters in a complex land surface model. *Agricultural and
24 Forest Meteorology*, 148(2), 268–287. <https://doi.org/10.1016/j.agrformet.2007.08.006>

25 Quaife, T., Lewis, P., Dekauwe, M., Williams, M., Law, B., Disney, M., & Bowyer, P. (2008).
26 Assimilating canopy reflectance data into an ecosystem model with an Ensemble Kalman
27 Filter. *Remote Sensing of Environment*, 112(4), 1347–1364.
28 <https://doi.org/10.1016/j.rse.2007.05.020>

29 Quegan, S., Le Toan, T., Chave, J., Dall, J., Exbrayat, J.-F., Minh, D. H. T., Lomas, M.,
30 D'Alessandro, M. M., Paillou, P., Papathanassiou, K., Rocca, F., Saatchi, S., Scipal, K.,
31 Shugart, H., Smallman, T. L., Soja, M. J., Tebaldini, S., Ulander, L., Villard, L., & Williams,
32 M. (2019). The European Space Agency BIOMASS mission: Measuring forest
33 above-ground biomass from space. *Remote Sensing of Environment*, 227, 44–60.
34 <https://doi.org/10.1016/j.rse.2019.03.032>

35 Racza, B., Dietze, M. C., Serbin, S. P., & Davis, K. J. (2018). What limits predictive certainty of
36 long-term carbon uptake? *Journal of Geophysical Research. Biogeosciences*, 123(12),
37 3570–3588. <https://doi.org/10.1029/2018jg004504>

38 Raiho, A. M., Nicklen, E. F., Foster, A. C., Roland, C. A., & Hooten, M. B. (2021). Bridging
39 implementation gaps to connect large ecological datasets and complex models. *Ecology
40 and Evolution*, 11(24), 18271–18287. <https://doi.org/10.1002/ece3.8420>

41 Raoult, N., Beylat, S., Salter, J. M., Hourdin, F., Bastrikov, V., Ottlé, C., & Peylin, P. (2024).
42 Exploring the potential of history matching for land surface model calibration. *Geoscientific
43 Model Development*, 17(15), 5779–5801. <https://doi.org/10.5194/gmd-17-5779-2024>

44 Raoult, N., Charbit, S., Dumas, C., Maignan, F., Ottlé, C., & Bastrikov, V. (2023). Improving

1 modelled albedo over the Greenland ice sheet through parameter optimisation and MODIS
2 snow albedo retrievals. *The Cryosphere*, 17(7), 2705–2724.
3 <https://doi.org/10.5194/tc-17-2705-2023>

4 Raoult, N., Edouard-Rambaut, L.-A., Vuichard, N., Bastrikov, V., Lansø, A. S., Guenet, B., &
5 Peylin, P. (2024). Using Free Air CO₂ Enrichment data to constrain land surface model
6 projections of the terrestrial carbon cycle. *Biogeosciences*, 21(4), 1017–1036.
7 <https://doi.org/10.5194/bg-21-1017-2024>

8 Raoult, N. M., Jupp, T. E., Cox, P. M., & Luke, C. M. (2016). Land-surface parameter
9 optimisation using data assimilation techniques: the adjULES system V1.0. *Geoscientific
10 Model Development*, 9(8), 2833–2852. <https://doi.org/10.5194/gmd-9-2833-2016>

11 Raoult, N., Ottlé, C., Peylin, P., Bastrikov, V., & Maugis, P. (2021). Evaluating and optimizing
12 surface soil moisture drydowns in the ORCHIDEE land surface model at in situ locations.
13 *Journal of Hydrometeorology*, 22(4), 1025–1043. <https://doi.org/10.1175/jhm-d-20-0115.1>

14 Rayner, P. J. (2010). *The current state of carbon-cycle data assimilation*. 2(4), 289–296.
15 https://scholar.google.com/citations?view_op=view_citation&hl=en&citation_for_view=H3up71wAAAAJ:isC4tDSrTZIC

16 Rayner, P. J., Koffi, E., Scholze, M., Kaminski, T., & Dufresne, J.-L. (2011). Constraining
17 predictions of the carbon cycle using data. *Philosophical Transactions. Series A,
18 Mathematical, Physical, and Engineering Sciences*, 369(1943), 1955–1966.
19 <https://doi.org/10.1098/rsta.2010.0378>

20 Rayner, P. J., Michalak, A. M., & Chevallier, F. (2019). Fundamentals of data assimilation
21 applied to biogeochemistry. *Atmospheric Chemistry and Physics*, 19(22), 13911–13932.
22 <https://doi.org/10.5194/acp-19-13911-2019>

23 Rayner, P. J., Scholze, M., Knorr, W., Kaminski, T., Giering, R., & Widmann, H. (2005). Two
24 decades of terrestrial carbon fluxes from a carbon cycle data assimilation system (CCDAS).
25 *Global Biogeochemical Cycles*, 19(2). <https://doi.org/10.1029/2004gb002254>

26 Reichstein, M., Camps-Valls, G., Stevens, B., Jung, M., Denzler, J., Carvalhais, N., & Prabhat.
27 (2019). Deep learning and process understanding for data-driven Earth system science.
28 *Nature*, 566(7743), 195–204. <https://doi.org/10.1038/s41586-019-0912-1>

29 Reick, C. H., Gayler, V., Goll, D., Hagemann, S., & Heidkamp, M. (2021).
30 https://pure.mpg.de/rest/items/item_3279802/component/file_3316522/content

31 Ricciuto, D. M., Butler, M. P., Davis, K. J., Cook, B. D., Bakwin, P. S., Andrews, A., & Teclaw, R.
32 M. (2008). Causes of interannual variability in ecosystem–atmosphere CO₂ exchange in a
33 northern Wisconsin forest using a Bayesian model calibration. *Agricultural and Forest
34 Meteorology*, 148(2), 309–327. <https://doi.org/10.1016/j.agrformet.2007.08.007>

35 Ricciuto, D. M., King, A. W., Dragoni, D., & Post, W. M. (2011). Parameter and prediction
36 uncertainty in an optimized terrestrial carbon cycle model: Effects of constraining variables
37 and data record length. *Journal of Geophysical Research*, 116(G1).
38 <https://doi.org/10.1029/2010jg001400>

39 Rödenbeck, C., Houweling, S., Gloor, M., & Heimann, M. (2003). CO₂ flux history 1982–2001
40 inferred from atmospheric data using a global inversion of atmospheric transport.
41 *Atmospheric Chemistry and Physics*, 3(6), 1919–1964.
42 <https://doi.org/10.5194/acp-3-1919-2003>

43 Rodríguez-Fernández, N., de Rosnay, P., Albergel, C., Richaume, P., Aires, F., Prigent, C., &

1 Kerr, Y. (2019). SMOS neural network Soil Moisture data assimilation in a Land surface
2 model and atmospheric impact. *Remote Sensing*, 11(11), 1334.
3 <https://doi.org/10.3390/rs11111334>

4 Rowland, L., Hill, T. C., Stahl, C., Siebicke, L., Burban, B., Zaragoza-Castells, J., Ponton, S.,
5 Bonal, D., Meir, P., & Williams, M. (2014). Evidence for strong seasonality in the carbon
6 storage and carbon use efficiency of an Amazonian forest. *Global Change Biology*, 20(3),
7 979–991. <https://doi.org/10.1111/gcb.12375>

8 Running, S., Mu, Q., & Zhao, M. (2021). *MODIS/Terra gross primary productivity 8-day L4*
9 *global 500m SIN grid V061* [Dataset]. NASA EOSDIS Land Processes Distributed Active
10 Archive Center. <https://doi.org/10.5067/MODIS/MOD17A2H.061>

11 Sacks, W. J., Schimel, D. S., Monson, R. K., & Braswell, B. H. (2006). Model-data synthesis of
12 diurnal and seasonal CO₂ fluxes at Niwot Ridge, Colorado: MODEL-DATA SYNTHESIS OF
13 CO₂ FLUXES. *Global Change Biology*, 12(2), 240–259.
14 <https://doi.org/10.1111/j.1365-2486.2005.01059.x>

15 Salmon, E., Jégou, F., Guenet, B., Jourdain, L., Qiu, C., Bastrikov, V., Guimbaud, C., Zhu, D.,
16 Ciais, P., Peylin, P., Gogo, S., Laggoun-Défarge, F., Aurela, M., Bret-Harte, M. S., Chen, J.,
17 Chojnicki, B. H., Chu, H., Edgar, C. W., Euskirchen, E. S., ... Ziemblińska, K. (2022).
18 Assessing methane emissions for northern peatlands in ORCHIDEE-PEAT revision 7020.
19 *Geoscientific Model Development*, 15(7), 2813–2838.
20 <https://doi.org/10.5194/gmd-15-2813-2022>

21 Saltelli, A., Ratto, M., Andres, T., Campolongo, F., Cariboni, J., Gatelli, D., Saisana, M., &
22 Tarantola, S. (2008). *Global Sensitivity Analysis: The Primer*. Wiley & Sons, Limited, John.
23 https://openlibrary.org/books/OL33376474M/Global_Sensitivity_Analysis

24 Sanderson, B. (2020). The role of prior assumptions in carbon budget calculations. *Earth*
25 *System Dynamics*, 11(2), 563–577. <https://doi.org/10.5194/esd-11-563-2020>

26 Sanderson, B. M., Knutti, R., Aina, T., Christensen, C., Faull, N., Frame, D. J., Ingram, W. J.,
27 Piani, C., Stainforth, D. A., Stone, D. A., & Allen, M. R. (2008). Constraints on Model
28 Response to Greenhouse Gas Forcing and the Role of Subgrid-Scale Processes. *Journal*
29 *of Climate*, 21(11), 2384–2400. <https://doi.org/10.1175/2008JCLI1869.1>

30 Santaren, D., Peylin, P., Bacour, C., Ciais, P., & Longdoz, B. (2014). Ecosystem model
31 optimization using in situ flux observations: benefit of Monte Carlo versus variational
32 schemes and analyses of the year-to-year model performances. *Biogeosciences*, 11(24),
33 7137–7158. <https://doi.org/10.5194/bg-11-7137-2014>

34 Santaren, D., Peylin, P., Viovy, N., & Ciais, P. (2007). Optimizing a process-based ecosystem
35 model with eddy-covariance flux measurements: A pine forest in southern France. *Global*
36 *Biogeochemical Cycles*, 21(2). <https://doi.org/10.1029/2006GB002834>

37 Sawada, Y. (2020). Machine learning accelerates parameter optimization and uncertainty
38 assessment of a land surface model. *Journal of Geophysical Research*, 125(20).
39 <https://doi.org/10.1029/2020jd032688>

40 Scholze, M., Buchwitz, M., Dorigo, W., Guanter, L., & Quegan, S. (2017). Reviews and
41 syntheses: Systematic Earth observations for use in terrestrial carbon cycle data
42 assimilation systems. *Biogeosciences*, 14(14), 3401–3429.
43 <https://doi.org/10.5194/bg-14-3401-2017>

44 Scholze, M., Kaminski, T., Knorr, W., Blessing, S., Vossbeck, M., Grant, J. P., & Scipal, K.

1 (2016). Simultaneous assimilation of SMOS soil moisture and atmospheric CO₂ in-situ
2 observations to constrain the global terrestrial carbon cycle. *Remote Sensing of*
3 *Environment*, 180, 334–345. <https://doi.org/10.1016/j.rse.2016.02.058>

4 Scholze, M., Kaminski, T., Knorr, W., Voßbeck, M., Wu, M., Ferrazzoli, P., Kerr, Y., Mialon, A.,
5 Richaume, P., Rodríguez-Fernández, N., Vittucci, C., Wigneron, J.-P., Mecklenburg, S., &
6 Drusch, M. (2019). Mean European carbon sink over 2010–2015 estimated by
7 simultaneous assimilation of atmospheric CO₂, soil moisture, and vegetation optical depth.
8 *Geophysical Research Letters*, 46(23), 13796–13803.
9 <https://doi.org/10.1029/2019gl085725>

10 Scholze, M., Kaminski, T., Rayner, P., Knorr, W., & Giering, R. (2007). Propagating uncertainty
11 through prognostic carbon cycle data assimilation system simulations.
12 <https://agupubs.onlinelibrary.wiley.com> › 2007JD008642
13 <https://doi.org/10.1029/2007JD008642>

14 Schürmann, G. J., Kaminski, T., Köstler, C., Carvalhais, N., Voßbeck, M., Kattge, J., Giering, R.,
15 Rödenbeck, C., Heimann, M., & Zaehle, S. (2016). Constraining a land-surface model with
16 multiple observations by application of the MPI-Carbon Cycle Data Assimilation System
17 V1.0. *Geoscientific Model Development*, 9(9), 2999–3026.
18 <https://doi.org/10.5194/gmd-9-2999-2016>

19 Scrucca, L. (2013). GA: A package for genetic algorithms in R. *Journal of Statistical Software*,
20 53(4), 1–37. <https://doi.org/10.18637/jss.v053.i04>

21 Seiler, C., Melton, J. R., Arora, V. K., Sitch, S., Friedlingstein, P., Anthoni, P., Goll, D., Jain, A.
22 K., Joetzjer, E., Lienert, S., Lombardozzi, D., Luyssaert, S., Nabel, J. E. M. S., Tian, H.,
23 Vuichard, N., Walker, A. P., Yuan, W., & Zaehle, S. (2022). Are terrestrial biosphere models
24 fit for simulating the global land carbon sink? *Journal of Advances in Modeling Earth
25 Systems*, 14(5). <https://doi.org/10.1029/2021ms002946>

26 Shan, X., Steele-Dunne, S., Huber, M., Hahn, S., Wagner, W., Bonan, B., Albergel, C., Calvet,
27 J.-C., Ku, O., & Georgievská, S. (2022). Towards constraining soil and vegetation dynamics
28 in land surface models: Modeling ASCAT backscatter incidence-angle dependence with a
29 Deep Neural Network. *Remote Sensing of Environment*, 279(113116), 113116.
30 <https://doi.org/10.1016/j.rse.2022.113116>

31 Shen, C., Appling, A. P., Gentine, P., Bandai, T., Gupta, H., Tartakovsky, A., Baity-Jesi, M.,
32 Fenicia, F., Kifer, D., Li, L., Liu, X., Ren, W., Zheng, Y., Harman, C. J., Clark, M., Farthing,
33 M., Feng, D., Kumar, P., Aboelyazeed, D., ... Lawson, K. (2023). Differentiable modelling to
34 unify machine learning and physical models for geosciences. *Nature Reviews Earth &
35 Environment*, 4(8), 552–567. <https://doi.org/10.1038/s43017-023-00450-9>

36 Shen, H., Wang, Y., Guan, X., Huang, W., Chen, J., Lin, D., & Gan, W. (2022). A spatiotemporal
37 constrained machine learning method for OCO-2 solar-induced chlorophyll fluorescence
38 (SIF) reconstruction. *IEEE Transactions on Geoscience and Remote Sensing: A Publication
39 of the IEEE Geoscience and Remote Sensing Society*, 60, 1–17.
40 <https://doi.org/10.1109/tgrs.2022.3204885>

41 Shiklomanov, A. N., Cowdery, E. M., Bahn, M., Byun, C., Jansen, S., Kramer, K., Minden, V.,
42 Niinemets, Ü., Onoda, Y., Soudzilovskaia, N. A., & Dietze, M. C. (2018). Does the leaf
43 economic spectrum hold within plant functional types? A Bayesian multivariate trait

1 meta-analysis. In *bioRxiv* (p. 475038). bioRxiv. <https://doi.org/10.1101/475038>

2 Shiklomanov, A. N., Dietze, M. C., Fer, I., Viskari, T., & Serbin, S. P. (2021). Cutting out the
3 middleman: calibrating and validating a dynamic vegetation model (ED2-PROSPECT5)
4 using remotely sensed surface reflectance. *Geoscientific Model Development*, 14(5),
5 2603–2633. <https://doi.org/10.5194/gmd-14-2603-2021>

6 Shi, Z., Allison, S. D., He, Y., Levine, P. A., Hoyt, A. M., Beem-Miller, J., Zhu, Q., Wieder, W. R.,
7 Trumbore, S., & Randerson, J. T. (2020). The age distribution of global soil carbon inferred
8 from radiocarbon measurements. *Nature Geoscience*, 13(8), 555–559.
9 <https://doi.org/10.1038/s41561-020-0596-z>

10 Shi, Z., Hoffman, F. M., Xu, M., Mishra, U., Allison, S. D., Zhou, J., & Randerson, J. T. (2024).
11 Global-scale convergence obscures inconsistencies in soil carbon change predicted by
12 Earth system models. *AGU Advances*, 5(2), e2023AV001068.
13 <https://doi.org/10.1029/2023av001068>

14 Schwartz-Ziv, R., & Armon, A. (2022). Tabular data: Deep learning is not all you need. *An*
15 *International Journal on Information Fusion*, 81, 84–90.
16 <https://doi.org/10.1016/j.inffus.2021.11.011>

17 Sitch, S., O'Sullivan, M., Robertson, E., Friedlingstein, P., Albergel, C., Anthoni, P., Arneth, A.,
18 Arora, V. K., Bastos, A., Bastrikov, V., Bellouin, N., Canadell, J. G., Chini, L., Ciais, P., Falk,
19 S., Harris, I., Hurt, G., Ito, A., Jain, A. K., ... Zaehle, S. (2024). Trends and drivers of
20 terrestrial sources and sinks of carbon dioxide: An overview of the TRENDY project. *Global*
21 *Biogeochemical Cycles*, 38(7), e2024GB008102. <https://doi.org/10.1029/2024gb008102>

22 Smallman, T. L., Miodowski, D. T., Neto, E. S., Koren, G., Ometto, J., & Williams, M. (2021).
23 Parameter uncertainty dominates C-cycle forecast errors over most of Brazil for the 21st
24 century. *Earth System Dynamics*, 12(4), 1191–1237.
25 <https://doi.org/10.5194/esd-12-1191-2021>

26 Smith, B. (2007). *LPJ-GUESS – an ecosystem modelling framework*.
27 https://www.baltex-research.eu/baltic2009/downloads/Literature/Specific/Smith_guess_software.pdf

29 Smith, C., Cummins, D. P., Fredriksen, H.-B., Nicholls, Z., Meinshausen, M., Allen, M., Jenkins,
30 S., Leach, N., Mathison, C., & Partanen, A.-I. (2024). fair-calibrate v1.4.1: calibration,
31 constraining and validation of the Fair simple climate model for reliable future climate
32 projections. In *EGUsphere*. <https://doi.org/10.5194/egusphere-2024-708>

33 Sobol', I. M. (2001). Global sensitivity indices for nonlinear mathematical models and their
34 Monte Carlo estimates. *Mathematics and Computers in Simulation*, 55(1-3), 271–280.
35 [https://doi.org/10.1016/s0378-4754\(00\)00270-6](https://doi.org/10.1016/s0378-4754(00)00270-6)

36 Song, H., Triguero, I., & Özcan, E. (2019). A review on the self and dual interactions between
37 machine learning and optimisation. *Progress in Artificial Intelligence*, 8(2), 143–165.
38 <https://doi.org/10.1007/s13748-019-00185-z>

39 Speich, M., Dormann, C. F., & Hartig, F. (2021). Sequential Monte-Carlo algorithms for Bayesian
40 model calibration – A review and method comparison. *Ecological Modelling*,
41 455(109608), 109608. <https://doi.org/10.1016/j.ecolmodel.2021.109608>

42 Stewart, L. M., Dance, S. L., & Nichols, N. K. (2008). Correlated observation errors in data
43 assimilation. *International Journal for Numerical Methods in Fluids*, 56(8), 1521–1527.
44 <https://doi.org/10.1002/fld.1636>

1 Stöckli, R., Rutishauser, T., Dragoni, D., O'Keefe, J., Thornton, P. E., Jolly, M., Lu, L., &
2 Denning, A. S. (2008). Remote sensing data assimilation for a prognostic phenology model:
3 DATA ASSIMILATION AND PHENOLOGY MODELING. *Journal of Geophysical Research*,
4 113(G4). <https://doi.org/10.1029/2008jg000781>

5 Sun, Y., Goll, D. S., Huang, Y., Ciais, P., Wang, Y.-P., Bastrikov, V., & Wang, Y. (2023). Machine
6 learning for accelerating process-based computation of land biogeochemical cycles. *Global
7 Change Biology*, 29(11), 3221–3234. <https://doi.org/10.1111/gcb.16623>

8 Talagrand, O., & Courtier, P. (1987). Variational assimilation of meteorological observations with
9 the adjoint vorticity equation. I: Theory: Variational assimilation. I: Theory. *Quarterly Journal
10 of the Royal Meteorological Society. Royal Meteorological Society (Great Britain)*, 113(478),
11 1311–1328. <https://doi.org/10.1002/qj.49711347812>

12 Tao, F., Houlton, B. Z., Huang, Y., Wang, Y.-P., Manzoni, S., Ahrens, B., Mishra, U., Jiang, L.,
13 Huang, X., & Luo, Y. (2024). Convergence in simulating global soil organic carbon by
14 structurally different models after data assimilation. *Global Change Biology*, 30(5), e17297.
15 <https://doi.org/10.1111/gcb.17297>

16 Tao, F., Zhou, Z., Huang, Y., Li, Q., Lu, X., Ma, S., Huang, X., Liang, Y., Hugelius, G., Jiang, L.,
17 Doughty, R., Ren, Z., & Luo, Y. (2020). Deep learning optimizes data-driven representation
18 of soil organic carbon in Earth system model over the conterminous United States.
19 *Frontiers in Big Data*, 3, 17. <https://doi.org/10.3389/fdata.2020.00017>

20 Tarantola, A. (1987). Inversion of travel times and seismic waveforms. In *Seismic Tomography*
21 (pp. 135–157). Springer Netherlands. https://doi.org/10.1007/978-94-009-3899-1_6

22 Tarantola, A. (2005). Back Matter. In *Inverse Problem Theory and Methods for Model Parameter
23 Estimation* (pp. 317–342). Society for Industrial and Applied Mathematics.
24 <https://doi.org/10.1137/1.9780898717921.bm>

25 Thomas, R. Q., Brooks, E. B., Jersild, A. L., Ward, E. J., Wynne, R. H., Albaugh, T. J.,
26 Dinon-Aldridge, H., Burkhardt, H. E., Domec, J.-C., Fox, T. R., Gonzalez-Benecke, C. A.,
27 Martin, T. A., Noormets, A., Sampson, D. A., & Teskey, R. O. (2017). Leveraging 35 years
28 of *Pinus taeda* research in the southeastern US to constrain forest carbon cycle predictions:
29 regional data assimilation using ecosystem experiments. *Biogeosciences*, 14(14),
30 3525–3547. <https://doi.org/10.5194/bg-14-3525-2017>

31 Thum, T., MacBean, N., Peylin, P., Bacour, C., Santaren, D., Longdoz, B., Loustau, D., & Ciais,
32 P. (2017). The potential benefit of using forest biomass data in addition to carbon and water
33 flux measurements to constrain ecosystem model parameters: Case studies at two
34 temperate forest sites. *Agricultural and Forest Meteorology*, 234-235, 48–65.
35 <https://doi.org/10.1016/j.agrformet.2016.12.004>

36 Tian, X., Minunno, F., Cao, T., Peltoniemi, M., Kalliokoski, T., & Mäkelä, A. (2020). Extending the
37 range of applicability of the semi-empirical ecosystem flux model PRELES for varying forest
38 types and climate. *Global Change Biology*, 26(5), 2923–2943.
39 <https://doi.org/10.1111/gcb.14992>

40 Torres-Rojas, L., Vergopolan, N., Herman, J. D., & Chaney, N. W. (2022). Towards an optimal
41 representation of sub-grid heterogeneity in land surface models. *Water Resources
42 Research*, 58(12). <https://doi.org/10.1029/2022wr032233>

43 Tramontana, G., Jung, M., Schwalm, C. R., Ichii, K., Camps-Valls, G., Ráduly, B., Reichstein,
44 M., Arain, M. A., Cescatti, A., Kiely, G., Merbold, L., Serrano-Ortiz, P., Sickert, S., Wolf, S.,

1 & Papale, D. (2016). Predicting carbon dioxide and energy fluxes across global FLUXNET
2 sites with regression algorithms. *Biogeosciences*, 13(14), 4291–4313.
3 <https://doi.org/10.5194/bg-13-4291-2016>

4 Tramontana, G., Migliavacca, M., Jung, M., Reichstein, M., Keenan, T. F., Camps-Valls, G.,
5 Ogee, J., Verrelst, J., & Papale, D. (2020). Partitioning net carbon dioxide fluxes into
6 photosynthesis and respiration using neural networks. *Global Change Biology*, 26(9),
7 5235–5253. <https://doi.org/10.1111/gcb.15203>

8 Trudinger, C. M., Raupach, M. R., Rayner, P. J., Kattge, J., Liu, Q., Pak, B., Reichstein, M.,
9 Renzullo, L., Richardson, A. D., Roxburgh, S. H., Styles, J., Wang, Y. P., Briggs, P., Barrett,
10 D., & Nikolova, S. (2007). OptIC project: An intercomparison of optimization techniques for
11 parameter estimation in terrestrial biogeochemical models. *Journal of Geophysical
12 Research: Biogeosciences*, 112(G2). <https://doi.org/10.1029/2006JG000367>

13 Trugman, A. T., Anderegg, L. D. L., Shaw, J. D., & Anderegg, W. R. L. (2020). Trait velocities
14 reveal that mortality has driven widespread coordinated shifts in forest hydraulic trait
15 composition. *Proceedings of the National Academy of Sciences of the United States of
16 America*, 117(15), 8532–8538. <https://doi.org/10.1073/pnas.1917521117>

17 Ustin, S. L., & Middleton, E. M. (2021). Current and near-term advances in Earth observation for
18 ecological applications. *Ecological Processes*, 10(1), 1.
19 <https://doi.org/10.1186/s13717-020-00255-4>

20 van Oijen, M. (2017). Bayesian methods for quantifying and reducing uncertainty and error in
21 forest models. *Current Forestry Reports*, 3(4), 269–280.
22 <https://doi.org/10.1007/s40725-017-0069-9>

23 Varney, R. M., Friedlingstein, P., Chadburn, S. E., Burke, E. J., & Cox, P. M. (2024). Soil
24 carbon-concentration and carbon-climate feedbacks in CMIP6 Earth system models.
25 *Biogeosciences*, 21(11), 2759–2776. <https://doi.org/10.5194/bg-21-2759-2024>

26 Vekuri, H., Tuovinen, J.-P., Kulmala, L., Papale, D., Kolari, P., Aurela, M., Laurila, T., Liski, J., &
27 Lohila, A. (2023). A widely-used eddy covariance gap-filling method creates systematic bias
28 in carbon balance estimates. *Scientific Reports*, 13(1), 1720.
29 <https://doi.org/10.1038/s41598-023-28827-2>

30 Verbeeck, H., Peylin, P., Bacour, C., Bonal, D., Steppe, K., & Ciais, P. (2011). Seasonal patterns
31 of CO₂fluxes in Amazon forests: Fusion of eddy covariance data and the ORCHIDEE
32 model. *Journal of Geophysical Research*, 116(G2). <https://doi.org/10.1029/2010jg001544>

33 Vergopolan, N., Chaney, N. W., Beck, H. E., Pan, M., Sheffield, J., Chan, S., & Wood, E. F.
34 (2020). Combining hyper-resolution land surface modeling with SMAP brightness
35 temperatures to obtain 30-m soil moisture estimates. *Remote Sensing of the Environment*,
36 242(111740), 111740. <https://doi.org/10.1016/j.rse.2020.111740>

37 Vergopolan, N., Chaney, N. W., Pan, M., Sheffield, J., Beck, H. E., Ferguson, C. R.,
38 Torres-Rojas, L., Sadri, S., & Wood, E. F. (2021). SMAP-HydroBlocks, a 30-m
39 satellite-based soil moisture dataset for the conterminous US. *Scientific Data*, 8(1), 264.
40 <https://doi.org/10.1038/s41597-021-01050-2>

41 Vrugt, J. A. (2016). Markov chain Monte Carlo simulation using the DREAM software package:
42 Theory, concepts, and MATLAB implementation. *Environmental Modelling & Software: With
43 Environment Data News*, 75, 273–316. <https://doi.org/10.1016/j.envsoft.2015.08.013>

44 Vrugt, J. A., ter Braak, C. J. F., Diks, C. G. H., Robinson, B. A., Hyman, J. M., & Higdon, D.

1 (2009). Accelerating Markov Chain Monte Carlo Simulation by Differential Evolution with
2 Self-Adaptive Randomized Subspace Sampling. *International Journal of Nonlinear*
3 *Sciences and Numerical Simulation*, 10(3). <https://doi.org/10.1515/IJNSNS.2009.10.3.273>

4 Vuichard, N., Messina, P., Luyssaert, S., Guenet, B., Zaehle, S., Ghattas, J., Bastrikov, V., &
5 Peylin, P. (2019). Accounting for carbon and nitrogen interactions in the global terrestrial
6 ecosystem model ORCHIDEE (trunk version, rev 4999): multi-scale evaluation of gross
7 primary production. *Geoscientific Model Development*, 12(11), 4751–4779.
8 <https://doi.org/10.5194/gmd-12-4751-2019>

9 Waller, J. A., Dance, S. L., & Nichols, N. K. (2016). Theoretical insight into diagnosing
10 observation error correlations using observation-minus-background and
11 observation-minus-analysis statistics. *Quarterly Journal of the Royal Meteorological*
12 *Society. Royal Meteorological Society (Great Britain)*, 142(694), 418–431.
13 <https://doi.org/10.1002/qj.2661>

14 Wang, H., Huo, X., Duan, Q., Liu, R., & Luo, S. (2023). Uncertainty quantification for the
15 Noah-MP land surface model: A case study in a grassland and sandy soil region. *Journal of*
16 *Geophysical Research Atmospheres*, 128(20). <https://doi.org/10.1029/2023jd038556>

17 Wang, J., Jiang, F., Wang, H., Qiu, B., Wu, M., He, W., Ju, W., Zhang, Y., Chen, J. M., & Zhou,
18 Y. (2021). Constraining global terrestrial gross primary productivity in a global carbon
19 assimilation system with OCO-2 chlorophyll fluorescence data. *Agricultural and Forest*
20 *Meteorology*, 304-305(108424), 108424. <https://doi.org/10.1016/j.agrformet.2021.108424>

21 Wang, N., Zhang, D., Chang, H., & Li, H. (2020). Deep learning of subsurface flow via
22 theory-guided neural network. *Journal of Hydrology*, 584(124700), 124700.
23 <https://doi.org/10.1016/j.jhydrol.2020.124700>

24 Wang, Y.-P., Leuning, R., Cleugh, H. A., & Coppin, P. A. (2001). Parameter estimation in surface
25 exchange models using nonlinear inversion: how many parameters can we estimate and
26 which measurements are most useful?: NONLINEAR PARAMETER ESTIMATION. *Global*
27 *Change Biology*, 7(5), 495–510. <https://doi.org/10.1046/j.1365-2486.2001.00434.x>

28 Watson-Parris, D. (2021). Machine learning for weather and climate are worlds apart.
29 *Philosophical Transactions. Series A, Mathematical, Physical, and Engineering Sciences*,
30 379(2194), 20200098. <https://doi.org/10.1098/rsta.2020.0098>

31 Watson-Parris, D., Williams, A., Deaconu, L., & Stier, P. (2021). Model calibration using ESEm
32 v1.1.0 – an open, scalable Earth system emulator. *Geoscientific Model Development*,
33 14(12), 7659–7672. <https://doi.org/10.5194/gmd-14-7659-2021>

34 Weng, E., & Luo, Y. (2011). Relative information contributions of model vs. data to short- and
35 long-term forecasts of forest carbon dynamics. *Ecological Applications: A Publication of the*
36 *Ecological Society of America*, 21(5), 1490–1505. <https://doi.org/10.1890/09-1394.1>

37 Weng, E., Luo, Y., Gao, C., & Oren, R. (2011). Uncertainty analysis of forest carbon sink
38 forecast with varying measurement errors: a data assimilation approach. *Journal of Plant*
39 *Ecology*, 4(3), 178–191. <https://doi.org/10.1093/jpe/rtr018>

40 Wesselkamp, M., Chantry, M., Pinnington, E., Choulga, M., Boussetta, S., Kalweit, M.,
41 Boedecker, J., Dormann, C. F., Pappenberger, F., & Balsamo, G. (2024). Advances in Land
42 Surface Model-based Forecasting: A comparative study of LSTM, Gradient Boosting, and
43 Feedforward Neural Network Models as prognostic state emulators. In *arXiv*
44 [*physics.ao-ph*]. arXiv. <http://arxiv.org/abs/2407.16463>

1 Whelan, M. E., Lennartz, S. T., Gimeno, T. E., Wehr, R., Wohlfahrt, G., Wang, Y., Kooijmans, L.
2 M. J., Hilton, T. W., Belviso, S., Peylin, P., Commane, R., Sun, W., Chen, H., Kuai, L.,
3 Mammarella, I., Maseyk, K., Berkelhammer, M., Li, K.-F., Yakir, D., ... Campbell, J. E.
4 (2018). Reviews and syntheses: Carbonyl sulfide as a multi-scale tracer for carbon and
5 water cycles. *Biogeosciences*, 15(12), 3625–3657.
6 <https://doi.org/10.5194/bg-15-3625-2018>

7 Williams, M., Schwarz, P. A., Law, B. E., Irvine, J., & Kurpius, M. R. (2005). An improved
8 analysis of forest carbon dynamics using data assimilation. *Global Change Biology*, 11(1),
9 89–105. <https://doi.org/10.1111/j.1365-2486.2004.00891.x>

10 Williamson, D., Goldstein, M., Allison, L., Blaker, A., Challenor, P., Jackson, L., & Yamazaki, K.
11 (2013). History matching for exploring and reducing climate model parameter space using
12 observations and a large perturbed physics ensemble. *Climate Dynamics*, 41(7),
13 1703–1729. <https://doi.org/10.1007/s00382-013-1896-4>

14 Wu, J.-L., Levine, M. E., Schneider, T., & Stuart, A. (2023). Learning about structural errors in
15 models of complex dynamical systems. In *arXiv [physics.comp-ph]*. arXiv.
16 <http://arxiv.org/abs/2401.00035>

17 Wu, M., Jiang, F., Scholze, M., Chen, D., Ju, W., Wang, S., Kaminski, T., Lu, Z., Vossbeck, M., &
18 Zheng, M. (2024). Regional responses of vegetation productivity to the two phases of
19 ENSO. *Geophysical Research Letters*, 51(8). <https://doi.org/10.1029/2024gl108176>

20 Wu, M., Scholze, M., Kaminski, T., Voßbeck, M., & Tagesson, T. (2020). Using SMOS soil
21 moisture data combining CO₂ flask samples to constrain carbon fluxes during 2010–2015
22 within a Carbon Cycle Data Assimilation System (CCDAS). *Remote Sensing of
23 Environment*, 240(111719), 111719. <https://doi.org/10.1016/j.rse.2020.111719>

24 Wu, M., Scholze, M., Voßbeck, M., Kaminski, T., & Hoffmann, G. (2018). Simultaneous
25 assimilation of remotely sensed Soil Moisture and FAPAR for improving terrestrial carbon
26 fluxes at multiple sites using CCDAS. *Remote Sensing*, 11(1), 27.
27 <https://doi.org/10.3390/rs11010027>

28 Wutzler, T., & Carvalhais, N. (2014). Balancing multiple constraints in model-data integration:
29 Weights and the parameter block approach. *Journal of Geophysical Research: Biogeosciences*, 119(11), 2112–2129. <https://doi.org/10.1002/2014jg002650>

30 Xiao, J., Davis, K. J., Urban, N. M., & Keller, K. (2014). Uncertainty in model parameters and
31 regional carbon fluxes: A model-data fusion approach. *Agricultural and Forest Meteorology*,
32 189–190, 175–186. <https://doi.org/10.1016/j.agrformet.2014.01.022>

33 Xie, K., Liu, P., Zhang, J., Han, D., Wang, G., & Shen, C. (2021). Physics-guided deep learning
34 for rainfall-runoff modeling by considering extreme events and monotonic relationships.
35 *Journal of Hydrology*, 603(127043), 127043. <https://doi.org/10.1016/j.jhydrol.2021.127043>

36 Xu, T., White, L., Hui, D., & Luo, Y. (2006). Probabilistic inversion of a terrestrial ecosystem
37 model: Analysis of uncertainty in parameter estimation and model prediction. *Global
38 Biogeochemical Cycles*, 20(2). <https://doi.org/10.1029/2005GB002468>

39 Yang, T., Sun, F., Gentine, P., Liu, W., Wang, H., Yin, J., Du, M., & Liu, C. (2019). Evaluation and
40 machine learning improvement of global hydrological model-based flood simulations.
41 *Environmental Research Letters*, 14(11), 114027.
42 <https://doi.org/10.1088/1748-9326/ab4d5e>

43 Yatheendradas, S., & Kumar, S. (2022). A novel machine learning-based gap-filling of

1 fine-resolution remotely sensed snow cover fraction data by combining downscaling and
2 regression. *Journal of Hydrometeorology*, 23(5), 637–658.
3 <https://doi.org/10.1175/jhm-d-20-0111.1>

4 Zaehle, S., Friedlingstein, P., & Friend, A. D. (2010). Terrestrial nitrogen feedbacks may
5 accelerate future climate change: CARBON-NITROGEN FEEDBACKS AFFECT CLIMATE.
6 *Geophysical Research Letters*, 37(1). <https://doi.org/10.1029/2009gl041345>

7 Zaehle, S., Friend, A. D., Friedlingstein, P., Dentener, F., Peylin, P., & Schulz, M. (2010). Carbon
8 and nitrogen cycle dynamics in the O-CN land surface model: 2. Role of the nitrogen cycle
9 in the historical terrestrial carbon balance: NITROGEN EFFECTS ON GLOBAL C
10 CYCLING. *Global Biogeochemical Cycles*, 24(1). <https://doi.org/10.1029/2009gb003522>

11 Zeng, H., Elnashar, A., Wu, B., Zhang, M., Zhu, W., Tian, F., & Ma, Z. (2022). A framework for
12 separating natural and anthropogenic contributions to evapotranspiration of
13 human-managed land covers in watersheds based on machine learning. *The Science of the
14 Total Environment*, 823(153726), 153726. <https://doi.org/10.1016/j.scitotenv.2022.153726>

15 Zhang, H., Hendricks Franssen, H.-J., Han, X., Vrugt, J. A., & Vereecken, H. (2017). State and
16 parameter estimation of two land surface models using the ensemble Kalman filter and the
17 particle filter. *Hydrology and Earth System Sciences*, 21(9), 4927–4958.
18 <https://doi.org/10.5194/hess-21-4927-2017>

19 Zhang, J., Chung, H. S.-H., & Lo, W.-L. (2007). Clustering-Based Adaptive Crossover and
20 Mutation Probabilities for Genetic Algorithms. *IEEE Transactions on Evolutionary
21 Computation*, 11(3), 326–335. <https://doi.org/10.1109/TEVC.2006.880727>

22 Zhang, Y., Joiner, J., Alemohammad, S. H., Zhou, S., & Gentine, P. (2018). A global spatially
23 contiguous solar-induced fluorescence (CSIF) dataset using neural networks.
24 *Biogeosciences*, 15(19), 5779–5800.
25 <https://bg.copernicus.org/articles/15/5779/2018/bg-15-5779-2018.html>

26 Zhao, H., & Kowalski, J. (2022). Bayesian active learning for parameter calibration of landslide
27 run-out models. *Landslides*, 19(8), 2033–2045. <https://doi.org/10.1007/s10346-022-01857-z>

28 Zhao, W. L., Gentine, P., Reichstein, M., Zhang, Y., Zhou, S., Wen, Y., Lin, C., Li, X., & Qiu, G. Y.
29 (2019). Physics-constrained machine learning of evapotranspiration. *Geophysical Research
30 Letters*, 46(24), 14496–14507. <https://doi.org/10.1029/2019gl085291>

31 Zhou, A., Hawkins, L., & Gentine, P. (2024). Proof-of-concept: Using ChatGPT to Translate and
32 Modernize an Earth System Model from Fortran to Python/JAX. In *arXiv [cs.DC]*. arXiv.
33 <http://arxiv.org/abs/2405.00018>

34 Zhu, H., Wu, M., Jiang, F., Vossbeck, M., Kaminski, T., Xing, X., Wang, J., Ju, W., & Chen, J. M.
35 (2023). Assimilation of Carbonyl Sulfide (COS) fluxes within the adjoint-based data
36 assimilation system—Nanjing University Carbon Assimilation System (NUCAS v1.0). In
37 *EGUphere* (pp. 1–35). <https://doi.org/10.5194/egusphere-2023-1955>

38 Ziehn, T., Scholze, M., & Knorr, W. (2012). On the capability of Monte Carlo and adjoint
39 inversion techniques to derive posterior parameter uncertainties in terrestrial ecosystem
40 models: COMPARISON OF INVERSION TECHNIQUES. *Global Biogeochemical Cycles*,
41 26(3). <https://doi.org/10.1029/2011gb004185>

42 Zobitz, J. M., Moore, D. J. P., Quaife, T., Braswell, B. H., Bergeson, A., Anthony, J. A., &
43 Monson, R. K. (2014). Joint data assimilation of satellite reflectance and net ecosystem
44 exchange data constrains ecosystem carbon fluxes at a high-elevation subalpine forest.

1 *Agricultural and Forest Meteorology*, 195-196, 73–88.

2 <https://doi.org/10.1016/j.agrformet.2014.04.011>

3 Zuo, H., Balmaseda, M. A., Tietsche, S., Mogensen, K., & Mayer, M. (2019). The ECMWF
4 operational ensemble reanalysis–analysis system for ocean and sea ice: a description of
5 the system and assessment. *Ocean Science*, 15(3), 779–808.

6 <https://doi.org/10.5194/os-15-779-2019>

7

Parameter Estimation in Land Surface Models: Challenges and Opportunities with Data Assimilation and Machine Learning

⁴ Nina Raoult^{1*}, Natalie Douglas², Natasha MacBean³, Jana Kolassa^{4,5}, Tristan Quaife², Andrew G. Roberts⁶, Rosie Fisher⁷, Istem Fer⁸, Cédric Bacour⁹, Katherine Dagon¹⁰, Linnia Hawkins¹¹, Nuno Carvalhais^{12,13,14}, Elizabeth Cooper¹⁵, Michael C. Dietze¹⁶, Pierre Gentine¹¹, Thomas Kaminski¹⁸, Daniel Kennedy¹⁹, Hannah M. Liddy^{20, 21}, David J.P. Moore²², Philippe Peylin⁹, Ewan Pinnington²³, Benjamin Sanderson⁷, Marko Scholze²⁴, Christian Seiler²⁵, T. Luke Smallman²⁶, Noemi Vergopolan²⁷, Toni Viskari²⁸, Mathew Williams²⁶, John Zobitz²⁹

¹⁰

¹¹ ¹Department of Mathematics and Statistics, Faculty of Environment, Science and Economy, University of Exeter, Exeter, UK

¹³ ²National Centre for Earth Observation, Department of Meteorology, University of Reading, Reading, UK

¹⁴ ³Departments of Geography and Environment & Biology, Western University, Canada

¹⁵ ⁴Global Modeling and Assimilation Office, NASA Goddard Space Flight Center, Greenbelt, MD, USA

¹⁶ ⁵Science Systems and Applications, Inc., Lanham, MD, USA

¹⁷ ⁶Computing and Data Sciences, Boston University, Boston, MA 02215 USA

¹⁸ ⁷CICERO, Norway

¹⁹ ⁸Finnish Meteorological Institute, Helsinki, Finland

²⁰ ⁹Laboratoire des Sciences du Climat et de l'Environnement, LSCE/IPSL, CEA-CNRS-UVSQ, Gif-sur-Yvette, France

²¹ ¹⁰NSF National Center for Atmospheric Research, Boulder, CO, USA

²² ¹¹Earth and Environmental Engineering Department, Columbia University, New York, NY 10027, USA

²³ ¹²Max Planck Institute for Biogeochemistry, Hans Knöll Strasse 10, 07745 Jena, Germany;

²⁴ ¹³Departamento de Ciências e Engenharia do Ambiente, DCEA, Faculdade de Ciências e Tecnologia, FCT,

²⁵ Universidade Nova de Lisboa, 2829-516 Caparica, Portugal

²⁶ ¹⁴ELLIS Unit Jena, Jena, Germany

²⁷ ¹⁵UK Centre for Ecology and Hydrology, Wallingford, UK

²⁸ ¹⁶Department of Earth & Environment, Boston University, Boston, MA 02215 USA

²⁹ ¹⁷Earth and Environmental Engineering Department, Columbia University, New York, NY 10027, USA

³⁰ ¹⁸The Inversion Lab, Hamburg, Germany

³¹ ¹⁹NSF National Center for Atmospheric Research, Boulder, CO, USA

³² ²⁰Columbia Climate School, Columbia University, New York, NY, USA

³³ ²¹NASA Goddard Institute for Space Studies, New York, NY, USA.

³⁴ ²²School of Natural Resources and the Environment, University of Arizona, Tucson, AZ, 85721, USA

³⁵ ²³European Centre for Medium-Range Weather Forecasts, Shinfield Park, Reading, UK

³⁶ ²⁴Department of Physical Geography and Ecosystem Science, Lund University, Lund, Sweden

³⁷ ²⁵School of Environmental Studies, Queen's University, Kingston, ON, K7L3N6, Canada

³⁸ ²⁶School of GeoSciences and National Centre for Earth Observation, University of Edinburgh, Edinburgh, EH9 3FF

³⁹ ²⁷Earth Environment and Planetary Sciences, Rice University, Houston, TX 77006, USA

⁴⁰ ²⁸European Commission Joint Research Center, Ispra, 21027 VA, Italy

⁴¹ ²⁹Department of Mathematics, Statistics, and Computer Science, Augsburg University, Minneapolis, MN 55454 USA

⁴² *now at European Centre for Medium-Range Weather Forecasts, Shinfield Park, Reading, UK

1 Key points (max 140 characters each)

- 2 • Data assimilation has been shown to be a powerful tool for reducing land surface model
- 3 parametric uncertainty.
- 4 • Machine learning can facilitate parameter estimation by enhancing computational
- 5 efficiency and replacing poorly represented processes.
- 6 • Collaboration is key to advancing land surface model calibration and data assimilation,
- 7 promoting knowledge exchange and standard methods.

8 Abstract (max 250 words)

9 Accurately predicting terrestrial ecosystem responses to climate change is crucial for
10 addressing global challenges. This relies on mechanistic modelling of ecosystem processes
11 through Land Surface Models (LSMs). Despite their importance, LSMs face significant
12 uncertainties due to poorly constrained parameters, especially in carbon cycle predictions. This
13 paper reviews the progress made in using data assimilation (DA) for LSM parameter
14 optimisation, focusing on carbon-water-vegetation interactions, as well as discussing the
15 technical challenges faced by the community. These challenges include identifying sensitive
16 model parameters and their prior distributions, characterising errors due to observation biases
17 and model-data inconsistencies, developing observation operators to interface between the
18 model and the observations, tackling spatial and temporal heterogeneity as well as dealing with
19 large and multiple datasets, and including the spin-up and historical period in the assimilation
20 window. We then outline how machine learning (ML) can help address these issues, proposing
21 different avenues for future work that integrate ML and DA to reduce uncertainties in LSMs. We
22 conclude by highlighting future priorities, including the need for international collaborations, to
23 fully leverage the wealth of available Earth observation datasets, harness machine learning
24 advances, and enhance the predictive capabilities of LSMs.

25 Plain language summary (max 200 words)

26 Improving the accuracy of land surface models (LSMs) is crucial for reducing uncertainties in
27 climate change projections. Parameter data assimilation, which fine-tunes model parameters to
28 better match observed data, is key to enhancing LSM performance. However, the complexity of
29 LSMs poses challenges for global optimisation. Advances in computational power, novel
30 datasets, and machine learning (ML) offer promising solutions to improve these models. ML can
31 streamline the data assimilation process, handling large datasets and reducing computational
32 demands. This article discusses the progress made in LSM parameter estimation and the
33 challenges faced by the community. We then discuss how machine learning can help address
34 these challenges and outline future priorities. International collaboration, fostered by initiatives
35 like the Analysis, Integration and Modeling of the Earth System Land Data Assimilation Working
36 Group and the International Land Model Forum, is essential for accelerating progress,
37 facilitating knowledge exchange, and developing standardised methods for more accurate
38 climate modelling.

¹ 1. Introduction and premise

² Our world faces unprecedented climate change, water scarcity, and food security challenges. To
³ tackle these issues effectively, we need to predict the responses of terrestrial ecosystem
⁴ dynamics to future global change. This strongly relies on our ability to accurately model the
⁵ underlying processes at the global scale. Such global-scale, mechanistic or process-based
⁶ models of the terrestrial biosphere, often embedded in Earth system models (wherein they are
⁷ called Land Surface Models – LSMs; Blyth et al., 2021), mathematically represent complex
⁸ interacting ecosystem vegetation, carbon, water and energy cycling processes over half-hourly
⁹ to centennial time scales. Thus, for a given atmospheric CO₂ or anthropogenic emissions
¹⁰ scenario (including emissions from land use change), LSMs are used to predict the response of
¹¹ terrestrial ecosystems to climate change, rising CO₂ and land use change, and the resultant
¹² feedbacks to climate. LSMs are also indispensable tools in assessing climate change mitigation
¹³ strategies, for example, to assess how effective nature-based solutions such as reforestation
¹⁴ will be in curbing rising CO₂ emissions.

¹⁵

¹⁶ Representing all the requisite processes corresponding to interacting vegetation,
¹⁷ biogeochemistry, water and energy cycles mechanistically (and accurately) in LSMs over a wide
¹⁸ range of timescales, from sub-daily flux exchanges with the atmosphere to decadal-century
¹⁹ timescales representative of changes in biomass and soil carbon pools required for
²⁰ carbon-climate feedbacks, is critical for robust and reliable projections (Watson-Parris, 2021).
²¹ However, LSMs are highly complex and subject to large uncertainties, both in terms of missing
²² processes, inadequate representation of processes, and poorly constrained parameters.
²³ Furthermore, when trying to address model structural uncertainty, implementing new processes
²⁴ tends to introduce additional parameters and, therefore, more parameter uncertainty. As a
²⁵ result, LSMs often diverge significantly in their representation of many terrestrial processes
²⁶ (Gier et al., 2024; Green et al., 2024; Varney et al., 2024). Consequently, their predictions of
²⁷ important ecosystem responses under future climate change scenarios often vary widely. For
²⁸ example, LSMs disagree on the magnitude of the land carbon sink (Koven et al., 2022; Shi et
²⁹ al., 2024), and the potential constraints on CO₂ fertilisation due to water (Green et al., 2019) and
³⁰ nutrient (Davies-Barnard et al., 2022) limitations.

³¹

³² Parametric uncertainty is one of the largest sources of uncertainty in all types of land models (simple,
³³ intermediate and full complexity models), particularly for predictions of carbon cycling,
³⁴ vegetation dynamics and climate-carbon cycle feedbacks (Booth et al., 2012; Dietze, 2017;
³⁵ Fisher et al., 2019; Smallman et al., 2021). Indeed, it has been shown for one LSM that even
³⁶ perturbing a single carbon flux related parameter within its range of uncertainty can result in a
³⁷ projection spread in atmospheric CO₂ by 2100 that is larger than running the model under
³⁸ different emissions scenarios (Booth et al., 2012). We urgently need to reduce this uncertainty
³⁹ to ensure we can utilise the full potential of LSMs—parameter optimisation is one way to
⁴⁰ achieve this.

⁴¹

⁴² Many processes in LSMs (as well as processes in ecosystem models, see Table A1 for all
⁴³ process-based models mentioned in the paper) are controlled by parameters that represent the

1 functioning of individual elements of the system. While some of these parameters can be
2 directly observed (e.g. photosynthetic capacity, wood density, rooting depth, hydraulic and
3 thermal properties of snow and soil, bark thickness, tissue nutrient stoichiometry), many
4 parameters either cannot be easily measured (e.g., rooting depth) or are essentially only
5 “effective” parameters in that they have no physical meaning. Even those parameters that can
6 be directly measured can often only be observed at scales that differ from the grid resolution of
7 most global-scale LSM simulations (typically 0.5 degrees or greater). As a result, LSM
8 predictions – particularly for vegetation and carbon cycle related processes – can be highly
9 sensitive to parameter choices (in addition to model parameterisation or structural uncertainties)
10 (Booth et al., 2012; Buotte et al., 2021; Exbrayat et al., 2014; Fisher et al., 2019; Oberpriller et
11 al., 2022; Smallman et al., 2021; Zaehle, Friedlingstein, et al., 2010).

12

13 Historically, LSM parameters have simply been manually tuned (adjusted by hand to produce
14 more realistic model behaviour or to better fit a given important model variable to a given
15 dataset). Manual tuning of LSM parameters was often the only option given the required rapid
16 pace of LSM development, the lack of available data at the correct scales for LSM parameter
17 optimisation, or the computational demand of optimising the large number of parameters
18 (typically >200) in LSMs with many complex, interacting processes. However, in the last two
19 decades, the hurdles associated with performing rigorous LSM parameter optimisation (as
20 opposed to tuning) have diminished to the point that it has become feasible: many datasets
21 have become available at LSM-relevant scales, and the computational cost of running LSMs
22 has decreased (although it remains a challenge – see Sect. 3). LSM groups have therefore
23 started to optimise a selection of parameters using statistically robust data assimilation (DA)
24 methods.

25

26 DA methods are powerful as they allow observational data to be combined with numerical
27 methods to optimise estimates of chosen variables at the time of observations, either to update
28 the state (state estimation) or to optimise internal parameters (parameter estimation) while
29 accounting for uncertainties in both the model and the data (Rayner et al., 2019). However, the
30 distinct requirements of LSMs compared to the atmospheric and ocean components of ESMs
31 result in subtle but important differences in how DA techniques are applied. The atmospheric
32 and ocean components of ESMs rely on fluid dynamic models, where the underlying
33 fundamental laws are relatively well understood, even if complex to simulate, and many of the
34 model parameters are known physical quantities that can be observed. Therefore, DA activities
35 using atmospheric or ocean components of ESMs have thus far been heavily focused on
36 numerical weather forecasting (NWP) and reanalysis applications, for which estimating and
37 correcting the optimal model state at each time step is the primary goal (de Rosnay et al., 2022;
38 Hersbach et al., 2018; Zuo et al., 2019). In LSMs, however, parametric and structural
39 uncertainties dominate their spread (Bonan & Doney, 2018; Draper, 2021; Luo et al., 2015).
40 LSM parameters are often linked to biological processes and organismal traits and are
41 dependent on plant functional type (PFT). Therefore, these parameters have a wide range of
42 possible values where they have been measured (in addition to a lack of data on parameters for
43 some PFTs and the role of “effective” parameters as discussed above). Characterising and

1 simplifying the diversity of life into relatively few parameters is thus a challenge faced in LSM
2 development that is less of an issue for atmospheric and ocean modeling.

3 Early efforts in global model calibration in the 1990s and 2000s focused on optimising
4 vegetation and carbon cycle parameters of simplified or intermediate complexity land, carbon, or
5 ecosystem models. These studies, such as Knorr & Heimann's (1995) work optimising
6 parameters of the Simple Diagnostic Biosphere Model (SDBM) using site CO₂ measurements,
7 laid the groundwork for DA-focused land model parameter optimisation. Knorr & Heimann's
8 (1995) study was followed by further studies constrain carbon flux related processes in simple
9 and intermediate complexity ecosystem models like BETHY (Rayner et al., 2005; Scholze et al.,
10 2007), using frameworks referred to carbon cycle data assimilation systems (CCDASs). Parallel
11 to this, there was significant progress in using local eddy-covariance flux tower measurements
12 to optimise parameters related to photosynthesis, respiration, and energy flux in ecosystem
13 models at the site level (e.g., Moore et al., 2008; Sacks et al., 2006; Y.-P. Wang et al., 2001;
14 Williams et al., 2005). Two key intercomparison projects, OptIC and REFLEX, played a pivotal
15 role in assessing various data assimilation techniques for parameter estimation in simple and
16 intermediate complexity land, carbon cycle or ecosystem models (Fox et al., 2009; Trudinger et
17 al., 2007).

18 Parameter optimisation of computational expensive land models using DA started in the late
19 2000s (Medvigy et al., 2009; Rayner, 2010; Santaren et al., 2007). These studies used similar
20 data (*in situ* fluxes and biomass) and similar experimental configurations (site scale
21 optimisations) as past studies with simple and intermediate complexity models but often with
22 different DA methods due to the increase in computational expense of running much more
23 complex models (Sect. 2). Building on the formative DA work with the SDBM (Kaminski et al.,
24 2002) and BETHY models (Rayner et al., 2005), other LSM groups also started using global
25 networks of *in situ* atmospheric CO₂ mole concentration data for constraining regional to global
26 scale surface net CO₂ exchange (Kaminski et al., 2013; Peylin et al., 2016; Schürmann et al.,
27 2016). Testing of DA configuration at site scale (data type, sampling interval, record length, and
28 combinations of data - e.g., carbon fluxes and stocks or carbon fluxes) continued with all types
29 of land models (Bastrikov et al., 2018; Bloom et al., 2016; Bloom & Williams, 2015; Braswell et
30 al., 2005; Dietze et al., 2014; Keenan et al., 2013; Medvigy et al., 2009; Moore et al., 2008;
31 Ricciuto et al., 2008, 2011; Santaren et al., 2014; Thum et al., 2017; Weng et al., 2011; Weng &
32 Luo, 2011; Wutzler & Carvalhais, 2014; Xu et al., 2006). One example was the emergence of
33 "multi-site" experiments – parameter estimation studies in which data from multiple sites (often
34 grouped by PFT) were included simultaneously in the assimilation, with the retrieved
35 parameters then compared to those from assimilations with only individual site data (see Sect.
36 3.4 for further discussion). These were initially performed against data from the global
37 FLUXNET network for a range of intermediate and full complexity LSMs, including many LSMs
38 used within ESMs (e.g., Carvalhais et al., 2008, 2010; Groenendijk et al., 2011; Kato et al.,
39 2013; Knorr et al., 2010; Wu et al., 2018; Xiao et al., 2014, ORCHIDEE: Kuppel et al., 2012,
40 2014; JULES: Alton, 2013; Raoult et al., 2016; Noah: Chaney et al., 2016; CLM: Post et al.,
41 2017). With the advent of satellite products, remote sensing indicators of vegetation dynamics
42 (phenology and photosynthetic uptake) began to be employed to constrain model parameters at
43 various spatial scales, including reflectance (Shiklomanov et al., 2021); vegetation indices

1 (Migliavacca et al., 2009; NDVI – MacBean et al., 2015), FAPAR (Bacour et al., 2015; Forkel et
2 al., 2014, 2019; Kaminski et al., 2012; Knorr et al., 2010; Stöckli et al., 2008; Zobitz et al., 2014),
3 solar-induced fluorescence (SIF; (Bacour et al., 2019; Forkel et al., 2019; Knorr et al., 2024;
4 MacBean et al., 2018; Norton et al., 2018, 2019; J. Wang et al., 2021), aboveground biomass
5 and burned area (Forkel et al., 2019). Over the past decade, parameter estimation has
6 advanced to constrain the terrestrial carbon, water, and energy cycles simultaneously, driven by
7 new remote sensing data on total column-integrated CO_2 fluxes (XCO_2), satellite-derived
8 vegetation optical depth, soil moisture, snow cover, and river flow measurements, which have
9 been successfully integrated, for example, into BETHY (Scholze et al., 2016), the new
10 community D&B model developed by the European Space Agency (ESA)'s Carbon Cluster
11 (Knorr et al., 2024); JULES (Pinnington et al., 2018, 2021), and ORCHIDEE (Raoult et al.,
12 2021). Further details on the history of parameter optimisation in all types of land models are
13 provided in Rayner (2010), Kaminski et al. (2013), Scholze et al. (2017), Rayner et al. (2019),
14 Baatz et al. (2021), and MacBean, Bacour, et al. (2022).

15 While substantial progress in complex LSM parameter optimisation has been made (particularly
16 for constraining parameters of short timescale vegetation dynamics and carbon fluxes, as
17 described above), a number of challenges hindering objective calibration of the full
18 high-dimensional LSM parameter space remain. Despite advances in the use of analytical
19 techniques to dramatically reduce the time for LSM simulations (Luo et al., 2022; Sun et al.,
20 2023), these highly complex models still have computational requirements – even for one global
21 scale simulation – that are too high for efficient multi-site to global DA experiments. This is true
22 even for “offline” simulations (i.e., LSM simulations forced with climate reanalysis data, as
23 opposed to “online” cases when LSMs are run within the whole ESM). High dimensionality and
24 computational cost make it difficult to calibrate LSMs using conventional statistical approaches
25 like Markov Chain Monte Carlo. Methods used with simpler models often fail with LSMs due to
26 their complexity. These challenges have also meant that LSMs currently struggle to fully
27 leverage the large amount of data from ground networks and Earth observation platforms for
28 calibration.

29

30 As an LSM community, thus far, we have no overall strategy for how to proceed towards a
31 system that allows for objective parameter estimation. However, this field is rapidly expanding
32 and we are in a unique position to learn from each other, especially in relation to the technical
33 challenges we face with computational expensive LSM parameter DA. Efforts to build a Land
34 Data Assimilation Community (<https://land-da-community.github.io/>) by the Analysis, Integration
35 and Modeling of the Earth System (AIMES) Land Data Assimilation Working Group (MacBean,
36 Liddy, et al., 2022) and the International Land Model Forum (ILMF –
37 <https://hydro-jules.org/international-land-modeling-forum-ilmf>) have precipitated this sharing of
38 knowledge through online workshops and town halls. Capitalising on this momentum is vital
39 given the importance of this problem. The rapid advancements in machine learning (ML) and
40 the increasing availability of global earth observations and networks of *in situ* data create new
41 opportunities for advancing land/earth system modelling with the help of DA.

42

43 In this paper, we summarise the current state of parameter estimation in land surface modelling,

1 starting with DA methods, before outlining the different challenges and opportunities our
2 community faces. We then highlight how some of these challenges can be potentially addressed
3 by capitalising on emerging ML techniques and increasing computational capabilities. Finally,
4 we propose future priorities for advancing the field given the urgent need for more accurate and
5 precise LSM projections. We focus on the techniques and challenges related to optimising
6 carbon-vegetation-water interactions in full complexity LSMs but also discuss parameter DA and
7 ML methods applied to intermediate complexity land, carbon cycle and ecosystem models.

8

9 This paper complements Kumar et al. (2022) which addresses land surface model data
10 assimilation in the context of state estimation, with a focus on vegetation and hydrology
11 processes. A water cycle-focused perspective, tackling both state and parameter estimation, is
12 offered by De Lannoy et al. (2022).

13 2. Data assimilation methods for parameter 14 estimation in land surface models

15

16 LSMs have many parameters that need to be calibrated to accurately reflect the real world
17 (ideally based on observations) and to increase confidence in their future projections. Expert
18 knowledge and empirical measurements of some LSM parameters provide approximate values
19 or their respective ranges. However, due to uncertainties in observations and processes, and
20 the conceptual nature of most parameters, the exact values of LSM parameters are inherently
21 difficult to determine. Instead, we make use of the abundance of observational data indirectly
22 related to the parameters via the processes they are related to, and thus the problem of
23 parameter estimation in LSMs becomes the solution to the inverse problem (Tarantola, 1987,
24 2005): *find the parameter set Θ given the observations y such that $y \approx G(\Theta)$* . In the context of
25 parameter estimation, G includes a mapping from parameters to states and propagates states
26 through time via a forward model as well as an observation operator (Kaminski & Mathieu,
27 2017) that maps states to observation space.

28

29 Typically, a unique solution to the exact inverse problem does not exist and often the logical step
30 is to cast the approximate inverse problem into a loss minimisation effort that locates the
31 argument of a cost function that minimises the discrepancy between y and $G(\Theta)$. However,
32 many techniques of this type only provide point estimates (i.e., a single solution), which have
33 significant limitations when applied to LSM calibration. LSMs are inherently complex, involving
34 many interacting processes, uncertain observations, and non-linear relationships. By focusing
35 only on the best-fit parameters, point estimates ignore the range of plausible values that could
36 explain the data equally well. This can lead to overconfident predictions, underestimating the
37 variability and uncertainty in model outcomes, which is crucial for understanding the full
38 spectrum of possible future climate scenarios. Instead, we want to be able to account for
39 uncertainties in the model, data, and parameters, and reduce the uncertainty in the parameters
40 by creating observationally-constrained posterior distributions.

41

1 Hence, an approach more desirable for its ability to quantify the uncertainty in the estimated
2 parameters and its inherent natural regularisation, is the Bayesian approach. Bayesian methods
3 include information on the prior distribution of the parameters $p(\Theta)$ to define an entire posterior
4 distribution:

5
$$p(\Theta|y) \propto p(y|\Theta)p(\Theta) \quad (1)$$

6 where Θ is regarded as a random variable as opposed to a fixed value to be estimated. In this
7 case, the maximum a posteriori (MAP) estimate - the argument that maximises the posterior
8 distribution (i.e., its mode) - provides a point estimate for Θ and is equivalent to a loss
9 minimisation estimate regularised with prior parameter information under Gaussian
10 assumptions. Under such assumptions, maximising the posterior distribution corresponds to
11 minimising the so-called variational cost function:

12
$$J(\Theta) = \frac{1}{2}[(G(\Theta) - y)^T R^{-1}(G(\Theta) - y) + (\Theta - \Theta_b)^T B^{-1}(\Theta - \Theta_b)], \quad (2)$$

13 where R and B are the model/data and prior error covariance matrix, respectively, and Θ_b are
14 the prior parameter values.

15

16 With the emergence of novel ground and satellite observation sets came the advent and
17 development of techniques to implement them in a field of mathematics originally coined Data
18 Assimilation (DA) (Talagrand & Courtier, 1987). Along with the differences in the aforementioned
19 approaches to solving the inverse problem, these methods also differ in the nature of the
20 temporal assimilation of the available observations. DA methods that assimilate all available
21 observations over a given time window are known as batch (or offline/smoothers) techniques
22 whereas those that incorporate the observations at the time they become available are referred
23 to as sequential (or online/filters). There is some confusion in the community regarding the
24 terminology used when describing DA methods, for example, the false dichotomies sometimes
25 used between “variational and sequential” and “optimisation-based versus Bayesian” - these
26 dichotomies have been marred over time with hybridisation and the continual development of
27 the techniques. Rayner et al. (2019) have made a significant effort to harmonise the notation
28 and clarify overlapping terminology within the community.

29

30 Although DA is primarily used in numerical weather forecasting to correct the model state, in
31 LSMs, DA is often employed to reduce parametric uncertainty, a process referred to as
32 parameter data assimilation (PDA). Techniques used in numerical weather forecasting can be
33 adapted for parameter estimation in LSMs. One of the key methods is 4DVar, which involves
34 minimising Eq. 2 (called 4DVar to contrast with 3DVar, where the observations are instead
35 compared to a single model output at a time). The next part of this section looks a little deeper
36 into methods used to reduce this cost function, as well as outlining alternative DA methods that
37 extract the full posterior distribution.

38

39 **Methods for reducing cost functions:**

40 Methods commonly used to minimise the cost (e.g., Eq. 2) require numerical optimisation due to
41 their complex structure and these can usually be grouped into local gradient-descent or global
42 random search techniques. Although more computationally efficient, gradient-descent methods
43 require the gradient of the cost function (either exact, which requires differentiating the entire
44 LSM - see Sect. 3.7, or approximated when exact is not possible or desirable) and they can

1 result in the location of a local minimum. A common gradient-based minimisation method used
2 in LSM parameter estimation is the quasi-Newton algorithm L-BFGS-B (limited memory
3 Broyden–Fletcher–Goldfarb–Shanno algorithm with bound constraints - Byrd et al., 1995). This
4 approach can leverage exact gradients derived from either the tangent linear (forward sensitivity
5 propagation) or adjoint (backward sensitivity propagation) of the model. These gradients can be
6 obtained by hand or using automatic differentiation software (Gelbrecht et al., 2023; Griewank,
7 1997). While L-BFGS-B is powerful when exact gradients are available, practical
8 challenges—such as the complexity and computational burden of maintaining the tangent
9 linear/adjoint (see Sect. 3.7)—often necessitate alternatives. To address this, approximate
10 gradient methods can be employed. One approach is to estimate gradients using finite
11 difference, calculating the change in model output relative to changes in parameters. This
12 method is especially useful for parameters related to threshold functions, such as those
13 controlling phenology. However, the choice of perturbation size to be applied to each parameter
14 individually is crucial, as inappropriate values can lead to inaccuracies. In cases where gradient
15 information is difficult to obtain or unreliable, derivative-free methods offer a solution. The
16 Nelder-Mead simplex algorithm (Nelder & Mead, 1965), for instance, iteratively adjusts a
17 simplex (geometric shape) in parameter space to converge towards the minimum of a cost
18 function, eliminating the need for direct gradient calculations. Additionally, more advanced
19 approaches, such as the ensemble-based 4DVar (4DEnVar) algorithm proposed by Liu et al.
20 (2008) use an ensemble of model trajectories to approximate gradient information via a control
21 variable transform.

22

23 Alternatively, global search methods can be used to minimise the cost function. These methods
24 use techniques that try to scan the entire parameter space in some defined way to avoid this
25 pitfall but often require heavy computational power to do so. These global search methods can
26 be categorised as Monte Carlo (MC), since they are methods that make use of repeated trials
27 (or sampling) generated using random numbers (Owen, 2013). An example of such a method is
28 the genetic algorithm (Goldberg & Holland, 1988; Haupt & Haupt, 2004), which is based on the
29 laws of natural selection and belongs to the class of evolutionary algorithms.

30

31 Although these gradient-descent and global search methods are very efficient in finding an
32 optimal point-estimate of the parameters that minimise the given cost function, usually they do
33 not directly offer information about the posterior error statistics. Nevertheless, it is possible to
34 exploit information about the curvature of the cost function (via the Hessian) at the optimum to
35 obtain such information, but this is typically more complicated than deriving gradient information
36 and more costly in the case of global search.

37

38 **Methods to extract the full posterior distribution:**

39 In contrast to methods that obtain point-estimates for the parameters, other approaches aim to
40 extract useful information from the full posterior distribution $P(\Theta|y)$, usually at a much higher
41 computational expense and tend to be applied to computationally inexpensive LSMs, carbon
42 cycle, and ecosystem models. Similarly to global search algorithms for objective function
43 optimisation, as opposed to gradient-descent methods, these techniques are often Monte Carlo
44 in nature and hence also derivative-free (black-box).

1
2 Techniques include importance sampling (Kloek & Van Dijk, 1978), a relatively simple approach
3 that samples random values from the prior and accumulates accepted parameterisations based
4 on importance weights and aims to estimate expectations of interest such as mean, variance,
5 etc. This approach can run into limitations when the problem becomes more complicated (e.g.
6 dimensionality increases or target distribution gets more complex), as demonstrated by Ziehn et
7 al. (2012). When the computational budget permits, Markov Chain Monte Carlo (MCMC;
8 Hastings, 1970) algorithms have emerged as the gold standard for quantifying uncertainty in the
9 solution of Bayesian inverse problems. This class of iterative algorithms seeks to draw samples
10 from the posterior distribution $P(\Theta|y)$, which can in turn be used to estimate posterior statistics of
11 interest. The cost of such comprehensive uncertainty quantification is that standard MCMC
12 algorithms often require a large number ($> 10^4$ – 10^7) of iterations that build on previously
13 accepted values and so must be performed serially (i.e., not taking advantage of parallel
14 high-performance computing). This essentially means that the full LSM must be run using a new
15 parameter vector during each iteration, and while it is possible to run different
16 information-sharing chains in parallel to accelerate sampling around a global optimum (Vrugt,
17 2016), within chain iterative model evaluations still precludes parallelisation.

18
19 Particle filters provide an alternative to MCMC for sampling from the posterior distribution,
20 particularly in time-evolving systems. They represent the posterior using a set of particles,
21 updating them with each new data point. While computationally intensive and prone to particle
22 degeneracy, particle filters are useful for real-time tracking of system states and time-varying
23 parameters. However, many of the parameters in land surface models are linked to biological
24 processes and thus are subject to change over time due to acclimation, phenotypic plasticity,
25 adaptation and evolution. While some attempts have been made to explore the seasonal
26 variability in parameters (Rowland et al., 2014; Verbeeck et al., 2011), the majority of the
27 literature in land model parameter estimation so far operates on the assumption that parameters
28 are fixed in time. As such, particle filters are rarely used in PDA (Speich et al., 2021) (unless
29 part of joint state-parameter DA, for example, Zhang et al., 2017).

30

31 Applications in LSMs:

32 Due to the high number of required model evaluations, MCMC methods have primarily been
33 applied to computationally inexpensive land, carbon cycle, and ecosystem models, or to
34 calibrate isolated processes such as fitting parameters of a two-pool model of substrate
35 dependence in plant respiration (Jones et al., 2024) or parameters of the wetlands CH4
36 emissions module in the second generation dynamic global vegetation model LPJ-GUESS
37 (Kallingal et al., 2024). For example, MCMC methods have been used to estimate parameters
38 of the Simplified PnET (SIPNET) ecosystem model (Fer et al., 2018; M. Liu et al., 2015; Sacks
39 et al., 2006), TECOS (Xu et al., 2006), FöBAAR forest carbon cycle model (Keenan et al.,
40 2012), BETHY (Knorr & Kattge, 2005) and the DALEC suite of intermediate complexity
41 ecosystem models (Famiglietti et al., 2021; Keenan et al., 2011; D. Lu et al., 2017). DALEC is
42 also at the heart of the cutting-edge CARbon DAta MOdel fraMework (CARDAMOM) where the
43 full potential of MCMC-based carbon parameter estimation is performed (Bloom et al., 2016;
44 Exbrayat, Smallman, et al., 2018; Smallman et al., 2021).

1
2 While computationally expensive LSMs build on this foundation, their complexity and parameter
3 volume have made MCMC methods computationally prohibitive. Consequently, 4DVar has been
4 the preferred approach for these models. When the tangent linear or adjoint models have been
5 available (e.g., Bacour et al., 2015; Knorr et al., 2024; Kuppel et al., 2012; Raoult et al., 2016;
6 Schürmann et al., 2016), these have been directly used to minimise the cost function and
7 calculate the Hessian. Alternatively, the Nelder-Mead simplex algorithm (Pinnington et al.,
8 2018), finite differences (Bacour et al., 2019; Bastrikov et al., 2018; MacBean et al., 2015) and
9 4DEnVar (Pinnington et al., 2020) have all been used to circumvent the need of such models.
10 While some Monte Carlo approaches have been used to calibrate complex LSM
11 parameters—either for global search methods to minimise the cost function or to extract the full
12 posterior distribution—these are typically applied at the site scale and fall short of full global
13 calibrations. Examples include the adaptive population importance sampler used to calibrate the
14 JSBACH model (Mäkelä et al., 2019), the genetic algorithm used to calibrate ORCHIDEE
15 (Bastrikov et al., 2018), and multichain MCMC method DiffeRential Evolution Adaptive
16 Metropolis (DREAM(zs)) (Vrugt et al., 2009) used with CLM (Post et al., 2017) and LPJ-GUESS
17 (Bagnara et al., 2019).

18 3. Challenges

19 3.1 Selecting parameters and their prior distributions

20 A big challenge in parameter estimation studies is defining the experiment, starting with
21 selecting the parameters to be constrained and the prior distributions over which they are
22 allowed to vary. A common first step is to select from the (potentially quite large) number of
23 model parameters, a subset that is deemed the most influential in some sense. The excluded
24 parameters are then fixed at their nominal values, yielding a parameter space of reduced
25 dimension. This challenge is amplified by large numbers of interconnected parameters
26 influencing different parts of the model as parameters with strong enough covariances need to
27 be considered jointly. Furthermore, the strong co-variations between parameters and forcing
28 and boundary conditions further complicate the parameter selection process. It is vital to identify
29 the key internal parameters that have the most impact on a given model output because i) PDA
30 techniques are computationally demanding, scaling with the number of parameters used in the
31 optimisation, and ii) due to the high degree of equifinality in most parameter spaces (i.e.,
32 different parameter vectors giving the same fit to the observed data), attempting to estimate an
33 excessive number of parameters can lead to overfitting and a severe degradation in model
34 performance when the model is run in predictive mode. In other words, increasing model
35 complexity for improved prediction is only justified when there are adequate observational
36 constraints to its parameters (Famiglietti et al., 2021). Note that identifying key internal
37 parameters is not a solution in itself to the equifinality issue - it is still possible to have only two
38 key parameters and end up at equifinality.

39

1 Which model output and metric is tested fundamentally affects the crucial parameter selection if
2 relying primarily on sensitivity analysis. Furthermore, parameter sensitivity is often a function of
3 the parameter prior distributions, about which for many parameters we may have poor
4 knowledge. Indeed, a key distinction between a traditional sensitivity analysis, which may vary
5 all parameters by the same arbitrary amount (e.g. +/- 10%), and an uncertainty partitioning
6 analysis is whether the prior distributions accurately represent our knowledge about model
7 parameters prior to calibration (direct data constraints, formal expert elicitation, etc.) (Dietze et
8 al., 2014; LeBauer et al., 2013; Raczka et al., 2018).

9

10 The most common parameter sensitivity experiment is a one-factor-at-a-time parameter
11 perturbation experiment. However, this does not account for covariance between parameters,
12 which can vary along ecological tradeoffs and are known to strongly impact LSM outputs
13 (Prihodko et al., 2008). One solution to combat this is to use spatial pattern correlations as a
14 metric for parameter selection to ensure that the parameters selected are not highly correlated
15 (Dagon et al., 2020). More sophisticated methods include using the adjoint model to determine
16 local sensitivities and global sensitivity methods such as Morris (Morris, 1991) and the
17 variance-based Sobol (Saltelli et al., 2008; Sobol', 2001) and Fourier amplitude sensitivity tests
18 (FAST; Cukier et al., 1973). These methods have been applied to wide range of LSMs including
19 CABLE (Lu et al., 2013), CLASSIC (Deepak et al., 2024), CLM4.5(FATES) (Massoud et al.,
20 2019), JULES (Pianosi et al., 2017), Noah-MP (Wang et al., 2023) and ORCHIDEE
21 (Dantec-Nédélec et al., 2017; Novick et al., 2022). However, these methods can be hard to
22 implement (see Sect. 3.7 for the discussion about adjoint models) or require a large number of
23 model runs (e.g., $O(10,000)$ for Sobol). Nevertheless, once the adjoint or ensemble exists, it is
24 relatively easy to test the sensitivity of different model outputs.

25

26 In complex LSMs, even after selecting the most influential parameters, the large number of
27 vegetation (e.g., 15 plant functional types in ORCHIDEE) and soil texture classes (e.g., 13
28 USDA textural classes) used to represent the diversity of terrestrial ecosystems quickly
29 increases the dimensionality of global calibrations, as each parameter can be varied
30 independently. One way to tackle this issue is to assume that the parameter differences among
31 different groups vary proportionally and, therefore, optimise a parameter scaling factor instead
32 of targeting each parameter per group (Fer et al., 2018; McNeall et al., 2024). However, for
33 some plant traits, the "within functional type" uncertainty can be as large as the "across
34 functional type" uncertainty (e.g., Trugman et al., 2020), possibly due to the traits being either
35 weakly constrained by available data or genuinely plastic traits that vary spatially. In the latter
36 case, this variability suggests that localising parameters rather than using PFT-specific
37 parameterisations may be more appropriate. As such, methods that allow for independent
38 tuning of parameters within each PFT, or even localisation of parameters, may be necessary.
39 Scaling factors can also be used to target processes without needing to deeply explore detailed
40 parameterisations (e.g., Raoult et al., 2021) used a factor to scale the bare soil resistance to
41 evapotranspiration parameterisation in ORCHIDEE).

42

43 Selecting parameters is only one part of the problem - choosing the prior distributions is equally
44 important. In the existing LSM calibration literature, it is very common to assume uniform prior

1 distributions, either explicitly within Bayesian calibrations or implicitly when selecting uniform
2 range restrictions within parameter estimation using a naive objective function (unlike, for
3 example, classic variational DA techniques such as 4DVar which use an explicit Gaussian prior).
4 In these cases, uniform ranges are often based on informal “expert judgment” or ad hoc trial and
5 error. In some cases, parameter uncertainty ranges can be obtained from *in situ* measurements,
6 such as the TRY database (Kattge et al., 2020). Alternatively, the range can be set based on the
7 operational value of the parameter (e.g., $\pm 20\%$) - although this should only be done as a last
8 resort. When selecting ranges, extra considerations are needed to ensure that the ranges make
9 physical sense (e.g., not sampling negative values if the parameter needs to be positive), that
10 parameter dependencies are maintained (e.g., two parameters whose ratio should not surpass
11 a given threshold, or multiple parameters that must sum to one) and that plausible relationships
12 are retained (e.g., longevity of wood should be longer than that of foliage).

13

14 While uniform distributions are frequently chosen due to the lack of a more specific prior
15 distribution, and often to ensure the range is broad enough to cover edge cases, this approach
16 has significant drawbacks. Uniform priors rarely represent our actual prior knowledge of a
17 system, as they imply that all values within a range are equally likely, but values even a little bit
18 outside that range are impossible. In practice, parameter values in certain parts of parameter
19 space are often known a priori to be more plausible than others. An alternative to assuming
20 uniform prior distributions is to select from any of a plethora of other distributions, with such
21 choices usually driven by a combination of structural constraints (e.g., using zero-bound
22 distributions for non-negative parameters), formal syntheses and meta-analyses of trait data,
23 and structured expert-elicitation exercises (Dietze, 2017; Dietze et al., 2014; LeBauer et al.,
24 2013). However, selecting an inappropriate distribution can be as problematic as using a
25 uniform distribution, especially given that the true prior distribution is often not well known at the
26 start of the calibration process. This highlights the importance of conducting formal prior
27 predictive checks to validate assumptions before proceeding.

28

29 Priors constructed from trait data, where available, can often be quite well constrained, acting as
30 a form of data fusion (i.e. combining multiple constraints) and helping to constrain subsequent
31 calibrations to biologically-plausible parts of parameters space. Indeed, accounting for prior trait
32 knowledge can lead to very different conclusions about what parameters need to be included in
33 a calibration, as there are cases where very sensitive parameters may be well constrained a
34 priori (e.g., the parameter controlling the maximum rate of carboxylation - V_{Cmax}) while in other
35 cases much less sensitive, but unconstrained, parameters may plausibly span multiple orders of
36 magnitude and thus contribute more to overall model predictive uncertainty (Dietze, 2017;
37 LeBauer et al., 2013).

38

39 Informative non-uniform priors do not have to assume parameter independence; multivariate
40 priors can be constructed to capture known correlation structures and trait trade-offs, both
41 within- and across-PFTs (Shiklomanov et al., 2018). However, quantifying these correlations can
42 be a challenge, and so error covariances are often omitted in PDA, neglecting natural parameter
43 relationships. This simplification can result in an ill-posed inversion problem.

44

1 Finally, adopting informative non-uniform priors makes it easier to take advantage of the iterative
2 nature of Bayesian inference, where the posteriors from one round of model calibration can be
3 used as priors in the next round without requiring the recalibration of models to earlier data
4 constraints. Not only does this greatly simplify the updating of model calibrations as new data
5 becomes available, but it offers considerable computational advantages.

6

7 It is important to stress that no matter the method used for parameter estimation, solutions only
8 exist in the parameter space defined by the parameter selection and authorised prior ranges
9 (Williamson et al., 2013). Changing the number of parameters, their prior distributions, and/or
10 the model process representation will require new calibrations since the solution may differ due
11 to new parameter interactions and the equifinality of solutions.

12 3.2 Characterisation of model and data/observation errors

13 The state-of-the-art way to account for model and observation errors is through a Bayesian
14 framework. However, properly characterising these errors (especially data bias) can be a
15 challenge and potential model-data biases are not always properly treated with this formalism
16 (Cameron et al., 2022; MacBean et al., 2016). Model discrepancy, or model process error, refers
17 to the inherent inability of a model to replicate observations (Wu et al., 2023), stemming from
18 factors such as missing processes, choice of process representation, ecosystem heterogeneity,
19 stochastic processes (e.g., dispersal, recruitment, mortality, disturbance), biases in the model
20 forcing data, uncertainties in the initial model state, and the resolution of numerical solvers.
21 Observation error encompasses sampling variability, instrument inaccuracies, and any errors
22 involved in deriving the data products making up the observations. Furthermore, observation
23 error also usually includes a modelling step from the raw data measurement to any given
24 physical quantity (see Sect. 3.3). Due to the difficulty in separating model and observation
25 errors, they have often been combined in past studies. In fact, the mathematical formalisation
26 commonly used in PDA assumes that observation errors include model errors, thereby treating
27 model discrepancy as part of the observational error.

28

29 Although common, combining model error with data error can lead to an overestimation of
30 predictive uncertainty (van Oijen, 2017). Another approach to deal with model error is to ignore
31 it (i.e. assume the model structure is correct), however, this means only the input uncertainty is
32 propagated. A final approach is to treat model uncertainty as a separate parameter needing
33 calibration. If a prior for the model error uncertainties can be specified explicitly, model and data
34 error terms can theoretically be fitted separately. However, in practice, specifying an informative
35 prior on the model error term is challenging due to incomplete theoretical understanding of the
36 underpinning processes (Brynjarsdóttir & O'Hagan, 2014). Fortunately, it is often much easier to
37 specify an informative prior on the observation error, as these are frequently reported in data
38 products or estimable via sampling theory, and this is often useful to allow model error to be
39 separately identifiable.

40

41 There are a number of arguments for keeping process and observation error distinct. Model
42 process error propagates in space and time when making predictions, while observation error

1 does not. Additionally, addressing a large process error requires improving the model structure,
2 while addressing a large observation error calls for improving data quality. Furthermore,
3 calibrating models using cost functions that rely solely on fixed a priori observation errors can
4 distort parameter uncertainty estimates as well as the relative weight assigned to different data
5 constraints, as there's often no inherent reason to assume that model skill at predicting a
6 variable is proportional to the accuracy of its measurement. Indeed, it is easy to point to
7 examples where the uncertainty in our ability to model something differs in rank order from our
8 ability to measure that same thing (e.g., at local scale, model predictions of net ecosystem
9 exchange (NEE) are more uncertain than gross primary productivity (GPP: the flux of carbon
10 absorbed into the land surface due to photosynthesis), but observations of GPP are more
11 uncertain than NEE).

12

13 Quantifying both observation and model process error correlations, such as autocorrelated
14 measurement error, presents an additional challenge. These correlations yield non-diagonal
15 covariance structures, which are rarely well understood and are often ignored. Nevertheless,
16 accounting for these correlated errors has been shown to improve data assimilation results
17 (Waller et al., 2016), for example, by increasing the information content of observations (Stewart
18 et al., 2008). Since observation error correlations are more prevalent in dense observation
19 networks (Bannister et al., 2020), strategies to mitigate not modelling them include observation
20 thinning (reducing the number of observations assimilated in data-rich regions) and
21 super-lobbing (combining many observations into one (Lorenc, 1981)). Another common
22 approach to inflate variances is to reduce the weight of observations in data assimilation
23 (Chevallier, 2007; Kuppel et al., 2013). However, all these approaches are subjective and
24 potentially reject meaningful information (Cameron et al., 2022).

25

26 Finally, addressing systematic errors in models and data is becoming increasingly crucial as the
27 volume of data grows. With larger datasets, random errors tend to average out, leaving
28 systematic errors to dominate. These errors have long been recognised by the LSM calibration
29 community, such as when a model's ability to predict one variable worsens after assimilating
30 data for another. However, the underlying causes and potential solutions have not been widely
31 appreciated. Since all models are approximations, systematic errors in both models and data
32 require greater attention. To combat these biases, various approaches are emerging, ranging
33 from incorporating simple linear bias correction factors in the cost function (Cameron et al.,
34 2022; Fer et al., 2018) to more complex and flexible statistical models of bias, applied either
35 within the assimilation process or post-hoc (Kennedy & O'Hagan, 2001; Oberpriller et al., 2021).
36 Additionally, hybrid models that integrate machine learning with process-based models are
37 being explored as a means to address these challenges (see Sect. 4.2).

38

39 Ultimately, interconnected efforts, such as the characterisation of data errors together with the
40 data providers, post-PDA analysis of remaining model-data discrepancies, multi-model PDA
41 protocols that highlight relative model structural errors, and novel PDA algorithms are all
42 valuable in providing ways forward for discerning errors in data from those in model structure.

¹ 3.3 Developing observation operators

² The term “observation operator” refers to any transformation of the modelled quantity used to
³ allow comparison against observations (Kaminski & Mathieu, 2017). Note that what are often
⁴ called observations are themselves complex transformations of raw data measurements used to
⁵ estimate physical quantities comparable to the LSM output. For example, radiances observed
⁶ by a satellite at the top of the atmosphere can be translated into any number of land surface
⁷ data products, such as leaf area index. This processing can also be seen as a complex model,
⁸ such as the inversion of a radiative transfer scheme. Furthermore, these data are usually
⁹ prepared in such a way that they are available on the model grid.

¹⁰

¹¹ In some cases, it is possible to assume a one-to-one relationship between the model output and
¹² assimilated data, in which case the observation operator is the identity matrix. However, in all
¹³ other cases, an observation operator is required for DA, and the choice of observation operator
¹⁴ can significantly impact the results (Cooper et al., 2019). A common use of an observation
¹⁵ operator is to bridge the spatial scale between model and observations, either by aggregating
¹⁶ the gridded observations to the resolution of the model or vice-versa (Pinnington et al., 2021).
¹⁷ More complex examples of spatial scaling operators utilise a weighted averaging process to
¹⁸ match a more detailed description of the observation, such as modelling the point spread
¹⁹ function of satellite data, or the footprint of an eddy-covariance flux measurement. For example,
²⁰ Vergopolan et al. (2020) introduced a cluster-based observation operator that maps the
²¹ Gaussian footprint of satellite observations to the sub-grid scale of high-resolution LSMs. This
²² enables efficiently assimilating coarse soil moisture observations while bridging the spatial scale
²³ mismatch with fine-scale LSMs and ground observations (Vergopolan et al., 2021). In an
²⁴ application with flux tower data, Pinnington et al. (2017) partitioned the fluxes to observe
²⁵ different parts of the forest and run separate assimilation experiments for logged and unlogged
²⁶ forest stands.

²⁷

²⁸ In another example, atmospheric transport is used to map surface fluxes of gas species, such
²⁹ as CO₂, into atmospheric concentrations of that species at sampling points. In this way, flask
³⁰ measurements of CO₂ have been used to constrain parameters in models of the terrestrial
³¹ biosphere (Bacour et al., 2023; Kaminski et al., 2002, 2012; Knorr & Heimann, 1995; Peylin et
³² al., 2016; Rayner et al., 2005, 2011; Scholze et al., 2007) and to evaluate simulated net CO₂
³³ fluxes after optimising against eddy-covariance data (Kuppel et al., 2014). For non-reactive
³⁴ species, it is sufficient to have data on winds to drive the observation operator, but for reactive
³⁵ species such as CH₄, the process is more complex as atmospheric chemistry needs to be
³⁶ included.

³⁷

³⁸ Observation operators are also used to predict observed quantities that are not directly
³⁹ computed by the model itself. A recent example is the assimilation of SIF data, which is typically
⁴⁰ assumed to be a proxy for GPP. Examples of SIF observation operators include simple linear
⁴¹ relationships with GPP (Bloom et al., 2020; MacBean et al., 2018) through to more complex
⁴² operators based on the underlying photochemistry and radiative transfer in the canopy, either
⁴³ using empirical simplifications of those processes (Bacour et al., 2019) or using fully

1 mechanistic models for the operator (Norton et al., 2019). Another example is vegetation optical
2 depth which has been used to constrain above-ground biomass and leaf area index (Scholze et
3 al., 2019).

4

5 Scholze et al. (2016, 2019) also developed observation operators to map surface soil moisture
6 (SSM) retrievals to simulated volumetric soil moisture of the surface layer of BETHY, which were
7 also used by Wu et al. (2018, 2020, 2024). SSM is subject to large biases, which therefore
8 necessitates this type of transformation. Numerous models employ methods to map SSM to the
9 climatology of their model, for example through cumulative density function (CDF) matching.
10 Another approach is to focus solely on dynamics (e.g., dry downs, Raoult et al., 2021). The
11 dynamics approach is often used when assimilating vegetation indices, FAPAR or leaf area
12 index (LAI) — retrievals are normalised to estimate the seasonality of phenology instead of the
13 absolute values (MacBean et al., 2015). The optimisation then focuses on a reduced set of
14 phenology-related parameters, rather than including those related to photosynthesis (Bacour et
15 al., 2015).

16

17 Forward modelling of remote sensing data — i.e., the process of simulating remote sensing data
18 directly from the LSM outputs rather than assimilating processed satellite products — like in the
19 example of SIF, is the opposite approach to the assimilation of high-level satellite products such
20 as LAI or GPP. A key argument for taking this approach is that assumptions in the retrieval
21 process used in these products are likely inconsistent with the assumptions embedded in the
22 land surface model they are being assimilated into. A clear example of this is the use of satellite
23 GPP products which typically employ a production efficiency approach (e.g. the MODIS GPP
24 product, Running et al., 2021) whereas land surface models often use limiting-rate enzyme
25 kinetic schemes derived from those of Farquhar et al. (1980) and Collatz et al. (1992).
26 Furthermore, satellite-derived GPP estimates typically use environmental drivers such as
27 downwelling shortwave radiation which will almost certainly differ from those used to drive the
28 land surface model they are being assimilated into. Finally, there are often substantial
29 differences between the satellite-derived estimates (e.g. of GPP or LAI) where the assimilation
30 of any one product is likely biased with respect to the ‘truth’ (which is the primary reason for
31 using the seasonal dynamics rather than the actual values of time series data, as discussed in
32 the previous paragraph). Consequently, discrepancies between these high-level observations
33 and the values of the same variables predicted by a LSM may differ due to these factors and be
34 non-trivial to characterise.

35

36 It is appealing, therefore, to assimilate low-level products like SIF or canopy reflectance (Quaife
37 et al., 2008). For canopy reflectance, this typically requires the use of radiative transfer models
38 and is analogous to so-called “radiance assimilation” which is used extensively in numerical
39 weather prediction. In that way, any systematic error between the model and the observations
40 can be attributed to the land model (including the radiative transfer model) itself. For example,
41 Shiklomanov et al. (2021) modified the existing canopy radiative transfer model in the
42 Ecosystem Demography v2 model (ED2) to predict full hyperspectral waveforms, instead of just
43 aggregate visible, near-infrared, and thermal bands, and then used this observation operator to
44 calibrate ED2 against airborne AVIRIS imaging spectroscopy across the eastern temperate US.

1 Meunier et al. (2022) later used this observation operator in the development of a novel tropical
2 liana PFT. However, low-level satellite products often exhibit variability across domains that are
3 not inherently resolved by the land model, leading to some level of compromise between i)
4 adding complexity to the land model, ii) having an observation operator that is not completely
5 consistent with the underlying model or, iii) accepting that some of the variability in the
6 observations themselves will not be resolved. In the examples of SIF and canopy reflectance,
7 both vary with the relative geometry of the sun and sensor - correctly capturing that directional
8 variability using an observation operator that is physically consistent with the description of the
9 radiative transfer regime implemented in global land surface models (which typically only predict
10 total fluxes, i.e. integrated across the viewing hemisphere) is not currently possible.
11 Nevertheless, the selection and processing of observation data can help mitigate some of these
12 issues. For example, space-time binning of space-borne SIF data across multiple observation
13 geometries can limit the impact of directional effects and potentially increase the consistency
14 between model assumptions and the observed variables.

15

16 As observation operators become more complex, especially in the case of radiative transfer
17 calculations, they also become more computationally expensive. This is a clear example of
18 where machine learning may offer a unique opportunity within DA applications, as discussed in
19 Sect. 4.3.

20 3.4 Tackling spatial and temporal heterogeneity

21 The large variability in the surface properties of terrestrial ecosystems, arising from diverse
22 climates, soil properties, and variations in plant and soil species composition, plasticity, and
23 evolution, is an additional challenge in LSM parameter estimation. Calibration of the model at
24 one location may not be applicable at another. Moreover, most LSMs are too computationally
25 demanding to support calibration across large spatial domains. As such, it is important to
26 develop strategies to ensure results offer a good compromise across different locations, as well
27 as perform rigorous evaluation checks against data not used in the calibration.

28

29 A common approach to tackle this spatial heterogeneity is to perform “multi-site” optimisations,
30 grouping sites and performing a single optimisation over this group to obtain a more generic set
31 of parameters. The multi-site approach has been shown to be very effective, at times
32 out-performing site-specific optimisations (Kuppel et al., 2012; Raoult et al., 2016). Another
33 approach is to average the results of single-site optimisations. While usually less effective than
34 multi-site optimisations, this is often a more practical solution and can still result in an improved
35 parameter set. For example, Olivera-Guerra et al. (2024) found that the median values of
36 optimised parameters improved simulated land-surface temperature performance.

37

38 Both these approaches can be thought of as end-members (all sites the same versus all sites
39 different) in a continuum representing the statistical independence of calibrations across sites.
40 While only just beginning to be utilised to calibrate ecosystem models (Dokooohaki et al., 2022;
41 Fer, Shiklomanov, et al., 2021), hierarchical models have a long history of use in ecology as a
42 way of capturing this continuum, allowing parameters to vary across space and through time,

1 but constraining that variability with multivariate statistical models that describe that variability.
2 Since the across-site and within-site calibrations are fit simultaneously, this would allow LSM
3 models to “borrow strength” across sites (e.g., reducing equifinality as described above) without
4 forcing parameters to be the same everywhere. Hierarchical models also provide a formal
5 framework for accounting for the fact that out-of-sample predictions are more uncertain
6 (because their parameter vectors need to be predicted) than in-sample predictions at sites
7 where parameter vectors are known. To date, existing hierarchical ecosystem model calibrations
8 have assumed a simple “random effects” structure (i.e. different sites are drawn from the same
9 across-site distribution), but there are important opportunities to explore hierarchical models
10 with across-site spatiotemporal covariances (i.e., sites closer together should be more similar)
11 and across-site covariates (i.e., parameters that explain, and help predict, parameter variability).

12 A further alternative is the use of intermediate complexity models (e.g., DALEC), which, due to
13 their reduced computational complexity, can retrieve parameters at the pixel scale utilising
14 spatially continuous information from Earth Observation (EO) data and thus derive unique
15 information about the spatial variability of key underlying parameters, such as tissue residence
16 times (Bloom et al., 2016) and the impact of fire (Exbrayat, Smallman, et al., 2018). The
17 parameters and emergent ecosystem properties estimated from these models provide valuable
18 insights into the spatial variability and magnitude of parameters. This can reduce the parameter
19 space that needs to be searched when calibrating larger models. Furthermore, these optimised
20 parameters can be inserted into more complex models, enhancing their performance and
21 helping to better understand their internal dynamics (Caen et al., 2022).

22 Similarly, the interannual variability of atmospheric conditions means we also need to be careful
23 which period is used for the assimilation. Ideally, we want to calibrate over multiple years to
24 capture both the seasonal cycle and this interannual variability, while still retaining a number of
25 years for evaluation (although using different sites for calibration and evaluation can help to
26 relax this latter requirement). However, in practice, we are often limited by short time series
27 (e.g., only a few years for some *in situ* experiments and recently launched satellite missions),
28 data gaps, and the availability of meteorological forcing for corresponding periods, particularly
29 for *in situ* datasets.

30 3.5 Dealing with large and multiple observational datasets

31 Although EO instruments can provide global gridded datasets with which to calibrate the
32 models, fully exploiting these opportunities is challenging. Running experiments at the same
33 resolution as the satellite products (e.g., 500m MODIS resolution; Justice et al., 2002) requires
34 a lot of computational power and time, and we do not always have access to matching
35 meteorological forcing data. The resolution of products to be assimilated may also not be
36 meaningful for the objectives of the experiment. Additionally, when assimilating more than one
37 remote sensing data constraint, we must address multiple competing resolutions. This requires
38 decisions about scaling (see Sect. 3.3), determining which products are to be upscaled
39 (aggregated) versus downscaled (interpolated). Generally, satellite products are scaled to

1 match the chosen model grid, usually dictated by the resolution of the forcing data, although this
2 scaling can result in an over-generalisation or loss of information.

3

4 Furthermore, the quality of EO data can differ hugely across different regions since they are
5 impacted by atmospheric conditions (e.g., cloud cover) and topography, as well as the different
6 data processing algorithms and calibration/validation strategies used to develop the different
7 products. This can lead to regional and biome biases in the products that are very hard to
8 circumvent due to measurement limitations, potentially generating structural model biases.
9 Therefore, for many LSMs, it is common to select representative pixels for optimisation (e.g.,
10 MacBean et al., 2015), although defining what is representative is a challenge in itself. Once
11 selected, the representative pixel approach helps to i) reduce the dimensionality of the problem,
12 allowing for efficient and multi-data-stream calibrations, ii) focus on points with close to
13 homogenous coverage to be able to calibrate class-specific parameters (e.g., plant functional
14 types), and iii) define a different evaluation set of pixels with which to assess the optimisations,
15 especially sites with additional ground data. After selecting representative pixels, multi-pixel
16 optimisations are performed (as described in Sect. 3.4), focusing on estimating parameters for
17 different ecosystem/edaphic conditions by spanning the various model plant functional types
18 and soil textures all over the globe.

19

20 Another way to include more constraints to an optimisation is by calibrating against multiple data
21 streams. There is now an unprecedented wealth of *in situ* and EO data available, with even
22 more satellite missions and *in situ* field measurement sites being planned (Balsamo et al., 2018;
23 Ustin & Middleton, 2021). Different data streams offer information over different footprints and at
24 different spatial and temporal resolutions offering unique opportunities to constrain different
25 processes in the models. As LSMs become more complex through increased process
26 representation and greater interconnectedness between the different terrestrial cycles (e.g.,
27 water, energy, carbon, nitrogen), multi-data stream optimisations are becoming paramount to
28 provide adequate constraints since parameters are likely to impact different parts of the model.
29 By selecting only one specific data stream in an optimisation, we risk degrading the model's
30 overall predictive capacity if some of the optimised parameters are loosely constrained (Bacour
31 et al., 2015, 2023).

32

33 There are two possible approaches when assimilating multiple data streams. We can either
34 calibrate against each data stream in turn, often referred to as "stepwise" assimilation, or
35 include all data streams in one single optimisation, known as "simultaneous" assimilation.
36 Although mathematically equivalent when the posterior parameter uncertainties are properly
37 estimated and propagated in the stepwise case (MacBean et al., 2016; Peylin et al., 2016),
38 simultaneous assimilation is often preferable, since it ensures consistency (Kaminski et al.,
39 2012) and avoids issues linked to accurately propagating the information gained about the
40 parameter values from one step to the next. However, simultaneous optimisations may not
41 always be practical, especially when running a computationally demanding LSM experiment,
42 which is why the stepwise approach is often the pragmatic choice. In particular, there may be
43 technical difficulties associated with the different number of observations for each data stream
44 and the characterisation of error correlations between them (Bacour et al., 2023). Nevertheless,

1 it must be stressed that issues with unbalanced data streams are not solely due to imbalance
2 but stem from the model's inability to accommodate both data sources when structural errors
3 exist in either the model or the data (Oberpriller et al., 2021). In fact, properly quantifying and
4 accounting for the uncertainty in the model structural error and data bias leads to better results
5 than using ad-hoc methods such as reweighting different data streams (Cameron et al., 2022)
6 (see Sect. 3.2).

7 3.6 Including the spin-up and transient historical period in the 8 assimilation to better constrain land carbon sink projections

9 Many LSM simulations include both a spin-up phase that brings the prognostic variables
10 including vegetation state, soil carbon pools, and soil moisture content into equilibrium prior to
11 the industrial revolution (c. 1750). This is followed by a transient historical simulation where the
12 model is driven by changing climate forcing, rising CO₂ levels, nitrogen deposition, and
13 prescribed land management and land cover change since the equilibrium time point up to the
14 present day. Even with transient forcings, this historical period is likely not accurately simulated,
15 in part due to the lack of accurate historical climate and land use forcing data, in part because
16 “slow” carbon cycling parameters (e.g. carbon allocation or turnover rates) that control the
17 magnitude of the equilibrium carbon stock are poorly constrained, and in part because the
18 effects of key global change drivers on carbon storage (including recovery from disturbance) are
19 often missing or not reliably represented in models. The result is a large spread in the
20 magnitude and dynamics of various carbon pools and fluxes which underpin the current and
21 future projections of the land carbon sink (Arora et al., 2020; Friedlingstein et al., 2023).

22
23 To obtain reliable estimates of the current or future land carbon sink and trend in atmospheric
24 CO₂ we need accurate simulations of global carbon stock trajectories (i.e., *changes* in carbon
25 stocks). The trend in carbon stocks depends on the magnitude of carbon stocks post spin-up,
26 which in turn is strongly controlled by soil carbon pool turnover rates (Exbrayat, Bloom, et al.,
27 2018) (in addition to other parameters involved in soil carbon decomposition that moderate that
28 turnover rate). This is because for the CENTURY type model (Parton et al., 1987) used in many
29 LSMs, heterotrophic respiration is partly dependent on the size of carbon stocks. Global
30 sensitivity analyses (Sect. 3.1) of soil carbon cycle models performed for multiple different
31 biomes worldwide have rarely been performed (though see Huang et al., 2018) due to the
32 computational expense of running long-timescale simulations needed to model carbon stock
33 trajectories. For the same reason, relatively few past parameter DA studies with computationally
34 expensive LSMs at multi-site or global scale have included these slow-acting carbon cycle
35 parameters in their assimilation experiments. However, we know from past DA studies that
36 optimising “fast” carbon cycle flux related parameters related to photosynthesis, phenology, and
37 ecosystem respiration has limited impact on regional to global scale carbon stocks (MacBean,
38 Bacour, et al., 2022), as expected, while “slow” carbon cycle process parameters (such as those
39 related to carbon allocation to different biomass pools, or biomass and soil carbon pool turnover
40 times) are important for constraining long-term carbon stock trajectories (Thum et al., 2017).

41

1 To optimise the “slow” acting carbon cycle parameters involved in carbon allocation, biomass
2 turnover and soil carbon cycling, LSM assimilation experiments would need to include the
3 spin-up and transient runs in the assimilation, which would be prohibitively costly given the
4 computational cost of LSM runs. Therefore, neither the spin-up or transient period (prior to the
5 assimilation window) are usually included in LSM assimilations (Peylin et al., 2016; Raoult et al.,
6 2016; Schürmann et al., 2016). This presents challenges for obtaining accurate model estimates
7 of carbon fluxes and stocks because an incorrect initial carbon stock will likely result in biased
8 parameter retrievals that are accounting for the model errors contributing to the incorrect initial
9 carbon stock. Note this is not the case for carbon cycle and ecosystem models that have much
10 faster run times and who have therefore been able to include biomass and soil carbon turnover
11 rates and other related “slow” carbon cycling parameters in their optimisations (e.g.,
12 CARDAMOM-DALEC – Bloom et al., 2016).

13

14 To make up for incorrect carbon pool magnitudes and the fact that including spin-up and
15 transient in the assimilation is not yet feasible, most past carbon cycle parameter DA studies
16 have included scalars on the initial C pools in the optimisation, resulting in an improved fit to
17 NEE and atmospheric CO₂ data (e.g., η , Carvalhais et al. (2008, 2010); K_{soilC} in ORCHIDEE
18 PDA studies, e.g., Peylin et al. (2016); f_{slow} in CCDAS studies, Castro-Morales et al. (2019;
19 Schürmann et al., (2016)). These scalars alter the initial carbon pool size to account for model
20 and forcing errors mentioned above that contribute to incorrect soil carbon stock sizes. Studies
21 differ in how many such scalars to include, both in terms of which carbon pools to relax (all C
22 pools as in Santaren et al. (2007) versus slow and/or passive as in Peylin et al. (2016), whether
23 to scale aboveground biomass or not (Carvalhais et al., 2010), and to how many to use spatially
24 in global simulations (1 in CCDAS, Castro-Morales et al. (2019), Schürmann et al. (2016),
25 versus 30 regional factors used in ORCHIDEE studies, Bacour et al. (2023), Peylin et al.
26 (2016)). Other options for avoiding spin-up include directly initialising models with carbon stock
27 observations, and including parameter calibration within iterative state DA approaches.
28 However, in all of these cases, calibrating the “right” model parameters to the “wrong” model
29 pools is going to produce poor fits, complex sets of compensating errors, and potentially
30 incorrect hypothesis testing around alternative model structures.

31

32 Adjusting initial carbon stocks without optimising the “slow” carbon cycle parameters to which
33 the equilibrium carbon stock magnitude is sensitive is only useful if the purpose of the carbon
34 cycle assimilation experiment is to update model estimates of *current* carbon budgets. If the
35 desired goal is an accurate prediction of *future* carbon stock trajectories – for predicting carbon
36 mitigation potentials or carbon-climate feedbacks under different scenarios of climate and
37 disturbance trajectories – then simply adjusting initial carbon stocks is insufficient. In longer runs
38 (up to 2100 or 2300) those “slow” carbon cycling parameters that resulted in the original
39 incorrect carbon stock magnitude will start to push the model back to that original (inaccurate)
40 equilibrium, resulting in an artificial trend in the modelled carbon pools (and resultant biases in
41 carbon fluxes and land carbon sink estimates). Thus, for long term projections of carbon-climate
42 feedbacks, all parameters that are important for carbon pool trajectories need to be included in
43 the assimilations. This means that longer time windows (lasting several hundreds to thousands
44 of years) governing the periods over which these “slower” carbon cycle parameters operate will

1 need to be included in the assimilation experiments (Raiho et al., 2021; Thum et al., 2017). This
2 will materially increase the computational cost of an experiment enough to be prohibitive for
3 computationally expensive LSMs with current simulation protocols and assimilation algorithms.
4 Methods for increasing the simulation speed (e.g., model emulation - see Sect. 4.2) will
5 potentially solve the issue of prohibitive computational cost for these longer-term assimilation
6 experiments. One opportunity for accelerating the spin-up is by adopting the matrix approach,
7 where carbon balance equations are expressed as a single matrix equation without altering any
8 processes of the original model, which has now been applied to multiple LSMs and used for
9 both parameter sensitivity analyses and data assimilation (Hararuk et al., 2014; Huang et al.,
10 2018; Luo et al., 2022; Tao et al., 2020, 2024). Intermediate complexity ecosystem models may
11 be able to assist by providing much constrained priors of soil carbon pool turnover times (and
12 other parameters to which equilibrium/initial carbon stock magnitude are sensitive) (Bloom et al.,
13 2016).

14

15 This problem is specific to long-term, slowly changing carbon (and other nutrient like nitrogen
16 and phosphorus) stocks: e.g., for water storage (e.g., soil moisture), usually only a few years
17 are required either for spin-up or to adjust to a given perturbation. Therefore, for
18 hydrology-focused simulations both the spin-up and historical period spanning the perturbation
19 from equilibrium can be included in the experiment. In fact, by including this shorter spinup, the
20 assimilation also gives an estimate of the initial state (e.g., soil moisture, Pinnington et al.,
21 (2021); snow albedo, Raoult et al. (2023)). While carbon cycling is interlinked with water and
22 energy cycles, long-term carbon stock trajectories are insensitive to short-term fluctuations in
23 soil moisture.

24

25 In addition to longer assimilation time windows, assimilating measurements of aboveground
26 biomass or soil C stocks in conjunction with carbon fluxes provides a useful additional constraint
27 on carbon pools magnitude and trajectory (Thum et al., 2017). However, data on soil carbon
28 stocks are relatively scarce compared to carbon fluxes, highly uncertain, and often difficult to
29 link to the conceptual carbon pools in many CENTURY-type models (Parton et al. (1987),
30 though this is changing, Abramoff et al. (2018)). Additionally, these datasets often contain only
31 one or a few time points. While assimilating some information on carbon stocks is better than
32 not having any data, constraining long-term changes in C stocks will require multiple
33 observations of both above- and belowground C stocks over time (Raiho et al., 2021) (or data
34 representing rates of carbon cycling) in addition to nighttime and soil respiration data that so far
35 have typically not been utilised in LSM DA studies. Just how long a time series we need to
36 include to accurately estimate slow carbon cycle parameters will likely depend upon which
37 parameters are important for estimating future carbon stock trajectories over the timescales of
38 interest and the uncertainties associated with observations. More parameter sensitivity studies
39 are needed to assess which slow carbon cycling parameters control carbon stock trajectories at
40 different temporal scales (Raczka et al., 2018). Ideally, these sensitivity studies should be
41 performed with different scenarios of global change drivers, as changing inputs may alter the
42 relative importance of slow carbon cycling parameters. The community can learn from the
43 calibration and validation activities of soil biogeochemical models being approved for use in
44 voluntary carbon markets (Mathers et al., 2023).

¹ 3.7 Choice and implementation of minimisation algorithms

² To perform optimisations effectively, careful consideration must be given to the choice of
³ algorithm and its implementation. As discussed in Sect. 2, various algorithms are available,
⁴ each with distinct characteristics, such as local versus global optimisation, each having different
⁵ computational demands. Additionally, every algorithm comes with a variety of configurable
⁶ options. For instance, a Genetic Algorithm implementation by (Scrucca, 2013) offers a range of
⁷ functions for parent selection (6 options), crossover (5 options), and mutation (3 options),
⁸ resulting in 90 possible combinations. Users can also adjust crossover and mutation
⁹ probabilities. The success of the optimisation process greatly depends on how the optimisation
¹⁰ is implemented, which may vary on a case-by-case basis. Systematically testing all possible
¹¹ combinations is unfeasible due to the large computational demand of an LSM. A more efficient
¹² approach is to use an emulator (see Sect. 4.1) rather than an LSM to find an optimal
¹³ experimental design (Dagon et al., 2020); once the design has been identified, the optimisation
¹⁴ can be carried out using the LSM.

¹⁵ Furthermore, for gradient-based methods, implementing and maintaining the tangent linear or
¹⁶ adjoint model is a huge challenge in LSM DA. For complex LSMs, which are historically coded
¹⁷ in Fortran, the tangent linear and adjoint models can take years to develop, even when using
¹⁸ automatic differentiation software, since the code first needs to be cleaned and structural
¹⁹ adjustments need to be made to ensure the code is differentiable without changing the
²⁰ fundamental physics. For example, this may require replacing look-up tables with their
²¹ continuous formulations and reformulating minimum and maximum calculations to allow a
²² smooth transition at the edge (Schürmann et al., 2016). The years taken to derive the tangent
²³ linear/adjoint models mean they quickly become outdated, especially with big community
²⁴ models like JULES and ORCHIDEE, where new processes are added approximately every six
²⁵ months. For JULES, the adjoint was developed for v2.2 of the model (Raoult et al., 2016),
²⁶ whereas JULES is currently at v7.3 at the time of writing. Similarly, while the tangent linear
²⁷ exists for ORCHIDEE, it exists for an old version of the model (AR5) that predates the addition
²⁸ of a multi-layered soil hydrology scheme and nitrogen cycle. To address this issue, the
²⁹ ORCHIDEE DA team has been developing a tool to do the required preprocessing of any
³⁰ version of ORCHIDEE so the tangent linear version of the model can be easily derived using
³¹ Transformation of Algorithms in Fortran (Giering, 2010). On the other hand, BETHY's lower
³² complexity has allowed it to be kept compliant with automatic differentiation software for
³³ decades, which provided efficient derivative code of the up-to-date version of the model. This is
³⁴ also the case for its successor D&B (Knorr et al., 2024), which is the model component of the
³⁵ European Space Agency supported TCASS system, and for the Nanjing University Carbon
³⁶ Assimilation System (NUCAS, Zhu et al., 2023). Alternatively, models written directly in an
³⁷ auto-differentiable language (Julia or python-JAX; see Sect. 5.4) alleviate this issue (Gelbrecht
³⁸ et al., 2023; C. Shen et al., 2023). Although these languages have slower computational
³⁹ performance than Fortran, these new languages often also facilitate the use of graphic
⁴⁰ processing units (GPU), e.g., through packages like pyTorch (Paszke et al., 2019).

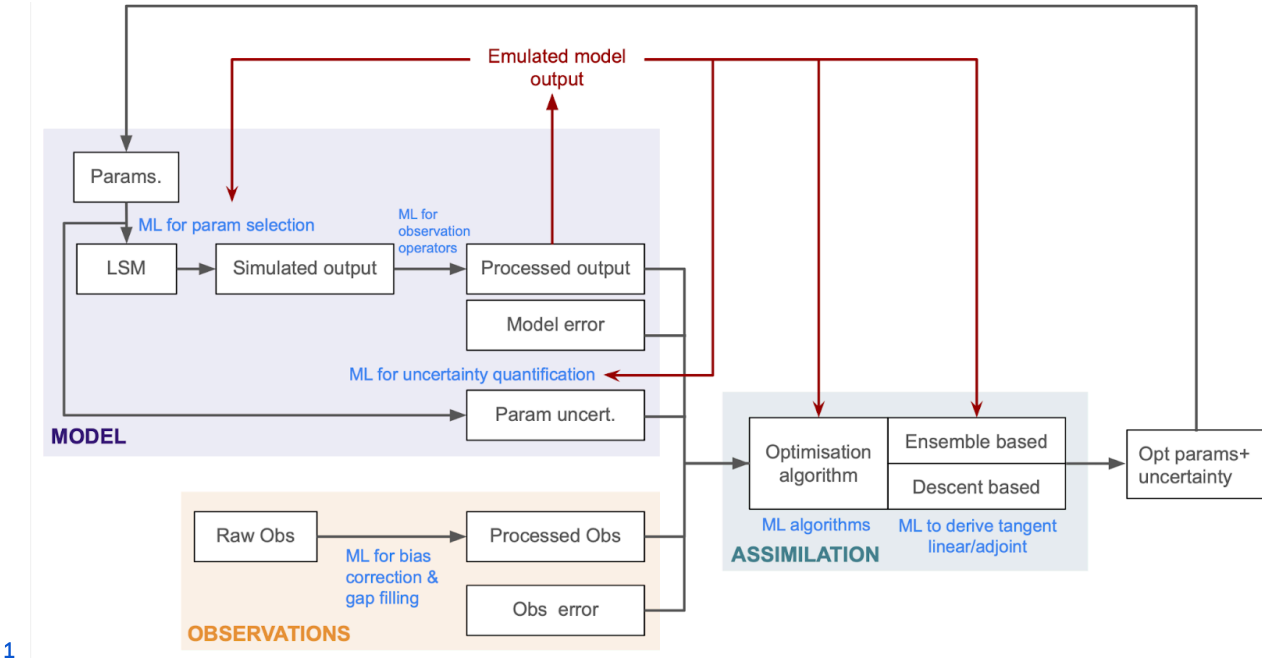
1 As discussed in Sect. 2, in the absence of the tangent linear or adjoint model, one can use finite
2 differences. However, this necessitates the selection of an appropriate step size for accuracy
3 and convergence speed, which will differ based on the sensitivities of the parameter estimated.
4 Other methods to bypass the need for tangent linear and adjoint models include LAVENDAR's
5 ensemble 4DVar approach (Pinnington et al., 2020) or the use of emulators, which can be used
6 to either avoid gradient-based approaches in favour of Monte Carlo ones, make numerical
7 approximations of gradients viable, or both (e.g., Hamiltonian MCMC). However, these
8 algorithms also come with a number of hyperparameters that need to be selected including the
9 number of ensembles and convergence criteria.

10 4. Opportunities through machine learning for 11 parameter estimation

12 Despite the challenges and knowledge gaps discussed above, our community has never been
13 in a better position to calibrate land surface models and rigorously diagnose their uncertainties.
14 We now have access to large observational datasets at high spatio-temporal resolutions and
15 increased computational capacity and efficiency. These factors, combined with recent advances
16 in machine learning (ML), potentially allow us to make significant progress in model calibration.
17

18 The recent surge in ML has been evident in every aspect of society with the most relevant
19 examples coming from numerical weather prediction (Lam et al., 2023) or remote sensing (Lary
20 et al., 2016). These examples can help us identify ways in which ML can assist with land PDA.
21 In this section, we specifically focus on how ML can help us address the current challenges and
22 limitations in land PDA outlined above, as well as areas where ML has the potential to improve
23 the DA workflow (Fig. 1). With the large number of studies currently being published in the field
24 of machine learning, we only provide a short overview of the relevant literature. In the context of
25 ML for PDA, we can broadly group the existing studies and applications into four categories: i)
26 the use of ML to emulate the relationship between LSM parameters and its outputs or
27 performance (Sect. 4.1), ii) the creation of 'hybrid models' in which ML replaces or complements
28 a component of a larger LSM (Sect. 4.2), iii) the use of ML to improve or pre-process
29 observation datasets prior to their use in PDA (Sect. 4.3), and iv) the use of ML to optimise the
30 parameter estimation process itself (Sect. 4.4).

31



1

2 **Figure 1:** Examples of where ML can facilitate each part of the land surface model PDA workflow

3 4.1 Parameter perturbation emulators

4 The computational cost of high-complexity LSMs hinders the use of the more computationally
 5 demanding PDA techniques such as MCMC. However, machine learning methods can mitigate
 6 a portion of these computational burdens. By building a statistical relationship between input
 7 parameter settings and the LSM output or an aggregate of the LSM output (for instance over
 8 time or space), the LSM output can be estimated for a new set of input parameters. The
 9 statistical relationship serves as a computationally efficient surrogate model for the expensive
 10 LSM and is most frequently called an emulator (although this term is not exclusive to this
 11 application), while surrogate, meta-model, or reduced-order model are also used to refer to this
 12 tool. Indeed, emulators already have a rich history in climate sciences (Knutti et al., 2003;
 13 Sanderson et al., 2008; Watson-Parris, 2021).

14

15 Parameter Sampling Strategies

16 The training of an emulator requires an ensemble of LSM simulations with perturbations to the
 17 input parameters often called a perturbed parameter ensemble (PPE, see McNeall et al. (2024)
 18 and Kennedy et al. (2024) for PPEs constructed for JULES and CLM, respectively). The design
 19 of the initial PPE depends on the intended use; for uncertainty quantification, it is often
 20 preferable to sparsely sample the entire parameter space using Latin hypercube sampling
 21 (McKay et al., 1979). However, for calibration applications, it can be more cost effective to use a
 22 non-random and targeted sampling strategy, such as active learning which tries to optimise the
 23 selection of the next sample (e.g., Zhao & Kowalski, 2022). Alternatively, an Ensemble Kalman
 24 Filter approach (Evensen, 2003) can be used to place the initial design points in regions of
 25 significant posterior mass to optimise the calibration process (e.g., (Cleary et al., 2021). When
 26 building emulators for model calibration it can be particularly effective to treat this as an iterative

1 design process, whereby an initial set of parameter vectors (e.g., Latin hypercube) is used to
2 generate a rough idea of where in parameter space the optimum lies, then additional parameter
3 vectors are sampled from this region, refining the emulator in a way conceptually similar to a
4 nested grid in parameter space (Fer et al., 2018). How to optimally propose points in parameter
5 space remains an important research question.

6

7 Emulation Methods

8 There are many ML methods appropriate for emulating the LSM response to parameter
9 modifications. When it comes to the calibration problem specifically, an alternative to emulating
10 the LSM output is to directly emulate the cost function itself (i.e., the response surface of model
11 error as a function of parameter value) which is much lower dimensional and often much
12 smoother than the model output itself (Cheng et al., 2023, 2024; Dagon et al., 2020; Fer et al.,
13 2018; Fer, Shiklomanov, et al., 2021).

14

15 Gaussian processes are commonly applied as they are well-suited to interpolate non-linear
16 surfaces in data-scarce settings and moreover provide a measure of prediction uncertainty that
17 can be used to quantify the emulator uncertainty. However, since the computational cost of
18 Gaussian processes dramatically increases with the size of the dataset, they are less feasible
19 for larger datasets. One option is to develop sparse Gaussian processes, as demonstrated by
20 Baker et al. (2022). Running JULES at a 1km resolution over Great Britain, they exploit the fact
21 that LSMs typically do not exchange information laterally between grid cells (river routing is
22 generally done as a separate step) to select a subset of coordinates representative of different
23 parameter settings and forcing data regimes.

24

25 Another popular method for emulating LSMs are neural networks (NNs), as they are
26 straightforward and fast to implement (Hatfield et al., 2021), with fast evaluation speeds and
27 good predictive skill within the bounds of the training data. However, NNs are sensitive to biases
28 in the selection of the training data as well as the tuning of the algorithm hyperparameters,
29 which means that they generally cannot extrapolate to scenarios beyond the training data or be
30 transferred to new datasets without performance degradation (Shwartz-Ziv & Armon, 2022). (D.
31 Lu & Ricciuto, 2019) used singular value decomposition with Bayesian optimisation to create a
32 reduced number of surrogate models for carbon modelling parameter perturbation. Their
33 approach showed minimal accuracy loss, making it effective for extensive parameter space
34 exploration and uncertainty quantification. Other examples of NNs used to emulate LSMs
35 include, Dagon et al. (2020), where a series of artificial feed-forward NNs were trained to
36 emulate CLM5 output given important biophysical parameter values and Meyer et al. (2022),
37 where an NN was trained to emulate the ensemble mean of several urban LSMs combining the
38 strengths of the different into one ML model. While artificial NNs do not provide a probabilistic
39 prediction, new methods are emerging such as neural processes (e.g., (Garnelo et al., 2018) or
40 randomised prior networks (Bhouri et al., 2023). Regression trees can also be extended to
41 include probabilistic prediction such as with NGBoost (Duan et al., 2020) or XGBoost (Donnerer,
42 2024), as used for example to emulate ELM-FATES (Li et al., 2023). XGBoost has been shown
43 to generally outperform NNs while requiring little parameter tuning and is able to achieve robust
44 performance even when extrapolating to scenarios beyond the training data (Grinsztajn et al.,

1 2022; Shwartz-Ziv & Armon, 2022). A disadvantage of tree-based methods is their slower
2 evaluation speeds and the fact that they are not differentiable, which can limit their usability for
3 certain applications (e.g., coupled DA, Hatfield et al., 2021). Long-Short Term Memory (LSTM)
4 methods, which for example have been applied to ECLand (Boussetta et al., 2021), include
5 memory mechanisms by leveraging long-term dependencies in the training data time series,
6 allowing them to effectively emulate model processes across different time scales without
7 performance loss at longer lead times (as is the case for XGBoost for example, (Wesselkamp et
8 al., 2024). This makes them particularly suited for the emulation of large-scale forecasting
9 systems that encompass physical processes acting at different time scales (e.g., Datta &
10 Faroughi, 2023; Guo et al., 2021; Wesselkamp et al., 2024).

11

12 Computational Cost Reduction

13 Once an emulator is trained it becomes computationally feasible to apply PDA techniques that
14 require a large number of samples from a prior parameter distribution, e.g., MCMC. Fer et al.,
15 (2018) showed how emulators sped up an MCMC optimisation for the relatively simple SIPNET
16 model by over two orders of magnitude (>100x). Further applying their method to the more
17 complex Ecosystem Demography model v2 (ED2), whose complexity precluded it from a direct
18 application of the MCMC methodology for parameter tuning, they found that emulators helped
19 achieve a >20,000x increase in speed (27 hr versus a predicted 74 years by traditional MCMC).
20 Similarly, Sawada (2020) and Cleary et al. (2021) both used emulators to perform Bayesian
21 inversion using the otherwise costly MCMC approach to sample the approximate posterior
22 parameter distribution after calibration. Torres-Rojas et al. (2022) combine surrogate modelling
23 with a multi-objective Pareto efficiency analysis to infer LSM's optimal subgrid parameters at 1%
24 of the computational cost. The emulators were trained on forward model runs used to initially
25 calibrate the model using Ensemble Kalman sampling - a derivative-free optimisation method.
26 Coining the method "Calibrate, emulate, sample", Cleary et al. (2021) showed how the method
27 could be successfully applied to models of different complexity, while other groups have also
28 demonstrated the suitability of ensemble approaches for parameter selection (e.g., Couvreux et
29 al., 2021).

30

31 History Matching

32 Emulators are commonly used in the field of uncertainty quantification, and one key method
33 from this field that is gaining traction in land surface modelling is the so-called history matching
34 (HM) method (Hourdin et al., 2023). This method is not about finding the most likely parameter
35 values, but rather ruling out implausible ones based on some given metrics (Williamson et al.,
36 2013). Using emulators to facilitate computation, HM is commonly applied using successive
37 iterations (also known as iterative refocusing) to reduce parameter space and retain the least
38 implausible parameters. Like the cost function used in variational DA, the implausibility takes the
39 observation and model structure errors into account. While these errors are still hard to
40 determine (Peatier et al., 2023), it is arguably less dangerous to get them wrong here than in the
41 DA case - if the errors are overestimated, HM gives a clear diagnostic of this being the case, for
42 example, by ruling out little to no parameter space. If the errors are underestimated, HM will rule
43 everything out, suggesting the errors have been misspecified, whereas, in other optimisation
44 approaches, we would still get a solution even if one does not exist. HM also allows the user to

1 test many different metrics to see if parameters can capture specific features, similar to
2 multi-objective optimisations, giving a clear diagnosis of model structure error. HM has
3 successfully been tested with some of the major high-complexity LSMs: CLM (Dagon et al.,
4 2020), JULES (Baker et al., 2022; McNeall et al., 2024), and ORCHIDEE (Raoult, Beylat, et al.,
5 2024), for example. These studies highlight how HM can be used to identify sensitive
6 parameters, redefine ranges of variation and identify non-Gaussian relationships between
7 parameters. This information could potentially be used to determine the prior error covariances
8 (i.e., to set up the background error covariance matrix in variational DA) or provide ecological
9 constraints to an optimisation.

10 4.2 Hybrid modelling

11 ML can also be used in a hybrid modelling approach to substitute components of the physical
12 model with an ML approximation (Eyring et al., 2024). The appeal of the hybrid approach is that
13 it can address known model inadequacies and computational bottlenecks in a targeted manner
14 while retaining the use of physical process knowledge and constraints where they are reliable.
15 For example, the hybrid approach can mitigate model structural errors, by replacing model
16 processes that are missing or poorly understood with data-driven substitutes, assuming
17 adequate data exists (Arsenault et al., 2018; Reichstein et al., 2019). At the same time, the
18 hybrid approach can add physical constraints to the ML model components, thus maintaining
19 physical consistency and interpretability (e.g., Beucler et al., 2021; Kraft et al., 2022; Reichstein
20 et al., 2019). ML and process models can be combined in a number of different ways, including
21 i) substituting a specific model parameterisation with an ML approximation, ii) deriving spatial
22 parameterisations that better capture observed physical behaviour, iii) training on model-data
23 residuals to predict process-model biases and characterise structural errors, and iv) replace
24 computationally costly parts of the model. Hybrid modelling has been implemented successfully
25 in a number of LSM applications, including for streamflow (Yang et al., 2019), evapotranspiration
26 (W. L. Zhao et al., 2019), subsurface flow (N. Wang et al., 2020), rainfall-runoff modelling (Xie et
27 al., 2021), as well as more generally for the prediction of sea surface temperatures (de Bézenac
28 et al., 2019), atmospheric convection (Gentine et al., 2018), and high impact weather events
29 (McGovern et al., 2017). As with all parameter estimation methods, hybrid modelling can be
30 subject to parameters compensating for model structural errors or errors in parameters outside
31 the calibration set (see also Sect. 4.2). This can be counteracted through the use of multivariate
32 independent observation constraints in the calibration.

33

34 Substitution of Uncertain or Missing Parameterisations and Processes

35 In the context of land DA, hybrid modelling has been used to improve the representation of
36 complex processes, such as the representation of human processes and their impact, which are
37 often not represented in their full complexity or missing completely in traditional LSMs. ML
38 approaches trained in an aggregate manner (e.g., one NN trained on all locations) and using a
39 combination of observations and process-model outputs can effectively account for human
40 processes by mapping observations into the model climatology (thus removing global biases).
41 At the same time, they can retain the independent information on human processes that is
42 inherent in the observations but typically removed in traditional bias correction approaches (e.g.,

1 Kumar et al., 2012). Kolassa et al. (2017) used an artificial NN observation operator trained on
2 brightness temperature observations from the Soil Moisture Active Passive (SMAP) mission and
3 GEOS land model outputs to assimilate soil moisture information, which introduced the impact
4 of irrigation and tile drainage in a model that does not normally represent these processes.
5 Assem et al. (2017) developed a Deep Convolutional NN, trained on historic water flow and
6 water level observations, to predict water flow in urban areas from runoff estimates generated
7 by a physical LSM. Hybrid modelling can also be used in cases when the naturally occurring
8 physical processes are poorly understood. For example, Arsenault et al. (2018) used an ANN
9 with a combination of remote sensing observations and model predicted states to generate
10 improved estimates of snow depth within the Land Information System.

11

12 Improved Spatial Parameterisations

13 Hybrid modelling techniques have also been used successfully to generate model
14 parameterisations that better capture the parameter spatial distribution and thus the observed
15 physical behaviour (Tao et al., 2020, 2024). Process-model parameterisations can be limited by
16 observation sparsity, which can lead to ad hoc decisions when assigning parameter values
17 globally. Similarly, many global LSMs significantly simplify biogeochemical and physical
18 mechanisms into empirical parametric functions. Hybrid modelling can address these issues by
19 mapping environmental variables into model parameters or using high-resolution, high-fidelity
20 model simulations to derive new parameterisations for coarse-resolution models (e.g., Gentine
21 et al., 2018). Bao et al. (2023) replaced the traditional PFT-based parameterisation of a light use
22 efficiency model with an ecosystem-property-based parameterisation derived from a multi-layer
23 perceptron NN to better capture the spatial variability of GPP within PFTs. Several studies have
24 used a hybrid ML approach to improve the representation of evapotranspiration in LSMs, either
25 by directly estimating evapotranspiration (Zhao et al., 2019) from observations or by inferring
26 related prognostic variables, such as the stomatal and aerodynamic resistances (ElGhawi et al.,
27 2023), or transpiration stress (Koppa et al., 2022). In each case, the hybrid model was able to
28 learn unknown latent processes and thus outperform traditional physics-based schemes.

29

30 Model Error Identification/Characterisation

31 Additionally, hybrid modelling implementations can serve as effective diagnostic tools to identify
32 model errors. For an independently evaluated ML approximation, systematic differences
33 between predictions from a physical model component and its ML counterpart can provide
34 insights into missing or flawed model process representations as well as identify inadequate
35 model parameters (e.g., McGovern et al., 2017), especially when the ML model is not only
36 trained to represent the model outputs but uses other observational constraints in the learning
37 phase. For example, Finn et al. (2023) and Gregory et al. (2023) used an ML trained on
38 model-data residuals to predict model biases and characterise structural errors, while Gregory
39 et al. (2024) extended this approach to implement an online bias correction within a DA
40 framework. Similarly, Farchi et al. (2021, 2023) integrated a deep-learning step into a DA
41 framework to create a hybrid model that dynamically learns and corrects model errors at each
42 DA time step.

43

44

1 Computational Cost Reduction

2 Finally, hybrid modelling can be used to replace computationally costly parts of the model. For
3 example, emulating the spinup, which can account for up to 98% of computational time in
4 complex LSMs, would greatly alleviate challenges linked to this bottleneck (see Sect. 3.6). A
5 successful undertaking by Sun et al. (2023) showed how bagging decision trees (an ensemble
6 ML method based on (Breiman, 1996) could be used to emulate the spin-up of the ORCHIDEE
7 LSM. Koppa et al. (2022) developed a deep learning-based hybrid model combining a
8 process-based land surface model with remotely-sensed observations to estimate global
9 evaporation. They showed how hybrid models can significantly improve predictive accuracy
10 while reducing the computational cost.

11

12 Data Requirements

13 Hybrid modelling has the potential to be very powerful, but it is also susceptible to issues linked
14 to equifinality (Kraft et al., 2022; Sawada, 2020). We note that any ML approaches need
15 substantial data to perform well and thus the ML components in the hybrid part need to be
16 targeting processes for which data is plentiful. ML approaches often have a large number of
17 parameters in their training which gives them a larger degree of flexibility that can compensate
18 for errors in physical models, but can also lead to overfitting.

19 4.3 Observation Processing

20 There are many examples of using ML to improve or pre-process the observational datasets
21 that can be assimilated into LSMs, especially from the field of remote sensing. Many of these
22 novel datasets have yet to be exploited in the LSM parameter estimation studies, presenting
23 exciting new opportunities.

24

25 Observation Operators

26 One such application is the use of ML-generated observation operators to translate
27 satellite-observed radiances into model states or parameters (see challenges raised in Sect.
28 3.3). The use of ML techniques in this context has several advantages: i) ML-based observation
29 operators are relatively simple to implement compared to physically-based approaches, which
30 often involve the inversion of radiative transfer models, ii) they are able to easily accommodate
31 the simultaneous assimilation of multiple observation types, iii) they can inherently correct
32 climatological biases between model and observations, and iv) they facilitate the assimilation of
33 radiance observations rather than retrieval products, thus reducing errors stemming from
34 possible inconsistencies between retrieval algorithm assumptions and models. Due to these
35 advantages, ML-based observation operators have been applied in several land data
36 assimilation studies, including for soil moisture (Kolassa et al., 2017; Rodríguez-Fernández et
37 al., 2019), leaf area index (Durbha et al., 2007), snow water equivalent (Kwon et al., 2019), and
38 as a combined forward model for soil moisture and LAI (Shan et al., 2022).

39

40 Retrieval Algorithms

41 Similarly, ML approaches have been used to develop data-driven retrieval algorithms in cases
42 where physical retrieval algorithms are very complex. For example, Chen et al. (2022), Gentine

1 & Alejomhammad (2018), Shen et al. (2022) and Zhang et al. (2018) each used ML to estimate
2 SIF from MODIS radiances, OCO-2, and TROPOMI observations, respectively. Alejomhammad
3 et al. (2017) developed an ML approach to retrieve global, monthly GPP estimates from
4 GOME-2 SIF observations only.

5

6 **Gap-Filling**

7 ML approaches can also be used to improve observation datasets by making them more
8 suitable for data assimilation applications. One approach is to use ML to generate gap-filled
9 observations or generate higher temporal resolution datasets. For example, Yatheendradas &
10 Kumar (2022) used an ML approach to create a gap-filled, high-resolution dataset of observed
11 snow cover fraction and Fang et al. (2019) used a deep learning Long Short-Term Memory
12 framework to predict daily “SMAP Level-3 like” soil moisture estimates from atmospheric forcing
13 data and static physiographic attributes. Vekuri et al. (2023) used extreme gradient boosting to
14 gap-fill eddy covariance data reducing the northern biases in the data found after using more
15 traditional gap-filling methods. Nevertheless, one must exert caution when using gap-filled data
16 (or other model-derived data, such as retrieval products) for parameter estimation, since they
17 are dependent on the assumptions of the selected gap-filling method. Furthermore, gap-filled
18 data can artificially inflate sample size, which leads to falsely precise parameter estimates.

19

20 **Upscaling**

21 Another approach is to use ML to map local observations to the global scale to mitigate
22 representativeness issues that can arise from the assimilation of local observations. For
23 example, studies by Beer et al. (2010), Joiner et al. (2018), Jung et al. (2011) and Tramontana
24 et al. (2016) all have used ML approaches in combination with remote sensing observations to
25 generate global estimates of carbon and energy fluxes from local flux-tower observations.
26 Vergopolan et al. (2021) used a high-resolution LSM and an ML Bayesian merging scheme
27 trained on in-situ soil moisture data to learn LSM and SMAP satellite biases and obtain 30m
28 satellite-based soil moisture estimates over the contiguous United States. One caveat to using
29 ML to upscale point observations is that large discrepancies can exist between different data
30 products based on the same observations, highlighting the need for thorough evaluation and
31 uncertainty assessment of ML-based products.

32

33 **Derived Quantities**

34 Finally, ML can be used to improve the algorithms used to generate observation datasets. For
35 example, Tramontana et al. (2020) used a combined neural network approach that accounts for
36 the influence of soil property and micrometeorological drivers to generate improved estimates of
37 the partitioning of observed NEE into GPP and ecosystem respiration (RECO), while Zeng et al.
38 (2022) used an ML approach to separate the natural and anthropogenic contributions to
39 satellite-estimated evapotranspiration.

40 **4.4 Optimisation process**

41 Since optimisation is a key component to both ML and DA, there are many algorithms common
42 to both fields including gradient-based and evolutionary algorithms (Sect. 2). Indeed, the strong

1 mathematical similarities between ML and DA mean that both fields can learn from each other
2 and share methodologies (Geer, 2021). ML approaches can be used to improve optimisation
3 algorithms themselves by helping speed up the search process and improve the quality of
4 solutions (Song et al., 2019). Furthermore, ML can be used to automatically choose the setting
5 of adjustable parameters found in some optimisation algorithms. For example, clustering
6 methods can be used to set the population size, crossover probability and mutation probability
7 parameters in genetic algorithms (Zhang et al., 2007) and maintain population diversity.
8 Tree-based random forest models have been used to dynamically construct, search, and prune
9 the parameter space to efficiently optimise ML structure and hyperparameters (Akiba et al.,
10 2019). ML techniques can also be used to choose the best-performing algorithm for a particular
11 optimisation problem (Kerschke et al., 2019). While the emerging ML methods are promising,
12 they are very novel and - to the best of our knowledge - have not yet been applied to optimising
13 the parameter estimation algorithm hyperparameters themselves.

14

15 Finally, a novel and emerging use of ML is the use of large language models (e.g. ChatGPT).
16 Modern open-source coding languages like Julia and Python through the Google JAX library
17 (Bradbury et al., 2018) can be automatically differentiated to generate the tangent linear model
18 (see Sect. 2). Many high-complexity LSMs are written in Fortran code; large language models
19 can help translate Fortran code to more modern languages (Zhou et al., 2024), facilitating the
20 derivative of such models. Alternatively, we can use neural networks to emulate the tangent
21 linear and adjoint models since neural networks can be differentiated trivially (Hatfield et al.,
22 2021).

23

24 Table 1: Summary of challenges outlined in Sect. 3 and their ML opportunities

PDA challenge	ML opportunity
Selecting parameters and their prior distributions (Sect. 3.1)	
<ul style="list-style-type: none">- Identifying which model parameters to optimise is challenging, due to high dimensionality and strong parameter covariances.- Choosing prior distributions for parameters is crucial yet difficult, requiring detailed structural insights and data.	<ul style="list-style-type: none">- Emulators can reduce the computational demand of running models with many different parameter settings needed for sensitivity analyses (Sect. 4.1).- Emulators can be used to facilitate uncertainty quantification, for example, through history matching (Sect. 4.1).
Characterisation of model and data/observation errors (Sect. 3.2)	
<ul style="list-style-type: none">- Model errors are difficult to quantify due to uncertainties in process representation, missing processes, and the challenge of specifying an informative prior.- Quantifying data errors is tricky because of sampling variability, instrument inaccuracies, and complex error correlations that are often ignored.	<ul style="list-style-type: none">- Hybrid modelling can be used to replace model processes that are missing or poorly understood, helping to diagnose model structural errors (Sect. 4.2).- ML methods can be used to generate improved estimates of derived quantities, thus reducing observation errors (Sect. 4.3).

Developing observation operators (Sect. 3.3)	
<ul style="list-style-type: none"> - Matching model outputs to observations require transformations that can introduce biases. 	<ul style="list-style-type: none"> - ML-generated observation operators can be used to directly translate satellite-observed radiances into model states or parameters (Sect. 4.3).
Tackling spatial and temporal heterogeneity (Sect. 3.4)	
<ul style="list-style-type: none"> - Variability in surface properties, driven by diverse climates, soils, and ecosystems, complicates parameter estimation across locations. - High computational demands make it difficult to calibrate LSMs across large spatial domains. - Temporal variability and short data series hinder the capture of both seasonal cycles and long-term trends. 	<ul style="list-style-type: none"> - Hybrid modelling can be used to improve spatial parameterisations (Sect. 4.2). - Emulators can help reduce the computational demand of running the model over large domains (Sect. 4.1). - Long Short-Term Memory encoder-decoder networks consider long-term dependencies and therefore may help capture seasonal and interannual trends (Sect. 4.1).
Dealing with large and multiple observational datasets (Sect. 3.5)	
<ul style="list-style-type: none"> - Scaling satellite products to match model grids can lead to information loss. - Products may be subject to regional biases due to varying data quality and processing methods. - Assimilating multiple data streams in model calibrations presents challenges in consistency, error characterisation, and balancing different data sources. 	<ul style="list-style-type: none"> - ML methods can be used to upscale sparse observational data (e.g., flux tower observations) or map satellite observations to a model grid (Sect. 4.3). - ML can be applied to improve the algorithms used to produce observational datasets (Sect. 4.3). - ML-based observation operators are able to easily accommodate multiple observation types and adjust their respective impacts in the assimilation (Sect. 4.3).
Including the historical period in the assimilation window (Sect. 3.6)	
<ul style="list-style-type: none"> - Spin-up and transient parts of model runs can be computationally demanding. 	<ul style="list-style-type: none"> - Hybrid modelling can be used to replace computationally costly parts of the model (Sect. 4.2).
Choice and implementation of minimisation algorithms (Sect. 3.7)	
<ul style="list-style-type: none"> - Algorithms requiring a large number of model runs are computationally costly and therefore rarely applied to complex LSMs. - For different algorithms, there can be a large number of configuration options and tuneable hyperparameters. 	<ul style="list-style-type: none"> - ML can enhance computational efficiency, enabling the use of algorithms that require numerous model runs (Sect. 4.1). - ML can help find the best configurations and hyperparameters to use when optimising (Sect. 4.4).

<ul style="list-style-type: none"> - Maintaining tangent linear/adjoint models for gradient-based optimisation in complex LSMs is challenging. 	<ul style="list-style-type: none"> - Large language models can be used to translate LSMs to modern coding languages that are easier to differentiate and can better exploit GPU. Alternatively, we can emulate the LSM using NNs, which are easily differentiable (Sect. 4.4).
---	---

¹ 5. Future priorities

² Moving beyond the ML avenues outlined in the previous section and summarised in Table 1,
³ here, we discuss the opportunities and future priorities where land PDA promises to have some
⁴ large impacts, building on recent successes. We argue that more funding for technical DA
⁵ studies and software engineering support would significantly aid this work.

⁶ 5.1 Testing novel datasets and experimental configurations

⁷ In addition to the traditional datasets used to optimise LSM parameters, our data-rich world
⁸ offers access to a wide array of data streams enabling new and exciting constraints on multiple
⁹ different processes in LSMs (as have been used for parameter DA in smaller scale ecosystem
¹⁰ and ecology models). These include (to name a few):

- ¹¹ • **Manipulation experiments:** For example, elevated CO₂ experiments can be used to constrain the fertilisation effect at nitrogen-limited sites (Thomas et al., 2017; Jiang et al., 2020; Mahmud et al., 2018; Raoult, Edouard-Rambaut, et al., 2024).
- ¹⁴ • **Data about soil carbon stocks:** Data from the International Soil Carbon Network (Harden et al., 2018; Nave et al., 2016) and the global soil respiration database (Jian et al., 2021) can provide valuable insights. Similarly, soil radiocarbon measurements (Lawrence et al., 2020) can help constrain rates of soil carbon cycling (Shi et al., 2020) and carbon isotope concentrations can be used to improve simulated soil organic matter decomposition (Mäkelä et al., 2022).
- ²⁰ • **Tree ring data:** Annual biomass increments derived from tree ring widths can help infer carbon accumulation (Babst et al., 2014; Jeong et al., 2021). Similarly, tree ring isotopic data (carbon and oxygen) can act as constraints for leaf physiology and growth (Barichivich et al., 2021).
- ²⁴ • **Other aboveground biomass products:** Products from the ESA BIOMASS mission (Quegan et al., 2019) help constrain carbon allocation and woody biomass turnover parameters (Smallman et al., 2021). Similarly, land-use and land-cover products (e.g., MapBiomas Collection 3.1, based on Landsat) can be used to create regrowth curves (Heinrich et al., 2021, 2023), which together with forest inventory data, can help constrain disturbance processes.
- ³⁰ • **Additional remote sensing datasets:** New datasets, such as full-waveform lidar data from the GEDI (Global Ecosystem Dynamics Investigation) mission (Dubayah et al., 2020), can help constrain canopy structural parameters, including canopy height (Potapov et al., 2021). Similarly, improved observations of land surface temperature and total

1 surface/groundwater content from GRACE instruments also can offer additional
2 constraints on the energy and water cycles.

3 • **Trace gas flux measurements:** Carbonyl sulfide measurements (Whelan et al., 2018)
4 can be used to constrain GPP and stomatal conductance (Abadie et al., 2023). There is
5 also a growing number of nitrous oxide flux measurements (Nicolini et al., 2013), which
6 can be used to calibrate LSMs that include nitrogen cycles. Methane flux measurements,
7 such as those over peatlands ((Salmon et al., 2022), can also be utilised to improve the
8 representation of methane production processes.

9 By combining these data and implementing novel DA approaches described in this paper, we
10 can aspire to assess how this information influences both short-term and long-term forecasts
11 and reduces model discrepancies. The focus should be on refining core processes driving
12 ecosystem-scale carbon and water fluxes and testing their responses to global change, beyond
13 just fitting historical data.

14

15 As with all past carbon cycle DA studies, before novel datasets can be reliably used in a DA
16 experiment, it will take time to test the best approaches for how to best use these data streams
17 within a DA experimental framework. It should be standard practice to run synthetic DA
18 experiments to test which observational characteristics (temporal sampling interval, record
19 length, observation uncertainty, choice of minimisation algorithm and its configuration, etc. –
20 Sect. 3.7) are required to retrieve the correct parameter values with the strong assumption that
21 there is no modelling bias. Synthetic experiments, also known as “twin” experiments, use
22 “pseudo data” that have been output from the model and modified according to known
23 observational characteristics (see REFLEX and Optic experiments; Trudinger et al., 2007; Fox
24 et al., 2009). As these data are model outputs, the “true” value of the parameters is known.
25 Synthetic DA experiments can also be used prior to data collection, where they can help
26 optimise sampling over space, time, and sampling design. Indeed, calibration has yet to be
27 adequately integrated into the broader literature on model-driven observing system simulation
28 experiments. To improve this, advocating for standardised community benchmark protocols and
29 datasets could address different challenges, such as assessing resistance to noise and
30 evaluating forcing variability. Results from such community-driven experimental setups could
31 reveal common challenges and development opportunities, enhancing the robustness and
32 effectiveness of DA methods across the field (see Sect. 5.4).

33

34 Additional tests of DA experimental configuration that are rarely performed (or rarely reported in
35 the literature) should include testing i) how parameters retrieved at individual sites compare to
36 parameters retrieved when including multiple sites in the assimilation (Kuppel et al., 2012;
37 Raoult et al., 2016) or using hierarchical approaches (Fer, Shiklomanov, et al., 2021; Tian et al.,
38 2020)(see Sect. 3.4), ii) the utility of PFT dependent parameters versus alternative approaches
39 for grouping parameters (e.g., regionally dependent PFTs - e.g. Dahlin et al., 2017; Bao et al.,
40 2023), iii) how retrieved parameters vary with the forcing dataset used in the simulations, iv)
41 how retrieved values depend on which parameters and/or PFTs are optimised or which terms to
42 include in the cost function, and v) how retrieved parameters vary in space and time within PFTs
43 and what this tells us about missing processes, among other factors. A critical test of any
44 parameterisation process is that the newly trained model must have improved predictive skill for

1 independent data. For example, Famiglietti et al. (2021) demonstrated that different data
2 combinations impact the resultant predictive skill and that the amount of data used in model
3 calibration must be commensurate with the complexity of the model. Such technical tests are
4 required each time a new process is optimised or a novel dataset is used in the assimilation.
5 Building DA frameworks to include this technical testing will give confidence in using retrieved
6 parameter values in operational versions of the models.

7 5.2 Moving towards land surface–atmospheric transport and full 8 Earth system model coupling in data assimilation

9 Atmospheric CO₂ mole fraction measurements collected at tall towers around the world have
10 proven valuable in improving NEE predictions at regional to global scales within a carbon cycle
11 DA framework (Bacour et al., 2023; Castro-Morales et al., 2019; Kaminski et al., 2002, 2012,
12 2013; Knorr & Heimann, 1995; Koffi et al., 2012; Peylin et al., 2016; Rayner et al., 2005;
13 Scholze et al., 2007, 2016; Schürmann et al., 2016). While atmospheric CO₂ data provide a
14 direct constraint on net surface CO₂ exchange, reliable representation of terrestrial carbon
15 sources and sinks ideally requires accurate simulations of the gross carbon fluxes. However,
16 while global scale estimates of GPP are available for model evaluation or assimilation purposes
17 (Joiner et al., 2018; Nelson et al., 2024) the currently available RECO products are still subject
18 to large uncertainties. For instance, empirically upscaled RECO from eddy covariance
19 measurements provided by FLUXCOM are inconsistent with inversion-based products in the
20 tropics, possibly due to low sampling density in the region (Jung et al., 2020). *In situ* data are
21 sparse and site history does not reflect larger-scale disturbance adequately. One benefit of
22 assimilating atmospheric CO₂ concentration data is that it is one of the only datasets that can
23 provide a large spatial scale constraint (albeit indirect) on RECO because it is heavily influenced
24 by soil carbon stocks; thus, assimilating atmospheric CO₂ data presents an opportunity to
25 improve the representation of both soil carbon flux and stock trajectories in LSMs, which is
26 crucial for future predictions regarding the carbon sink capacity of terrestrial ecosystems.

27
28 However, the assimilation of atmospheric CO₂ data requires coupling LSMs with atmospheric
29 transport models in order to scale the simulated land surface fluxes to atmospheric CO₂
30 concentrations at specified vertical levels (for station data) or integrated over the atmospheric
31 column (for space-borne data). The observational constraints of atmospheric CO₂ data on LSM
32 parameters is also more "diffuse" than when assimilating surface observations. This is due to
33 the inclusion of additional modelling errors associated with the atmospheric model itself (physics
34 and spatial/vertical discretisation) and with the other CO₂ fluxes required as inputs (mainly
35 ocean fluxes, fossil fuel emissions, and biomass burning). The coupling also presents technical
36 and computational challenges. Compared to LSMs, the derivation of the tangent linear and
37 adjoint models of atmospheric transport models is more straightforward (Kaminski et al., 1999;
38 Meirink et al., 2008; Rödenbeck et al., 2003), but their implementation increases the
39 computational load. One approach to overcome this issue is to use pre-calculated transport
40 fields of the sensitivity of mean atmospheric concentrations at selected stations to the surface
41 net CO₂ flux (see Peylin et al. (2016); or Bacour et al. (2023) for further details). However, this
42 method has limited spatial and temporal coverage due to the finite time period of the

1 precalculated sensitivities (estimating these sensitivities is also technically and computationally
2 expensive). Assimilation of space-borne retrievals of XCO₂ (column-averaged carbon dioxide)
3 with global coverage and pre-computed transport in SDBM and BETHY was demonstrated by
4 Kaminski et al. (2010) and Kaminski & Mathieu (2017). Recent advances in the utilisation of
5 graphics accelerators (Chevallier et al., 2023) offer hope for a significant reduction in
6 computational times and the development of full coupling between LSMs and atmospheric
7 transport models in the near future.

8

9 While coupling to an atmospheric transport model at least permits the use of atmospheric CO₂
10 data in parameter DA experiments, the ultimate goal for LSM parameter calibration is within a
11 fully coupled ESM. This would allow representation of carbon-climate and land-atmosphere
12 feedbacks within the optimisations. To date, there has been limited assessment of whether
13 posterior parameter values from offline DA experiments compare to retrieved values from fully
14 coupled runs (nor how retrieved values vary when different offline climate reanalysis forcing
15 products are used). To achieve this goal, LSM DA groups should learn from advances made in
16 the NWP community (de Rosnay et al., 2022). As discussed at length in this review, while
17 computational cost has so far been a prohibiting factor in achieving full ESM coupling, new ML
18 techniques for model emulation (Sect. 4.1) (Watson-Parris et al., 2021) and automatic
19 differentiation of model code (Gelbrecht et al., 2023) should help considerably in alleviating this
20 problem (see Sect. 3.7 for remaining challenges).

21 5.3 Identifying and improving structural errors and model 22 representation

23 The best estimates of different parameters are very dependent on the experimental setup and
24 so few of the optimised parameter values are actually used in the operational version of each
25 LSM—although this is something to strive for in future efforts. Indeed, even when calibrated
26 parameters have been shown to improve model performance, getting them to be the new
27 defaults in coupled models is non-trivial (Kyker-Snowman et al., 2022). Instead, the main
28 strength of parameter estimation for LSMs and, therefore, its main purpose thus far, has been to
29 identify structural errors. If we cannot match observations within the bounds of their known
30 uncertainties by simply changing the parameter values, this suggests that a process is poorly
31 represented or missing from the model. This critical information is then fed back to the model
32 developers to ensure changes are made to the model, before restarting the cycle of model
33 calibration. Although this exchange is key in developing any LSM, it is rarely published.
34 Nevertheless, a few documented examples from the ORCHIDEE land surface model workflow
35 exist. MacBean et al. (2015) demonstrated that temperate broadleaved temperature thresholds
36 for senescence in the ORCHIDEE LSM were too low. The newly optimised parameters have
37 since been included in ORCHIDEE trunk versions. Salmon et al. (2022) found that when
38 constraining parameters of the ORCHIDEE LSM against methane emissions in northern
39 peatlands, the process providing enough active carbon for methanogenesis was missing. Raoult
40 et al. (2023) found by assimilating MODIS snow albedo over Greenland that a three-layered ice
41 sheet model was insufficient to simulate accurately both the snow albedo and runoff rates,
42 leading to further discretisation of the model.

1
2 However, careful consideration is needed to avoid equating the status quo of making changes to
3 models—often involving increased complexity—with progress in model development. While
4 identifying and addressing structural errors is crucial, introducing new processes or refining
5 existing ones can sometimes lead to models that are more complex without necessarily
6 improving their predictive power. It is important to strike a balance between enhancing model
7 accuracy and maintaining model parsimony. Overly complex models can become difficult to
8 validate and manage, potentially obscuring rather than clarifying underlying processes.
9 Therefore, the goal should be to make thoughtful adjustments that improve model performance
10 while ensuring that the added complexity is justified by significant improvements in accuracy or
11 functionality. This approach ensures that models remain robust and efficient and that any
12 modifications contribute meaningfully to their overall effectiveness.

13
14 As parameter estimation methods and systems become more developed, we can run more
15 experiments to quantify and reduce uncertainty due to poorly constrained parameters using
16 different driving datasets and versions of the model that account for different representations of
17 processes. In the wider climate science literature, there exist promising approaches to provide
18 objective assessments of structural and parametric components of model error (Peatier et al.,
19 2023). Moreover, the proposed move to more modular LSMs (Fisher & Koven, 2020) will also
20 allow for different processes in the model to be isolated and calibrated sequentially, reducing the
21 scale of parameter subspaces to be calibrated and enabling better testing of alternative
22 hypotheses (e.g., different stomatal optimisation theories) and facilitate collaboration across
23 different modelling groups.

24 5.4 International collaboration: intercomparison studies and 25 shared toolboxes

26 Efforts by AIMES and ILMF to build a Land Data Assimilation Community have significantly
27 advanced knowledge sharing through online workshops and town halls, highlighting the
28 importance of continued collaboration. The goal is to facilitate cross-group interaction for DA
29 methods training, knowledge exchange on technical DA developments and calibrated model
30 intercomparison projects. The learning curve associated with learning DA for land surface
31 modelling is steep. This is exacerbated by the lack of community-wide educational materials
32 (although some resources exist, see <https://land-da-community.github.io/training/> for a selective
33 list, last accessed 27th August 2024). Understanding of DA methods is also hampered by the
34 fact that technical studies testing different DA configurations are generally buried in
35 supplementary materials or not published at all. Parameter DA system intercomparison studies
36 would help to determine how much parameter uncertainty is contributing to the spread in model
37 projections. This would signal to the wider LSM community that parameter uncertainty
38 quantification and reduction are needed to improve future projections of carbon-climate
39 feedbacks and land-atmosphere interactions. One desirable outcome may be to create and
40 share statistical toolboxes utilising community cyberinfrastructure, for example, following the
41 pioneering example of PEcAn (Predictive Ecosystem Analyzer; Fer, Gardella, et al., 2021;
42 LeBauer et al., 2013), which offers a complete end-to-end informatic structure, as well as

1 open-source land surface model benchmarking tools (iLAMB: Collier et al., 2018; Seiler et al.,
2 2022). While LSMs with established DA systems may not switch to a community toolbox, such
3 shared toolboxes will facilitate knowledge sharing, intercomparison studies and training of early
4 career researchers. Simultaneously, if LSMs with established DA systems made more of their
5 tools available within established community toolboxes, it would help reduce redundant
6 research efforts and make the adoption of such tools easier. This is one of the big lessons we
7 can learn as a community from the recent boom in ML. In addition to the improved hardware
8 (e.g., GPUs), new algorithms and huge datasets, one of the reasons ML has been so successful
9 is because the research has been done with a collaborative spirit and developed using
10 open-source frameworks (e.g., TensorFlow, PyTorch, JAX).

11 5.5 Propagation of error reductions to constrain climate 12 predictions

13 Many studies have successfully constrained parameter uncertainty in LSMs, leading to reduced
14 uncertainty in contemporary land-atmosphere carbon fluxes. However, this reduction in
15 uncertainty has not been fully propagated to constrain future projections. There is a clear
16 opportunity to take this extra step to enable observationally constrained probabilistic statements
17 to be made about the future of the land biosphere. Such efforts are already commonplace in
18 ensembles of reduced complexity models (Sanderson, 2020; Smith et al., 2024), where large
19 ensembles of future projections are computationally trivial, but the difficulty of spinning up slow
20 carbon pool processes and ocean circulation in ESMs remains a challenge for probabilistic
21 coupled projections with ESMs (without flux corrections, (Irvine et al., 2013)). However, with
22 increased computational power, we are acquiring the capability to run LSMs as ensembles
23 rather than relying on a single realisation, thereby enabling us to better capture the uncertainty
24 of model predictions (Arora et al., 2023).

25
26 By sampling from the posterior distributions after a PDA experiment, we can generate ensemble
27 simulations which can be used to explore future scenarios and idealised experiments (e.g.
28 1%/yr CO₂ concentration increase) and quantify constrained distributions of carbon-climate-CO₂
29 feedbacks. For example, by weighting the probability of each of the ensemble members, we can
30 create probability density functions of future land carbon storage for different locations, thus
31 narrowing the associated uncertainty of the future land sink and subsequently leading to more
32 accurate calculations of carbon budget estimates. Although this can easily be done for simpler
33 models where MCMC can be applied, for computational demanding models, there are two
34 critical yet distinct questions in this area that need addressing. The first is how to generate joint
35 posterior distributions for large models, which likely requires the use of emulators (see Sect.
36 4.1). The second is how to intelligently select parameter vectors from those distributions.
37 Currently, simple models might propagate uncertainty by using 100-1000 ensemble members,
38 but protocols like that used in the Coupled Model Intercomparison Project (CMIP) are not yet
39 adopting such large ensembles, again due to computational expense and constraints on data
40 storage. As a climate community, we should be striving to move towards using data-constrained
41 ensemble simulations in CMIP or the TRENDY model intercomparison project (Sitch et al.,
42 2024) to quantify uncertainties in model predictions reported in the Intergovernmental Panel on

¹ Climate Change (IPCC) 8th Assessment Report, the annual Global Carbon Budget (GCB) and
² other emerging frameworks quantifying land carbon trajectories. Therefore, we must develop
³ methods to maximise the propagation and partitioning of uncertainty with a limited number of
⁴ ensemble runs. Constraining parameter uncertainty via improved DA and ML techniques should
⁵ also help to reduce inter-model spread in CMIP and TRENDY, as model differences are likely
⁶ partly attributable to variations in parameter values between models.

⁷

⁸ Other international frameworks that oversee policies and socioeconomic management of
⁹ terrestrial carbon stocks – such as the voluntary carbon market and national emissions reporting
¹⁰ for Nationally Determined Contributions under the Paris Agreement – already require estimates
¹¹ of model uncertainty; however, so far the models used in voluntary carbon market offset project
¹² verification tend to be of simple to intermediate complexity, and not full complexity LSMs. Better
¹³ estimating uncertainty in LSMs via methods such as parameter DA should therefore facilitate
¹⁴ their use in a wider range of policy and carbon management initiatives.

¹⁵ 6. Summary and conclusion

¹⁶ Improving the accuracy of land surface models (LSMs) is of vital importance since land surface
¹⁷ feedbacks on climate change represent one of the largest sources of uncertainty in climate
¹⁸ change projections. Parameter data assimilation is critical for enhancing the performance and
¹⁹ reliability of these LSMs. This process involves determining the best estimates of model
²⁰ parameters, and their uncertainties, that best align the model outputs with observed data.
²¹ Effective parameter estimation helps in capturing the complex dynamics of land-atmosphere
²² interactions and improves the model's ability to simulate real-world phenomena. However, LSMs
²³ used to predict future climate scenarios (e.g., when coupled to Earth System Models) are
²⁴ complex in nature leading to many challenges when performing global scale optimisations.
²⁵ Nevertheless, advances in computational capability, novel datasets and emerging technologies
²⁶ offer promising avenues for improving parameter accuracy and model calibration.

²⁷ Machine learning (ML) clearly has a pivotal part to play in the future of land surface model data
²⁸ assimilation, helping to streamline the assimilation process, manage large datasets and speed
²⁹ up otherwise computationally demanding processes. International collaboration is crucial in this
³⁰ endeavour, as shared knowledge and resources can significantly accelerate the advancement
³¹ of LSM calibration and data assimilation. Efforts to build a Land Data Assimilation Community,
³² such as those by the AIMES Land Data Assimilation Working Group and the International Land
³³ Model Forum, have already made substantial progress in facilitating cross-group interactions.
³⁴ These collaborative platforms are essential for training, knowledge exchange, and the
³⁵ development of standardised methodologies, ultimately leading to more accurate LSMs.

¹ Acknowledgements

² This manuscript is the result of efforts by the Analysis, Integration, and Modeling of the Earth
³ System (AIMES) Land DA Working Group annual virtual workshops
⁴ (<https://aimesproject.org/lawg/>) and initiatives to build a Land DA Community
⁵ (<https://land-da-community.github.io>). NR has been supported by a H2020 Marie
⁶ Skłodowska-Curie Actions grant (no. 101026422). ND and TQ would like to acknowledge
⁷ funding from the UKRI National Centre for Earth Observation, under the International Science
⁸ Programme (NE/X006328/1). AR and MD acknowledge funding from NSF MSB 2406258 and
⁹ MD further acknowledges funding from NASA CMS 80NSSC21K0965. KD, LH and PG would
¹⁰ like to acknowledge funding from the National Science Foundation (NSF) Science and
¹¹ Technology Center (STC) Learning the Earth with Artificial Intelligence and Physics (LEAP),
¹² Award # 2019625-STC. KD further acknowledges support from the U.S. Department of Energy,
¹³ Office of Biological & Environmental Research (BER), under Award DE-SC0022070, the
¹⁴ National Science Foundation (NSF) under IA 1947282, and the National Center for Atmospheric
¹⁵ Research (NCAR) through Cooperative Agreement No. 1852977 NM acknowledges support
¹⁶ from the Wolfe-Western Fellowship At-Large for Outstanding Newly Recruited Research
¹⁷ Scholars Endowment Fund. IF acknowledges funding from the Research Council of Finland
¹⁸ (grant number 337552) and Horizon Europe, HORIZON-MISS-2022-SOIL-01-05. TLS was
¹⁹ funded by the National Centre for Earth Observation, under the LTSS programme
²⁰ (NE/R016518/1) and the UK's EO Climate Information Service (NE/X019071/1). MS
²¹ acknowledges support from three Swedish strategic research areas: Modelling the Regional
²² and Global Earth system (MERGE), the e-science collaboration (eSSENCE), and Biodiversity
²³ and Ecosystems in a Changing Climate (BECC).

²⁴ Open research

²⁵ **Data Availability statement:** This article discusses the challenges and priorities in the field of
²⁶ parameter estimation for land data assimilation, and the opportunities offered by machine
²⁷ learning—it does not include the specific use of any particular software or results involving
²⁸ specific data products.

²⁹

¹ Appendix

² The process-based models mentioned through the paper are listed in Table A1. This list cover
³ wide spectrum of land models ranging in complexity and computational demand, including
⁴ LSMs that simulate interactions between carbon, water, and energy cycles, often incorporating
⁵ other biogeochemical cycles (e.g., nitrogen cycling) and dynamic vegetation processes;
⁶ stand-alone DGVMs that have more complex representation of vegetation demography
⁷ (so-called vegetation demographic models, VDMs) but may not fully represent energy and
⁸ hydrology components; and ecosystem models that primarily represent carbon cycling and
⁹ simple representations of vegetation and hydrology processes but may lack the full mechanistic
¹⁰ representation of energy and hydrological processes or vegetation dynamics seen in LSMs and
¹¹ VDMs.

¹² **Table A1.** References for the process-based models mentioned in this article.

Acronym	Full name	Model reference
BETHY	Biosphere Energy Transfer Hydrology	Knorr (2000)
CABLE	Community Atmosphere Biosphere Land Exchange	Kowalczyk et al., (2006)
CARDAMOM	CARbon DATA MOdel fraMework	Bloom et al. (2016); Smallman et al. (2021)
CLASSIC	Canadian Land Surface Scheme Including Biogeochemical Cycles	Melton et al. (2020)
CLM	Community Land Model	Lawrence et al. (2019)
D&B	DALEC & BETHY	Knorr et al. (2024)
DALEC	Data Assimilation Linked Ecosystem Carbon	Williams et al. (2005)
ED	Ecosystem Demography	Ma et al. (2022); Moorcroft et al. (2001)
ECLand	European Centre for Medium-range Weather Forecasts Land model (based on CHTESSEL: Carbon-Hydrology Tiled Scheme for Surface Exchanges over Land)	Boussetta et al. (2021)

FATES	Functionally Assembled Terrestrial Ecosystem Simulator	Fisher et al. (2015); Koven et al. (2020)
FöBAAR	Forest Biomass, Assimilation, Allocation and Respiration	Keenan et al. (2012)
JULES	Joint UK Land Environment Simulator	Best et al. (2011); Clark et al. (2011)
JSBACH	Jena Scheme for Biosphera-Atmosphere Coupling in Hamburg	Mauritsen et al (2019); Reick et al. (2021)
LPJ-GUESS	Lund-Potsdam-Jena General Ecosystem Simulator	Smith (2007)
Noah	-	Ek et al. (2003)
ORCHIDEE	Organising Carbon and Hydrology In Dynamic Ecosystems	Krinner et al. (2005); Vuichard et al. (2019); Zaehle, Friend, et al. (2010)
SDBM	Simple Diagnostic Biosphere Model	Knorr & Heimann (1995)
SIPNET	Simplified Photosynthesis and Evapotranspiration	Braswell et al. (2005)
TECOS	terrestrial ecosystem	Xu et al., (2006)

1 References

2 Abadie, C., Maignan, F., Remaud, M., Kohonen, K.-M., Sun, W., Kooijmans, L., Vesala, T.,
3 Seibt, U., Raoult, N., Bastrikov, V., Belviso, S., & Peylin, P. (2023). Carbon and water fluxes
4 of the boreal evergreen needleleaf forest biome constrained by assimilating ecosystem
5 carbonyl sulfide flux observations. *Journal of Geophysical Research. Biogeosciences*,
6 128(7), e2023JG007407. <https://doi.org/10.1029/2023jg007407>

7 Abramoff, R., Xu, X., Hartman, M., O'Brien, S., Feng, W., Davidson, E., Finzi, A., Moorhead, D.,
8 Schimel, J., Torn, M., & Mayes, M. A. (2018). The Millennial model: in search of measurable
9 pools and transformations for modeling soil carbon in the new century. *Biogeochemistry*,
10 137(1-2), 51–71. <https://doi.org/10.1007/s10533-017-0409-7>

11 Akiba, T., Sano, S., Yanase, T., Ohta, T., & Koyama, M. (2019). Optuna: A Next-generation
12 Hyperparameter Optimization Framework. In *arXiv [cs.LG]*. arXiv.
13 <http://arxiv.org/abs/1907.10902>

14 Alejomhammad, S. H., Fang, B., Konings, A. G., Aires, F., Green, J. K., Kolassa, J., Miralles, D.,
15 Prigent, C., & Gentine, P. (2017). Water, Energy, and Carbon with Artificial Neural Networks
16 (WECANN): A statistically-based estimate of global surface turbulent fluxes and gross
17 primary productivity using solar-induced fluorescence. *Biogeosciences*, 14(18), 4101–4124.
18 <https://doi.org/10.5194/bg-14-4101-2017>

19 Alton, P. B. (2013). From site-level to global simulation: Reconciling carbon, water and energy
20 fluxes over different spatial scales using a process-based ecophysiological land-surface
21 model. *Agricultural and Forest Meteorology*, 176, 111–124.
22 <https://doi.org/10.1016/j.agrformet.2013.03.010>

23 Arora, V. K., Katavouta, A., Williams, R. G., Jones, C. D., Brovkin, V., Friedlingstein, P.,
24 Schwinger, J., Bopp, L., Boucher, O., Cadule, P., Chamberlain, M. A., Christian, J. R.,
25 Delire, C., Fisher, R. A., Hajima, T., Ilyina, T., Joetzjer, E., Kawamiya, M., Koven, C. D., ...
26 Ziehn, T. (2020). Carbon–concentration and carbon–climate feedbacks in CMIP6 models
27 and their comparison to CMIP5 models. *Biogeosciences*, 17(16), 4173–4222.
28 <https://doi.org/10.5194/bg-17-4173-2020>

29 Arora, V. K., Seiler, C., Wang, L., & Kou-Giesbrecht, S. (2023). Towards an ensemble-based
30 evaluation of land surface models in light of uncertain forcings and observations.
31 *Biogeosciences*, 20(7), 1313–1355. <https://doi.org/10.5194/bg-20-1313-2023>

32 Arsenault, K. R., Kumar, S. V., Geiger, J. V., Wang, S., Kemp, E., Mocko, D. M., Beaudoing, H.
33 K., Getirana, A., Navari, M., Li, B., Jacob, J., Wegiel, J., & Peters-Lidard, C. D. (2018). The
34 Land surface Data Toolkit (LDT v7.2) – a data fusion environment for land data assimilation
35 systems. *Geoscientific Model Development*, 11(9), 3605–3621.
36 <https://doi.org/10.5194/gmd-11-3605-2018>

37 Assem, H., Ghariba, S., Makrai, G., Johnston, P., Gill, L., & Pilla, F. (2017). Urban water flow
38 and water level prediction based on deep learning. In *Machine Learning and Knowledge
39 Discovery in Databases* (pp. 317–329). Springer International Publishing.
40 https://doi.org/10.1007/978-3-319-71273-4_26

41 Baatz, R., Hendricks Franssen, H. J., Euskirchen, E., Sihi, D., Dietze, M., Ciavatta, S., Fennel,
42 K., Beck, H., De Lannoy, G., Pauwels, V. R. N., Raiho, A., Montzka, C., Williams, M.,
43 Mishra, U., Poppe, C., Zacharias, S., Lausch, A., Samaniego, L., Van Looy, K., ...

1 Vereecken, H. (2021). Reanalysis in earth system science: Toward terrestrial ecosystem
2 reanalysis. *Reviews of Geophysics* (Washington, D.C.: 1985), 59(3), e2020RG000715.
3 <https://doi.org/10.1029/2020rg000715>

4 Babst, F., Bouriaud, O., Alexander, R., Trouet, V., & Frank, D. (2014). Toward consistent
5 measurements of carbon accumulation: A multi-site assessment of biomass and basal area
6 increment across Europe. *Dendrochronologia*, 32(2), 153–161.
7 <https://doi.org/10.1016/j.dendro.2014.01.002>

8 Bacour, C., MacBean, N., Chevallier, F., Léonard, S., Koffi, E. N., & Peylin, P. (2023).
9 Assimilation of multiple datasets results in large differences in regional- to global-scale NEE
10 and GPP budgets simulated by a terrestrial biosphere model. *Biogeosciences*, 20(6),
11 1089–1111. <https://doi.org/10.5194/bg-20-1089-2023>

12 Bacour, C., Maignan, F., MacBean, N., Porcar-Castell, A., Flexas, J., Frankenberg, C., Peylin,
13 P., Chevallier, F., Vuichard, N., & Bastrikov, V. (2019). Improving estimates of gross primary
14 productivity by assimilating solar-induced fluorescence satellite retrievals in a terrestrial
15 biosphere model using a process-based SIF model. *Journal of Geophysical Research: Biogeosciences*, 124(11), 3281–3306. <https://doi.org/10.1029/2019jg005040>

17 Bacour, C., Peylin, P., MacBean, N., Rayner, P. J., Delage, F., Chevallier, F., Weiss, M.,
18 Demarty, J., Santaren, D., Baret, F., Berveiller, D., Dufrêne, E., & Prunet, P. (2015). Joint
19 assimilation of eddy covariance flux measurements and FAPAR products over temperate
20 forests within a process-oriented biosphere model. *Journal of Geophysical Research: Biogeosciences*, 120(9), 1839–1857. <https://doi.org/10.1002/2015JG002966>

22 Bagnara, M., Silveyra Gonzalez, R., Reifenberg, S., Steinkamp, J., Hickler, T., Werner, C.,
23 Dormann, C. F., & Hartig, F. (2019). An R package facilitating sensitivity analysis, calibration
24 and forward simulations with the LPJ-GUESS dynamic vegetation model. *Environmental Modelling & Software: With Environment Data News*, 111, 55–60.
26 <https://doi.org/10.1016/j.envsoft.2018.09.004>

27 Baker, E., Harper, A. B., Williamson, D., & Challenor, P. (2022). Emulation of high-resolution
28 land surface models using sparse Gaussian processes with application to JULES.
29 *Geoscientific Model Development*, 15(5), 1913–1929.
30 <https://doi.org/10.5194/gmd-15-1913-2022>

31 Balsamo, G., Agusti-Panareda, A., Albergel, C., Arduini, G., Beljaars, A., Bidlot, J., Blyth, E.,
32 Bousserez, N., Boussetta, S., Brown, A., Buizza, R., Buontempo, C., Chevallier, F.,
33 Choulga, M., Cloke, H., Cronin, M. F., Dahoui, M., De Rosnay, P., Dirmeyer, P. A., ... Zeng,
34 X. (2018). Satellite and in situ observations for advancing global Earth surface modelling: A
35 review. *Remote Sensing*, 10(12), 2038. <https://doi.org/10.3390/rs10122038>

36 Bannister, R. N., Chipilski, H. G., & Martinez-Alvarado, O. (2020). Techniques and challenges in
37 the assimilation of atmospheric water observations for numerical weather prediction
38 towards convective scales. *Quarterly Journal of the Royal Meteorological Society*,
39 146(726), 1–48. <https://doi.org/10.1002/qj.3652>

40 Bao, S., Alonso, L., Wang, S., Gensheimer, J., De, R., & Carvalhais, N. (2023). Toward robust
41 parameterizations in ecosystem-level photosynthesis models. *Journal of Advances in
42 Modeling Earth Systems*, 15(8). <https://doi.org/10.1029/2022ms003464>

43 Barichivich, J., Peylin, P., Launois, T., Daux, V., Risi, C., Jeong, J., & Luysaert, S. (2021). A
44 triple tree-ring constraint for tree growth and physiology in a global land surface model.

1 *Biogeosciences*, 18(12), 3781–3803. <https://doi.org/10.5194/bg-18-3781-2021>

2 Bastrikov, V., MacBean, N., Bacour, C., Santaren, D., Kuppel, S., & Peylin, P. (2018). Land
3 surface model parameter optimisation using in situ flux data: Comparison of gradient-based
4 versus random search algorithms (a case study using ORCHIDEE v1. 9.5. 2). *Geoscientific
5 Model Development*, 11(12), 4739–4754. <https://gmd.copernicus.org/articles/11/4739/2018/>

6 Beer, C., Reichstein, M., Tomelleri, E., Ciais, P., Jung, M., Carvalhais, N., Rödenbeck, C., Arain,
7 M. A., Baldocchi, D., Bonan, G. B., Bondeau, A., Cescatti, A., Lasslop, G., Lindroth, A.,
8 Lomas, M., Luyssaert, S., Margolis, H., Oleson, K. W., Roupsard, O., ... Papale, D. (2010).
9 Terrestrial gross carbon dioxide uptake: global distribution and covariation with climate.
10 *Science (New York, N.Y.)*, 329(5993), 834–838. <https://doi.org/10.1126/science.1184984>

11 Best, M. J., Pryor, M., Clark, D. B., Rooney, G. G., Essery, R., Ménard, C. B., & Harding R.
12 (2011). The Joint UK Land Environment Simulator (JULES), model description—Part 1:
13 energy and water fluxes. *Geoscientific Model Development*, 4(3), 677–699.
14 <https://gmd.copernicus.org/articles/4/677/2011/>

15 Beucler, T., Pritchard, M., Rasp, S., Ott, J., Baldi, P., & Gentine, P. (2021). Enforcing analytic
16 constraints in neural networks emulating physical systems. *Physical Review Letters*, 126(9),
17 098302. <https://doi.org/10.1103/PhysRevLett.126.098302>

18 Bhouri, M. A., Joly, M., Yu, R., Sarkar, S., & Perdikaris, P. (2023). Scalable Bayesian
19 optimization with randomized prior networks. *Computer Methods in Applied Mechanics and
20 Engineering*, 417, 116428. <https://doi.org/10.1016/j.cma.2023.116428>

21 Bloom, A. A., Bowman, K. W., Liu, J., Konings, A. G., Worden, J. R., Parazoo, N. C., Meyer, V.,
22 Reager, J. T., Worden, H. M., Jiang, Z., Quetin, G. R., Smallman, T. L., Exbrayat, J.-F., Yin,
23 Y., Saatchi, S. S., Williams, M., & Schimel, D. S. (2020). Lagged effects regulate the
24 inter-annual variability of the tropical carbon balance. *Biogeosciences*, 17(24), 6393–6422.
25 <https://doi.org/10.5194/bg-17-6393-2020>

26 Bloom, A. A., Exbrayat, J.-F., van der Velde, I. R., Feng, L., & Williams, M. (2016). The decadal
27 state of the terrestrial carbon cycle: Global retrievals of terrestrial carbon allocation, pools,
28 and residence times. *Proceedings of the National Academy of Sciences of the United
29 States of America*, 113(5), 1285–1290. <https://doi.org/10.1073/pnas.1515160113>

30 Bloom, A. A., & Williams, M. (2015). Constraining ecosystem carbon dynamics in a data-limited
31 world: integrating ecological “common sense” in a model–data fusion framework.
32 *Biogeosciences*, 12(5), 1299–1315. <https://doi.org/10.5194/bg-12-1299-2015>

33 Blyth, E. M., Arora, V. K., Clark, D. B., Dadson, S. J., De Kauwe, M. G., Lawrence, D. M.,
34 Melton, J. R., Pongratz, J., Turton, R. H., Yoshimura, K., & Yuan, H. (2021). Advances in
35 land surface modelling. *Current Climate Change Reports*, 7(2), 45–71.
36 <https://doi.org/10.1007/s40641-021-00171-5>

37 Bonan, G. B., & Doney, S. C. (2018). Climate, ecosystems, and planetary futures: The challenge
38 to predict life in Earth system models. *Science (New York, N.Y.)*, 359(6375).
39 <https://doi.org/10.1126/science.aam8328>

40 Booth, B. B. B., Jones, C. D., Collins, M., Totterdell, I. J., Cox, P. M., Sitch, S., Huntingford, C.,
41 Betts, R. A., Harris, G. R., & Lloyd, J. (2012). High sensitivity of future global warming to
42 land carbon cycle processes. *Environmental Research Letters*, 7(2), 024002.
43 <https://doi.org/10.1088/1748-9326/7/2/024002>

44 Boussetta, S., Balsamo, G., Arduini, G., Dutra, E., McNorton, J., Choulga, M., Agustí-Panareda,

1 A., Beljaars, A., Wedi, N., Munoz-Sabater, J., de Rosnay, P., Sandu, I., Hadade, I., Carver,
2 G., Mazzetti, C., Prudhomme, C., Yamazaki, D., & Zsoter, E. (2021). ECLand: The ECMWF
3 land surface modelling system. *Atmosphere*, 12(6), 723.
4 <https://doi.org/10.3390/atmos12060723>

5 Bradbury, J., Frostig, R., Hawkins, P., Johnson, M. J., Leary, C., Maclaurin, D., Necula, G.,
6 Paszke, A., VanderPlas, J., Wanderman-Milne, S., & Zhang, Q. (2018). JAX: *composable*
7 *transformations of Python+NumPy programs* (Version 0.3.13). <http://github.com/google/jax>

8 Braswell, B. H., Sacks, W. J., Linder, E., & Schimel, D. S. (2005). Estimating diurnal to annual
9 ecosystem parameters by synthesis of a carbon flux model with eddy covariance net
10 ecosystem exchange observations. *Global Change Biology*, 11(2), 335–355.
11 <https://doi.org/10.1111/j.1365-2486.2005.00897.x>

12 Breiman, L. (1996). Bagging predictors. *Machine Learning*, 24(2), 123–140.
13 <https://doi.org/10.1007/bf00058655>

14 Brynjarsdóttir, J., & O'Hagan, A. (2014). Learning about physical parameters: the importance of
15 model discrepancy. *Inverse Problems*, 30(11), 114007.
16 <https://doi.org/10.1088/0266-5611/30/11/114007>

17 Buotte, P. C., Koven, C. D., Xu, C., Shuman, J. K., Goulden, M. L., Levis, S., & Kueppers L.
18 (2021). Capturing functional strategies and compositional dynamics in vegetation
19 demographic models. *Biogeosciences*, 18(14), 4473–4490.
20 <https://bg.copernicus.org/articles/18/4473/2021/bg-18-4473-2021.html>

21 Byrd, R. H., Lu, P., Nocedal, J., & Zhu, C. (1995). A limited memory algorithm for bound
22 constrained optimization. *SIAM Journal on Scientific Computing: A Publication of the*
23 *Society for Industrial and Applied Mathematics*, 16(5), 1190–1208.
24 <https://doi.org/10.1137/0916069>

25 Caen, A., Smallman, T. L., de Castro, A. A., Robertson, E., von Randow, C., Cardoso, M., &
26 Williams, M. (2022). Evaluating two land surface models for Brazil using a full carbon cycle
27 benchmark with uncertainties. *Climate Resilience and Sustainability*, 1(1).
28 <https://doi.org/10.1002/clr2.10>

29 Cameron, D., Hartig, F., Minnuno, F., Oberpriller, J., Reineking, B., Van Oijen, M., & Dietze, M.
30 (2022). Issues in calibrating models with multiple unbalanced constraints: the significance
31 of systematic model and data errors. *Methods in Ecology and Evolution*, 13(12),
32 2757–2770. <https://doi.org/10.1111/2041-210x.14002>

33 Carvalhais, N., Reichstein, M., Ciais, P., Collatz, G. J., Mahecha, M. D., Montagnani, L., Papale,
34 D., Rambal, S., & Seixas, J. (2010). Identification of vegetation and soil carbon pools out of
35 equilibrium in a process model via eddy covariance and biometric constraints:
36 ECOSYSTEM C POOLS APART FROM EQUILIBRIUM. *Global Change Biology*, 16(10),
37 2813–2829. <https://doi.org/10.1111/j.1365-2486.2010.02173.x>

38 Carvalhais, N., Reichstein, M., Seixas, J., James Collatz, G., Pereira, J. S., Berbigier, P.,
39 Carrara, A., Granier, A., Montagnani, L., Papale, D., Rambal, S., Sanz, M. J., & Valentini, R.
40 (2008). Implications of the carbon cycle steady state assumption for biogeochemical
41 modeling performance and inverse parameter retrieval. *Global Biogeochemical Cycles*,
42 22(2). <https://doi.org/10.1029/2007GB003033>

43 Castro-Morales, K., Schürmann, G., Köstler, C., Rödenbeck, C., Heimann, M., & Zaehle, S.
44 (2019). Three decades of simulated global terrestrial carbon fluxes from a data assimilation

1 system confronted with different periods of observations. *Biogeosciences* , 16(15),
2 3009–3032. <https://doi.org/10.5194/bg-16-3009-2019>

3 Chaney, N. W., Herman, J. D., Ek, M. B., & Wood, E. F. (2016). Deriving global parameter
4 estimates for the Noah land surface model using FLUXNET and machine learning. *Journal*
5 *of Geophysical Research: Atmospheres*, 121(22), 13,218–13,235.
6 <https://doi.org/10.1002/2016JD024821>

7 Cheng, Y., Wang, W., Dettò, M., Fisher, R., & Shoemaker, C. (2024). Calibrating tropical forest
8 coexistence in ecosystem demography models using Multi-objective optimization through
9 population-based parallel surrogate search. *Journal of Advances in Modeling Earth*
10 *Systems*, 16(8), e2023MS004195. <https://doi.org/10.1029/2023ms004195>

11 Cheng, Y., Xia, W., Dettò, M., & Shoemaker, C. A. (2023). A framework to calibrate ecosystem
12 demography models within earth system models using parallel surrogate global
13 optimization. *Water Resources Research*, 59(1), e2022WR032945.
14 <https://doi.org/10.1029/2022wr032945>

15 Chen, X., Huang, Y., Nie, C., Zhang, S., Wang, G., Chen, S., & Chen, Z. (2022). A long-term
16 reconstructed TROPOMI solar-induced fluorescence dataset using machine learning
17 algorithms. *Scientific Data*, 9(1), 427. <https://doi.org/10.1038/s41597-022-01520-1>

18 Chevallier, F. (2007). Impact of correlated observation errors on inverted CO₂ surface fluxes
19 from OCO measurements. *Geophysical Research Letters*, 34(24).
20 <https://doi.org/10.1029/2007gl030463>

21 Chevallier, F., Lloret, Z., Cozic, A., Takache, S., & Remaud, M. (2023). Toward high-resolution
22 global atmospheric inverse modeling using graphics accelerators. *Geophysical Research*
23 *Letters*, 50(5). <https://doi.org/10.1029/2022gl102135>

24 Clark, D. B., Mercado, L. M., Sitch, S., Jones, C. D., Gedney, N., Best, M. J., & Cox P. (2011).
25 The Joint UK Land Environment Simulator (JULES), model description—Part 2: carbon
26 fluxes and vegetation dynamics. *Geoscientific Model Development*, 4(3), 701–722.
27 <https://gmd.copernicus.org/articles/4/701/2011/>

28 Cleary, E., Garbuno-Íñigo, A., Lan, S., Schneider, T., & Stuart, A. M. (2021). Calibrate, emulate,
29 sample. *Journal of Computational Physics*, 424, 109716.
30 <https://doi.org/10.1016/j.jcp.2020.109716>

31 Collatz, G. J., Ribas-Carbo, M., & Berry, J. A. (1992). Coupled photosynthesis-stomatal
32 conductance model for leaves of C₄ plants. *Functional Plant Biology: FPB*, 19(5), 519.
33 <https://doi.org/10.1071/pp9920519>

34 Collier, N., Hoffman, F. M., Lawrence, D. M., Keppel-Aleks, G., Koven, C. D., Riley, W. J., Mu,
35 M., & Randerson, J. T. (2018). The international land model benchmarking (ILAMB) system:
36 Design, theory, and implementation. *Journal of Advances in Modeling Earth Systems*,
37 10(11), 2731–2754. <https://doi.org/10.1029/2018ms001354>

38 Cooper, E. S., Dance, S. L., García-Pintado, J., Nichols, N. K., & Smith, P. J. (2019).
39 Observation operators for assimilation of satellite observations in fluvial inundation
40 forecasting. *Hydrology and Earth System Sciences*, 23(6), 2541–2559.
41 <https://doi.org/10.5194/hess-23-2541-2019>

42 Couvreux, F., Hourdin, F., Williamson, D., Roehrig, R., Volodina, V., Villefranque, N., Rio, C.,
43 Audouin, O., Salter, J., Bazile, E., Brient, F., Favot, F., Honnert, R., Lefebvre, M.-P.,
44 Madeleine, J.-B., Rodier, Q., & Xu, W. (2021). Process-based climate model development

1 harnessing machine learning: I. a calibration tool for parameterization improvement. *Journal*
2 *of Advances in Modeling Earth Systems*, 13(3). <https://doi.org/10.1029/2020ms002217>

3 Cukier, R. I., Fortuin, C. M., Shuler, K. E., Petschek, A. G., & Schaibly, J. H. (1973). Study of the
4 sensitivity of coupled reaction systems to uncertainties in rate coefficients. I Theory. *The*
5 *Journal of Chemical Physics*, 59(8), 3873–3878. <https://doi.org/10.1063/1.1680571>

6 Dagon, K., Sanderson, B. M., Fisher, R. A., & Lawrence, D. M. (2020). A machine learning
7 approach to emulation and biophysical parameter estimation with the Community Land
8 Model, version 5. *Advances in Statistical Climatology Meteorology and Oceanography*, 6(2),
9 223–244. <https://doi.org/10.5194/ascmo-6-223-2020>

10 Dahlin, K. M., Ponte, D. D., Setlock, E., & Nagelkirk, R. (2017). Global patterns of drought
11 deciduous phenology in semi-arid and savanna-type ecosystems. *Ecography*, 40(2),
12 314–323. <https://doi.org/10.1111/ecog.02443>

13 Dantec-Nédélec, S., Ottlé, C., Wang, T., Guglielmo, F., Maignan, F., Delbart, N., Valdayskikh, V.,
14 Radchenko, T., Nekrasova, O., Zakharov, V., & Jouzel, J. (2017). Testing the capability of
15 ORCHIDEE land surface model to simulate Arctic ecosystems: Sensitivity analysis and
16 site-level model calibration. *Journal of Advances in Modeling Earth Systems*, 9(2),
17 1212–1230. <https://doi.org/10.1002/2016ms000860>

18 Datta, P., & Faroughi, S. A. (2023). A multihead LSTM technique for prognostic prediction of soil
19 moisture. *Geoderma*, 433(116452), 116452.
20 <https://doi.org/10.1016/j.geoderma.2023.116452>

21 Davies-Barnard, T., Zaehle, S., & Friedlingstein, P. (2022). Assessment of the impacts of
22 biological nitrogen fixation structural uncertainty in CMIP6 earth system models.
23 *Biogeosciences*, 19(14), 3491–3503. <https://doi.org/10.5194/bg-19-3491-2022>

24 de Bézenac, E., Pajot, A., & Gallinari, P. (2019). Deep learning for physical processes:
25 incorporating prior scientific knowledge. *Journal of Statistical Mechanics*, 2019(12), 124009.
26 <https://doi.org/10.1088/1742-5468/ab3195>

27 Deepak, R., Seiler, C., & Monahan, A. H. (2024). A global sensitivity analysis of parameter
28 uncertainty in the CLASSIC model. *Atmosphere-Ocean*, 0(0), 1–13.
29 <https://doi.org/10.1080/07055900.2024.2396426>

30 De Lannoy, G. J. M., Bechtold, M., Albergel, C., Brocca, L., Calvet, J.-C., Carrassi, A., Crow, W.,
31 T., de Rosnay, P., Durand, M., Forman, B., Geppert, G., Girotto, M., Hendricks Franssen,
32 H.-J., Jonas, T., Kumar, S., Lievens, H., Lu, Y., Massari, C., Pauwels, V. R. N., ...
33 Steele-Dunne, S. (2022). Perspective on satellite-based land data assimilation to estimate
34 water cycle components in an era of advanced data availability and model sophistication.
35 *Frontiers in Water*, 4. <https://doi.org/10.3389/frwa.2022.981745>

36 de Rosnay, P., Browne, P., de Boisséson, E., Fairbairn, D., Hirahara, Y., Ochi, K., Schepers, D.,
37 Weston, P., Zuo, H., Alonso-Balmaseda, M., Balsamo, G., Bonavita, M., Borman, N.,
38 Brown, A., Chrust, M., Dahoui, M., Chiara, G., English, S., Geer, A., ... Rabier, F. (2022).
39 Coupled data assimilation at ECMWF: current status, challenges and future developments.
40 *Quarterly Journal of the Royal Meteorological Society*, 148(747), 2672–2702.
41 <https://doi.org/10.1002/qj.4330>

42 Dietze, M. C. (2017). *Ecological Forecasting*. Princeton University Press.
43 <https://doi.org/10.1515/9781400885459>

44 Dietze, M. C., Serbin, S. P., Davidson, C., Desai, A. R., Feng, X., Kelly, R., Kooper, R., LeBauer,

1 D., Mantooth, J., McHenry, K., & Wang, D. (2014). A quantitative assessment of a terrestrial
2 biosphere model's data needs across North American biomes. *Journal of Geophysical*
3 *Research. Biogeosciences*, 119(3), 286–300. <https://doi.org/10.1002/2013jg002392>

4 Dokoochaki, H., Morrison, B. D., Raiho, A., Serbin, S. P., Zarada, K., Dramko, L., & Dietze, M.
5 (2022). Development of an open-source regional data assimilation system in PEcAn v.
6 1.7.2: application to carbon cycle reanalysis across the contiguous US using SIPNET.
7 *Geoscientific Model Development*, 15(8), 3233–3252.
8 <https://doi.org/10.5194/gmd-15-3233-2022>

9 Donnerer, C. (n.d.). *xgboost-distribution: Probabilistic prediction with XGBoost*. Github.
10 Retrieved August 15, 2024, from <https://github.com/CDonnerer/xgboost-distribution>

11 Draper, C. S. (2021). Accounting for land model error in numerical weather prediction ensemble
12 systems: toward ensemble-based coupled land/atmosphere data assimilation. *Journal of*
13 *Hydrometeorology*, 22(8), 2089–2104. <https://doi.org/10.1175/jhm-d-21-0016.1>

14 Duan, T., Anand, A., Ding, D. Y., Thai, K. K., Basu, S., Ng, A., & Schuler, A. (13–18 Jul 2020).
15 NGBoost: Natural Gradient Boosting for Probabilistic Prediction. In H. D. Iii & A. Singh
16 (Eds.), *Proceedings of the 37th International Conference on Machine Learning* (Vol. 119,
17 pp. 2690–2700). PMLR. <https://proceedings.mlr.press/v119/duan20a.html>

18 Dubayah, R., Blair, J. B., Goetz, S., Fatoyinbo, L., Hansen, M., Healey, S., Hofton, M., Hurt, G.,
19 Kellner, J., Luthcke, S., Armston, J., Tang, H., Duncanson, L., Hancock, S., Jantz, P.,
20 Marselis, S., Patterson, P. L., Qi, W., & Silva, C. (2020). The Global Ecosystem Dynamics
21 Investigation: High-resolution laser ranging of the Earth's forests and topography. *Egyptian*
22 *Journal of Remote Sensing and Space Sciences*, 1, 100002.
23 <https://doi.org/10.1016/j.srs.2020.100002>

24 Durbha, S. S., King, R. L., & Younan, N. H. (2007). Support vector machines regression for
25 retrieval of leaf area index from multiangle imaging spectroradiometer. *Remote Sensing of*
26 *Environment*, 107(1-2), 348–361. <https://doi.org/10.1016/j.rse.2006.09.031>

27 Ek, M. B., Mitchell, K. E., Lin, Y., Rogers, E., Grunmann, P., Koren, V., Gayno, G., & Tarpley, J.
28 D. (2003). Implementation of Noah land surface model advances in the National Centers for
29 Environmental Prediction operational mesoscale Eta model. *Journal of Geophysical*
30 *Research*, 108(D22). <https://doi.org/10.1029/2002jd003296>

31 ElGhawi, R., Kraft, B., Reimers, C., Reichstein, M., Körner, M., Gentine, P., & Winkler, A. J.
32 (2023). Hybrid modeling of evapotranspiration: inferring stomatal and aerodynamic
33 resistances using combined physics-based and machine learning. *Environmental Research*
34 *Letters*, 18(3), 034039. <https://doi.org/10.1088/1748-9326/acbbe0>

35 Evensen, G. (2003). The Ensemble Kalman Filter: theoretical formulation and practical
36 implementation. *Ocean Dynamics*, 53(4), 343–367.
37 <https://doi.org/10.1007/s10236-003-0036-9>

38 Exbrayat, J.-F., Bloom, A. A., Falloon, P., Ito, A., Smallman, T. L., & Williams, M. (2018).
39 Reliability ensemble averaging of 21st century projections of terrestrial net primary
40 productivity reduces global and regional uncertainties. *Earth System Dynamics*, 9(1),
41 153–165. <https://doi.org/10.5194/esd-9-153-2018>

42 Exbrayat, J.-F., Pitman, A. J., & Abramowitz, G. (2014). Response of microbial decomposition to
43 spin-up explains CMIP5 soil carbon range until 2100. *Geoscientific Model Development*,
44 7(6), 2683–2692. <https://doi.org/10.5194/gmd-7-2683-2014>

1 Exbrayat, J.-F., Smallman, T. L., Bloom, A. A., Hutley, L. B., & Williams, M. (2018). Inverse
2 determination of the influence of fire on vegetation carbon turnover in the pantropics. *Global*
3 *Biogeochemical Cycles*, 32(12), 1776–1789. <https://doi.org/10.1029/2018gb005925>

4 Eyring, V., Collins, W. D., Gentine, P., Barnes, E. A., Barreiro, M., Beucler, T., Bocquet, M.,
5 Bretherton, C. S., Christensen, H. M., Dagon, K., Gagne, D. J., Hall, D., Hammerling, D.,
6 Hoyer, S., Iglesias-Suarez, F., Lopez-Gomez, I., McGraw, M. C., Meehl, G. A., Molina, M.
7 J., ... Zanna, L. (2024). Pushing the frontiers in climate modelling and analysis with
8 machine learning. *Nature Climate Change*, 14(9), 916–928.
9 <https://doi.org/10.1038/s41558-024-02095-y>

10 Famiglietti, C. A., Smallman, T. L., Levine, P. A., Flack-Prain, S., Quetin, G. R., Meyer, V.,
11 Parazoo, N. C., Stettz, S. G., Yang, Y., Bonal, D., Bloom, A. A., Williams, M., & Konings, A.
12 G. (2021). Optimal model complexity for terrestrial carbon cycle prediction. *Biogeosciences*
13 , 18(8), 2727–2754. <https://doi.org/10.5194/bg-18-2727-2021>

14 Fang, K., Pan, M., & Shen, C. (2019). The value of SMAP for long-term soil moisture estimation
15 with the help of deep learning. *IEEE Transactions on Geoscience and Remote Sensing: A*
16 *Publication of the IEEE Geoscience and Remote Sensing Society*, 57(4), 2221–2233.
17 <https://doi.org/10.1109/tgrs.2018.2872131>

18 Farchi, A., Chrust, M., Bocquet, M., Laloyaux, P., & Bonavita, M. (2023). Online model error
19 correction with neural networks in the incremental 4D-Var framework. *Journal of Advances*
20 *in Modeling Earth Systems*, 15(9), e2022MS003474.
21 <https://doi.org/10.1029/2022ms003474>

22 Farchi, A., Laloyaux, P., Bonavita, M., & Bocquet, M. (2021). Using machine learning to correct
23 model error in data assimilation and forecast applications. *Quarterly Journal of the Royal*
24 *Meteorological Society. Royal Meteorological Society (Great Britain)*, 147(739), 3067–3084.
25 <https://doi.org/10.1002/qj.4116>

26 Farquhar, G. D., von Caemmerer, S., & Berry, J. A. (1980). A biochemical model of
27 photosynthetic CO₂ assimilation in leaves of C 3 species. *Planta*, 149(1), 78–90.
28 <https://doi.org/10.1007/BF00386231>

29 Fer, I., Gardella, A. K., Shiklomanov, A. N., Campbell, E. E., Cowdery, E. M., De Kauwe, M. G.,
30 Desai, A., Duveneck, M. J., Fisher, J. B., Haynes, K. D., Hoffman, F. M., Johnston, M. R.,
31 Kooper, R., LeBauer, D. S., Mantooth, J., Parton, W. J., Poulter, B., Quaife, T., Raiho, A., ...
32 Dietze, M. C. (2021). Beyond ecosystem modeling: A roadmap to community
33 cyberinfrastructure for ecological data-model integration. *Global Change Biology*, 27(1),
34 13–26. <https://doi.org/10.1111/gcb.15409>

35 Fer, I., Kelly, R., Moorcroft, P. R., Richardson, A. D., Cowdery, E. M., & Dietze, M. C. (2018).
36 Linking big models to big data: efficient ecosystem model calibration through Bayesian
37 model emulation. *Biogeosciences* , 15(19), 5801–5830.
38 <https://doi.org/10.5194/bg-15-5801-2018>

39 Fer, I., Shiklomanov, A., Novick, K. A., Gough, C. M., Altaf Arain, M., Chen, J., Murphy, B.,
40 Desai, A. R., & Dietze, M. C. (2021). Capturing site-to-site variability through Hierarchical
41 Bayesian calibration of a process-based dynamic vegetation model. In *bioRxiv* (p.
42 2021.04.28.441243). <https://doi.org/10.1101/2021.04.28.441243>

43 Finn, T. S., Durand, C., Farchi, A., Bocquet, M., Chen, Y., Carrassi, A., & Dansereau, V. (2023).
44 Deep learning subgrid-scale parametrisations for short-term forecasting of sea-ice

1 dynamics with a Maxwell elasto-brittle rheology. *The Cryosphere*, 17(7), 2965–2991.
2 <https://doi.org/10.5194/tc-17-2965-2023>

3 Fisher, R. A., & Koven, C. D. (2020). Perspectives on the future of land surface models and the
4 challenges of representing complex terrestrial systems. *Journal of Advances in Modeling
Earth Systems*, 12(4). <https://doi.org/10.1029/2018ms001453>

5 Fisher, R. A., Muszala, S., Verteinstein, M., Lawrence, P., Xu, C., McDowell, N. G., Knox, R. G.,
6 Koven, C., Holm, J., Rogers, B. M., Spessa, A., Lawrence, D., & Bonan, G. (2015). Taking
7 off the training wheels: the properties of a dynamic vegetation model without climate
8 envelopes, CLM4.5(ED). *Geoscientific Model Development*, 8(11), 3593–3619.
9 <https://doi.org/10.5194/gmd-8-3593-2015>

10 Fisher, R. A., Wieder, W. R., Sanderson, B. M., Koven, C. D., Oleson, K. W., Xu, C., Fisher, J.
11 B., Shi, M., Walker, A. P., & Lawrence, D. M. (2019). Parametric controls on vegetation
12 responses to biogeochemical forcing in the CLM5. *Journal of Advances in Modeling Earth
13 Systems*, 11(9), 2879–2895. <https://doi.org/10.1029/2019ms001609>

14 Forkel, M., Carvalhais, N., Schaphoff, S., v. Bloh, W., Migliavacca, M., Thurner, M., & Thonicke,
15 K. (2014). Identifying environmental controls on vegetation greenness phenology through
16 model–data integration. *Biogeosciences*, 11(23), 7025–7050.
17 <https://doi.org/10.5194/bg-11-7025-2014>

18 Forkel, M., Drüke, M., Thurner, M., Dorigo, W., Schaphoff, S., Thonicke, K., von Bloh, W., &
19 Carvalhais, N. (2019). Constraining modelled global vegetation dynamics and carbon
20 turnover using multiple satellite observations. *Scientific Reports*, 9(1), 18757.
21 <https://doi.org/10.1038/s41598-019-55187-7>

22 Fox, A., Williams, M., Richardson, A. D., Cameron, D., Gove, J. H., Quaife, T., Ricciuto, D.,
23 Reichstein, M., Tomelleri, E., Trudinger, C. M., & Van Wijk, M. T. (2009). The REFLEX
24 project: Comparing different algorithms and implementations for the inversion of a terrestrial
25 ecosystem model against eddy covariance data. *Agricultural and Forest Meteorology*,
26 149(10), 1597–1615. <https://doi.org/10.1016/j.agrformet.2009.05.002>

27 Friedlingstein, P., O'Sullivan, M., Jones, M. W., Andrew, R. M., Bakker, D. C. E., Hauck, J.,
28 Landschützer, P., Le Quéré, C., Luijckx, I. T., Peters, G. P., Peters, W., Pongratz, J.,
29 Schwingshackl, C., Sitch, S., Canadell, J. G., Ciais, P., Jackson, R. B., Alin, S. R., Anthoni,
30 P., ... Zheng, B. (2023). Global Carbon Budget 2023. *Earth System Science Data*, 15(12),
31 5301–5369.
32 <https://doi.org/10.5194/essd-15-5301-202310.5194/essd-15-5301-2023-supplement>

33 Garnelo, M., Schwarz, J., Rosenbaum, D., Viola, F., Rezende, D. J., Ali Eslami, S. M., & Teh, Y.
34 W. (2018). Neural Processes. In *arXiv [cs.LG]*. arXiv. <http://arxiv.org/abs/1807.01622>

35 Geer, A. J. (2021). Learning earth system models from observations: machine learning or data
36 assimilation? *Philosophical Transactions. Series A, Mathematical, Physical, and
37 Engineering Sciences*, 379(2194), 20200089. <https://doi.org/10.1098/rsta.2020.0089>

38 Gelbrecht, M., White, A., Bathiany, S., & Boers, N. (2023). Differentiable programming for Earth
39 system modeling. *Geoscientific Model Development*, 16(11), 3123–3135.
40 <https://doi.org/10.5194/gmd-16-3123-2023>

41 Gentine, P., & Aleomohammad, S. H. (2018). Reconstructed solar-induced fluorescence: A
42 machine learning vegetation product based on MODIS surface reflectance to reproduce
43 GOME-2 solar-induced fluorescence. *Geophysical Research Letters*, 45(7), 3136–3146.

1 <https://doi.org/10.1002/2017GL076294>

2 Gentine, P., Pritchard, M., Rasp, S., Reinaudi, G., & Yacalis, G. (2018). Could machine learning
3 break the convection parameterization deadlock? *Geophysical Research Letters*, 45(11),
4 5742–5751. <https://doi.org/10.1029/2018gl078202>

5 Gier, B. K., Schlund, M., Friedlingstein, P., Jones, C. D., Jones, C., Zaehle, S., & Eyring, V.
6 (2024). Representation of the terrestrial carbon cycle in CMIP6. In *arXiv [physics.ao-ph]*.
7 arXiv. <https://doi.org/10.5194/egusphere-2024-277>

8 Giering, R. (2010). *Transformation of algorithms in Fortran Version 1.15 (TAF Version 1.9. 70)*.

9 Goldberg, D. E., & Holland, J. H. (1988). Genetic Algorithms and Machine Learning. *Machine
Learning*, 3(2/3), 95–99. <https://doi.org/10.1023/a:1022602019183>

10 Green, J. K., Seneviratne, S. I., Berg, A. M., Findell, K. L., Hagemann, S., Lawrence, D. M., &
11 Gentine, P. (2019). Large influence of soil moisture on long-term terrestrial carbon uptake.
12 *Nature*, 565(7740), 476–479. <https://doi.org/10.1038/s41586-018-0848-x>

13 Green, J. K., Zhang, Y., Luo, X., & Keenan, T. F. (2024). Systematic underestimation of canopy
14 conductance sensitivity to drought by Earth System Models. *AGU Advances*, 5(1),
15 e2023AV001026. <https://doi.org/10.1029/2023av001026>

16 Gregory, W., Bushuk, M., Adcroft, A., Zhang, Y., & Zanna, L. (2023). Deep learning of
17 systematic sea ice model errors from data assimilation increments. *Journal of Advances in
Modeling Earth Systems*, 15(10), e2023MS003757. <https://doi.org/10.1029/2023ms003757>

18 Gregory, W., Bushuk, M., Zhang, Y., Adcroft, A., & Zanna, L. (2024). Machine learning for online
19 sea ice bias correction within global ice-ocean simulations. *Geophysical Research Letters*,
20 51(3), e2023GL106776. <https://doi.org/10.1029/2023gl106776>

21 Griewank, A. (1997). *On Automatic Differentiation*.
22 https://www.researchgate.net/publication/2703247_On_Automatic_Differentiation

23 Grinsztajn, L., Oyallon, E., & Varoquaux, G. (2022). Why do tree-based models still outperform
24 deep learning on tabular data? In *arXiv [cs.LG]*. arXiv. <http://arxiv.org/abs/2207.08815>

25 Groenendijk, M., Dolman, A. J., Ammann, C., Arneth, A., Cescatti, A., Dragoni, D., Gash, J. H.
26 C., Gianelle, D., Gioli, B., Kiely, G., Knohl, A., Law, B. E., Lund, M., Marcolla, B., van der
27 Molen, M. K., Montagnani, L., Moors, E., Richardson, A. D., Roupsard, O., ... Wohlfahrt, G.
28 (2011). Seasonal variation of photosynthetic model parameters and leaf area index from
29 global Fluxnet eddy covariance data. *Journal of Geophysical Research: Biogeosciences*,
30 116(G4). <https://doi.org/10.1029/2011JG001742>

31 Guo, Y., Yu, X., Xu, Y.-P., Chen, H., Gu, H., & Xie, J. (2021). AI-based techniques for multi-step
32 streamflow forecasts: application for multi-objective reservoir operation optimization and
33 performance assessment. *Hydrology and Earth System Sciences*, 25(11), 5951–5979.
34 <https://doi.org/10.5194/hess-25-5951-2021>

35 Hararuk, O., Xia, J., & Luo, Y. (2014). Evaluation and improvement of a global land model
36 against soil carbon data using a Bayesian Markov chain Monte Carlo method. *Journal of
37 Geophysical Research. Biogeosciences*, 119(3), 403–417.
38 <https://doi.org/10.1002/2013jg002535>

39 Harden, J. W., Hugelius, G., Ahlström, A., Blankinship, J. C., Bond-Lamberty, B., Lawrence, C.
40 R., Loisel, J., Malhotra, A., Jackson, R. B., Ogle, S., Phillips, C., Ryals, R., Todd-Brown, K.,
41 Vargas, R., Vergara, S. E., Cotrufo, M. F., Keiluweit, M., Heckman, K. A., Crow, S. E., ...
42 Nave, L. E. (2018). Networking our science to characterize the state, vulnerabilities, and

1 management opportunities of soil organic matter. *Global Change Biology*, 24(2),
2 e705–e718. <https://doi.org/10.1111/gcb.13896>

3 Hastings, W. K. (1970). Monte Carlo sampling methods using Markov chains and their
4 applications. *Biometrika*, 57(1), 97–109. <https://doi.org/10.1093/biomet/57.1.97>

5 Hatfield, S., Chantry, M., Dueben, P., Lopez, P., Geer, A., & Palmer, T. (2021). Building
6 tangent-linear and adjoint models for data assimilation with neural networks. *Journal of*
7 *Advances in Modeling Earth Systems*, 13(9). <https://doi.org/10.1029/2021ms002521>

8 Haupt, R. L., & Haupt, S. E. (2004). *Practical genetic algorithms* (2nd ed.) [PDF]. John Wiley &
9 Sons. <https://doi.org/10.1002/0471671746>

10 Heinrich, V. H. A., Dalagnol, R., Cassol, H. L. G., Rosan, T. M., de Almeida, C. T., Silva Junior,
11 C. H. L., Campanharo, W. A., House, J. I., Sitch, S., Hales, T. C., Adami, M., Anderson, L.
12 O., & Aragão, L. E. O. C. (2021). Large carbon sink potential of secondary forests in the
13 Brazilian Amazon to mitigate climate change. *Nature Communications*, 12(1), 1785.
14 <https://doi.org/10.1038/s41467-021-22050-1>

15 Heinrich, V. H. A., Vancutsem, C., Dalagnol, R., Rosan, T. M., Fawcett, D., Silva-Junior, C. H. L.,
16 Cassol, H. L. G., Achard, F., Jucker, T., Silva, C. A., House, J., Sitch, S., Hales, T. C., &
17 Aragão, L. E. O. C. (2023). The carbon sink of secondary and degraded humid tropical
18 forests. *Nature*, 615(7952), 436–442. <https://doi.org/10.1038/s41586-022-05679-w>

19 Hersbach, H., de Rosnay, P., Bell, B., Schepers, D., Simmons, A., Soci, C., Abdalla, S.,
20 Alonso-Balmaseda, M., Balsamo, G., Bechtold, P., Berrisford, P., Bidlot, J.-R., de
21 Boisséson, E., Bonavita, M., Browne, P., Buizza, R., Dahlgren, P., Dee, D., Dragani, R., ...
22 Zuo, H. (2018). Operational global reanalysis: progress, future directions and synergies with
23 NWP | ERA Report Series. *ECMWF*.
24 <https://www.ecmwf.int/en/elibrary/80922-operational-global-reanalysis-progress-future-directions-and-synergies-nwp>

25

26 Hourdin, F., Ferster, B., Deshayes, J., Mignot, J., Musat, I., & Williamson, D. (2023). Toward
27 machine-assisted tuning avoiding the underestimation of uncertainty in climate change
28 projections. *Science Advances*, 9(29), eadf2758. <https://doi.org/10.1126/sciadv.adf2758>

29 Huang, Y., Zhu, D., Ciais, P., Guenet, B., Huang, Y., Goll, D. S., Guimbertea, M., Jornet-Puig,
30 A., Lu, X., & Luo, Y. (2018). Matrix-based sensitivity assessment of soil organic carbon
31 storage: A case study from the ORCHIDEE-MICT model. *Journal of Advances in Modeling*
32 *Earth Systems*, 10(8), 1790–1808. <https://doi.org/10.1029/2017MS001237>

33 Irvine, P. J., Gregoire, L. J., Lunt, D. J., & Valdes, P. J. (2013). An efficient method to generate a
34 perturbed parameter ensemble of a fully coupled AOGCM without flux-adjustment.
35 *Geoscientific Model Development*, 6(5), 1447–1462.
36 <https://doi.org/10.5194/gmd-6-1447-2013>

37 Jeong, J., Barichivich, J., Peylin, P., Haverd, V., McGrath, M. J., Vuichard, N., Evans, M. N.,
38 Babst, F., & Luyssaert, S. (2021). Using the International Tree-Ring Data Bank (ITRDB)
39 records as century-long benchmarks for global land-surface models. *Geoscientific Model*
40 *Development*, 14(9), 5891–5913.
41 <https://doi.org/10.5194/gmd-14-5891-202110.5194/gmd-14-5891-2021-supplement>

42 Jiang, M., Medlyn, B. E., Drake, J. E., Duursma, R. A., Anderson, I. C., Barton, C. V. M., Boer,
43 M. M., Carrillo, Y., Castañeda-Gómez, L., Collins, L., Crous, K. Y., De Kauwe, M. G., Dos
44 Santos, B. M., Emmerson, K. M., Facey, S. L., Gherlenda, A. N., Gimeno, T. E., Hasegawa,

1 S., Johnson, S. N., ... Ellsworth, D. S. (2020). The fate of carbon in a mature forest under
2 carbon dioxide enrichment. *Nature*, 580(7802), 227–231.
3 <https://doi.org/10.1038/s41586-020-2128-9>

4 Jian, J., Vargas, R., Anderson-Teixeira, K., Stell, E., Herrmann, V., Horn, M., Kholod, N.,
5 Manzon, J., Marchesi, R., Paredes, D., & Bond-Lamberty, B. (2021). A restructured and
6 updated global soil respiration database (SRDB-V5). *Earth System Science Data*, 13(2),
7 255–267. <https://doi.org/10.5194/essd-13-255-2021>

8 Joiner, J., Yoshida, Y., Zhang, Y., Duveiller, G., Jung, M., Lyapustin, A., Wang, Y., & Tucker, C. J.
9 (2018). Estimation of Terrestrial Global Gross Primary Production (GPP) with Satellite
10 Data-Driven Models and Eddy Covariance Flux Data. *Remote Sensing*, 10(9), 1346.
11 <https://doi.org/10.3390/rs10091346>

12 Jones, S., Mercado, L. M., Bruhn, D., Raoult, N., & Cox, P. M. (2024). Night-time decline in plant
13 respiration is consistent with substrate depletion. *Communications Earth & Environment*,
14 5(1), 1–9. <https://doi.org/10.1038/s43247-024-01312-y>

15 Jung, M., Reichstein, M., Margolis, H. A., Cescatti, A., Richardson, A. D., Arain, M. A., Arneth,
16 A., Bernhofer, C., Bonal, D., Chen, J., Gianelle, D., Gobron, N., Kiely, G., Kutsch, W.,
17 Lasslop, G., Law, B. E., Lindroth, A., Merbold, L., Montagnani, L., ... Williams, C. (2011).
18 Global patterns of land-atmosphere fluxes of carbon dioxide, latent heat, and sensible heat
19 derived from eddy covariance, satellite, and meteorological observations. *Journal of*
20 *Geophysical Research*, 116(G00J07). <https://doi.org/10.1029/2010jg001566>

21 Jung, M., Schwalm, C., Migliavacca, M., Walther, S., Camps-Valls, G., Koirala, S., Anthoni, P.,
22 Besnard, S., Bodesheim, P., Carvalhais, N., Chevallier, F., Gans, F., Goll, D. S., Haverd, V.,
23 Köhler, P., Ichii, K., Jain, A. K., Liu, J., Lombardozzi, D., ... Reichstein, M. (2020). Scaling
24 carbon fluxes from eddy covariance sites to globe: synthesis and evaluation of the
25 FLUXCOM approach. *Biogeosciences*, 17(5), 1343–1365.
26 <https://doi.org/10.5194/bg-17-1343-2020>

27 Justice, C., Townshend, J., Vermote, E., Masuoka, E., Wolfe, R., Saleous, N., Roy, D., &
28 Morisette, J. (2002). An overview of MODIS Land data processing and product status.
29 *Remote Sensing of Environment*, 83, 3–15. [https://doi.org/10.1016/S0034-4257\(02\)00084-6](https://doi.org/10.1016/S0034-4257(02)00084-6)

30 Kallingal, J. T., Scholze, M., Miller, P. A., Lindström, J., Rinne, J., Aurela, M., Vestin, P., &
31 Weslien, P. (2024). Assimilating multi-site eddy-covariance data to calibrate the CH₄
32 wetland emission module in a terrestrial ecosystem model. In *EGUsphere* (pp. 1–32).
33 <https://doi.org/10.5194/egusphere-2024-373>

34 Kaminski, T., Heimann, M., & Giering, R. (1999). A coarse grid three-dimensional global inverse
35 model of the atmospheric transport: 1. Adjoint model and Jacobian matrix. *Journal of*
36 *Geophysical Research*, 104(D15), 18535–18553. <https://doi.org/10.1029/1999jd900147>

37 Kaminski, T., Knorr, W., Rayner, P., & Heimann, M. (2002). Assimilating atmospheric data into a
38 terrestrial biosphere model: A case study of the seasonal cycle. *Global Biogeochem.*
39 *Cycles*, 16(4), 1066. <https://doi.org/10.1029/2001GB001463>

40 Kaminski, T., Knorr, W., Scholze, M., Gobron, N., Pinty, B., Giering, R., & Mathieu, P.-P. (2012).
41 Consistent assimilation of MERIS FAPAR and atmospheric CO₂ into a terrestrial vegetation
42 model and interactive mission benefit analysis. *Biogeosciences*, 9(8), 3173–3184.
43 <https://doi.org/10.5194/bg-9-3173-2012>

44 Kaminski, T., Knorr, W., Schürmann, G., Scholze, M., Rayner, P. J., Zaehle, S., Blessing, S.,

1 Dorigo, W., Gayler, V., Giering, R., Gobron, N., Grant, J. P., Heimann, M., Hooker-Stroud,
2 A., Houweling, S., Kato, T., Kattge, J., Kelley, D., Kemp, S., ... Ziehn, T. (2013). The
3 BETHY/JSBACH Carbon Cycle Data Assimilation System: experiences and challenges.
4 *Journal of Geophysical Research. Biogeosciences*, 118(4), 1414–1426.
5 <https://doi.org/10.1002/jgrg.20118>

6 Kaminski, T., & Mathieu, P.-P. (2017). Reviews and syntheses: Flying the satellite into your
7 model: on the role of observation operators in constraining models of the Earth system and
8 the carbon cycle. *Biogeosciences*, 14(9), 2343–2357.
9 <https://doi.org/10.5194/bg-14-2343-2017>

10 Kaminski, T., Scholze, M., & Houweling, S. (2010). Quantifying the benefit of A-SCOPE data for
11 reducing uncertainties in terrestrial carbon fluxes in CCDAS. *Tellus. Series B, Chemical and
12 Physical Meteorology*, 62(5), 784–796. <https://doi.org/10.1111/j.1600-0889.2010.00483.x>

13 Kato, T., Knorr, W., Scholze, M., Veenendaal, E., Kaminski, T., Kattge, J., & Gobron, N. (2013).
14 Simultaneous assimilation of satellite and eddy covariance data for improving terrestrial
15 water and carbon simulations at a semi-arid woodland site in Botswana. *Biogeosciences*,
16 10(2), 789–802. <https://doi.org/10.5194/bg-10-789-2013>

17 Kattge, J., Bönisch, G., Díaz, S., Lavorel, S., Prentice, I. C., Leadley, P., Tautenhahn, S.,
18 Werner, G. D. A., Aakala, T., Abedi, M., Acosta, A. T. R., Adamidis, G. C., Adamson, K.,
19 Aiba, M., Albert, C. H., Alcántara, J. M., Alcázar C, C., Aleixo, I., Ali, H., ... Wirth, C. (2020).
20 TRY plant trait database - enhanced coverage and open access. *Global Change Biology*,
21 26(1), 119–188. <https://doi.org/10.1111/gcb.14904>

22 Keenan, T. F., Carbone, M. S., Reichstein, M., & Richardson, A. D. (2011). The model-data
23 fusion pitfall: assuming certainty in an uncertain world. *Oecologia*, 167(3), 587–597.
24 <https://doi.org/10.1007/s00442-011-2106-x>

25 Keenan, T. F., Davidson, E. A., Munger, J. W., & Richardson, A. D. (2013). Rate my data:
26 quantifying the value of ecological data for the development of models of the terrestrial
27 carbon cycle. *Ecological Applications: A Publication of the Ecological Society of America*,
28 23(1), 273–286. <https://doi.org/10.1890/12-0747.1>

29 Keenan, T. F., Davidson, E., Moffat, A. M., Munger, W., & Richardson, A. D. (2012). Using
30 model-data fusion to interpret past trends, and quantify uncertainties in future projections, of
31 terrestrial ecosystem carbon cycling. *Global Change Biology*, 18(8), 2555–2569.
32 <https://doi.org/10.1111/j.1365-2486.2012.02684.x>

33 Kennedy, D., Dagon, K., Lawrence, D. M., Fisher, R. A., Sanderson, B. M., Collier, N., Hoffman,
34 F. M., Koven, C. D., Levis, S., Oleson, K. W., Zariski, C. M., Cheng, Y., Foster, A., Lu, X.,
35 Fowler, M., Hawkins, L., Kavoo, T., Kluzeck, E. B., Kumar, S., ... Luo, Y. (2024).
36 One-at-a-time parameter perturbation ensemble of the community land model, version 5.1.
37 In *ESS Open Archive*. <https://doi.org/10.22541/essar.172745082.24089296/v1>

38 Kennedy, M. C., & O'Hagan, A. (2001). Bayesian Calibration of Computer Models. *Journal of the
39 Royal Statistical Society Series B: Statistical Methodology*, 63(3), 425–464.
40 <https://doi.org/10.1111/1467-9868.00294>

41 Kerschke, P., Hoos, H. H., Neumann, F., & Trautmann, H. (2019). Automated Algorithm
42 Selection: Survey and Perspectives. *Evolutionary Computation*, 27(1), 3–45.
43 https://doi.org/10.1162/evco_a_00242

44 Kloek, T., & Van Dijk, H. K. (1978). Bayesian estimates of equation system parameters: an

1 application of integration by Monte Carlo. *Econometrica: Journal of the Econometric Society*.
2
3 https://www.jstor.org/stable/1913641?casa_token=1EgxpT-njfMAAAAAA:EPhlIE24zFcUOWFrDS_G8r0LMGluWx60_Ft7yeBlx9XViRf0sI27b3uD1MmKewRbJkO2Lcgb7G3kDQS-sQBi1vl tqRAyTEHOyQfEkAYw1W6Dtalc-PGm

6 Knorr, W. (2000). Annual and interannual CO₂ exchanges of the terrestrial biosphere:
7 process-based simulations and uncertainties: CO₂ exchanges of the terrestrial biosphere.
8 *Global Ecology and Biogeography: A Journal of Macroecology*, 9(3), 225–252.
9 <https://doi.org/10.1046/j.1365-2699.2000.00159.x>

10 Knorr, W., & Heimann, M. (1995). Impact of drought stress and other factors on seasonal land
11 biosphere CO₂ exchange studied through an atmospheric tracer transport model. *Tellus. Series B, Chemical and Physical Meteorology*, 47(4), 471–489.
13 <https://doi.org/10.1034/j.1600-0889.47.issue4.7.x>

14 Knorr, W., Kaminski, T., Scholze, M., Gobron, N., Pinty, B., Giering, R., & Mathieu, P.-P. (2010).
15 Carbon cycle data assimilation with a generic phenology model. *Journal of Geophysical Research*, 115(G4). <https://doi.org/10.1029/2009jg001119>

17 Knorr, W., & Kattge, J. (2005). Inversion of terrestrial ecosystem model parameter values
18 against eddy covariance measurements by Monte Carlo sampling. *Global Change Biology*,
19 11(8), 1333–1351. <https://doi.org/10.1111/j.1365-2486.2005.00977.x>

20 Knorr, W., Williams, M., Thum, T., Kaminski, T., Voßbeck, M., Scholze, M., Quaife, T.,
21 Smallmann, L., Steele-Dunne, S., Vreugdenhil, M., Green, T., Zähle, S., Aurela, M., Bouvet,
22 A., Buechi, E., Dorigo, W., El-Madany, T., Migliavacca, M., Honkanen, M., ... Drusch, M.
23 (2024). A comprehensive land surface vegetation model for multi-stream data assimilation,
24 D&B v1.0. In *EGUsphere*. <https://doi.org/10.5194/egusphere-2024-1534>

25 Knutti, R., Stocker, T. F., Joos, F., & Plattner, G.-K. (2003). Probabilistic climate change
26 projections using neural networks. *Climate Dynamics*, 21(3), 257–272.
27 <https://doi.org/10.1007/s00382-003-0345-1>

28 Koffi, E. N., Rayner, P. J., Scholze, M., & Beer, C. (2012). Atmospheric constraints on gross
29 primary productivity and net ecosystem productivity: Results from a carbon-cycle data
30 assimilation system. *Global Biogeochemical Cycles*, 26(1).
31 <https://doi.org/10.1029/2010gb003900>

32 Kolassa, J., Reichle, R. H., Liu, Q., Cosh, M., Bosch, D. D., Caldwell, T. G., Colliander, A.,
33 Collins, C. H., Jackson, T. J., Livingston, S. J., Moghaddam, M., & Starks, P. J. (2017). Data
34 assimilation to extract soil moisture information from SMAP observations. *Remote Sensing*,
35 9(11), 1179. <https://doi.org/10.3390/rs9111179>

36 Koppa, A., Rains, D., Hulsman, P., Poyatos, R., & Miralles, D. G. (2022). A deep learning-based
37 hybrid model of global terrestrial evaporation. *Nature Communications*, 13(1), 1912.
38 <https://doi.org/10.1038/s41467-022-29543-7>

39 Koven, C. D., Arora, V. K., Cadule, P., Fisher, R. A., Jones, C. D., Lawrence, D. M., Lewis, J.,
40 Lindsay, K., Mathesius, S., Meinshausen, M., Mills, M., Nicholls, Z., Sanderson, B. M.,
41 Séférian, R., Swart, N. C., Wieder, W. R., & Zickfeld, K. (2022). Multi-century dynamics of
42 the climate and carbon cycle under both high and net negative emissions scenarios. *Earth
43 System Dynamics*, 13(2), 885–909. <https://doi.org/10.5194/esd-13-885-2022>

44 Koven, C. D., Knox, R. G., Fisher, R. A., Chambers, J. Q., Christoffersen, B. O., Davies, S. J.,

1 Detto, M., Dietze, M. C., Faybushenko, B., Holm, J., Huang, M., Kovenock, M., Kueppers, L.
2 M., Lemieux, G., Massoud, E., McDowell, N. G., Muller-Landau, H. C., Needham, J. F.,
3 Norby, R. J., ... Xu, C. (2020). Benchmarking and parameter sensitivity of physiological and
4 vegetation dynamics using the Functionally Assembled Terrestrial Ecosystem Simulator
5 (FATES) at Barro Colorado Island, Panama. *Biogeosciences*, 17(11), 3017–3044.
6 <https://doi.org/10.5194/bg-17-3017-2020>

7 Kowalczyk, E. A., Wang, Y. P., Law, R. M., Davies, H. L., McGregor, J. L., Abramowitz, G. S.
8 (2006). *The CSIRO Atmosphere Biosphere Land Exchange (CABLE) model for use in*
9 *climate models and as an offline model*. Aspendale, Vic., CSIRO Marine and Atmospheric
10 Research. <https://doi.org/10.4225/08/58615C6A9A51D>

11 Kraft, B., Jung, M., Körner, M., Koirala, S., & Reichstein, M. (2022). Towards hybrid modeling of
12 the global hydrological cycle. *Hydrology and Earth System Sciences*, 26(6), 1579–1614.
13 <https://doi.org/10.5194/hess-26-1579-2022>

14 Krinner, G., Viovy, N., de Noblet-Ducoudré, N., Ogée, J., Polcher, J., Friedlingstein, P., Ciais, P.,
15 Sitch, S., & Prentice, I. C. (2005). A dynamic global vegetation model for studies of the
16 coupled atmosphere-biosphere system: DVGM FOR COUPLED CLIMATE STUDIES.
17 *Global Biogeochemical Cycles*, 19(1). <https://doi.org/10.1029/2003gb002199>

18 Kumar, S., Kolassa, J., Reichle, R., Crow, W., de Lannoy, G., de Rosnay, P., MacBean, N.,
19 Giroto, M., Fox, A., Quaife, T., Draper, C., Forman, B., Balsamo, G., Steele-Dunne, S.,
20 Albergel, C., Bonan, B., Calvet, J.-C., Dong, J., Liddy, H., & Ruston, B. (2022). An agenda
21 for land data assimilation priorities: Realizing the promise of terrestrial water, energy, and
22 vegetation observations from space. *Journal of Advances in Modeling Earth Systems*,
23 14(11). <https://doi.org/10.1029/2022ms003259>

24 Kumar, S. V., Reichle, R. H., Harrison, K. W., Peters-Lidard, C. D., Yatheendradas, S., &
25 Santanello, J. A. (2012). A comparison of methods for a priori bias correction in soil
26 moisture data assimilation: BIAS CORRECTION IN SOIL MOISTURE DATA
27 ASSIMILATION. *Water Resources Research*, 48(3). <https://doi.org/10.1029/2010wr010261>

28 Kuppel, S., Chevallier, F., & Peylin, P. (2013). Quantifying the model structural error in carbon
29 cycle data assimilation systems. *Geoscientific Model Development*, 6(1), 45–55.
30 <https://gmd.copernicus.org/articles/6/45/2013/>

31 Kuppel, S., Peylin, P., Chevallier, F., Bacour, C., Maignan, F., & Richardson, A. D. (2012).
32 Constraining a global ecosystem model with multi-site eddy-covariance data.
33 *Biogeosciences*, 9(10), 3757–3776. <https://doi.org/10.5194/bg-9-3757-2012>

34 Kuppel, S., Peylin, P., Maignan, F., Chevallier, F., Kiely, G., Montagnani, L., & Cescatti, A.
35 (2014). Model–data fusion across ecosystems: From multisite optimizations to global
36 simulations. *Geoscientific Model Development*, 7(6), 2581–2597.
37 <https://gmd.copernicus.org/articles/7/2581/2014/>

38 Kwon, Y., Forman, B. A., Ahmad, J. A., Kumar, S. V., & Yoon, Y. (2019). Exploring the utility of
39 machine learning-based passive microwave brightness temperature data assimilation over
40 terrestrial snow in High Mountain Asia. *Remote Sensing*, 11(19), 2265.
41 <https://doi.org/10.3390/rs11192265>

42 Kyker-Snowman, E., Lombardozzi, D. L., Bonan, G. B., Cheng, S. J., Dukes, J. S., Frey, S. D.,
43 Jacobs, E. M., McNellis, R., Rady, J. M., Smith, N. G., Thomas, R. Q., Wieder, W. R., &
44 Grandy, A. S. (2022). Increasing the spatial and temporal impact of ecological research: A

1 roadmap for integrating a novel terrestrial process into an Earth system model. *Global
2 Change Biology*, 28(2), 665–684. <https://doi.org/10.1111/gcb.15894>

3 Lam, R., Sanchez-Gonzalez, A., Willson, M., Wirnsberger, P., Fortunato, M., Alet, F., Ravuri, S.,
4 Ewalds, T., Eaton-Rosen, Z., Hu, W., Merose, A., Hoyer, S., Holland, G., Vinyals, O., Stott,
5 J., Pritzel, A., Mohamed, S., & Battaglia, P. (2023). Learning skillful medium-range global
6 weather forecasting. *Science*, 382(6677), 1416–1421.
7 <https://doi.org/10.1126/science.adz2336>

8 Lary, D. J., Alavi, A. H., Gandomi, A. H., & Walker, A. L. (2016). Machine learning in
9 geosciences and remote sensing. *Geoscience Frontiers*, 7(1), 3–10.
10 <https://doi.org/10.1016/j.gsf.2015.07.003>

11 Lawrence, C. R., Beem-Miller, J., Hoyt, A. M., Monroe, G., Sierra, C. A., Stoner, S., Heckman,
12 K., Blankinship, J. C., Crow, S. E., McNicol, G., Trumbore, S., Levine, P. A., Vindušková, O.,
13 Todd-Brown, K., Rasmussen, C., Hicks Pries, C. E., Schädel, C., McFarlane, K., Doetterl,
14 S., ... Wagai, R. (2020). An open-source database for the synthesis of soil radiocarbon
15 data: International Soil Radiocarbon Database (ISRaD) version 1.0. *Earth System Science
16 Data*, 12(1), 61–76. <https://doi.org/10.5194/essd-12-61-2020>

17 Lawrence, D. M., Fisher, R. A., Koven, C. D., Oleson, K. W., Swenson, S. C., Bonan, G., Collier,
18 N., Ghimire, B., van Kampenhout, L., Kennedy, D., Kluzek, E., Lawrence, P. J., Li, F., Li, H.,
19 Lombardozzi, D., Riley, W. J., Sacks, W. J., Shi, M., Vertenstein, M., ... Zeng, X. (2019).
20 The community land model version 5: Description of new features, benchmarking, and
21 impact of forcing uncertainty. *Journal of Advances in Modeling Earth Systems*, 11(12),
22 4245–4287. <https://doi.org/10.1029/2018ms001583>

23 LeBauer, D. S., Wang, D., Richter, K. T., Davidson, C. C., & Dietze, M. C. (2013). Facilitating
24 feedbacks between field measurements and ecosystem models. *Ecological Monographs*,
25 83(2), 133–154. <https://doi.org/10.1890/12-0137.1>

26 Li, L., Fang, Y., Zheng, Z., Shi, M., Longo, M., Koven, C. D., Holm, J. A., Fisher, R. A.,
27 McDowell, N. G., Chambers, J., & Leung, L. R. (2023). A machine learning approach
28 targeting parameter estimation for plant functional type coexistence modeling using
29 ELM-FATES (v2.0). *Geoscientific Model Development*, 16(14), 4017–4040.
30 <https://doi.org/10.5194/gmd-16-4017-202310.5194/gmd-16-4017-2023-supplement>

31 Liu, C., Xiao, Q., & Wang, B. (2008). An ensemble-based four-dimensional variational data
32 assimilation scheme. Part I: Technical formulation and preliminary test. *Monthly Weather
33 Review*, 136(9), 3363–3373. <https://doi.org/10.1175/2008mwr2312.1>

34 Liu, M., He, H., Ren, X., Sun, X., Yu, G., Han, S., Wang, H., & Zhou, G. (2015). The effects of
35 constraining variables on parameter optimization in carbon and water flux modeling over
36 different forest ecosystems. *Ecological Modelling*, 303, 30–41.
37 <https://doi.org/10.1016/j.ecolmodel.2015.01.027>

38 Lorenc, A. C. (1981). A global three-dimensional multivariate statistical interpolation scheme.
39 *Monthly Weather Review*, 109(4), 701–721.
40 [https://doi.org/10.1175/1520-0493\(1981\)109<0701:agtdms>2.0.co;2](https://doi.org/10.1175/1520-0493(1981)109<0701:agtdms>2.0.co;2)

41 Lu, D., & Ricciuto, D. (2019). Efficient surrogate modeling methods for large-scale Earth system
42 models based on machine-learning techniques. *Geoscientific Model Development*, 12(5),
43 1791–1807. <https://doi.org/10.5194/gmd-12-1791-2019>

44 Lu, D., Ricciuto, D., Walker, A., Safta, C., & Munger, W. (2017). Bayesian calibration of

1 terrestrial ecosystem models: a study of advanced Markov chain Monte Carlo methods.
2 *Biogeosciences*, 14, 4295–4314. <https://doi.org/10.5194/BG-14-4295-2017>

3 Luo, Y., Huang, Y., Sierra, C. A., Xia, J., Ahlström, A., Chen, Y., Hararuk, O., Hou, E., Jiang, L.,
4 Liao, C., Lu, X., Shi, Z., Smith, B., Tao, F., & Wang, Y.-P. (2022). Matrix approach to land
5 carbon cycle modeling. *Journal of Advances in Modeling Earth Systems*, 14(7).
6 <https://doi.org/10.1029/2022ms003008>

7 Luo, Y., Keenan, T. F., & Smith, M. (2015). Predictability of the terrestrial carbon cycle. *Global
8 Change Biology*, 21(5), 1737–1751. <https://doi.org/10.1111/gcb.12766>

9 Lu, X., Wang, Y.-P., Ziehn, T., & Dai, Y. (2013). An efficient method for global parameter
10 sensitivity analysis and its applications to the Australian community land surface model
11 (CABLE). *Agricultural and Forest Meteorology*, 182-183, 292–303.
12 <https://doi.org/10.1016/j.agrformet.2013.04.003>

13 MacBean, N., Bacour, C., Raoult, N., Bastrikov, V., Koffi, E. N., Kuppel, S., Maignan, F., Ottlé,
14 C., Peaucelle, M., Santaren, D., & Peylin, P. (2022). Quantifying and reducing uncertainty in
15 global carbon cycle predictions: Lessons and perspectives from 15 years of data
16 assimilation studies with the ORCHIDEE terrestrial biosphere model. *Global
17 Biogeochemical Cycles*, 36(7), e2021GB007177. <https://doi.org/10.1029/2021gb007177>

18 MacBean, N., Liddy, H., Quaife, T., Kolassa, J., & Fox, A. (2022). Building a land data
19 assimilation community to tackle technical challenges in quantifying and reducing
20 uncertainty in land model predictions. *Bulletin of the American Meteorological Society*,
21 103(3), E733–E740. <https://doi.org/10.1175/bams-d-21-0228.1>

22 MacBean, N., Maignan, F., Bacour, C., Lewis, P., Peylin, P., Guanter, L., Köhler, P.,
23 Gómez-Dans, J., & Disney, M. (2018). Strong constraint on modelled global carbon uptake
24 using solar-induced chlorophyll fluorescence data. *Scientific Reports*, 8(1), 1973.
25 <https://doi.org/10.1038/s41598-018-20024-w>

26 MacBean, N., Maignan, F., Peylin, P., Bacour, C., Bréon, F.-M., & Ciais, P. (2015). Using satellite
27 data to improve the leaf phenology of a global terrestrial biosphere model. *Biogeosciences* ,
28 12(23), 7185–7208. <https://doi.org/10.5194/bg-12-7185-2015>

29 MacBean, N., Peylin, P., Chevallier, F., Scholze, M., & Schürmann, G. (2016). Consistent
30 assimilation of multiple data streams in a carbon cycle data assimilation system.
31 *Geoscientific Model Development*, 9(10), 3569–3588.
32 <https://doi.org/10.5194/gmd-9-3569-2016>

33 Mahmud, K., Medlyn, B. E., Duursma, R. A., Campany, C., & De Kauwe, M. G. (2018). Inferring
34 the effects of sink strength on plant carbon balance processes from experimental
35 measurements. *Biogeosciences* , 15(13), 4003–4018.
36 <https://doi.org/10.5194/bg-15-4003-2018>

37 Mäkelä, J., Arppe, L., Fritze, H., Heinonsalo, J., Karhu, K., Liski, J., Oinonen, M., Straková, P., &
38 Viskari, T. (2022). Implementation and initial calibration of carbon-13 soil organic matter
39 decomposition in the Yasso model. *Biogeosciences*, 19(17), 4305–4313.
40 <https://doi.org/10.5194/bg-19-4305-2022>

41 Mäkelä, J., Knauer, J., Aurela, M., Black, A., Heimann, M., Kobayashi, H., Lohila, A.,
42 Mammarella, I., Margolis, H., Markkanen, T., Susiluoto, J., Thum, T., Viskari, T., Zaehle, S.,
43 & Aalto, T. (2019). Parameter calibration and stomatal conductance formulation comparison
44 for boreal forests with adaptive population importance sampler in the land surface model

1 JSBACH. *Geoscientific Model Development*, 12(9), 4075–4098.
2 <https://doi.org/10.5194/gmd-12-4075-2019>

3 Ma, L., Hurtt, G., Ott, L., Sahajpal, R., Fisk, J., Lamb, R., & Sullivan. (2022). Global evaluation
4 of the Ecosystem Demography model (ED v3. 0). *Geoscientific Model Development*, 15(5),
5 1971–1994. <https://gmd.copernicus.org/articles/15/1971/2022/>

6 Massoud, E. C., Xu, C., Fisher, R. A., Knox, R. G., Walker, A. P., Serbin, S. P., Christoffersen, B.
7 O., Holm, J. A., Kueppers, L. M., Ricciuto, D. M., Wei, L., Johnson, D. J., Chambers, J. Q.,
8 Koven, C. D., McDowell, N. G., & Vrugt, J. A. (2019). Identification of key parameters
9 controlling demographically structured vegetation dynamics in a land surface model:
10 CLM4.5(FATES). *Geoscientific Model Development*, 12(9), 4133–4164.
11 <https://doi.org/10.5194/gmd-12-4133-2019>

12 Mathers, C., Black, C. K., Segal, B. D., Gurung, R. B., Zhang, Y., Easter, M. J., Williams, S.,
13 Motew, M., Campbell, E. E., Brummitt, C. D., Paustian, K., & Kumar, A. A. (2023). Validating
14 DayCent-CR for cropland soil carbon offset reporting at a national scale. *Geoderma*,
15 438(116647), 116647. <https://doi.org/10.1016/j.geoderma.2023.116647>

16 Mauritsen, T., Bader, J., & Becker, T. (2019). *Developments in the MPI-M Earth System Model
version 1.2 (MPI-ESM1.2) and Its Response to Increasing CO₂*.
17 <https://doi.org/10.1029/2018ms001400>

18 McGovern, A., Elmore, K. L., Gagne, D. J., II, Haupt, S. E., Karstens, C. D., Lagerquist, R.,
19 Smith, T., & Williams, J. K. (2017). Using artificial intelligence to improve real-time
20 decision-making for high-impact weather. *Bulletin of the American Meteorological Society*,
21 98(10), 2073–2090. <https://doi.org/10.1175/bams-d-16-0123.1>

22 McKay, M. D., Beckman, R. J., & Conover, W. J. (1979). A Comparison of Three Methods for
23 Selecting Values of Input Variables in the Analysis of Output from a Computer Code.
24 *Technometrics: A Journal of Statistics for the Physical, Chemical, and Engineering
Sciences*, 21(2), 239–245. <https://doi.org/10.2307/1268522>

25 McNeall, D., Robertson, E., & Wiltshire, A. (2024). Constraining the carbon cycle in
26 JULES-ES-1.0. *Geoscientific Model Development*, 17(3), 1059–1089.
27 <https://doi.org/10.5194/gmd-17-1059-2024>

28 Medvigy, D., Wofsy, S. C., Munger, J. W., Hollinger, D. Y., & Moorcroft, P. R. (2009). Mechanistic
29 scaling of ecosystem function and dynamics in space and time: Ecosystem Demography
30 model version 2. *Journal of Geophysical Research: Biogeosciences*, 114(G1).
31 <https://doi.org/10.1029/2008JG000812>

32 Meirink, J. F., Bergamaschi, P., & Krol, M. C. (2008). Four-dimensional variational data
33 assimilation for inverse modelling of atmospheric methane emissions: method and
34 comparison with synthesis inversion. *Atmospheric Chemistry and Physics*, 8(21),
35 6341–6353. <https://doi.org/10.5194/acp-8-6341-2008>

36 Melton, J. R., Arora, V. K., Wisernig-Cojoc, E., Seiler, C., Fortier, M., Chan, E., & Teckentrup, L.
37 (2020). CLASSIC v1.0: the open-source community successor to the Canadian Land
38 Surface Scheme (CLASS) and the Canadian Terrestrial Ecosystem Model (CTEM) – Part 1:
39 Model framework and site-level performance. *Geoscientific Model Development*, 13(6),
40 2825–2850. <https://doi.org/10.5194/gmd-13-2825-2020>

41 Meunier, F., Visser, M. D., Shiklomanov, A., Dietze, M. C., Guzmán Q, J. A., Sanchez-Azofeifa,
42 G. A., De Deurwaerder, H. P. T., Krishna Moorthy, S. M., Schnitzer, S. A., Marvin, D. C.,

1 Longo, M., Liu, C., Broadbent, E. N., Almeyda Zambrano, A. M., Muller-Landau, H. C.,
2 Detto, M., & Verbeeck, H. (2022). Liana optical traits increase tropical forest albedo and
3 reduce ecosystem productivity. *Global Change Biology*, 28(1), 227–244.
4 <https://doi.org/10.1111/gcb.15928>

5 Meyer, D., Grimmond, S., Dueben, P., Hogan, R., & van Reeuwijk, M. (2022). Machine learning
6 emulation of urban land surface processes. *Journal of Advances in Modeling Earth
7 Systems*, 14(3), e2021MS002744. <https://doi.org/10.1029/2021ms002744>

8 Migliavacca, M., Meroni, M., Busetto, L., Colombo, R., Zenone, T., Matteucci, G., Manca, G., &
9 Seufert, G. (2009). Modeling gross primary production of agro-forestry ecosystems by
10 assimilation of satellite-derived information in a process-based model. *Sensors (Basel,
11 Switzerland)*, 9(2), 922–942. <https://doi.org/10.3390/s90200922>

12 Moorcroft, P. R., Hurtt, G. C., & Pacala, S. W. (2001). A method for scaling vegetation dynamics:
13 the ecosystem demography model (ED). *Ecological Monographs*.
14 [https://doi.org/10.1890/0012-9615\(2001\)071\[0557:AMFSVD\]2.0.CO;2](https://doi.org/10.1890/0012-9615(2001)071[0557:AMFSVD]2.0.CO;2)

15 Moore, D. J. P., Hu, J., Sacks, W. J., Schimel, D. S., & Monson, R. K. (2008). Estimating
16 transpiration and the sensitivity of carbon uptake to water availability in a subalpine forest
17 using a simple ecosystem process model informed by measured net CO₂ and H₂O fluxes.
18 *Agricultural and Forest Meteorology*, 148(10), 1467–1477.
19 <https://doi.org/10.1016/j.agrformet.2008.04.013>

20 Morris, M. D. (1991). Factorial sampling plans for preliminary computational experiments.
21 *Technometrics: A Journal of Statistics for the Physical, Chemical, and Engineering
22 Sciences*, 33(2), 161–174. <https://doi.org/10.1080/00401706.1991.10484804>

23 Nave, L., Johnson, K., van Ingen, C., Agarwal, D., Humphrey, M., & Beekwilder, N. (2016).
24 *International Soil Carbon Network (ISCN) Database v3-1*.
25 <https://doi.org/10.17040/ISCN/1305039>

26 Nelder, J. A., & Mead, R. (1965). A simplex method for function minimization. *The Computer
27 Journal*, 7(4), 308–313. <https://doi.org/10.1093/comjnl/7.4.308>

28 Nelson, J. A., Walther, S., Gans, F., Kraft, B., Weber, U., Novick, K., Buchmann, N., Migliavacca,
29 M., Wohlfahrt, G., Šigut, L., Ibrom, A., Papale, D., Göckede, M., Duveiller, G., Knohl, A.,
30 Hörtnagl, L., Scott, R. L., Zhang, W., Hamdi, Z. M., ... Jung, M. (2024). X-BASE: the first
31 terrestrial carbon and water flux products from an extended data-driven scaling framework,
32 FLUXCOM-X. In *EGUspHERE*. <https://doi.org/10.5194/egusphere-2024-165>

33 Nicolini, G., Castaldi, S., Fratini, G., & Valentini, R. (2013). A literature overview of
34 micrometeorological CH₄ and N₂O flux measurements in terrestrial ecosystems.
35 *Atmospheric Environment (Oxford, England: 1994)*, 81, 311–319.
36 <https://doi.org/10.1016/j.atmosenv.2013.09.030>

37 Norton, A. J., Rayner, P. J., Koffi, E. N., & Scholze, M. (2018). Assimilating solar-induced
38 chlorophyll fluorescence into the terrestrial biosphere model BETHY-SCOPE v1.0: model
39 description and information content. *Geoscientific Model Development*, 11(4), 1517–1536.
40 <https://doi.org/10.5194/gmd-11-1517-2018>

41 Norton, A. J., Rayner, P. J., Koffi, E. N., Scholze, M., Silver, J. D., & Wang, Y.-P. (2019).
42 Estimating global gross primary productivity using chlorophyll fluorescence and a data
43 assimilation system with the BETHY-SCOPE model. *Biogeosciences*, 16(15), 3069–3093.
44 <https://doi.org/10.5194/bg-16-3069-2019>

1 Novick, K. A., Ficklin, D. L., Baldocchi, D., Davis, K. J., Ghezzehei, T. A., Konings, A. G.,
2 MacBean, N., Raoult, N., Scott, R. L., Shi, Y., Sulman, B. N., & Wood, J. D. (2022).
3 Confronting the water potential information gap. *Nature Geoscience*, 15(3), 158–164.
4 <https://doi.org/10.1038/s41561-022-00909-2>

5 Oberpriller, J., Cameron, D. R., Dietze, M. C., & Hartig, F. (2021). Towards robust statistical
6 inference for complex computer models. *Ecology Letters*, 24(6), 1251–1261.
7 <https://doi.org/10.1111/ele.13728>

8 Oberpriller, J., Herschlein, C., Anthoni, P., Arneth, A., Krause, A., Rammig, A., & Hartig. (2022).
9 Climate and parameter sensitivity and induced uncertainties in carbon stock projections for
10 European forests (using LPJ-GUESS 4.0). *Geoscientific Model Development*, 15(16),
11 6495–6519. <https://gmd.copernicus.org/articles/15/6495/2022/>

12 Olivera-Guerra, L.-E., Ottlé, C., Raoult, N., & Peylin, P. (2024). *Assimilating ESA-CCI Land
13 Surface Temperature into the ORCHIDEE Land Surface Model: Insights from a multi-site
14 study across Europe*. <https://doi.org/10.5194/egusphere-2024-546>

15 Owen, A. B. (2013). *Monte Carlo theory, methods and examples*. 16, 19–22.
16 https://scholar.google.com/citations?view_op=view_citation&hl=en&citation_for_view=owV8q1cAAAAJ:tOudhMTPpwUC

18 Parton, W. J., Schimel, D. S., Cole, C. V., & Ojima, D. S. (1987). Analysis of factors controlling
19 soil organic matter levels in Great Plains grasslands. *Soil Science Society of America
20 Journal. Soil Science Society of America*, 51(5), 1173–1179.
21 <https://doi.org/10.2136/sssaj1987.03615995005100050015x>

22 Paszke, A., Gross, S., Massa, F., Lerer, A., Bradbury, J., Chanan, G., Killeen, T., Lin, Z.,
23 Gimelshein, N., Antiga, L., Desmaison, A., Köpf, A., Yang, E., DeVito, Z., Raison, M.,
24 Tejani, A., Chilamkurthy, S., Steiner, B., Fang, L., ... Chintala, S. (2019). PyTorch: An
25 imperative style, high-performance deep learning library. *Neural Information Processing
26 Systems*, *abs/1912.01703*.
27 <https://papers.nips.cc/paper/9015-pytorch-an-imperative-style-high-performance-deep-learn>
28 ing-library

29 Peatier, S., Sanderson, B. M., & Terray, L. (2023). On the spatial calibration of imperfect climate
30 models. In *EGUspHERE*. <https://doi.org/10.5194/egusphere-2023-2269>

31 Peylin, P., Bacour, C., MacBean, N., Leonard, S., Rayner, P., Kuppel, S., Koffi, E., Kane, A.,
32 Maignan, F., Chevallier, F., Ciais, P., & Prunet, P. (2016). A new stepwise carbon cycle data
33 assimilation system using multiple data streams to constrain the simulated land surface
34 carbon cycle. *Geoscientific Model Development*, 9(9), 3321–3346.
35 <https://doi.org/10.5194/gmd-9-3321-2016>

36 Pianosi, F., Iwema, J., Rosolem, R., & Wagener, T. (2017). A multimethod global sensitivity
37 analysis approach to support the calibration and evaluation of land surface models. In
38 *Sensitivity Analysis in Earth Observation Modelling* (pp. 125–144). Elsevier.
39 <https://doi.org/10.1016/b978-0-12-803011-0.00007-0>

40 Pinnington, E., Amezcuia, J., Cooper, E., Dadson, S., Ellis, R., Peng, J., Robinson, E., Morrison,
41 R., Osborne, S., & Quaife, T. (2021). Improving soil moisture prediction of a high-resolution
42 land surface model by parameterising pedotransfer functions through assimilation of SMAP
43 satellite data. *Hydrology and Earth System Sciences*, 25(3), 1617–1641.
44 <https://doi.org/10.5194/hess-25-1617-2021>

1 Pinnington, E. M., Casella, E., Dance, S. L., Lawless, A. S., Morison, J. I. L., Nichols, N. K.,
2 Wilkinson, M., & Quaife, T. L. (2017). Understanding the effect of disturbance from selective
3 felling on the carbon dynamics of a managed woodland by combining observations with
4 model predictions. *J. Geophys. Res. Biogeosci.*, 122, 886–902.
5 <https://doi.org/10.1002/2017JG003760>

6 Pinnington, E., Quaife, T., & Black, E. (2018). Impact of remotely sensed soil moisture and
7 precipitation on soil moisture prediction in a data assimilation system with the JULES land
8 surface model. *Hydrology and Earth System Sciences*, 22(4), 2575–2588.
9 <https://hess.copernicus.org/articles/22/2575/2018/>

10 Pinnington, E., Quaife, T., Lawless, A., Williams, K., Arkebauer, T., & Scoby, D. (2020). The
11 Land Variational Ensemble Data Assimilation Framework: LAVENDAR v1.0.0. *Geoscientific
12 Model Development*, 13(1), 55–69. <https://doi.org/10.5194/gmd-13-55-2020>

13 Post, H., Vrugt, J. A., Fox, A., Vereecken, H., & Hendricks Franssen, H.-J. (2017). Estimation of
14 Community Land Model parameters for an improved assessment of net carbon fluxes at
15 European sites: Estimation of CLM Parameters. *Journal of Geophysical Research.
16 Biogeosciences*, 122(3), 661–689. <https://doi.org/10.1002/2015jg003297>

17 Potapov, P., Li, X., Hernandez-Serna, A., Tyukavina, A., Hansen, M. C., Kommareddy, A.,
18 Pickens, A., Turubanova, S., Tang, H., Silva, C. E., Armston, J., Dubayah, R., Blair, J. B., &
19 Hofton, M. (2021). Mapping global forest canopy height through integration of GEDI and
20 Landsat data. *Remote Sensing of Environment*, 253(112165), 112165.
21 <https://doi.org/10.1016/j.rse.2020.112165>

22 Prihodko, L., Denning, A. S., Hanan, N. P., Baker, I., & Davis, K. (2008). Sensitivity, uncertainty
23 and time dependence of parameters in a complex land surface model. *Agricultural and
24 Forest Meteorology*, 148(2), 268–287. <https://doi.org/10.1016/j.agrformet.2007.08.006>

25 Quaife, T., Lewis, P., Dekauwe, M., Williams, M., Law, B., Disney, M., & Bowyer, P. (2008).
26 Assimilating canopy reflectance data into an ecosystem model with an Ensemble Kalman
27 Filter. *Remote Sensing of Environment*, 112(4), 1347–1364.
28 <https://doi.org/10.1016/j.rse.2007.05.020>

29 Quegan, S., Le Toan, T., Chave, J., Dall, J., Exbrayat, J.-F., Minh, D. H. T., Lomas, M.,
30 D'Alessandro, M. M., Paillou, P., Papathanassiou, K., Rocca, F., Saatchi, S., Scipal, K.,
31 Shugart, H., Smallman, T. L., Soja, M. J., Tebaldini, S., Ulander, L., Villard, L., & Williams,
32 M. (2019). The European Space Agency BIOMASS mission: Measuring forest
33 above-ground biomass from space. *Remote Sensing of Environment*, 227, 44–60.
34 <https://doi.org/10.1016/j.rse.2019.03.032>

35 Racza, B., Dietze, M. C., Serbin, S. P., & Davis, K. J. (2018). What limits predictive certainty of
36 long-term carbon uptake? *Journal of Geophysical Research. Biogeosciences*, 123(12),
37 3570–3588. <https://doi.org/10.1029/2018jg004504>

38 Raiho, A. M., Nicklen, E. F., Foster, A. C., Roland, C. A., & Hooten, M. B. (2021). Bridging
39 implementation gaps to connect large ecological datasets and complex models. *Ecology
40 and Evolution*, 11(24), 18271–18287. <https://doi.org/10.1002/ece3.8420>

41 Raoult, N., Beylat, S., Salter, J. M., Hourdin, F., Bastrikov, V., Ottlé, C., & Peylin, P. (2024).
42 Exploring the potential of history matching for land surface model calibration. *Geoscientific
43 Model Development*, 17(15), 5779–5801. <https://doi.org/10.5194/gmd-17-5779-2024>

44 Raoult, N., Charbit, S., Dumas, C., Maignan, F., Ottlé, C., & Bastrikov, V. (2023). Improving

1 modelled albedo over the Greenland ice sheet through parameter optimisation and MODIS
2 snow albedo retrievals. *The Cryosphere*, 17(7), 2705–2724.
3 <https://doi.org/10.5194/tc-17-2705-2023>

4 Raoult, N., Edouard-Rambaut, L.-A., Vuichard, N., Bastrikov, V., Lansø, A. S., Guenet, B., &
5 Peylin, P. (2024). Using Free Air CO₂ Enrichment data to constrain land surface model
6 projections of the terrestrial carbon cycle. *Biogeosciences*, 21(4), 1017–1036.
7 <https://doi.org/10.5194/bg-21-1017-2024>

8 Raoult, N. M., Jupp, T. E., Cox, P. M., & Luke, C. M. (2016). Land-surface parameter
9 optimisation using data assimilation techniques: the adjULES system V1.0. *Geoscientific
10 Model Development*, 9(8), 2833–2852. <https://doi.org/10.5194/gmd-9-2833-2016>

11 Raoult, N., Ottlé, C., Peylin, P., Bastrikov, V., & Maugis, P. (2021). Evaluating and optimizing
12 surface soil moisture drydowns in the ORCHIDEE land surface model at in situ locations.
13 *Journal of Hydrometeorology*, 22(4), 1025–1043. <https://doi.org/10.1175/jhm-d-20-0115.1>

14 Rayner, P. J. (2010). *The current state of carbon-cycle data assimilation*. 2(4), 289–296.
15 https://scholar.google.com/citations?view_op=view_citation&hl=en&citation_for_view=H3up71wAAAAJ:isC4tDSrTZIC

16 Rayner, P. J., Koffi, E., Scholze, M., Kaminski, T., & Dufresne, J.-L. (2011). Constraining
17 predictions of the carbon cycle using data. *Philosophical Transactions. Series A,
18 Mathematical, Physical, and Engineering Sciences*, 369(1943), 1955–1966.
19 <https://doi.org/10.1098/rsta.2010.0378>

20 Rayner, P. J., Michalak, A. M., & Chevallier, F. (2019). Fundamentals of data assimilation
21 applied to biogeochemistry. *Atmospheric Chemistry and Physics*, 19(22), 13911–13932.
22 <https://doi.org/10.5194/acp-19-13911-2019>

23 Rayner, P. J., Scholze, M., Knorr, W., Kaminski, T., Giering, R., & Widmann, H. (2005). Two
24 decades of terrestrial carbon fluxes from a carbon cycle data assimilation system (CCDAS).
25 *Global Biogeochemical Cycles*, 19(2). <https://doi.org/10.1029/2004gb002254>

26 Reichstein, M., Camps-Valls, G., Stevens, B., Jung, M., Denzler, J., Carvalhais, N., & Prabhat.
27 (2019). Deep learning and process understanding for data-driven Earth system science.
28 *Nature*, 566(7743), 195–204. <https://doi.org/10.1038/s41586-019-0912-1>

29 Reick, C. H., Gayler, V., Goll, D., Hagemann, S., & Heidkamp, M. (2021).
30 https://pure.mpg.de/rest/items/item_3279802/component/file_3316522/content

31 Ricciuto, D. M., Butler, M. P., Davis, K. J., Cook, B. D., Bakwin, P. S., Andrews, A., & Teclaw, R.
32 M. (2008). Causes of interannual variability in ecosystem–atmosphere CO₂ exchange in a
33 northern Wisconsin forest using a Bayesian model calibration. *Agricultural and Forest
34 Meteorology*, 148(2), 309–327. <https://doi.org/10.1016/j.agrformet.2007.08.007>

35 Ricciuto, D. M., King, A. W., Dragoni, D., & Post, W. M. (2011). Parameter and prediction
36 uncertainty in an optimized terrestrial carbon cycle model: Effects of constraining variables
37 and data record length. *Journal of Geophysical Research*, 116(G1).
38 <https://doi.org/10.1029/2010jg001400>

39 Rödenbeck, C., Houweling, S., Gloor, M., & Heimann, M. (2003). CO₂ flux history 1982–2001
40 inferred from atmospheric data using a global inversion of atmospheric transport.
41 *Atmospheric Chemistry and Physics*, 3(6), 1919–1964.
42 <https://doi.org/10.5194/acp-3-1919-2003>

43 Rodríguez-Fernández, N., de Rosnay, P., Albergel, C., Richaume, P., Aires, F., Prigent, C., &

1 Kerr, Y. (2019). SMOS neural network Soil Moisture data assimilation in a Land surface
2 model and atmospheric impact. *Remote Sensing*, 11(11), 1334.
3 <https://doi.org/10.3390/rs11111334>

4 Rowland, L., Hill, T. C., Stahl, C., Siebicke, L., Burban, B., Zaragoza-Castells, J., Ponton, S.,
5 Bonal, D., Meir, P., & Williams, M. (2014). Evidence for strong seasonality in the carbon
6 storage and carbon use efficiency of an Amazonian forest. *Global Change Biology*, 20(3),
7 979–991. <https://doi.org/10.1111/gcb.12375>

8 Running, S., Mu, Q., & Zhao, M. (2021). *MODIS/Terra gross primary productivity 8-day L4
9 global 500m SIN grid V061* [Dataset]. NASA EOSDIS Land Processes Distributed Active
10 Archive Center. <https://doi.org/10.5067/MODIS/MOD17A2H.061>

11 Sacks, W. J., Schimel, D. S., Monson, R. K., & Braswell, B. H. (2006). Model-data synthesis of
12 diurnal and seasonal CO₂ fluxes at Niwot Ridge, Colorado: MODEL-DATA SYNTHESIS OF
13 CO₂ FLUXES. *Global Change Biology*, 12(2), 240–259.
14 <https://doi.org/10.1111/j.1365-2486.2005.01059.x>

15 Salmon, E., Jégou, F., Guenet, B., Jourdain, L., Qiu, C., Bastrikov, V., Guimbaud, C., Zhu, D.,
16 Ciais, P., Peylin, P., Gogo, S., Laggoun-Défarge, F., Aurela, M., Bret-Harte, M. S., Chen, J.,
17 Chojnicki, B. H., Chu, H., Edgar, C. W., Euskirchen, E. S., ... Ziemblińska, K. (2022).
18 Assessing methane emissions for northern peatlands in ORCHIDEE-PEAT revision 7020.
19 *Geoscientific Model Development*, 15(7), 2813–2838.
20 <https://doi.org/10.5194/gmd-15-2813-2022>

21 Saltelli, A., Ratto, M., Andres, T., Campolongo, F., Cariboni, J., Gatelli, D., Saisana, M., &
22 Tarantola, S. (2008). *Global Sensitivity Analysis: The Primer*. Wiley & Sons, Limited, John.
23 https://openlibrary.org/books/OL33376474M/Global_Sensitivity_Analysis

24 Sanderson, B. (2020). The role of prior assumptions in carbon budget calculations. *Earth
25 System Dynamics*, 11(2), 563–577. <https://doi.org/10.5194/esd-11-563-2020>

26 Sanderson, B. M., Knutti, R., Aina, T., Christensen, C., Faull, N., Frame, D. J., Ingram, W. J.,
27 Piani, C., Stainforth, D. A., Stone, D. A., & Allen, M. R. (2008). Constraints on Model
28 Response to Greenhouse Gas Forcing and the Role of Subgrid-Scale Processes. *Journal
29 of Climate*, 21(11), 2384–2400. <https://doi.org/10.1175/2008JCLI1869.1>

30 Santaren, D., Peylin, P., Bacour, C., Ciais, P., & Longdoz, B. (2014). Ecosystem model
31 optimization using in situ flux observations: benefit of Monte Carlo versus variational
32 schemes and analyses of the year-to-year model performances. *Biogeosciences*, 11(24),
33 7137–7158. <https://doi.org/10.5194/bg-11-7137-2014>

34 Santaren, D., Peylin, P., Viovy, N., & Ciais, P. (2007). Optimizing a process-based ecosystem
35 model with eddy-covariance flux measurements: A pine forest in southern France. *Global
36 Biogeochemical Cycles*, 21(2). <https://doi.org/10.1029/2006GB002834>

37 Sawada, Y. (2020). Machine learning accelerates parameter optimization and uncertainty
38 assessment of a land surface model. *Journal of Geophysical Research*, 125(20).
39 <https://doi.org/10.1029/2020jd032688>

40 Scholze, M., Buchwitz, M., Dorigo, W., Guanter, L., & Quegan, S. (2017). Reviews and
41 syntheses: Systematic Earth observations for use in terrestrial carbon cycle data
42 assimilation systems. *Biogeosciences*, 14(14), 3401–3429.
43 <https://doi.org/10.5194/bg-14-3401-2017>

44 Scholze, M., Kaminski, T., Knorr, W., Blessing, S., Vossbeck, M., Grant, J. P., & Scipal, K.

1 (2016). Simultaneous assimilation of SMOS soil moisture and atmospheric CO₂ in-situ
2 observations to constrain the global terrestrial carbon cycle. *Remote Sensing of*
3 *Environment*, 180, 334–345. <https://doi.org/10.1016/j.rse.2016.02.058>

4 Scholze, M., Kaminski, T., Knorr, W., Voßbeck, M., Wu, M., Ferrazzoli, P., Kerr, Y., Mialon, A.,
5 Richaume, P., Rodríguez-Fernández, N., Vittucci, C., Wigneron, J.-P., Mecklenburg, S., &
6 Drusch, M. (2019). Mean European carbon sink over 2010–2015 estimated by
7 simultaneous assimilation of atmospheric CO₂, soil moisture, and vegetation optical depth.
8 *Geophysical Research Letters*, 46(23), 13796–13803.
9 <https://doi.org/10.1029/2019gl085725>

10 Scholze, M., Kaminski, T., Rayner, P., Knorr, W., & Giering, R. (2007). Propagating uncertainty
11 through prognostic carbon cycle data assimilation system simulations.
12 <https://agupubs.onlinelibrary.wiley.com> › 2007JD008642
13 <https://doi.org/10.1029/2007JD008642>

14 Schürmann, G. J., Kaminski, T., Köstler, C., Carvalhais, N., Voßbeck, M., Kattge, J., Giering, R.,
15 Rödenbeck, C., Heimann, M., & Zaehle, S. (2016). Constraining a land-surface model with
16 multiple observations by application of the MPI-Carbon Cycle Data Assimilation System
17 V1.0. *Geoscientific Model Development*, 9(9), 2999–3026.
18 <https://doi.org/10.5194/gmd-9-2999-2016>

19 Scrucca, L. (2013). GA: A package for genetic algorithms in R. *Journal of Statistical Software*,
20 53(4), 1–37. <https://doi.org/10.18637/jss.v053.i04>

21 Seiler, C., Melton, J. R., Arora, V. K., Sitch, S., Friedlingstein, P., Anthoni, P., Goll, D., Jain, A.
22 K., Joetzjer, E., Lienert, S., Lombardozzi, D., Luyssaert, S., Nabel, J. E. M. S., Tian, H.,
23 Vuichard, N., Walker, A. P., Yuan, W., & Zaehle, S. (2022). Are terrestrial biosphere models
24 fit for simulating the global land carbon sink? *Journal of Advances in Modeling Earth
25 Systems*, 14(5). <https://doi.org/10.1029/2021ms002946>

26 Shan, X., Steele-Dunne, S., Huber, M., Hahn, S., Wagner, W., Bonan, B., Albergel, C., Calvet,
27 J.-C., Ku, O., & Georgievská, S. (2022). Towards constraining soil and vegetation dynamics
28 in land surface models: Modeling ASCAT backscatter incidence-angle dependence with a
29 Deep Neural Network. *Remote Sensing of Environment*, 279(113116), 113116.
30 <https://doi.org/10.1016/j.rse.2022.113116>

31 Shen, C., Appling, A. P., Gentine, P., Bandai, T., Gupta, H., Tartakovsky, A., Baity-Jesi, M.,
32 Fenicia, F., Kifer, D., Li, L., Liu, X., Ren, W., Zheng, Y., Harman, C. J., Clark, M., Farthing,
33 M., Feng, D., Kumar, P., Aboelyazeed, D., ... Lawson, K. (2023). Differentiable modelling to
34 unify machine learning and physical models for geosciences. *Nature Reviews Earth &
35 Environment*, 4(8), 552–567. <https://doi.org/10.1038/s43017-023-00450-9>

36 Shen, H., Wang, Y., Guan, X., Huang, W., Chen, J., Lin, D., & Gan, W. (2022). A spatiotemporal
37 constrained machine learning method for OCO-2 solar-induced chlorophyll fluorescence
38 (SIF) reconstruction. *IEEE Transactions on Geoscience and Remote Sensing: A Publication
39 of the IEEE Geoscience and Remote Sensing Society*, 60, 1–17.
40 <https://doi.org/10.1109/tgrs.2022.3204885>

41 Shiklomanov, A. N., Cowdery, E. M., Bahn, M., Byun, C., Jansen, S., Kramer, K., Minden, V.,
42 Niinemets, Ü., Onoda, Y., Soudzilovskaia, N. A., & Dietze, M. C. (2018). Does the leaf
43 economic spectrum hold within plant functional types? A Bayesian multivariate trait

1 meta-analysis. In *bioRxiv* (p. 475038). bioRxiv. <https://doi.org/10.1101/475038>

2 Shiklomanov, A. N., Dietze, M. C., Fer, I., Viskari, T., & Serbin, S. P. (2021). Cutting out the
3 middleman: calibrating and validating a dynamic vegetation model (ED2-PROSPECT5)
4 using remotely sensed surface reflectance. *Geoscientific Model Development*, 14(5),
5 2603–2633. <https://doi.org/10.5194/gmd-14-2603-2021>

6 Shi, Z., Allison, S. D., He, Y., Levine, P. A., Hoyt, A. M., Beem-Miller, J., Zhu, Q., Wieder, W. R.,
7 Trumbore, S., & Randerson, J. T. (2020). The age distribution of global soil carbon inferred
8 from radiocarbon measurements. *Nature Geoscience*, 13(8), 555–559.
9 <https://doi.org/10.1038/s41561-020-0596-z>

10 Shi, Z., Hoffman, F. M., Xu, M., Mishra, U., Allison, S. D., Zhou, J., & Randerson, J. T. (2024).
11 Global-scale convergence obscures inconsistencies in soil carbon change predicted by
12 Earth system models. *AGU Advances*, 5(2), e2023AV001068.
13 <https://doi.org/10.1029/2023av001068>

14 Schwartz-Ziv, R., & Armon, A. (2022). Tabular data: Deep learning is not all you need. *An
15 International Journal on Information Fusion*, 81, 84–90.
16 <https://doi.org/10.1016/j.inffus.2021.11.011>

17 Sitch, S., O'Sullivan, M., Robertson, E., Friedlingstein, P., Albergel, C., Anthoni, P., Arneth, A.,
18 Arora, V. K., Bastos, A., Bastrikov, V., Bellouin, N., Canadell, J. G., Chini, L., Ciais, P., Falk,
19 S., Harris, I., Hurt, G., Ito, A., Jain, A. K., ... Zaehle, S. (2024). Trends and drivers of
20 terrestrial sources and sinks of carbon dioxide: An overview of the TRENDY project. *Global
21 Biogeochemical Cycles*, 38(7), e2024GB008102. <https://doi.org/10.1029/2024gb008102>

22 Smallman, T. L., Miodowski, D. T., Neto, E. S., Koren, G., Ometto, J., & Williams, M. (2021).
23 Parameter uncertainty dominates C-cycle forecast errors over most of Brazil for the 21st
24 century. *Earth System Dynamics*, 12(4), 1191–1237.
25 <https://doi.org/10.5194/esd-12-1191-2021>

26 Smith, B. (2007). *LPJ-GUESS – an ecosystem modelling framework*.
27 [https://www.baltex-research.eu/baltic2009/downloads/Literature/Specific/Smith_guess_soft
ware.pdf](https://www.baltex-research.eu/baltic2009/downloads/Literature/Specific/Smith_guess_soft
ware.pdf)

29 Smith, C., Cummins, D. P., Fredriksen, H.-B., Nicholls, Z., Meinshausen, M., Allen, M., Jenkins,
30 S., Leach, N., Mathison, C., & Partanen, A.-I. (2024). fair-calibrate v1.4.1: calibration,
31 constraining and validation of the Fair simple climate model for reliable future climate
32 projections. In *EGUsphere*. <https://doi.org/10.5194/egusphere-2024-708>

33 Sobol', I. M. (2001). Global sensitivity indices for nonlinear mathematical models and their
34 Monte Carlo estimates. *Mathematics and Computers in Simulation*, 55(1-3), 271–280.
35 [https://doi.org/10.1016/s0378-4754\(00\)00270-6](https://doi.org/10.1016/s0378-4754(00)00270-6)

36 Song, H., Triguero, I., & Özcan, E. (2019). A review on the self and dual interactions between
37 machine learning and optimisation. *Progress in Artificial Intelligence*, 8(2), 143–165.
38 <https://doi.org/10.1007/s13748-019-00185-z>

39 Speich, M., Dormann, C. F., & Hartig, F. (2021). Sequential Monte-Carlo algorithms for Bayesian
40 model calibration – A review and method comparison. *Ecological Modelling*,
41 455(109608), 109608. <https://doi.org/10.1016/j.ecolmodel.2021.109608>

42 Stewart, L. M., Dance, S. L., & Nichols, N. K. (2008). Correlated observation errors in data
43 assimilation. *International Journal for Numerical Methods in Fluids*, 56(8), 1521–1527.
44 <https://doi.org/10.1002/fld.1636>

1 Stöckli, R., Rutishauser, T., Dragoni, D., O'Keefe, J., Thornton, P. E., Jolly, M., Lu, L., &
2 Denning, A. S. (2008). Remote sensing data assimilation for a prognostic phenology model:
3 DATA ASSIMILATION AND PHENOLOGY MODELING. *Journal of Geophysical Research*,
4 113(G4). <https://doi.org/10.1029/2008jg000781>

5 Sun, Y., Goll, D. S., Huang, Y., Ciais, P., Wang, Y.-P., Bastrikov, V., & Wang, Y. (2023). Machine
6 learning for accelerating process-based computation of land biogeochemical cycles. *Global
7 Change Biology*, 29(11), 3221–3234. <https://doi.org/10.1111/gcb.16623>

8 Talagrand, O., & Courtier, P. (1987). Variational assimilation of meteorological observations with
9 the adjoint vorticity equation. I: Theory: Variational assimilation. I: Theory. *Quarterly Journal
10 of the Royal Meteorological Society. Royal Meteorological Society (Great Britain)*, 113(478),
11 1311–1328. <https://doi.org/10.1002/qj.49711347812>

12 Tao, F., Houlton, B. Z., Huang, Y., Wang, Y.-P., Manzoni, S., Ahrens, B., Mishra, U., Jiang, L.,
13 Huang, X., & Luo, Y. (2024). Convergence in simulating global soil organic carbon by
14 structurally different models after data assimilation. *Global Change Biology*, 30(5), e17297.
15 <https://doi.org/10.1111/gcb.17297>

16 Tao, F., Zhou, Z., Huang, Y., Li, Q., Lu, X., Ma, S., Huang, X., Liang, Y., Hugelius, G., Jiang, L.,
17 Doughty, R., Ren, Z., & Luo, Y. (2020). Deep learning optimizes data-driven representation
18 of soil organic carbon in Earth system model over the conterminous United States.
19 *Frontiers in Big Data*, 3, 17. <https://doi.org/10.3389/fdata.2020.00017>

20 Tarantola, A. (1987). Inversion of travel times and seismic waveforms. In *Seismic Tomography*
21 (pp. 135–157). Springer Netherlands. https://doi.org/10.1007/978-94-009-3899-1_6

22 Tarantola, A. (2005). Back Matter. In *Inverse Problem Theory and Methods for Model Parameter
23 Estimation* (pp. 317–342). Society for Industrial and Applied Mathematics.
24 <https://doi.org/10.1137/1.9780898717921.bm>

25 Thomas, R. Q., Brooks, E. B., Jersild, A. L., Ward, E. J., Wynne, R. H., Albaugh, T. J.,
26 Dinon-Aldridge, H., Burkhardt, H. E., Domec, J.-C., Fox, T. R., Gonzalez-Benecke, C. A.,
27 Martin, T. A., Noormets, A., Sampson, D. A., & Teskey, R. O. (2017). Leveraging 35 years
28 of *Pinus taeda* research in the southeastern US to constrain forest carbon cycle predictions:
29 regional data assimilation using ecosystem experiments. *Biogeosciences*, 14(14),
30 3525–3547. <https://doi.org/10.5194/bg-14-3525-2017>

31 Thum, T., MacBean, N., Peylin, P., Bacour, C., Santaren, D., Longdoz, B., Loustau, D., & Ciais,
32 P. (2017). The potential benefit of using forest biomass data in addition to carbon and water
33 flux measurements to constrain ecosystem model parameters: Case studies at two
34 temperate forest sites. *Agricultural and Forest Meteorology*, 234-235, 48–65.
35 <https://doi.org/10.1016/j.agrformet.2016.12.004>

36 Tian, X., Minunno, F., Cao, T., Peltoniemi, M., Kalliokoski, T., & Mäkelä, A. (2020). Extending the
37 range of applicability of the semi-empirical ecosystem flux model PRELES for varying forest
38 types and climate. *Global Change Biology*, 26(5), 2923–2943.
39 <https://doi.org/10.1111/gcb.14992>

40 Torres-Rojas, L., Vergopolan, N., Herman, J. D., & Chaney, N. W. (2022). Towards an optimal
41 representation of sub-grid heterogeneity in land surface models. *Water Resources
42 Research*, 58(12). <https://doi.org/10.1029/2022wr032233>

43 Tramontana, G., Jung, M., Schwalm, C. R., Ichii, K., Camps-Valls, G., Ráduly, B., Reichstein,
44 M., Arain, M. A., Cescatti, A., Kiely, G., Merbold, L., Serrano-Ortiz, P., Sickert, S., Wolf, S.,

1 & Papale, D. (2016). Predicting carbon dioxide and energy fluxes across global FLUXNET
2 sites with regression algorithms. *Biogeosciences*, 13(14), 4291–4313.
3 <https://doi.org/10.5194/bg-13-4291-2016>

4 Tramontana, G., Migliavacca, M., Jung, M., Reichstein, M., Keenan, T. F., Camps-Valls, G.,
5 Ogee, J., Verrelst, J., & Papale, D. (2020). Partitioning net carbon dioxide fluxes into
6 photosynthesis and respiration using neural networks. *Global Change Biology*, 26(9),
7 5235–5253. <https://doi.org/10.1111/gcb.15203>

8 Trudinger, C. M., Raupach, M. R., Rayner, P. J., Kattge, J., Liu, Q., Pak, B., Reichstein, M.,
9 Renzullo, L., Richardson, A. D., Roxburgh, S. H., Styles, J., Wang, Y. P., Briggs, P., Barrett,
10 D., & Nikolova, S. (2007). OptIC project: An intercomparison of optimization techniques for
11 parameter estimation in terrestrial biogeochemical models. *Journal of Geophysical
12 Research: Biogeosciences*, 112(G2). <https://doi.org/10.1029/2006JG000367>

13 Trugman, A. T., Anderegg, L. D. L., Shaw, J. D., & Anderegg, W. R. L. (2020). Trait velocities
14 reveal that mortality has driven widespread coordinated shifts in forest hydraulic trait
15 composition. *Proceedings of the National Academy of Sciences of the United States of
16 America*, 117(15), 8532–8538. <https://doi.org/10.1073/pnas.1917521117>

17 Ustin, S. L., & Middleton, E. M. (2021). Current and near-term advances in Earth observation for
18 ecological applications. *Ecological Processes*, 10(1), 1.
19 <https://doi.org/10.1186/s13717-020-00255-4>

20 van Oijen, M. (2017). Bayesian methods for quantifying and reducing uncertainty and error in
21 forest models. *Current Forestry Reports*, 3(4), 269–280.
22 <https://doi.org/10.1007/s40725-017-0069-9>

23 Varney, R. M., Friedlingstein, P., Chadburn, S. E., Burke, E. J., & Cox, P. M. (2024). Soil
24 carbon-concentration and carbon-climate feedbacks in CMIP6 Earth system models.
25 *Biogeosciences*, 21(11), 2759–2776. <https://doi.org/10.5194/bg-21-2759-2024>

26 Vekuri, H., Tuovinen, J.-P., Kulmala, L., Papale, D., Kolari, P., Aurela, M., Laurila, T., Liski, J., &
27 Lohila, A. (2023). A widely-used eddy covariance gap-filling method creates systematic bias
28 in carbon balance estimates. *Scientific Reports*, 13(1), 1720.
29 <https://doi.org/10.1038/s41598-023-28827-2>

30 Verbeeck, H., Peylin, P., Bacour, C., Bonal, D., Steppe, K., & Ciais, P. (2011). Seasonal patterns
31 of CO₂fluxes in Amazon forests: Fusion of eddy covariance data and the ORCHIDEE
32 model. *Journal of Geophysical Research*, 116(G2). <https://doi.org/10.1029/2010jg001544>

33 Vergopolan, N., Chaney, N. W., Beck, H. E., Pan, M., Sheffield, J., Chan, S., & Wood, E. F.
34 (2020). Combining hyper-resolution land surface modeling with SMAP brightness
35 temperatures to obtain 30-m soil moisture estimates. *Remote Sensing of the Environment*,
36 242(111740), 111740. <https://doi.org/10.1016/j.rse.2020.111740>

37 Vergopolan, N., Chaney, N. W., Pan, M., Sheffield, J., Beck, H. E., Ferguson, C. R.,
38 Torres-Rojas, L., Sadri, S., & Wood, E. F. (2021). SMAP-HydroBlocks, a 30-m
39 satellite-based soil moisture dataset for the conterminous US. *Scientific Data*, 8(1), 264.
40 <https://doi.org/10.1038/s41597-021-01050-2>

41 Vrugt, J. A. (2016). Markov chain Monte Carlo simulation using the DREAM software package:
42 Theory, concepts, and MATLAB implementation. *Environmental Modelling & Software: With
43 Environment Data News*, 75, 273–316. <https://doi.org/10.1016/j.envsoft.2015.08.013>

44 Vrugt, J. A., ter Braak, C. J. F., Diks, C. G. H., Robinson, B. A., Hyman, J. M., & Higdon, D.

1 (2009). Accelerating Markov Chain Monte Carlo Simulation by Differential Evolution with
2 Self-Adaptive Randomized Subspace Sampling. *International Journal of Nonlinear*
3 *Sciences and Numerical Simulation*, 10(3). <https://doi.org/10.1515/IJNSNS.2009.10.3.273>

4 Vuichard, N., Messina, P., Luyssaert, S., Guenet, B., Zaehle, S., Ghattas, J., Bastrikov, V., &
5 Peylin, P. (2019). Accounting for carbon and nitrogen interactions in the global terrestrial
6 ecosystem model ORCHIDEE (trunk version, rev 4999): multi-scale evaluation of gross
7 primary production. *Geoscientific Model Development*, 12(11), 4751–4779.
8 <https://doi.org/10.5194/gmd-12-4751-2019>

9 Waller, J. A., Dance, S. L., & Nichols, N. K. (2016). Theoretical insight into diagnosing
10 observation error correlations using observation-minus-background and
11 observation-minus-analysis statistics. *Quarterly Journal of the Royal Meteorological*
12 *Society. Royal Meteorological Society (Great Britain)*, 142(694), 418–431.
13 <https://doi.org/10.1002/qj.2661>

14 Wang, H., Huo, X., Duan, Q., Liu, R., & Luo, S. (2023). Uncertainty quantification for the
15 Noah-MP land surface model: A case study in a grassland and sandy soil region. *Journal of*
16 *Geophysical Research Atmospheres*, 128(20). <https://doi.org/10.1029/2023jd038556>

17 Wang, J., Jiang, F., Wang, H., Qiu, B., Wu, M., He, W., Ju, W., Zhang, Y., Chen, J. M., & Zhou,
18 Y. (2021). Constraining global terrestrial gross primary productivity in a global carbon
19 assimilation system with OCO-2 chlorophyll fluorescence data. *Agricultural and Forest*
20 *Meteorology*, 304-305(108424), 108424. <https://doi.org/10.1016/j.agrformet.2021.108424>

21 Wang, N., Zhang, D., Chang, H., & Li, H. (2020). Deep learning of subsurface flow via
22 theory-guided neural network. *Journal of Hydrology*, 584(124700), 124700.
23 <https://doi.org/10.1016/j.jhydrol.2020.124700>

24 Wang, Y.-P., Leuning, R., Cleugh, H. A., & Coppin, P. A. (2001). Parameter estimation in surface
25 exchange models using nonlinear inversion: how many parameters can we estimate and
26 which measurements are most useful?: NONLINEAR PARAMETER ESTIMATION. *Global*
27 *Change Biology*, 7(5), 495–510. <https://doi.org/10.1046/j.1365-2486.2001.00434.x>

28 Watson-Parris, D. (2021). Machine learning for weather and climate are worlds apart.
29 *Philosophical Transactions. Series A, Mathematical, Physical, and Engineering Sciences*,
30 379(2194), 20200098. <https://doi.org/10.1098/rsta.2020.0098>

31 Watson-Parris, D., Williams, A., Deaconu, L., & Stier, P. (2021). Model calibration using ESEm
32 v1.1.0 – an open, scalable Earth system emulator. *Geoscientific Model Development*,
33 14(12), 7659–7672. <https://doi.org/10.5194/gmd-14-7659-2021>

34 Weng, E., & Luo, Y. (2011). Relative information contributions of model vs. data to short- and
35 long-term forecasts of forest carbon dynamics. *Ecological Applications: A Publication of the*
36 *Ecological Society of America*, 21(5), 1490–1505. <https://doi.org/10.1890/09-1394.1>

37 Weng, E., Luo, Y., Gao, C., & Oren, R. (2011). Uncertainty analysis of forest carbon sink
38 forecast with varying measurement errors: a data assimilation approach. *Journal of Plant*
39 *Ecology*, 4(3), 178–191. <https://doi.org/10.1093/jpe/rtr018>

40 Wesselkamp, M., Chantry, M., Pinnington, E., Choulga, M., Boussetta, S., Kalweit, M.,
41 Boedecker, J., Dormann, C. F., Pappenberger, F., & Balsamo, G. (2024). Advances in Land
42 Surface Model-based Forecasting: A comparative study of LSTM, Gradient Boosting, and
43 Feedforward Neural Network Models as prognostic state emulators. In *arXiv*
44 [*physics.ao-ph*]. arXiv. <http://arxiv.org/abs/2407.16463>

1 Whelan, M. E., Lennartz, S. T., Gimeno, T. E., Wehr, R., Wohlfahrt, G., Wang, Y., Kooijmans, L.
2 M. J., Hilton, T. W., Belviso, S., Peylin, P., Commane, R., Sun, W., Chen, H., Kuai, L.,
3 Mammarella, I., Maseyk, K., Berkelhammer, M., Li, K.-F., Yakir, D., ... Campbell, J. E.
4 (2018). Reviews and syntheses: Carbonyl sulfide as a multi-scale tracer for carbon and
5 water cycles. *Biogeosciences*, 15(12), 3625–3657.
6 <https://doi.org/10.5194/bg-15-3625-2018>

7 Williams, M., Schwarz, P. A., Law, B. E., Irvine, J., & Kurpius, M. R. (2005). An improved
8 analysis of forest carbon dynamics using data assimilation. *Global Change Biology*, 11(1),
9 89–105. <https://doi.org/10.1111/j.1365-2486.2004.00891.x>

10 Williamson, D., Goldstein, M., Allison, L., Blaker, A., Challenor, P., Jackson, L., & Yamazaki, K.
11 (2013). History matching for exploring and reducing climate model parameter space using
12 observations and a large perturbed physics ensemble. *Climate Dynamics*, 41(7),
13 1703–1729. <https://doi.org/10.1007/s00382-013-1896-4>

14 Wu, J.-L., Levine, M. E., Schneider, T., & Stuart, A. (2023). Learning about structural errors in
15 models of complex dynamical systems. In *arXiv [physics.comp-ph]*. arXiv.
16 <http://arxiv.org/abs/2401.00035>

17 Wu, M., Jiang, F., Scholze, M., Chen, D., Ju, W., Wang, S., Kaminski, T., Lu, Z., Vossbeck, M., &
18 Zheng, M. (2024). Regional responses of vegetation productivity to the two phases of
19 ENSO. *Geophysical Research Letters*, 51(8). <https://doi.org/10.1029/2024gl108176>

20 Wu, M., Scholze, M., Kaminski, T., Voßbeck, M., & Tagesson, T. (2020). Using SMOS soil
21 moisture data combining CO₂ flask samples to constrain carbon fluxes during 2010–2015
22 within a Carbon Cycle Data Assimilation System (CCDAS). *Remote Sensing of
23 Environment*, 240(111719), 111719. <https://doi.org/10.1016/j.rse.2020.111719>

24 Wu, M., Scholze, M., Voßbeck, M., Kaminski, T., & Hoffmann, G. (2018). Simultaneous
25 assimilation of remotely sensed Soil Moisture and FAPAR for improving terrestrial carbon
26 fluxes at multiple sites using CCDAS. *Remote Sensing*, 11(1), 27.
27 <https://doi.org/10.3390/rs11010027>

28 Wutzler, T., & Carvalhais, N. (2014). Balancing multiple constraints in model-data integration:
29 Weights and the parameter block approach. *Journal of Geophysical Research: Biogeosciences*, 119(11), 2112–2129. <https://doi.org/10.1002/2014jg002650>

30 Xiao, J., Davis, K. J., Urban, N. M., & Keller, K. (2014). Uncertainty in model parameters and
31 regional carbon fluxes: A model-data fusion approach. *Agricultural and Forest Meteorology*,
32 189–190, 175–186. <https://doi.org/10.1016/j.agrformet.2014.01.022>

33 Xie, K., Liu, P., Zhang, J., Han, D., Wang, G., & Shen, C. (2021). Physics-guided deep learning
34 for rainfall-runoff modeling by considering extreme events and monotonic relationships.
35 *Journal of Hydrology*, 603(127043), 127043. <https://doi.org/10.1016/j.jhydrol.2021.127043>

36 Xu, T., White, L., Hui, D., & Luo, Y. (2006). Probabilistic inversion of a terrestrial ecosystem
37 model: Analysis of uncertainty in parameter estimation and model prediction. *Global
38 Biogeochemical Cycles*, 20(2). <https://doi.org/10.1029/2005GB002468>

39 Yang, T., Sun, F., Gentile, P., Liu, W., Wang, H., Yin, J., Du, M., & Liu, C. (2019). Evaluation and
40 machine learning improvement of global hydrological model-based flood simulations.
41 *Environmental Research Letters*, 14(11), 114027.
42 <https://doi.org/10.1088/1748-9326/ab4d5e>

43 Yatheendradas, S., & Kumar, S. (2022). A novel machine learning-based gap-filling of

1 fine-resolution remotely sensed snow cover fraction data by combining downscaling and
2 regression. *Journal of Hydrometeorology*, 23(5), 637–658.
3 <https://doi.org/10.1175/jhm-d-20-0111.1>

4 Zaehle, S., Friedlingstein, P., & Friend, A. D. (2010). Terrestrial nitrogen feedbacks may
5 accelerate future climate change: CARBON-NITROGEN FEEDBACKS AFFECT CLIMATE.
6 *Geophysical Research Letters*, 37(1). <https://doi.org/10.1029/2009gl041345>

7 Zaehle, S., Friend, A. D., Friedlingstein, P., Dentener, F., Peylin, P., & Schulz, M. (2010). Carbon
8 and nitrogen cycle dynamics in the O-CN land surface model: 2. Role of the nitrogen cycle
9 in the historical terrestrial carbon balance: NITROGEN EFFECTS ON GLOBAL C
10 CYCLING. *Global Biogeochemical Cycles*, 24(1). <https://doi.org/10.1029/2009gb003522>

11 Zeng, H., Elnashar, A., Wu, B., Zhang, M., Zhu, W., Tian, F., & Ma, Z. (2022). A framework for
12 separating natural and anthropogenic contributions to evapotranspiration of
13 human-managed land covers in watersheds based on machine learning. *The Science of the
14 Total Environment*, 823(153726), 153726. <https://doi.org/10.1016/j.scitotenv.2022.153726>

15 Zhang, H., Hendricks Franssen, H.-J., Han, X., Vrugt, J. A., & Vereecken, H. (2017). State and
16 parameter estimation of two land surface models using the ensemble Kalman filter and the
17 particle filter. *Hydrology and Earth System Sciences*, 21(9), 4927–4958.
18 <https://doi.org/10.5194/hess-21-4927-2017>

19 Zhang, J., Chung, H. S.-H., & Lo, W.-L. (2007). Clustering-Based Adaptive Crossover and
20 Mutation Probabilities for Genetic Algorithms. *IEEE Transactions on Evolutionary
21 Computation*, 11(3), 326–335. <https://doi.org/10.1109/TEVC.2006.880727>

22 Zhang, Y., Joiner, J., Alemohammad, S. H., Zhou, S., & Gentine, P. (2018). A global spatially
23 contiguous solar-induced fluorescence (CSIF) dataset using neural networks.
24 *Biogeosciences*, 15(19), 5779–5800.
25 <https://bg.copernicus.org/articles/15/5779/2018/bg-15-5779-2018.html>

26 Zhao, H., & Kowalski, J. (2022). Bayesian active learning for parameter calibration of landslide
27 run-out models. *Landslides*, 19(8), 2033–2045. <https://doi.org/10.1007/s10346-022-01857-z>

28 Zhao, W. L., Gentine, P., Reichstein, M., Zhang, Y., Zhou, S., Wen, Y., Lin, C., Li, X., & Qiu, G. Y.
29 (2019). Physics-constrained machine learning of evapotranspiration. *Geophysical Research
30 Letters*, 46(24), 14496–14507. <https://doi.org/10.1029/2019gl085291>

31 Zhou, A., Hawkins, L., & Gentine, P. (2024). Proof-of-concept: Using ChatGPT to Translate and
32 Modernize an Earth System Model from Fortran to Python/JAX. In *arXiv [cs.DC]*. arXiv.
33 <http://arxiv.org/abs/2405.00018>

34 Zhu, H., Wu, M., Jiang, F., Vossbeck, M., Kaminski, T., Xing, X., Wang, J., Ju, W., & Chen, J. M.
35 (2023). Assimilation of Carbonyl Sulfide (COS) fluxes within the adjoint-based data
36 assimilation system—Nanjing University Carbon Assimilation System (NUCAS v1.0). In
37 *EGUphere* (pp. 1–35). <https://doi.org/10.5194/egusphere-2023-1955>

38 Ziehn, T., Scholze, M., & Knorr, W. (2012). On the capability of Monte Carlo and adjoint
39 inversion techniques to derive posterior parameter uncertainties in terrestrial ecosystem
40 models: COMPARISON OF INVERSION TECHNIQUES. *Global Biogeochemical Cycles*,
41 26(3). <https://doi.org/10.1029/2011gb004185>

42 Zobitz, J. M., Moore, D. J. P., Quaife, T., Braswell, B. H., Bergeson, A., Anthony, J. A., &
43 Monson, R. K. (2014). Joint data assimilation of satellite reflectance and net ecosystem
44 exchange data constrains ecosystem carbon fluxes at a high-elevation subalpine forest.

1 *Agricultural and Forest Meteorology*, 195-196, 73–88.

2 <https://doi.org/10.1016/j.agrformet.2014.04.011>

3 Zuo, H., Balmaseda, M. A., Tietsche, S., Mogensen, K., & Mayer, M. (2019). The ECMWF
4 operational ensemble reanalysis–analysis system for ocean and sea ice: a description of
5 the system and assessment. *Ocean Science*, 15(3), 779–808.

6 <https://doi.org/10.5194/os-15-779-2019>

7